COORDINATION CHEMISTRY OF IRIDIUM AND PLATINUM COMPLEXES AS MODEL HOMOGENEOUS CATALYSTS

by

ILANA ENGELBRECHT

A thesis submitted to meet the requirements for the degree of

PHILOSOPHIAE DOCTOR

In the

DEPARTMENT OF CHEMISTRY

FACULTY OF NATURAL AND AGRICULTURAL SCIENCES

At the

UNIVERSITY OF THE FREE STATE

PROMOTOR: PROF. ANDREAS ROODT

CO-PROMOTOR: PROF. HENDRIK G. VISSER

FEBRUARY 2013

Acknowledgements

Firstly, all the glory and honour to my Heavenly Father who equipped me with wisdom, insight and perseverance to make my success possible. Thank you for the countless blessing that You have bestowed on me, for I am nothing without You.

Thank you to Prof. André Roodt for all the opportunities, patience and endless enthusiasm for chemistry. You are truly an inspiration and it is an honour to be known as one of your students.

To Prof. Deon Visser, thank you for all your guidance, encouragement and support. Your patience and willingness to give advice is greatly appreciated.

Thank you to all my colleagues in the Inorganic group for all the laughter and jokes. Thank you for all the advice and for sharing your knowledge.

Thank you to Prof. Roodt, Prof. Peter Comba and the INKABA yeAfrica program for the opportunity to study abroad in Germany.

To my parents, Barnie and Salomé Engelbrecht, without your unconditional love and sacrifices throughout the years, none of this would be possible. I am truly grateful for everything you have done for me. To my sister, Sarina, who is always willing to listen and who has made this journey easier, I thank you. Thank you to my grandmother, Sarah Nel, for entrusting the virtuous values that our family lives by.

Financial assistance from the Department of Science and Technology (DST) of South Africa, the NRF (National Research Foundation), the DST-NRF centre of excellence (c*change), SASOL, INKABA yeAfrica and the University of the Free State are gratefully acknowledged.

~~~~~~~

The most exciting phrase to hear in science, the one that heralds the most discoveries, is not "Eureka!" (I found it!), but "hmm, that's funny..."
~~~~~~~

Table of contents

Abbreviations and symbols VIII

Chapter 1:

Introduction and aim

1.1 Introduction 1

1.1.1 Homogeneous catalysis 1

1.1.2 Background on metals 2

1.2 Aim of this study 6

Chapter 2:

Literature Study

2.1 Introduction 10

2.2 Catalysis 11

2.3 Hydroformylation 13

2.3.1 Introduction 13

2.3.2 Mechanism 14

2.4 Ligand properties 16

2.4.1 Electronic effect 16

2.4.2 Steric effect 17

2.5 Effects of ligands in catalysis 17

2.5.1 Steric implication of ligands 17

2.5.2 Natural bite angle of *bis*-chelating ligands 22

Chapter 3:

Synthesis and characterization of PNP-ligands and corresponding metal coordinated complexes

3.1 Introduction 29

3.2 Chemicals and apparatus 30

3.3 Synthesis of reagents 31

3.3.1 *cis*-(η^4-Cycloocta-1,5-diene-dichloridoplatinum(II)) ([Pt(cod)Cl_2]) 31

3.3.2 *cis*-(η^4-Cycloocta-1,5-diene-dichloridopalladium(II)) ([Pd(cod)Cl_2]) 31

3.3.3 (Acetylacetonato)dicarbonylrhodium(I) ([Rh(acac)(CO_2)]) 31

3.4 Synthesis of bis(diphenylphosphino)amine ligands 32

3.4.1 *N,N*-Bis(diphenylphosphino)cyclopropanamine (1) 32

3.4.2 *N,N*-Bis(diphenylphosphino)cyclobutanamine (2) 32

3.4.3 *N,N*-Bis(diphenylphosphino)cyclopentanamine (3) 33

3.4.4 *N,N*-Bis(diphenylphosphino)cyclohexanamine (4) 33

3.5 Synthesis of Pt(II)-PNP complexes 34

3.5.1 Bis[*N,N*-bis(diphenylphosphanyl)cyclopropanamine-κ^2P,P']platinum(II) bis(trifluoromethanesulfonate) 34

3.5.2 Bis[*N,N*-bis(diphenylphosphanyl)cyclobutanamine-κ^2P,P']platinum(II) bis(trifluoromethanesulfonate) 34

3.5.3 Bis[*N,N*-bis(diphenylphosphanyl)cyclopentanamine-κ^2P,P']platinum(II) bis(trifluoromethanesulfonate) 35

3.5.4 Bis[*N,N*-bis(diphenylphosphanyl)cyclohexanamine-κ^2P,P']platinum(II) bis(hexafluoridophosphate) 35

3.5.5 Bis[*N,N*-bis(diphenylphosphanyl)-*n*-pentylamine-κ^2P,P']platinum(II) bis(hexafluoridophosphate) 36

3.6 Synthesis of Pd(II)-PNP complexes 36

3.6.1 Bis[*N,N*-bis(diphenylphosphanyl)cyclopropanamine-κ^2P,P']palladium(II) bis(hexafluoridophosphate) 36

3.6.2 Bis[*N,N*-bis(diphenylphosphanyl)cyclobutanamine-κ^2P,P']palladium(II) bis(hexafluoridophosphate) 37

3.6.3 Bis[*N,N*-bis(diphenylphosphanyl)cyclopentanamine-κ^2P,P']palladium(II) bis(hexafluoridophosphate) 37

3.6.4 Bis[*N,N*-bis(diphenylphosphanyl)cyclohexanamine-κ^2P,P']palladium(II) bis(hexafluorophosphate) 38

3.7 Discussion 38

Chapter 4:

Single crystal X-ray crystallographic study of bis(diphenylphosphino)amine ligands

4.1 Introduction 41

4.2 Experimental 44

4.3 *N,N-Bis*(diphenylphosphanyl)cyclopropanamine (1) 46

4.4 *N,N-Bis*(diphenylphosphanyl)cyclobutanamine (2) 50

4.5 *N,N-Bis*(diphenylphosphanyl)cyclopentylamine (3) 54

4.6 Discussion 59

Chapter 5:

Single crystal X-ray crystallographic study of Pt(II)-PNP and Pd(II)-PNP complexes

5.1 Introduction 62

5.2 Experimental 64

5.3 Bis[*N,N*-bis(diphenylphosphanyl)cyclopropanamine-κ^2P,P']platinum(II) bis(trifluoromethanesulfonate) 67

5.4 Bis[*N*,*N*-bis(diphenylphosphanyl)cyclobutanamine-κ^2P,P']platinum(II) bis(trifluoromethanesulfonate) 71

5.5 Bis[*N*,*N*-bis(diphenylphosphanyl)cyclopentanamine-κ^2P,P']platinum(II) bis(trifluoromethanesulfonate) 76

5.6 Bis[*N*,*N*-bis(diphenylphosphanyl)cyclohexylamine-κ^2P,P']platinum(II) bis(hexafluoridophosphate) dichloromethane disolvate 80

5.7 Bis[*N*,*N*-bis(diphenylphosphanyl)-*n*-pentylamine-κ^2P,P']platinum(II) bis(hexafluoridophosphate) dichloromethane disolvate 85

5.8 Bis[*N*,*N*-bis(diphenylphosphanyl)cyclopropyl-κ^2P,P']palladium(II) bis(hexafluoridophosphate) 89

5.9 Discussion 92

Chapter 6:

Theoretical study of non-coordinated PNP-ligands and Pt(II)/Pd(II) PNP-coordinated complexes

6.1 Introduction 95

6.2 Experimental 96

6.3 Theoretical calculations of non-coordinated PNP-ligands 98

6.3.1 PNP-*c*Prop (1 *vs* 1*) 98

6.3.2 PNP-*c*But (2 *vs* 2*) 100

6.3.3 PNP-*c*Pent (3 *vs* 3*) 102

6.4 Theoretical calculations of [Pt(PNP-alkyl)$_2$] complexes 104

6.4.1 [Pt(PNP-*c*Prop)$_2$] (4 *vs* 4*) 104

6.4.2 [Pt(PNP-*c*Pent)$_2$] (5 *vs* 5*) 106

6.4.3 [Pt(PNP-*c*Hex)$_2$] (6 *vs* 6*) 108

6.4.4 [Pd(PNP-*c*Prop)$_2$] (7 *vs* 7*) 111

6.5 Discussion 113

6.5.1 Non-coordinated PNP-ligands 113
6.5.2 [Pt/Pd(PNP-alkyl)$_2$] complexes 115
6.5.3 Phenyl ring orientations for [Pt/Pd(PNP-alkyl)$_2$] complexes 117
6.6 Conclusion 121

Chapter 7:
Catalytic Hydroformylation of 1-octene
7.1 Introduction 122
7.2 Experimental 123
7.2.1 General 123
7.2.2 Catalytic hydroformylation 123
7.2.3 High pressure FT-IR (HP IR) experiments 124
7.2.4 General hydroformylation results calculations 124
7.3 Results and discussion 125
7.3.1 Rhodium catalyzed hydroformylation of 1-octene 126
7.3.1.1 Effect of the metal precursor and ligand ratio's on catalytic activity 131
7.3.1.2 Effect of temperature and syngas ratio's on catalytic activity 131
7.3.1.3 Effect of reaction variables on catalyst activity 132
7.3.1.4 HP IR study 134
7.3.2 Iridium catalyzed hydroformylation of 1-octene 138
7.4 Conclusion 141

Chapter 8:
Evaluation of study
8.1 Introduction 146
8.2 Evaluation 146

8.2.1 Synthesis and single crystal X-ray crystallographic study 146
8.2.2 Computational study 147
8.2.3 Catalytic selectivity *vs.* crystallographic data 148
8.3 Future work 148

Summary 150
Opsomming 152
Appendix A 154
Appendix B 201

Abbreviations and symbols

Label	Definition
$\theta_{N\text{-}sub}$	Effective Tolman-based N-substituent steric effect
PNP	Bis(diphenylphosphino)alkylamine
°C	Degrees Celsius
K	Kelvin
g	Gram
M	$Mol.dm^{-3}$
Z	Number of asymmetric units per unit cell
Å	Angström
°	Degrees
π	Pi
σ	Sigma
α	Alpha
β	Beta
γ	Gamma
θ	Theta
CO	Carbonyl
Ph	Phenyl
T or temp.	Temperature
NMR	Nuclear magnetic resonance
ppm	(Unit of chemical shift) Parts per million
CD_2Cl_2	Deuterated dichloromethane
$CDCl_3$	Deuterated chloroform
TMS	Tetramethylsilane
δ	Chemical shift
s	Singlet
d	Doublet
m	Multiplet
IR	Infrared spectroscopy
HP IR	High pressure infrared spectroscopy
ν	Stretching frequency on IR
DCM	Dichloromethane
DFT	Density functional theory
RMS	Root Mean Square
*n*Et	Bis(diphenylphosphino)ethylamine
*n*Prop	bis(diphenylphosphino)propylamine
*n*But	Bis(diphenylphosphino)butylamine
*n*Pent	Bis(diphenylphosphino)pentylamine
*c*Prop	Bis(diphenylphosphino)cyclopropylamine
*c*But	Bis(diphenylphosphino)cyclobutylamine
*c*Pent	Bis(diphenyl-phosphino)cyclopentylamine
*i*Prop	Bis(diphenylphosphino)isopropylamine
*c*Hex	Bis(diphenylphosphino)cyclohexylamine
Dimp	Bis(diphenylphosphino)1,2-dimethylpropylamine
*t*But	Bis(diphenylphosphino)*tert*-butylamine
Trimp	Bis(diphenylphosphino)1,2,2-trimethylpropylamine

1 Introduction and aim

In this chapter...

A brief history of homogeneous catalysis and background information on selected platinum group metals are presented. The aim of this study is also discussed in detail.

1.1 Introduction

1.1.1 Homogeneous catalysis

A catalyst is defined as a substance that increases the rate of a chemical reaction without itself undergoing any permanent chemical change. Homogeneous catalysis refers to a catalytic system in which the reactants and catalyst of the reaction is in the same phase, most often the liquid phase.[1,2] Examples of this are enzymes in biochemical reactions or transition-metal complexes used in the liquid phase for catalyzing organic reactions in industry.[3] One of the first man-made catalytic processes, the "lead chamber process", was developed in the 1750's for the production of sulphuric acid.3 Many homogeneous catalyzed processes have since been employed successfully in various industrial areas, including nickel hydrocyanation (Dupont),[4] Wacker synthesis of acetaldehyde using a $PdCl_2$ catalyst,[5,6,7] and the BASF, Monsato and Cativa catalysed carbonylation of methanol[8,9] to name a few.

---

[1] G.C. Bond, *Heterogeneous catalysis*, Oxford: Claredon Press, 1974.
[2] J.T. Richardson, *Principles of Catalyst Development*, New York: Plenum Press, 1989.
[3] P.W.N.M van Leeuwen, *Homogeneous Catalysis: Understanding the Art*, Dordrecht: Kluwer Academic Publishers, 2004.
[4] F.A. Cotton, G. Wilkinson, P.L. Gaus, *Basic Inorganic Chemistry*, 3rd Ed., New York: John Wiley & Sons, Inc., 1995.
[5] J. Smidt, W. Hafner, R. Jira, J. Sedlmeier, R. Sieber, R. Rüttinger, H. Kojer, *Angew. Chem.*, 71 (1959) 176.
[6] J. Smidt, W. Hafner, R. Jira, R. Sieber, J. Sedlmeier, A. Sabel, *Angew. Chem.*, 74 (1962) 93.
[7] J.E. Baeckvall, B. Akermark, S.O. Ljunggren, *J. Am. Chem. Soc.*, 101 (1979) 2411.
[8] C.E. Hickey, P.M. Maitlis, *J. Chem. Soc. Chem. Commun.*, 1984, 1609.
[9] C.M. Lukehart, *Fundamental Transition Metal Organometallic Chemistry*, California: Brooks/Cole Publishing Company, 1985.

The mechanism of the catalytic cycle in homogeneous catalysis can be studied in much detail to deliberate the influencing steric and electronic properties of the catalyst. In recent years it has been shown that the ligand effects in homogeneous catalysis by metal complexes are extremely important, inspiring a lot of research in this area.[10,11] A variety of products can be obtained from a single metal by merely changing the ligands around the metal centre. It is therefore possible to optimize the homogeneous catalyst by tailoring it through its chemical and structural basis. The ligand effects on catalytic processes will be discussed in more detail in the next chapter.

1.1.2 Background on metals

Selected platinum group metals (PGM's)

The platinum group metals (PGM's)[12] – platinum, ruthenium, rhodium, palladium, osmium, iridium – are "d" block elements with partly filled *d* or *f* shells in any of their chemically important oxidation states. The empty *d* orbitals offer the possibility of binding suitable neutral molecules to the metal centre. The outstanding properties of these PGMs include high melting points, high lustre, resistance to corrosion as well as catalytic tendencies used in the chemical, electrical and petroleum refining industries. The major source of PGM's today is located in South Africa.[13] The platinum metals tend to occur in the same mineral desposits,[14] and generally with small amounts of gold, copper, silver, nickel, iron, and other metals. They often occur as natural alloys such as osmiridium which consists of iridium, osmium and small amounts of the other metals.

[10] R.G. Wilkins, Kinetics and Mechanisms of Reactions of Transition Metal Complexes, VCH, New York, 2nd Ed, 1991.
[11] A. Roodt, S. Otto, G. Steyl, *Coord. Chem. Rev.*, 245 (2003) 121.
[12] L.B. Hunt, F.M. Lever, *Platinum Metals Rev.*, 13 (4) (1969) 126.
[13] H.V. Eales, *A First Introduction to the Geology of the Bushveld Complex*, Pretoria: Council of GeoScience, 2001, 73.
[14] D.C. Harris, L.J. Cabri, The Canadian Mineralogist, 29 (1991) 231.

In the finely divided state, platinum is an excellent catalyst, having long been used in the process for producing sulphuric acid. It is also used as a catalyst in cracking petroleum products. The platinum compound, *cis*platin ([*cis*-$(PtCl_2(NH_3)_2]$) was the first of a series of square-planar platinum(II) chemotherapy drugs. Platinum's most common oxidation states are +2 and +4 while the +1 and +3 oxidation states are less common.[15,16]

In 1803, in the course of his study of platinum, Wollaston isolated and identified palladium (Pd) from the mother liquor remaining after platinum had been precipitated as $[(NH_4)_2PtCl_6]$ from its solution in *aqua regia*. He named it after the newly discovered asteroid, Pallas, itself named after the Greek goddess of wisdom. Palladium is a soft silver-white metal that resembles platinum. It is the least dense and has the lowest melting point of the platinum group metals. Palladium is used in the catalytic control of car exhaust emissions and when finely divided it forms a good catalyst and is used to speed up hydrogenation and dehydrogenation reactions, as well as petroleum cracking. The largest single use for palladium is in the manufacture of electronic components, but it is also used in dentistry and the jewellery trade. Common oxidation states of palladium are 0,+1, +2 and +4.[15,16]

The transition metal rhodium (Rh), was discovered between 1803 and 1804 by William Hyde Wollaston in crude platinum ore from South America. Rhodium is one of the least abundant metals in the earth's crust and was named after the word *rodon*, meaning rose.[17] It is primarily used as an alloying agent for hardening platinum and palladium. It is extensively used in chemical synthesis as an important catalyst and to control car exhaust emissions.[18]

[15] R.C. Weast, *Handbook of Chemistry and Physics*, 60th Ed., CRC Press, 1979.
[16] N.N. Greenwood, A. Earnshaw, *Chemistry of the Elements*, 2nd Ed., Pergamon Press, 1997.
[17] B. Carincorss, *Field Guide to Rocks and Minerals in South Africa*, Cape Town: Struik Publishers, 2004.
[18] J.D. Lee, *Concise Inorganic Chemistry*, 4th Ed., London: Chapman & Hall, 1991.

CHAPTER 1

In 1925, Manchot and König did the first synthesis of a rhodium-carbon bond[19] by treatment of [$RhCl_3$] with carbon monoxide, yielding a red crystalline compound. This compound was incorrectly characterized as [$Rh_2Cl_2O.3CO$] and only correctly characterized 18 years later by Hieber and Lagally as the rhodiumdichlorotetracarbonyl dimer [$Rh_2Cl_2(CO)_4$].[20]

The two most common states oxidation states are +1 and +3. Rh(I) has a d^8 electron configuration and a square planar 4-coordinate or a bipyrimidal 5-coordinate conformation. The Rh(III) oxidation state has a d^6 electron configuration and an octahedral conformation.[21,22] The oxidative addition and reductive elimination reactions from Rh(I) to Rh(III) and *vice versa*, has transformed the catalytic industry and has produced many fascinating reactions over the years.

Well-known catalytic processes such as hydroformylation, hydrogenation and carbonylation have mostly used cobalt or rhodium as catalysts with a combination of various ligand systems. The original cobalt catalyst used in hydroformylation, [$Co_2(CO)_8$],[23] was later replaced by the rhodium catalyst, [$RhHCO(PPh_3)_3$].[24] In the old process a cobalt salt was used, but was later modified to a cobalt salt plus a tertiary phoshine as the catalyst precursor. The phosphine-modified cobalt-based system was developed by Shell specifically for linear alcohol syntheses. [$Rh_4(CO)_{12}$] is another very active Rh catalyst, but has poor selectivity proving that the presence of phosphine ligands increase selectivity. The highly phosphine-substituted rhodium catalyst, [$RhHCO(PPh_3)_3$], is a more active, highly selective catalyst reacting under milder pressures and lower temperatures than the earlier Co-catalyzed reaction.[25]

[19] W. Manchot, J. König, *Chem. Ber.*, 58B (1925) 2173.
[20] W. Hieber, H.Z. Lagally, *Anorg. Allg. Chem.*, 96 (1943) 251.
[21] S.S. Basson, J.G. Leipoldt, A. Roodt, J.A. Venter, *Inorg. Chim. Acta.*, 118 (1986) L45.
[22] B. Cornils, W.A. Hermann, *Applied Homogenous Catalysis*, VHC publishers, Weinhein. 1996.
[23] C. Elschenbroich, A. Salzer, *Organometallics: A Concise Introduction*, New York: VCH Publishers, 1989.
[24] J.A. Osborn, G. Wilkinson, J.F. Young, *Chem. Commun.*, 1965, 17.
[25] R. Ugo, *Aspects of Homogenous Catalysis*, Vol 2, Dordrecht, Holland: D. Reidel Publ. Comp., 1974.

INTRODUCTION AND AIM

Iridium was discovered in the same year as rhodium and share many resemblances in their chemistry. Iridium (Ir), named after *iris*, the Greek term meaning *rainbow*, due to its highly coloured salts, was discovered by Smithson Tennant in 1803 when he studied the black *aqua regia* insoluble residue of crude platinum.[26] Iridium is not attacked by *aqua regia* nor by any of the acids, but certain molten salts, such as NaCl and NaCN, are corrosive towards iridium. It is extremely hard and the most corrosion-resistant metal known, making it very hard to machine, form, or to work with. Natural iridium contains two stable isotopes, ^{191}Ir and ^{193}Ir with a natural abundance of 37.3 % and 62.7 %, respectively. Iridium is the densest element known apart from osmium and many applications of this metal rely on its inertness. Iridium has found use in making crucibles and apparatus for application at high temperatures, electrical coating and as a hardening agent for platinum.[27] Iridium can exist in a variety of oxidation states from -1 ($[Ir(CO)_3(PPh_3)]^-$) to +6 ($[IrF_6]$), with the most common oxidation states being +1, +3 and +4.[28] Ir(I) oxidation state has a d^8 electron configuration and usually forms either square-planar 4-coordinated or trigonal bipyrimidal 5-coordinated complexes that are stabilized by π-bonding ligands such as tertiary phosphines or carbonyl groups. The vast majority of the Ir(III) oxidation state, with d^6 electron configuration, have 6-coordinated octahedral geometries.[26]

The interest of iridium coordination compounds remain in the catalysis field and in its luminescent properties. The iridium analogue of Wilkinson's compound, $[IrCl(PPh_3)_3]$, illustrates the differences that can arise between two very similar metals. $[IrCl(PPh_3)_3]$ cannot be used as a hydrogenation catalyst because the ligands are strongly bonded to the metal center. PPh_3 does not dissociate from $[IrH_2Cl(PPh_3)_3]$ so the alkene is unable to bind. Without alkene binding, hydrogen transfer from the metal to the alkene cannot occur.[29] Iridium analogues of Rh hydrogenation catalysts are less labile and less active than the Rh series and consequently attention was focused on stable iridium hydrides for the study of transition intermediates of Rh catalysts.

[26] D.N. MacLennan, E.J. Simmonds, *Chemistry of Precious Metals*, Weinheim: Chapman & Hall, 1992.
[27] D.R. Lide, *Handbook of Chemistry and Physics*, Boca Raton, FL: CRC Press, 2005.
[28] N.N. Greenwood, *Chemistry of the Elements*, 2nd Ed., Oxford: Butterworth-Heinemann, 1997.
[29] J.A. Osborn, F.H. Jardine, J.F.Young, G. Wilkinson, *J. Chem. Soc. (A)*, (1966) 1711.

Iridium compounds are in some instances the most active catalysts available and in the cases where it may not yield the most active catalysts, iridium complexes nevertheless yield important information about the structure and reactivity of important catalytic intermediates.

1.2 Aim of this study

Hydroformylation or the "oxo reaction" was discovered by Otto Roelen in 1938. The basic reaction converts alkenes into aldehydes by addition of a hydrogen atom and formyl (CHO) group to a C=C double bond.[30] The aldehydes can then be converted to alcohols for the production of polyvinylchloride (PVC), polyalkenes and detergents. High selectivity for the desired linear aldehyde can be achieved through an optimal choice of catalyst, ligand and process conditions.[31,32]

The first phosphine-substituted rhodium catalysts, $[RhHCO(PPh_3)_3]$, for use in the hydroformylation of olefins, attracted much attention due to high activity, selectivity and mild reaction conditions. Since then, numerous new modifying phosphine and phosphite ligands have been applied in many catalytic reactions.[25,33,34,35,36] Chelating diphosphine ligand systems as well as sterically bulky ligands have been shown to lead to higher reactivity and selectivity.[37,38,39,40] The difference in steric bulk with the varying of alkyl moieties on the N atom

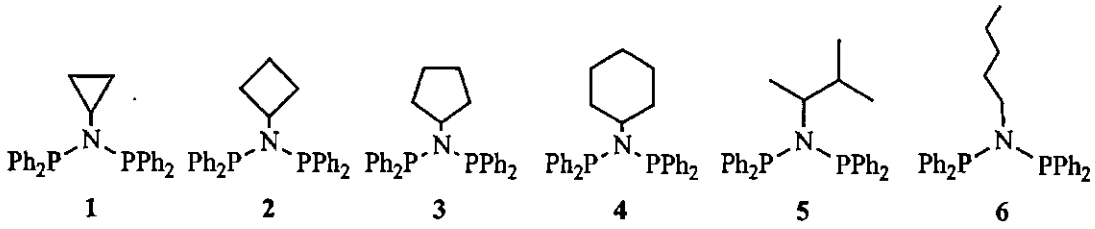
[30] D.W.A. Sharpe, *The Penguin Dictionary of Chemistry*, 3rd Ed., England: Penguin Books Ltd., 2003.
[31] R.G. Wilkins, Kinetics and Mechanisms of Reactions of Transition Metal Complexes, VCH, New York, 2nd edn, 1991.
[32] A. Roodt, S. Otto, G. Steyl, *Coord. Chem. Rev.*, 245 (2003) 121.
[33] H. Janecko, A.M. Trzeciak, J.J. Ziolkowski, *J. Mol. Cat.*, 26 (1984) 355.
[34] A. van Rooy, J.N.H. de Bruijn, C.F. Roobeek, P.C. Kamer, P.W.N.M. van Leeuwen, *J. Organomet. Chem.*, 507 (1996) 69.
[35] P.W.N.M. van Leeuwen and C.F. Roobeek, *J. Organomet. Chem.*, 258 (1983) 343.
[36] A. Polo, J. Real, C. Claver, S. Castillon, J.C. Bayon, *J. Chem. Soc., Chem. Commun.*, (1990) 600.
[37] R. Kadyrov, D. Heller and R. Selke, *Tetrahedron: Asymmetry*, 9 (1998) 329.
[38] Z. Freixa, M. M. Pereira, J. C. Bayon, A. M. S. Silva, J. A. R. Salvador, A. M. Beja, J. A. Paixao and M. Ramos, *Tetrahedron: Asymmetry*, 12 (2001) 1083.
[39] M.J. Overett, K. Blann, A. Bollmann, J.T. Dixon, F. Hess, E. Killian, H. Maumela, D.H. Morgan, A. Neveling, S. Otto, *Chem. Commun.*, (2005) 622.
[40] A.J. Rucklidge, D.S. McGuinness, R.P. Tooze, A.M.Z. Slawin, J.D.A. Pelletier, M.J. Hanton, P.B. Webb, *Organometallics*, 26 (2007) 2782.

of bidentate diphosphinoamine (PNP) ligands was found to be the predominant factor in selectivity in ethylene tetramerisation[41,42,43,44,45]

Based on this information, the study was concerned with investigating the use of PNP-ligands with various substituents on the nitrogen atom in the hydroformylation of α-olefins. The main objective of this study was focussed on the synthesis, solid state characterization and computational study to ensure an overarching correlation of the general behaviour of these ligand systems.

Thus, various PNP ligands (see **Scheme 1.1**) have been synthesized and single crystal X-ray crystallographic studies instigated to further evaluate any correlations. A comparison of the crystallographic data of the PNP ligands with varying activity and selectivity, when complexed with Rh(I) and Ir(I) during the hydroformylation of olefins, could provide valuable information for future ligand design and explaining catalytic behaviour. Complexing other metal cations (e.g. Pt(II) and Pd(II)) with the various PNP-ligands will provide further information on the coordination mode of these ligands, since Rh(I) and Ir(I) are notoriously unstable and difficult to crystallize.

[41] K, Blann, A. Bollmann, H. de Bod, J.T. Dixon, E. Killian, P. Nongodlwana, M.C. Maumela, H. Maumela, A.E. McConnell, D.H. Morgan, M.J. Overett, M. Prétorius, S. Kuhlmann, P. Wasserscheid, *J. Catal.*, 249 (2007) 244.
[42] M.J. Overett, K. Blann, A. Bollmann, J.T. Dixon, F. Hess, E. Killian, H. Maumela, D.H. Morgan, A. Neveling, S. Otto, *Chem. Commun.*, (2005) 622.
[43] K. Blann, A. Bollmann, J.T. Dixon, F.H. Hess, E. Killian, H. Maumela, D.H. Morgan, A. Neveling, S. Otto, M. J. Overett, *Chem. Commun.*, (2005) 620.
[44] S. Kuhlmann, K. Blann, A. Bollmann, J.T. Dixon, E. Killian, M.C. Maumela, H. Maumela, D.H. Morgan, M. Prétorius, N. Taccardi, P. Wasserscheid, *J. Catal.*, 245 (2007) 277.
[45] E. Killian, K. Blann, A. Bollmann, J.T. Dixon, S.E. Kuhlmann, M.C. Maumela, H. Maumela, D.H. Morgan, P. Nongodlwana, M.J. Overett, M. Prétorius, K. Höfener, P. Wasserscheid, *J. Mol. Catal. Chem.*, 270 (2007) 214.



Scheme 1.1: Diphosphinoamine ligands (PNP-ligands) synthesized, characterized and used in this study. (1) *N,N*-Bis(diphenylphosphanyl)cyclo-propylamine (PNP-*c*Prop); (2) *N,N*-Bis(diphenylphosphanyl)cyclobutanamine (PNP-*c*But); (3) *N,N*-Bis(diphenylphosphanyl)-cyclopentanamine (PNP-*c*Pent); (4) *N,N*-Bis(diphenylphosphanyl)cyclohexanamine (PNP-*c*Hex); (5) *N,N*-Bis(diphenyl-phosphanyl)-1,2-dimethylpropylamine (PNP-Dimprop)[46]; (6) *N,N*-Bis(diphenylphosphanyl)-*n*-pentylamine (PNP-*n*Pent).[47]

An additional part of this investigation involves the theoretical calculations of the crystal structures of the non-coordinated ligands and metal-PNP complexes. These structures could provide a more in-depth understanding of the observed structures from the crystallographic data. The theoretical structures, obtained by DFT calculations, are reported and compared with the crystallographic data of the corresponding structures.

Proceeding from the previous paragraphs, the following stepwise goals were set for this study:

1. To synthesize a range of diphosphinoamine ligands and collect single crystal X-ray crystallographic data of the non-coordinated PNP-ligands.
2. Synthesizing metal-PNP compounds (metal = Pt(II) and Pd(II)) and collect single crystal X-ray crystallographic data.
3. Perform theoretical calculations of the various free PNP-ligands and metal-PNP complexes and compare the optimized structures with the corresponding crystal structures.
4. Compare the crystallographic data of the variety of PNP-ligands with the catalytic selectivity and activity, during the hydroformylation of 1-octene, and evaluate any possible correlations.
5. Develop a systematic approach to evaluating catalysis by incorporating X-ray crystallographic data and theoretical calculations in order to improve future ligand design methods.

[46] N. Cloete, H.G. Visser, A. Roodt, J.T. Dixon, K. Blann, K. *Acta Cryst.*, E64 (2008) o480.
[47] N.Cloete, PhD thesis, University of the Free State, 2009.

INTRODUCTION AND AIM

In the following chapter a brief literature review of the discovery and development of the catalytic hydroformylation process is presented, followed by the systematic presentation and discussion of the experimental results.

2 Literature Study

In this chapter...

A brief history on the discovery and development of the hydroformylation process will be discussed. An overview of fundamental ligand properties applying to the chemistry involved is also included.

2.1 Introduction

One of the largest and most important homogeneous catalyzed industrial processes is hydroformylation for the production of aldehydes from alkenes. Most of these resulting aldehydes are hydrogenated to alcohols, having applications in plasticizer alcohols, detergents, wood preservatives and surfactants.[1] The process has received considerable attention since its discovery in 1938,[2] bringing forth continues improvement in catalyst design, activity, selectivity and reaction conditions. Originally, a cobalt catalyst was used, $[Co_2(CO)_8]$,[3] to be replaced later by the more efficient phosphine substituted rhodium catalyst, $[RhHCO(PPh_3)_3]$.1 Ligand design has especially received a great deal of attention, since phosphine ligands made a distinct impact on the reactivity of the popular Wilkinson hydrogenation catalyst, $[RhCl(PPh_3)_3]$.[4] Numerous phosphine ligands have since been applied in many catalytic reactions, all the more unmistakably signifying that changes in the ligand environment induce different steric and electronic properties into the catalyst system.[5,6]

---

[1] P.W.N.M van Leeuwen, C. Claver (Eds.), *Rhodium Catalyzed Hydroformylation*, Kluwer Academics Publishers, Dordrecht, 2000.
[2] D.W.A. Sharpe, *The Penguin Dictionary of Chemistry*, 3rd Ed., England: Penguin Books Ltd., 2003.
[3] C. Elschenbroich, A. Salzer, *Organometallics: A Concise Introduction*, New York: VCH Publishers, 1989.
[4] J.A. Osborn, G. Wilkinson, J.F. Young, *J. Chem. Soc., Chem. Commun.*, (1965) 17.
[5] R.G. Wilkins, Kinetics and Mechanisms of Reactions of Transition Metal Complexes, VCH, New York, 2nd edn, 1991.
[6] A. Roodt, S. Otto, G. Steyl, *Coord. Chem. Rev.*, 245 (2003) 121.

2.2 Catalysis

The chemical industry is primarily based on the production of economically important chemicals through the catalytic combination of small molecules (C_2H_4, CO, H_2, H_2O and NH_3) to produce larger molecules (ethylene glycol, acetaldehyde, acetic acid and acrylonitrile)[7]. Homogeneous catalysis refers to a catalytic system in which the reactants and catalyst of the reaction are in the same phase, most often the liquid phase. Phase boundaries however, do exist in heterogeneous catalysis.[8,9] Homogeneous catalysis is more stereoselective, but heterogeneous catalysis is still used for most petrochemical processes.[10] This is because heterogeneous catalysts are more stable at higher temperatures and are easily separated from the substrate phase. In homogeneous catalysis, the catalytic cycle mechanism can be studied in much detail to deliberate the influencing steric and electronic properties of the catalyst, unlike heterogeneous catalysis. It is therefore, possible to optimise the homogeneous catalyst by tailoring it through its chemical and structural basis.

Coordinative unsaturated square-planar group 9 and 10 complexes can partake in a series of elementary reactions that are key steps in the catalytic synthesis of organic products.[11,12] In general, the key reactions of a catalytic cycle include:[13,14]

- Creation of a "vacant site"
- Olefin insertion
- Carbonyl insertion
- β-hydrogen elimination
- Nucleophilic addition to coordinated ligands
- Oxidative addition
- Reductive elimination
- *Cis* migration

[7] K.F. Purcell, J.C. Kotz, *An Introduction to Inorganic Chemistry*, Philadelphia: Saunders College Publishing, 1980.
[8] G.C. Bond, *Heterogeneous catalysis*, Oxford: Claredon Press, 1974.
[9] J.T. Richardson, *Principles of Catalyst Development*, New York: Plenum Press, 1989.
[10] G.W. Parshall, R.E. Putscher, *J. Chem. Educ.*, 63 (1986) 189.
[11] F.A. Cotton, G. Wilkinson, *Advanced Inorganic Chemistry*, 5th Ed., New York: John Wiley & Sons, Inc., 1980.
[12] J. Halpern, *Inorg. Chim. Acta.*, 50 (1980) 11.
[13] W. Koga, K. Morokuma, *Chem. Rev.*, 91 (1991) 823.
[14] D.F. Schriver, P.W. Atkins, C.H. Langford, *Inorganic Chemistry*, 2nd Ed., Oxford University, Oxford, 1994.

CHAPTER 2

Some well known examples of homogeneous catalytic processes utilizing transition metal catalysts combined with a variety of ligand systems are listed below:

- The making of sulphuric acid *via* the old catalytic "lead chamber process"[15]
- Wacker synthesis of acetaldehyde from olefins using a $PdCl_2$ catalyst and air[16,17,18]
- Hydrocyanation of alkenes using nickel phosphite complexes[19]
- Hydroformylation of olefins using cobalt or rhodium catalysts[20]
- The BASF, Monsanto and Cativa catalyzed carbonylation of methanol[21,22]
- The hydrogenation of unsaturated compounds using Wilkinson's catalyst $RhCl(PPh_3)_3$, $RhCl_3(Py)_3$ etc[23]
- Metathesis of alkenes with Schrock's and Grubbs' catalysts[24,25,26]
- Olefin oligomerization – in particular tri- and tetramerisation[27]

However, the prime focus of this PhD study is on ligand effects in the hydroformylation reaction. Thus, the latter will be described in more detail, followed by ligand effects thereafter.

---

[15] P.W.N.M. Van Leeuwen, *Homogeneous Catalysis: Understanding the Art*, Dordrecht: Kluwer Academic Publishers, 2004.
[16] J. Smidt, W. Hafner, R. Jira, J. Sedlmeier, R. Sieber, R. Rüttinger, H. Kojer, *Angew. Chem.*, 71 (1959) 176.
[17] J. Smidt, W. Hafner, R. Jira, R. Sieber, J. Sedlmeier, A. Sabel, *Angew. Chem.*, 74 (1962) 93.
[18] J.E. Baeckvall, B. Akermark, S.O. Ljunggren, *J. Am. Chem. Soc.*, 101 (1979) 2411.
[19] F.A. Cotton, G. Wilkinson, P.L. Gaus, *Basic Inorganic Chemistry*, 3rd Ed., New York: John Wiley & Sons, Inc., 1995.
[20] W.A. Hermann, B. Cornils, *Angew. Chem., Int. Ed.*, 36 (1997) 1048.
[21] C.E. Hickey, P.M. Maitlis, *J. Chem. Soc. Chem. Commun.*, (1984) 1609.
[22] C.M. Lukehart, *Fundamental Transition Metal Organometallic Chemistry*, California: Brooks/Cole Publishing Company, 1985.
[23] R.H. Crabtree, *The Organometallic Chemistry of the Transition Metals*, New York, John Wiley & Sons., 1988.
[24] R.R. Schrock, J.S. Murdzek, G.C. Bazan, J. Robbins, M. DiMare, M. O'Regan, *J. Am. Chem. Soc.*, 112 (1990) 3875.
[25] R.H. Grubbs, *Tetrahedron*, 60 (2004) 7117.
[26] R.H. Grubbs, S. Chang, *Tetrahedron*, 54 (1998) 4413.
[27] J.T. Dixon, C. Grové, A. Ranwell, WO 01/83447 (Sasol Tehnology (Pty) Ltd), November 8, 2001.

2.3 Hydroformylation

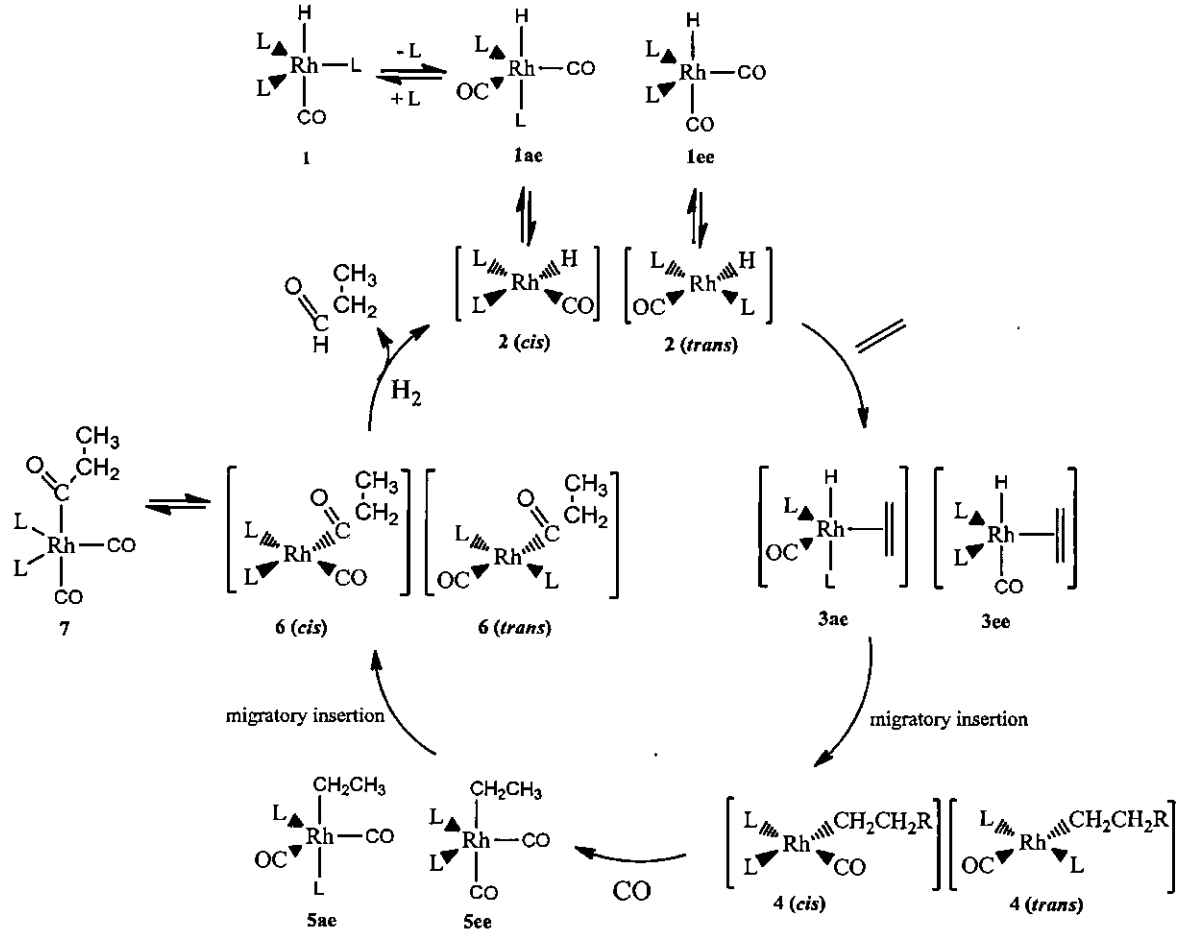
2.3.1 Introduction

Despite the fact that hydroformylation has been extensively studied, it still attracts considerable attention due to the rich and complex chemistry associated with this reaction, especially where catalyst design is concerned.1[28] Studies are directed towards gaining fresh insights into the reaction mechanism for improving rate and selectivity using, amongst others, new modifying phosphine and phosphite[29,30,31,32] ligands, other than PPh_3. The numerous steps within the reaction mechanism present a delicate balance between elements such as the rate of the reaction, on the one hand, and at the same time the ratio between linear and branched aldehydes on the other, all influenced differently by the steric hindrance and electronic properties of the ligand, thus presenting great challenges for designing a catalyst that positively influences throughout the hydroformylation process.[33,34]

[28] B.R. James, P.W.N.M. van leeuwen (Eds.), *Catalysis by Metal Comlexes Series*, vol. 22, Kluwer Academic Publisheres, Dordrecht, 2000.
[29] H. Janecko, A.M. Trzeciak, J.J. Ziolkowski, *J. Mol. Cat.*, 26 (1984) 355.
[30] A. van Rooy, J.N.H. de Bruijn, C.F. Roobeek, P.C. Kamer, P.W.N.M. van Leeuwen, *J. Organomet. Chem.*, 507 (1996) 69.
[31] P.W.N.M. van Leeuwen and C.F. Roobeek, *J. Organomet. Chem.*, 258 (1983) 343.
[32] A. Polo, J. Real, C. Claver, S. Castillon, J.C. Bayon, *J. Chem. Soc., Chem. Commun.*, (1990) 600.
[33] M. Haumann, R. Meijboom, J.R. Moss, A. Roodt, *Dalton Trans.*, (2004) 1679.
[34] R. Meijboom, M. Haumann, A. Roodt, L. Damoense, *Helvetica Chimica Acta*, 88 (2005) 676.

2.3.2 Mechanism

The generally accepted mechanism (**Scheme 2.1**) for the hydroformylation process was first proposed by Heck[35] and corresponds to Wilkinson's dissociative mechanism.[36,37,38]



Scheme 2.1: The basic catalytic cycle for the hydroformylation of propylene (only *n*-product pathway shown) using a rhodium-phosphine based catalyst.[15]

[35] R.F. Heck, *Acc. Chem. Res.*, 2 (1969) 10.
[36] J.F. Young, J.A. Osborn, F.A. Jardine, G. Wilkinson, *J. Chem. Soc. Chem. Commun.*, 1965, 131.
[37] J.A. Osborn, G. Wilkinson, D. Evans, *J. Chem. Soc. (A)*, 1968, 3133.
[38] D. Evans, G. Yagupsky, G. Wilkinson, *J. Chem. Soc. (A)*, 1968, 2660.

For $[RhH(CO)(PPh_3)_3]$ (**1**) as pre-catalyst and PPh_3 as ligand, the initial step is the generation of a 16-electron square intermediate, **2**, from the 18-electron precursor, **1ae** and **1ee**. This is followed by alkene coordination, **3**, and hydrogen transfer to give the alkyl species **4**. CO addition and migratory insertion give the acyl derivative, **6**, which subsequently undergoes oxidative addition of molecular hydrogen and the reductive elimination of the aldehyde product, and regeneration of the unsaturated intermediate, **2**.

Initial treatment of $[RhH(CO)(PPh_3)_3]$ (**1**) with carbon monoxide in the presence of PPh_3 forms $[RhH(CO)_2(PPh_3)_2]$ complexes (**1ae** and **1ee**) in which both phosphine ligands can coordinate in the equatorial positions (ee) or one in the axial and the other in the equatorial position (ae).[39] Dissociation of either equatorial L or equatorial CO leads to the active square-planar intermediates which have phosphines in the *cis* or *trans* configuration respectively (**2**). It is known that dissociation of the equatorial ligands from trigonal bipyramids is normally preferred. Coordination of the alkene to complex **2** gives again two isomeric (**3ae** and **3ee**) forms having a hydride in an apical position. Complexes **3ae** and **3ee** undergoes migratory insertion to give square-planar alkyl complexes (**4**), which are respectively *cis* or *trans*.

The regioselectivityl towards linear or branched aldehydes is determined by the alkene insertion at the trigonal bipyramidal five-coordinate intermediate (**3**) which depends on the orientation of the PPh_3 ligands in the active specie (**2**), governed by the initial CO treatment of the pre-catalyst, $[RhH(CO)(PPh_3)_3]$, (**1**). Syn-gas pressures and metal-ligand ratios also play an important role in the overall performance of the catalyst. With low PPh_3 concentrations, $[Rh(CO)_2H(PPh_3)_2]$ (**1**) is the predominant resting state and the active specie (**2**) is formed by CO dissociation, which is inhibited by increased CO concentration. Also, deactivation of the catalyst can occur with an excess of CO over H_2 in which complex **6** forms the five-coordinate dicarbonyl acyl complexes, **7**, which cannot react with hydrogen, therefore inhibiting the hydroformylation process.[40] With high concentrations of bulky ligands, $[Rh(CO)H(PPh_3)_3]$ (**1**) is the resting state and dissociation of a phosphine must occur to form the unsaturated intermediates, **2**, which can be suppressed by increased PPh_3 concentrations. Regeneration of rhodium hydrides from dormant dirhodium

[39] J.M. Brown, A.G. Kent, *J. Chem. Soc. Perkin Trans. II*, 1987, 1597.
[40] C.K. Brown, G. Wilkinson, *J. Chem. Soc. (A)*, 1970, 2753.

impurities, caused by low hydrogen pressures and high rhodium concentrations, can be achieved by increased H_2 pressures. Sterically bulky ligands can also cause steric hindrance reducing the tendency of alkene binding severely slowing down the reaction rate of the hydroformylation process or preventing it completely.

The rhodium catalyst can also be added as a number of pre-catalysts such as: $[Rh_4(CO)_{10}]$, $[Rh(acac)(CO)_2]$, $[Rh(acac)(CO)(PPh_3)]$, $[RhH(CO)(PPh_3)_3]$ or similar complexes which, in some cases, also have an effect on the activity and selectivity. The active catalyst can also display hydrogenation activity resulting in alcohols being obtained at the end of the reaction through *in situ* hydrogenation of the aldehyde. As is evident from the complexity of the catalytic cycle, an ongoing tug of war is ever present between the vast amounts of variables present. Thus, it is important that sufficient knowledge be obtained regarding the fundamental principles applying to the chemistry involved. Ligands govern the magnitude of the catalytic system effects, so in order for new complexes to be developed, properties such as solubility, reactivity and steric bulk of various ligands must be clearly understood to enable intelligent adjustments to be made for inducing the effects of choice.

2.4 Ligand properties

2.4.1 Electronic effect

Infrared carbonyl frequencies can be used for measuring electronic properties of ligands during coordination to a particular metal, described by Strohmeier.[41] A carbonyl ligand in a catalyst can be easily identified on an IR spectrum and is used to determine the σ-basicity and π-acidity of phosphorus ligands. The electron density on the metal centre increases with strong σ–donor ligands, causing a substantial back-donation to the CO ligands, increasing the M-C bond length and shortening the C-O bond of the carbonyl, thus lowering the IR frequency. The opposite is true for strong π-acceptor ligands as they compete with the CO ligand for electron back-donation causing the CO stretching frequency to remain high.[6,42,43]

[41] W. Strohmeier, F.J. Müller, *Chem. Ber.* 100 (1967) 2812.
[42] C.A. Tolman, *Chem. Rev.*, 77 (1977) 313.
[43] A. Muller, S. Otto, A. Roodt, *Dalton Trans.*, (2008) 650.

2.4.2 Steric effect

Tolman's cone angle is the most widely used method in defining a reliable steric parameter that indicates the amount of space a phosphorus based ligand system occupies. Tolman proposed the measurement of the steric bulk of a phosphine ligand by use of CPK models. From the metal centre, 2.28 Å from the phosphorus atom, a cylindrical cone is constructed which just touches the van der Waals radii of the outermost atoms of the model. The cone angle, θ, measured is the desired steric parameter. In the case of non-symmetrical phosphorus ligands this cone angle, θ, can be calculated by the following equation:

$$\theta = (2/3)\sum_{i=1}^{3} \theta_i/2 \qquad 2.1$$

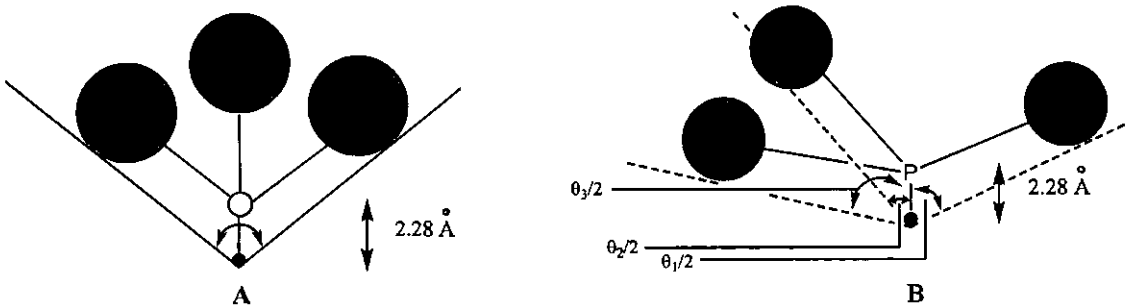


Figure 2.1: Cone angle measurements of symmetrical (A) and unsymmetrical (B) ligands.[42]

2.5 Effects of ligands in catalysis

2.5.1 Steric implication of ligands

Ligand design plays an important role in the performance of the catalyst. Detailed investigation of the bonding and reactivity of the ligand is of utmost importance as reactivity of organotransition metal complexes is dependent on the ligand environment of the metal.[44,45] Subtle changes in the electronic and steric effects of the ligand influences activity and selectivity

[44] P.W.N.M van Leeuwen, K. Morokuma, J.H. van Lenthe (Eds.), *Theoretical Aspects of Homogeneous Catalysis, Applications of Ab Initio Molecular Orbital Theory*, Kluwer Academic Publishers, Dordrecht, 1995.
[45] F. Maseras, A. Lledós (Eds.), *Computational Modeling of Homogeneous Catalysis*, Kluwer Academic Publishers, Dordrecht, 2002.

so that catalyst performance can be directed and in some cases even predicted. Extensive research has been devoted to fine-tuning of the catalysts, by means of ligand modification, towards certain selectivity and reactivity. The Tolman cone angle[42] is still the most widely used model to describe and quantify the steric demand of a ligand.[46] This is due to, amongst others, the easy calculation of this parameter from molecular models or crystallographic data.

Steric effects are extremely important for phosphine- and phosphite-modified hydroformylation of alkenes. The first example of phosphite-modified rhodium-catalyzed hydroformylation of α-olefins was reported by Pruett and Smith.[47] It showed that the use of bulky phosphite ligands leads to higher reactivity[48,49] and increases the coordinative unsaturation of the rhodium,[50,51] making them very attractive in hydroformylation chemistry. It also opened new doors for normally unreactive branched alkenes[52] to be hydroformylated in the presence of a bulky phosphite-modified catalyst under milder conditions than those involving the conventional PPh_3-modified catalyst.[53,54] In rhodium-catalyzed hydroformylation using bulky *tris*(2-*tert*-butyl-4-methylphenyl) phosphite as ligand, the very large cone angle (θ = 172 °) was recognized as the reason for increased rates when substrates such as 1,2- and 2,2-dialkylalkenes where hydroformylated[53] as opposed to PPh_3 as ligand.[53] The bulky *mono*-phosphite is capable of hydroformylating a range of substrates[55] with very high rates of up to 160 000 mol (mol Rh)$^{-1}$ h^{-1} observed for 1-octene as substrate with moderate selectivity towards the linear aldehyde.[56]

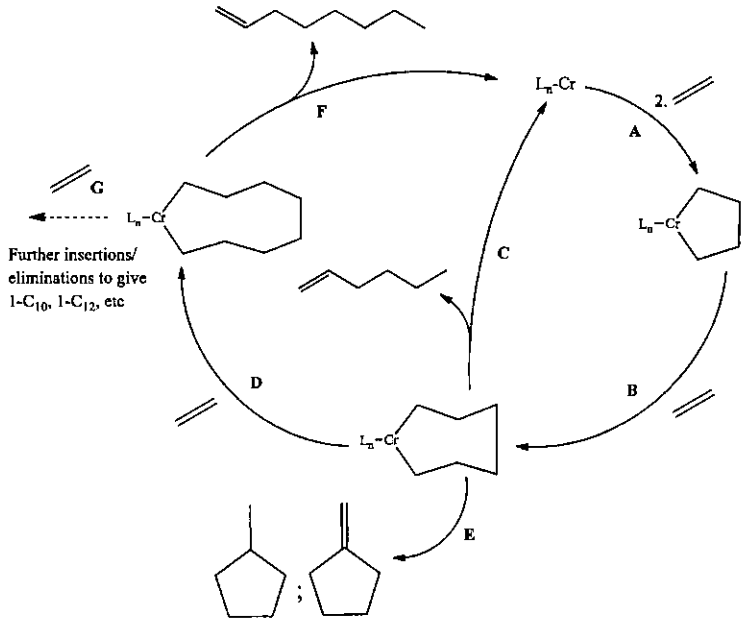
Another good example of the effect of the steric parameters of ligands is the kinetic reaction systems illustrated by the oxidative addition reaction of $[(\eta^5\text{-}C_5H_5)Co(CO)(L)]$

[46] K.A. Bunten, L. Chen, A.L. Fernandez, A.J. Poë, *Coord. Chem. Rev.*, 233 (2002) 41.
[47] R. L. Pruett and J. A. Smith, *J. Org. Chem.*, 34 (1969) 327.
[48] R. Kadyrov, D. Heller and R. Selke, *Tetrahedron: Asymmetry*, 9 (1998) 329.
[49] Z. Freixa, M. M. Pereira, J. C. Bayon, A. M. S. Silva, J. A. R. Salvador, A. M. Beja, J. A. Paixao and M. Ramos, *Tetrahedron: Asymmetry*, 12 (2001) 1083.
[50] T. Yoshida, T. Okano, Y. Ueda and S. Otsuka, *J. Am. Chem. Soc.*, 103 (1981) 3411.
[51] M. A. Freeman and D. A. Young, *Inorg. Chem.*, 25 (1986) 1556.
[52] A. van Rooy, J.N.H. de Bruijn, K.F. Roobeek, P.C.J. Kamer, P.W.N.M. van Leeuwen, *J. Organomet. Chem.*, 507 (1996) 69.
[53] P.W.N.M. van Leeuwen and C.F. Roobeek, *J. Organomet. Chem.*, 258 (1983) 343.
[54] T. Jongsma, G. Challa and P.W.N.M. van Leeuwen, *J. Organomet. Chem.*, 421 (1991) 121.
[55] A. Polo, J. Real, C. Claver, S. Castillon and J.C. Bayon, *J. Chem. Soc., Chem. Commun.*, (1990) 600.
[56] A. van Rooy, E.N. Orij, P.C.J. Kamer and P.W.N.M. van Leeuwen, *Organometallics*, 14 (1995) 34.

A variety of techniques have been developed in order to rapidly evaluate ligands' electronic properties, for example, measuring the coupling constants between ^{31}P and other NMR active nuclei[59,60,61] such as ^{11}B, ^{195}Pt or ^{77}Se. The $^{1}J_{P\text{-}Se}$ coupling constant is a good measure of phosphine basicity, irrespective of the size of the phosphine ligand.60 This method, demonstrated by Allen *et al.*, involves the rapid oxidative addition of $SeCN^-$ to tertiary phosphine ligands to easily produce phosphine selenides,[62] providing a simple and fast way to evaluate the electronic properties of a specific phosphorous ligand. The $^{1}J_{P\text{-}Se}$ coupling constants of phosphine selenides together with the cone angle (slightly modified Tolman cone angle) was successfully used in determining the steric and electronic parameters for the bicyclic phosphine ligands.[63] These parameters were evaluated together with catalytic behaviour of these systems as catalysts in the hydroformylation of alkenes. Such elemental evaluations are important to gain insights to more active and selective catalyst designs.

Tetramerisation of ethylene to 1-octene (**Scheme 2.3**) is another catalytic process that showed to be greatly influenced by the steric properties of the ligand. Selective tetramerisation was demonstrated using a chromium source, diphenylphosphinoamine ligand of the general structure $(Ph_2P)_2N\text{-}R$ and a methylaluminoxane (MAO) based activator.[64] It was found that the steric bulk of the substituent on the N-atom was the predominant factor that influenced catalyst productivity and selectivity (**Table 2.1**) in such a way that it is possible to shift between 1-hexene and 1-octene selectivities by slight modifications of the ligands.[65,66]

[59] A.H. Cowley, M.C. Damasco, *J. Am. Chem. Soc.*, 93 (1971) 6815.
[60] D.W. Allen, B.F. Taylor, *J. Chem. Soc. Dalton Trans.*, (1982) 51.
[61] D.W. Allen, I.W. Nowel, B.F. Taylor, *J. Chem. Soc. Dalton Trans.*, (1985) 2505.
[62] P. Nicpon, D.W. Meek, *Inorg. Chem.*, 5 (1966) 1297.
[63] P.N. Bungu, S. Otto, *J. Organomet. Chem.*, 692 (2007) 3370.
[64] A. Bollmann, K. Blann, J.T. Dixon, F.M. Hess, E. Kilian, H. Maumela, D.S. McGuinness, D.H. Morgan, A. Nevelling, S. Otto, M. Overett, A.M.Z. Slawin, P. Wasserscheid, S. Kuhlmann, *J. Am. Chem. Soc.*, 126 (2004) 14712.
[65] K. Blann, A. Bollmann, J.T. Dixon, F.H. Hess, E. Killian, H. Maumela, D.H. Morgan, A. Neveling, S. Otto, M. J. Overett, *Chem. Commun.*, (2005) 620.
[66] M.J. Overett, K. Blann, A. Bollmann, J.T. Dixon, F. Hess, E. Killian, H. Maumela, D.H. Morgan, A. Neveling, S. Otto, *Chem. Commun.*, (2005) 622.



Scheme 2.3: Cationic metallocycle mechanism proposed for the Cr/PNP ethylene tetramerisation system.[67]

Table 2.1: Selected ethylene oligomerisation catalytic data for various PNP ligand systems.[68]

PNP Ligand	% 1-C_6 [a]	% 1-C_8 [b]	% C_6 cyclics[c]
*n*Et	7.3	62.8	10.4
*n*Prop	7.8	60.2	10.9
*n*But	7.8	60.5	10.9
*n*Pent	6.9	58.2	10.1
*c*Prop	8.8	61.4	10.8
*c*But	9.3	60.1	10.0
*c*Pent	12.1	63.8	6.7
*i*Prop	12.8	69.4	4.1
*c*Hex	14.7	68.2	4.8
Dimp	21.1	66.6	3.6
*t*But	30.9	58.4	1.9
Trimp	44.4	44.6	1.2

[a] % 1-hexene of total liquid product at 45 bar, 60 °C [b] % 1-octene of total liquid product 45 bar, 60 °C [6], [c] % C6 cyclic side-product formation of total liquid product 45 bar, 60 °C

[67] A.J. Rucklidge, D.S. McGuinness, R.P. Tooze, A.M.Z. Slawin, J.D.A. Pelletier, M.J. Hanton, P.B. Webb, *Organometallics*, 26 (2007) 2782.
[68] N. Cloete, PhD Thesis, University of the Free State, South Africa, 2009.

2.5.2 Natural bite angle of *bis*-chelating ligands

Although steric evaluation of ligands is of utmost importance, it is not the only ligand property that has dramatic effects on catalytic processes. High selectivities in the hydroformylation of alkenes have been reported for both diphosphine and diphosphite modified rhodium catalysts.[71,72,74,75] Chelating diphosphine ligand systems have often been found to improve catalyst stability, giving rise to superior results than for the monophosphine and –phosphite systems. The bidentate ligands possess natural bite angles.[69] The concept of the natural bite angle is means to predict chelational preferences of bidentate ligands[70] and is determined only by ligand backbone constraints and not by metal valance angles.[71]

Ligands with larger bite angles are normally more flexible and have shown to produce better product ratios in hydroformylation, but can have negative effects on catalyst stability.[72,73,74,75] These bite angles affect the selectivity towards linear aldehydes as regioselectivity is determined by relative stabilities of the transition states during alkene insertion. Alkene coordination precedes a five-coordinate trigonal bipyramidal intermediate in which the bidentate ligand may be coordinated in either an equatorial-equatorial (ee) or an equatorial-axial (ea) fashion (**Scheme 2.1**).

Casey and co-workers[76] designed specific chelating diphosphine ligands (**Figure 2.2**) to intentionally coordinate in diequatorial (ee) or equatorial-axial (ea) positions to determine their effects on the regioselectivity of rhodium-catalyzed 1-hexene hydroformylation. In an ideal trigonal bipyramid, an ee complex would require a bite angle of 120° and ea 90°. Larger bite angles of 113 °, 107 ° and 85 ° for ligands BISBI (2,2'-*bis*[(diphenylphosphino)methyl]-1,1'-biphenyl), T-BDCP (*trans*-1,2-*bis*[(diphenylphosphino)methyl]cyclopropane) and DIPHOS

[69] R.H. Crabtree, *The Organometallic Chemistry of the Transition Metals*, Wiley, New York, 2001.
[70] C.P. Casey, G. T. Whiteker, *Isr. J. Chem.* 30 (1990) 299.
[71] C. Casey, G. Whiteker, M. Melville, L. Petrovich, J. Gavney, D. Powell, *J. Am. Chem. Soc*, 114 (1992) 5535.
[72] L. van der Veen, P. Keeven, G. Schoemaker, J. Reek, P. Kamer, P.W.N.M. van Leeuwen, M. Lutz, A. Spek, *Organometallics*, 19 (2000) 872.
[73] T.J. Devon, G.W. Phillips, T.A. Puckette, J.L. Stavinoha, J.J. van der Bilt, *Chem. Abstr.* 108 (1988) 7890.
[74] M. Kranenburg, Y.E.M. van der Burgt, P.C.J. Kamer, P.W.N.M. van Leeuwen, *Organometallics*, 14 (1995) 3081.
[75] A. van Rooy, P.C.J. Kamer, P.W.N.M. van Leeuwen, K. Goubitz, J. Fraanje, N. Veldman, A.K. Spek, *Organometallics*, 15 (1996) 835.
[76] C.P. Casey, E.L. Paulsen, E.W. Beuttenmueller, B.R. Proft, L.M. Petrovich, B.A. Matter, D.R. Powell, *J. Am. Chem. Soc.*, 119 (1997) 11817.

(1,2-*bis*(diphenylphosphino)ethane) respectively, influences the nature of the intermediates, which then influence the regioselectivity.[77,78,79] BISBI coordinates almost exclusively ee, T-BDCP occurs in a 2:1 ratio of ee:ea and DIPHOS are mostly ea.[71]

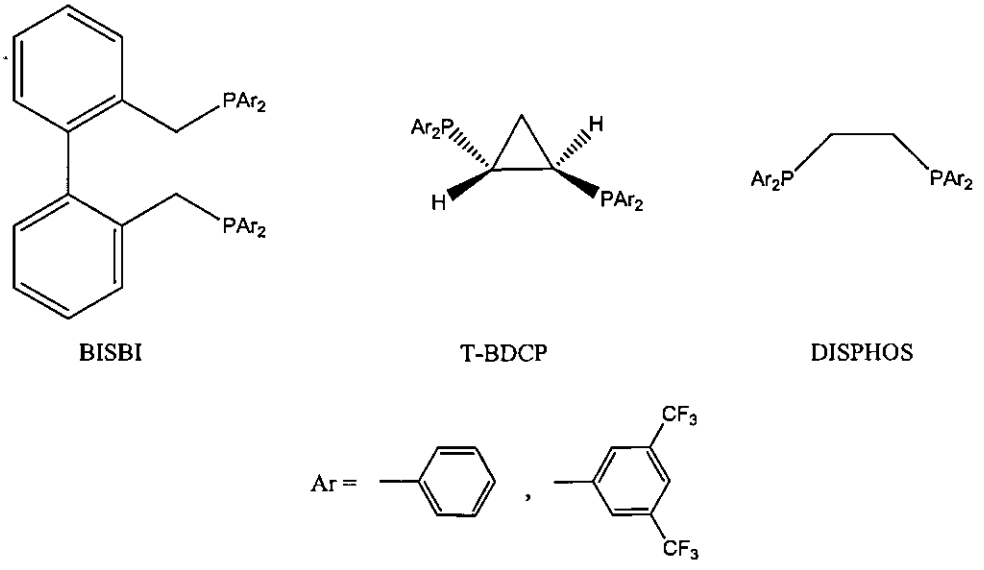


Figure 2.2: Diphosphine ligands used in rhodium-catalyzed hydroformylation of 1-hexene.[80]

Large bite angles thus favour the ee intermediate, disfavouring the branched pathway, in which the alkyl R group is forced to be *cis* to two phosphines. Smaller bite angles favour the ea intermediate, which does not disfavour the branched pathway to nearly the same extent. It was proposed by van Leeuwen that a larger bite angle would increase the steric bulk around the area where the olefin adds, thus favouring the linear product.[81] Addition of electron withdrawing and –donating groups to the backbone of the diphosphine ligands can also contribute to the preferred equatorial or axial coordination of the ligand to the metal centre, thus influencing linear aldehyde selectivity.[82,83] Electron withdrawing CF_3 groups on the aryl rings of BISBI-(3,5-CF_3) and T-BDCP-(3,5-CF_3) led to an increase in linear aldehydes, but led to a decrease in *n*-aldehyde

[77] C. Casey, L. Petrovich, *J. Am. Chem. Soc.*, 117 (1995) 6007.
[78] J. Brown, A.G.J. Kent, *Perkin Trans.*, 2 (1987) 1597.
[79] P. Dierkes, P.W.N.M. van Leeuwen, *J. Chem. Soc. Dalton Trans.*, (1999) 1519.
[80] P.D. Achord, P. Kiprof, B. Barker, *J. Mol. Structure: THEOCHEM*, 849 (2008) 103-111.
[81] L.A. van der Veen, M.D.K. Boele, F.R. Bregman, P.C. Kamer, P.W.N.M. van Leeuwen, K. Goubitz, J. Fraanje, J. Schenk, C. Bo, *J. Am. Chem. Soc.*, 120 (1998) 11616.
[82] C. Casey, E. Paulsen, E. Beuttenmueller, B. Profit, B. Matter, D. Powell, *J. Am. Chem. Soc.*, 121 (1999) 1985.
[83] J.D. Unruh, J.R. Christenson, *J. Mol. Catal.*, 14 (1982) 19.

regioselectivity in the apical position of DIPHOS-(3,5-CF_3) when compared with the phenyl-substituted analogues.

In another study, the phenyl groups of the thixantphos ligand, **Figure 2.3**, was modified with sterically similar electron withdrawing and electron-donating groups (*p*-$(CH_3)_2N$, *p*-CH_3O, *p*-H, *p*-F, *p*-Cl, or *p*-CF_3) and it was found that decreasing phosphine basicity favoured the ee intermediate.[81]

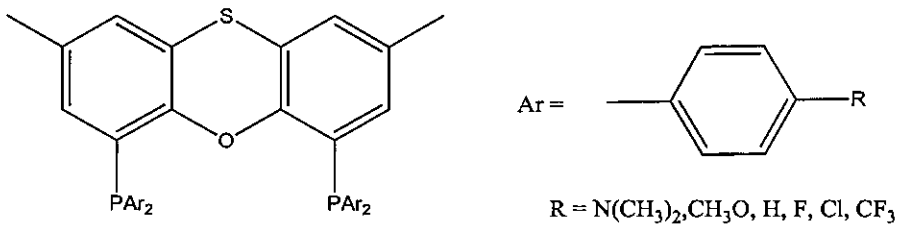


Figure 2.3: Thixantphos bidentate ligand.[80]

The [(diphosphine)Rh$(CO)_2$H] complexes occurred in ee:ea isomer ratio that shifted from one for the *p*-$(CH_3)_2N$-substituted ligand to more than nine for the *p*-CF_3-substituted ligand, showing the equilibrium compositions to be dependent on phosphine basicity. During hydroformylation of 1-octene and styrene an increase in l:b product ratio and activity was observed with a decrease in phosphine basicity. A selectivity of 92-93 % for linear aldehyde formation for 1-octene across all ligands also indicates that the chelation mode in the [(diphosphine)Rh$(CO)_2$H] complexes are not in itself the key parameter controlling regioselectivity.

Hydroformylation can also be achieved by employing platinum-disphosphine complexes in the presence of a $SnCl_2$ cocatalyst which has been investigated with particular interest towards asymmetric reactions where high stereoselectivity is established.[84] Platinum(II) complexes containing bidentate diphosphine ligands have demonstrated good activities and selectivities toward linear aldehydes.[85,86] Examples of these Pt/Sn systems show that catalytic efficiency is directly related to the bite angle.[87,88]

[84] E.V. Gusevskaya, E.N. dos Santo, R. Augusti, A. Dias, C.M. Foca, *J. Mol. Cat. Chem.*, 152 (2000) 15.
[85] R. van Duren, J. van der Vlugt, H. Kooijman, A.L. Apek, D. Vogt. *Dalton Trans.*, (2007) 1053.
[86] L.A. van der Veen, P.K. Keeven, P.C.J. Kamer, P.W.N.M. van Leeuwen, *Chem Commun.*, (2000) 333.
[87] T. Hayashi, T. Kawabata, T. Isoyama, I. Ogata, *Bull Chem. Soc. Jpn.*, 54 (1981) 3438.

Hayashi studied the hydroformylation of 1-pentene using [$PtCl_2(Ph_2P(CH_2)_nPh_2P)$] ($n$ = 1-6, 10) as ligand and it was found to depend strongly on the methylene chain length.[87] *Bis*(diphenylphosphino)methane and 1,2-*bis*(diphenylphosphino)ethane were almost completely ineffective, where diphosphine of n=3 had comparable rates as when using PPh_3 as ligand, as shown by Orchin *et al*[89] and Knifton *et al.*[90] A rate several times higher than when PPh_3 was used was observed with diphosphine n=4, achieving a maximum overall rate enhancement throughout the various chain lengths evaluated. When n exceeds four, the rate is rapidly reduced and gradually becomes ineffective. The linearity of 91-94 % was unvarying except in the case of n=3 in which the linearity was reduced to 69 % that could have been due to instability. A range of 1,4-*bis*(diphenylphosphino)butane derivatives were investigated to clarify the effect on the reaction rate and product distribution. This involved the bridging of the 2- and 3-carbons to construct a rigid and saturated ring skeleton (**Figure 2.4**).

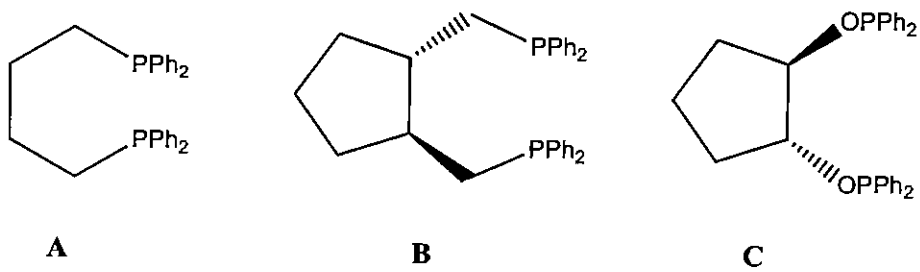


Figure 2.4: Some examples of the 1,4-*bis*(diphenylphosphino)butane ligand (**A**) and modification thereof by bridging of the 2- and 3-carbons for constructing saturated ring skeletons (**B** and **C**).[87]

It was found that the electronic effect of the bidentate ligands had no influence on the hydroformylation rate or product ratios as made clear by *trans*-1,2-*bis*(diphenylphosphinomethyl)cyclopentane (**B**) and *trans*-1,2-*bis*(diphenylphosphinooxy)cyclopentane (**C**) which are sterically similar but electronically different giving similar hydroformylation results. Thus, the rigidity and steric properties of the ring skeletons is the main factor for the effectiveness of the diphosphines as also seen by Knifton[90] with various *mono*-phosphine ligands.

[88] T. Hayashi, T. Kawabata, T. Isoyama, I. Ogata, *J. Chem. Soc. Chem. Commun.*, (1979) 462.
[89] C.Y. Hsu, M. Orchin, *J. Am. Chem. Soc.*, 97 (1975) 3553.
[90] I. Schwager, J.K. Knifton, *J. Catal.*, 45 (1976) 256.

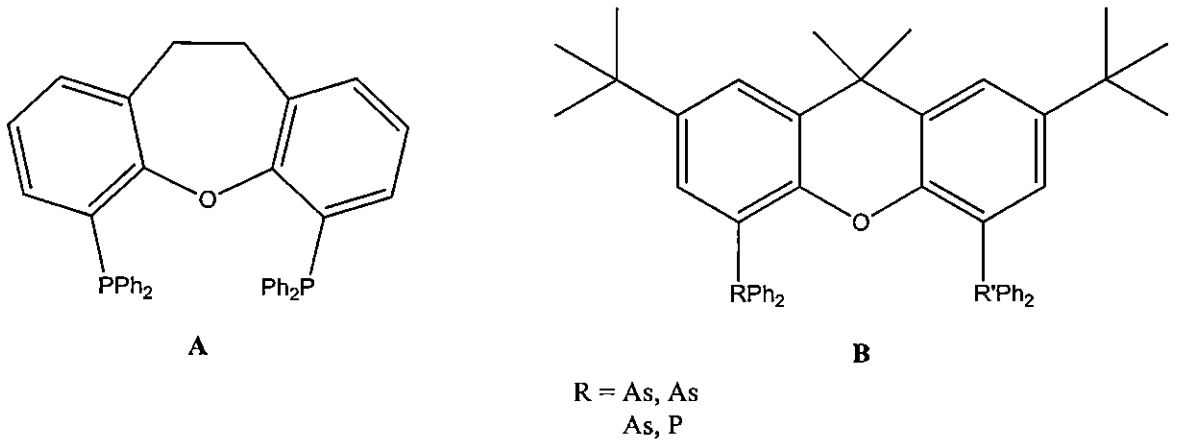
CHAPTER 2

Platinum(II) complexes containing diphosphinoamine *P,P'*-bidentate ligands of the type $[PtCl_2(R\text{-}N(PPh_2P)_2)]$ (R = benzyl, 2-picolyl and ^nPr) have shown to hydroformylate 1-octene, albeit at low activities and slightly higher regioselectivities towards linear aldehydes. The larger l:b aldehyde ratio is considerably higher than the linearity when using $[PtCl_2(dppp)]$, providing evidence that these catalysts impose a greater steric effect resulting in more linear products. When comparing the diphosphinoamine ligands to the previously mentioned Hayashi *et al*[87] diphosphine ligands, the small bite angle methylene bridged complex, $[PtCl_2(Ph_2P(CH_2)Ph_2P)]$, showed little to no hydroformylation activity simulating the same trend as the comparable bite angle of the platinum complexes containing diphosphinoamine ligands. The hydroformylation activity is at a maximum when the larger bite angle 1,4-*bis*(diphenylphosphino)butane ligand was used and further modification of a rigid ring skeleton at the 2- and 3-carbon influenced the rate and selectivity significantly, indicating that not only do steric bulkiness effect the hydroformylation process, but it appears that the bite angle is also a decisive factor in activity and selectivity.

In platinum/tin-catalyzed hydroformylation, the smaller natural bite angle of homoxantphos (**Figure 2.5 A**), showed a higher activity than the general xantphos ligand as can also be seen by work of Kawabata and Hayashi *et al.*[88] A relatively small bite angle of 102 ° for the homoxantphos (**Figure 2.5 A**) ligand produces a beneficial reaction rate that is 40 times higher than for the general xantphos ligand with a natural bite angle of 110 °. This is probably due to the difference in reactivity of the *cis* and *trans* isomers of platinum(II) complexes. In general *trans* coordination of phosphines in the square-planar platinum/tin–acyl complexes is thermodynamically favoured over *cis* coordination.[91,92,93] However, *cis* coordination of the phosphines is a prerequisite so ensure an active catalyst for migratory insertion reactions and hydrogenolysis to form the aldehyde product.[94,95,96] Diphosphines with narrow natural bite angles can only form the *cis* complex due to bite angle constraints and therefore yield an active hydroformylation catalyst. Wider bite angle diphosphines and *mono*-phosphines will give the

[91] A. Scrivanti, C. Botteghi, L. Toniolo and A. Berton, *J. Organomet.Chem.*, 344 (1988) 261.
[92] M. Gomez, G. Muller, D. Sainz, J. Sales and X. Solans, *Organometallics*, 10 (1991) 4036.
[93] G. K. Anderson and R. J. Cross, *Acc. Chem. Res.*, 17 (1984) 67.
[94] I. Tóth, T. Kegi, C. J. Elsevier and L. Kollar, *Inorg. Chem.*, 33 (1994) 5708.
[95] W. R. Rocha and W. B. De Almeida, *Organometallics*, 17 (1998) 1961.
[96] N. Koga and K. Morokuma, *Chem. Rev.*, 91 (1991) 823.

more stable *trans* platinum/tin-acyl complexes. Group 15 derivates of the xantphos ligand, xantphosarsine and xantarsine, (**Figure 2.5 B**) gave efficient platinum/tin catalyst for the hydroformylation of 1-octene. A remarkable increase in activity and selectivity was observed for the xantphosarsine ligand which despite a wide natural bite angle, has enhanced preference for *cis* co-ordinated platinum/tin complexes compared to xantphos with a similar bite angle.



A **B**

R = As, As
As, P

Figure 2.5: The homoxantphos ligand (A) and the arsine and mixed arsine/phosphine analogues of the xantphos ligand (B).[97]

The increase in activity with an increasing natural bite angle is only observed for ligands with narrow natural bite angles and is explained by the alkene and carbon monoxide insertion.[96,98,99] Rocha and De Almeida showed that the P-Pt-P bite angle increases from 106.8 ° to a maximum of 146.2 ° for the complex $[Pt(H)(PH_3)(SnCl_3)(C_2H_4)]$ during a theoretical study.[100] It can be concluded that widening of the natural bite angle enhances the alkene insertion reaction and, therefore, the hydroformylation rate. The natural bite also influences the selectivity for linear aldehyde formation in platinum/tin catalyst systems and the effect is comparable to that observed in the rhodium-diphosphine catalyzed hydroformylation and can be explained in a similar fashion. A wider bite angle leads to an increase in steric congestion around the platinum metal centre, and hence, to more selective formation of the sterically less hindered linear platinum alkyl species.

[97] L. van der Veen, P.K. Keeven, P.C.J. Kamer, P.W.N.M. van Leeuwen, *J. Chem, Soc., Dalton Trans.*, (2000) 2105.
[98] G. K. Anderson and G. J. Lumetta, *Organometallics*, 4 (1985) 1542.
[99] G. P. C. M. Dekker, C. J. Elsevier, K. Vrieze and P. W. N. M. van Leeuwen, *Organometallics*, 11 (1992) 1598.
[100] W. R. Rocha and W. B. De Almeida, *Organometallics*, 17 (1998) 1961.

CHAPTER 2

During nickel-phosphine catalyzed hydrocyanation of styrene, the bite angle proved to be of crucial importance towards activity and selectivity. Modified xantphos diphosphine ligands with an optimal bite angle of 105-106 ° gave very high selectivity and conversions of up to 95 %, while a slight increase to 109 ° or a decrease to 101 ° results in a significant drop in activity.[101]

The significance of these structural characteristics on ligand as well as metal catalyst design forms the key focus for this study on the hydroformylation of olefins. Furthermore, by selectively adjusting these parameters, one can better postulate the idealised factors for the design of the catalyst, when the main influencing properties are determined from such a comparative study.

[101] M. Kranenburg, P.C.J. Kamer, P.W.N.M. van Leeuwen, D. Vogtb, W. Keim, *J. Chem. Soc., Chem. Commun.*, (1995) 2177.

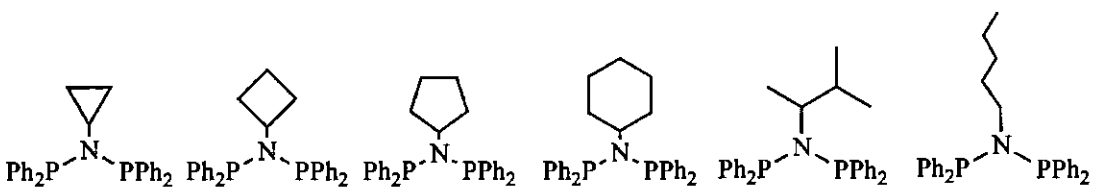
3 Synthesis and characterization of PNP-ligands and corresponding metal coordinated complexes

In this chapter...

The synthesis of a range of bis(diphenylphosphino)amine ligands are described as well as the coordination of these ligands to Pt(II) and Pd(II).

3.1 Introduction

A range of diphosphinoamine ligands (PNP-ligands) (**Scheme 3.1**) were synthesized in which only the substituent bonded to the nitrogen atom was stepwise manipulated from one compound to the next. These ligands were then coordinated to metal cations such as platinum(II) and palladium(II) to investigate the electronic and structural effects of the moiety changes of the PNP-ligands for the various compounds. The information gathered could be useful regarding kinetics and coordination intermediates formed during model hydroformylation reactions using rhodium and iridium catalyst systems. The difficulty associated with isolating unstable rhodium and iridium complexes, made platinum and palladium ideal alternative metal centres in order to study the solid state coordination of these PNP-ligands.



Scheme 3.1: Diphosphinoamine ligands (PNP-ligands) synthesized in this study. (1) *N,N*-Bis(diphenylphosphanyl)cyclopropylamine (PNP-*c*Prop); (2) *N,N*-Bis(diphenylphosphanyl)cyclobutanamine (PNP-*c*But); (3) *N,N*-Bis(diphenylphosphanyl)-cyclopentanamine (PNP-*c*Pent); (4) *N,N*-Bis(diphenylphosphanyl)cyclohexanamine (PNP-*c*Hex); (5) *N,N*-Bis(diphenylphosphanyl)-1,2-dimethylpropylamine (PNP-Dimprop)[1]; (6) *N,N*-Bis(diphenylphosphanyl)-*n*-pentylamine (PNP-*n*Pent).[2]

[1] N. Cloete, H.G. Visser, A. Roodt, J.T. Dixon, K. Blann, K. *Acta Cryst.*, E64 (2008) o480.

3.2 Chemicals and apparatus

All chemicals used for the preparation of the complexes were reagent grade. General reagents 1,5-cyclooctadiene, triethylamine and chlorodiphenylphosphine (Aldrich) were used as received. The metal complexes [K_4PtCl_4] and [$PdCl_2$] were obtained commercially from Next Chimica, South Africa. All solvents used, were of analytical grade and used as received, except where dry conditions were required. In these cases solvents were purified and dried according to literature procedures.[3] In the case of moisture and oxygen sensitive chemicals all reactions were performed under argon atmosphere using standard anaerobic conditions.

The PNP-ligands were synthesized by reacting the amine and diphenylphosphine chloride Ph_2PCl, as described in the literature.[4,5,6,7]

All infrared spectra were recorded as neat samples on a Digilab FTS 2000 Fourier transform spectrometer (ATR) utilizing a He-Ne laser at 632.6 nm, in the range of 3000 to 600 cm^{-1}. All NMR data were obtained on a Bruker AXS 600 MHz (operating at 600.28, 150.96 and 242.99 MHz for ^{1}H, ^{13}C and ^{31}P, respectively) or Bruker AXS 300 MHz (operating at 300.13 and 121.49 MHz for ^{1}H and ^{31}P, respectively) nuclear magnetic resonance spectrometer using the mentioned deuterated solvent. Chemical shifts, δ, are reported in ppm with ^{1}H spectra calibrated relative to the residual $CHCl_3$ (7.24 ppm) and CH_2Cl_2 (5.32 ppm) peaks. ^{13}C spectra were calibrated relative to the residual CH_2Cl_2 (53.84 ppm) peak and ^{31}P NMR spectra calibrated relative to 85% H_3PO_4 as external standard in a capillary (0 ppm). Coupling constants, *J*, are reported in Hertz.

[2] N.Cloete, PhD thesis, University of the Free State, 2009.
[3] D.D. Perrin, W.L.F. Armarego, Purification of Laboratory Chemicals, 3rd Edition, Pergamon Press, 1988.
[4] S.J. Dossett, A. Gillon, A.G. Orpen, J.S. Fleming, P.G. Pringle, D.F.Wass, M.D. Jones, *Chem. Commun.*, (2001) 699.
[5] M.S. Balakrishna, T.K. Prakasha, S.S. Krishnamurthy, *J. Organomet. Chem.*, 390 (2) (1990) 203.
[6] N.A. Cooley, S.M. Green, D.F. Wass, K. Heslop, A.G. Orpen, P. Pringle, *Organometallics*, 20 (2001) 4769.
[7] S. Kuhlmann, K. Blann, A. Bollmann, J.T. Dixon, E. Killian, M.C. Maumela, H. Maumela, D.H. Morgan, M. Pretorius, N. Taccardi, P. Wasserscheid, *J. Catal.*, 245 (2007) 279.

3.3 Synthesis of reagents

3.3.1 *cis*-(η^4-Cycloocta-1,5-diene-dichloridoplatinum(II)) ([Pt(cod)Cl_2])

K_2PtCl_4 (1.0 g, 2.4 mmol) was dissolved in a mixture of distilled water (16 ml) and n-propanol (11 ml). 1,5-Cyclooctadiene (2 ml, 2.4 mmol) and $SnCl_2$ (15.0 mg, 2.4 mmol) was added. The reaction mixture was stirred at room temperature for 48 hours. The solvent was evaporated overnight. The product was then extracted with boiling dichloromethane. The solution was allowed to evaporate slowly overnight forming light yellow crystals. Yield 0.865 g (96.0 %). δ_H (600 MHz $CDCl_3$) 2.28-2.30 (4 H, m, 2 CH_2), 2.69-2.72 (4 H, m, 2 CH_2), 5.61-5.64 (4 H, m, 4 CH).

3.3.2 *cis*-(η^4-Cycloocta-1,5-diene-dichloridopalladium(II)) ([Pd(cod)Cl_2])

$PdCl_2$ (2.0 g, 11.3 mmol) was dissolved in hot concentrated HCl (5 ml, 10 M). The solution was cooled to room temperature and diluted with ethanol (150 ml) and filtered. 1,5-Cyclooctadiene (3 ml, 11.3 mmol) was added to the filtrate with rapid stiring. The yellow product precipitated immediately and was stirred for a further 10 minutes. The solution was filtered and the precipitate was washed with diethyl ether (100 ml). Yield 2.93 g (91.0 %). δ_H (600 MHz $CDCl_3$) 2.60-2.63 (4 H, m, 2 CH_2); 2.88-2.91 (4 H, m, 2 CH_2); 5.29-5.33 (4 H, m, 4 CH).

3.3.3 (Acetylacetonato)dicarbonylrhodium(I) ([Rh(acac)(CO_2)])

Rhodium(III) trichloride hydrate (0.109g, 0.414 mmol) was dissolved in one drop of water and minimal DMF and refluxed at 185 °C for 30min. The light yellow solution was then cooled to room temperature and 2.1 eq acetylacetone (acac) (42.8 µl, 0.430 mmol) was added. The light pink product was precipitated with a large excess of ice-water and centrifuged. The water was decanted and the product dissolved in DCM and left overnight to crystallize. Yield 85.01 g (80.0 %). υ_{max}/cm^{-1} 1995, 2062 (CO).

3.4 Synthesis of bis(diphenylphosphino)amine ligands

3.4.1 *N,N*-Bis(diphenylphosphino)cyclopropanamine (1)

Cyclopropylamine (693 µl, 0.010 mol) was dissolved in dichloromethane (30 ml) after which the solution was placed on an ice bath. Triethylamine (4.21 ml, 0.030 mol) was added to the solution while stirring. Chlorodiphenylphosphine (3.70 ml, 0.020 mol) was added dropwise to the reaction mixture. The ice bath was removed after 1 h and the reaction mixture was allowed to stir at room temperature for a further 12 h. The reaction mixture was reduced to dryness under vacuo. A mixture of hexane (20 ml) and toluene (2 ml) was added to the remaining white powder and was passed through a column containing neutral activated alumina (35 g). The solvent of the eluent was removed under reduced pressure and the white precipitate was collected. Single colourless crystals suitable for X-ray crystallography were obtained from recrystallization from methanol. Yield 1.81 g (43 %). δ_H (600 MHz CD_2Cl_2) 0.35-0.40 (2 H, m, CH_2); 0.55-0.59 (2 H, m, CH_2); 2.62-2.67 (1 H, m, CH) 7.30-7.35 (12 H, m, ArH) 7.42-7.46 (8 H, m, ArH). δ_C (151 MHz CD_2Cl_2) 8.9 (t, C-C); 34.8 (t, N-C); 128.3 (s, ArC); 129.0 (s, ArC); 133.4 (t, ArC); 139.5 (t, P-C). δ_P (121 MHz CD_2Cl_2) 63.4 (s). υ_{max}/cm^{-1} 1431-1477 (ArC); 1308 (N-P); 1092 (N-C). C, H, N microanalysis: found (%): C 76.23, H 5.92, N 3.29; calculated for $C_{27}H_{25}NP_2$: C 76.19, H 5.9, N 3.30.

3.4.2 *N,N*-Bis(diphenylphosphino)cyclobutanamine (2)

The title compound, PNP-*c*But, was prepared in a similar fashion as PNP-*c*Prop in §3.4.1 using cyclobutylamine (854 µl, 0.010 mol). Yield 2.100 g (48%). δ_H (600 MHz CD_2Cl_2) 1.35-1.44 (1 H, m, CH_2); 1.61-1.68 (1 H, m, CH_2) 1.75-1.83 (2 H, m, CH_2); 2.49-2.57 (2 H, m, CH_2); 3.90-4.1 (1 H, m, CH); 7.12-7.83 (20 H, m, Ar). δ_C (151 MHz CD_2Cl_2) 15.2 (s, C-C); 33.1 (t, C-C); 56.9 (t, N-C); 128.4 (d, ArC); 128.9 (s, ArC); 133.0 (d, ArC); 140.0 (d, P-C). δ_P (121 MHz CD_2Cl_2) 49.3 (s). υ_{max}/cm^{-1} 1436-1500 (ArC); 1311 (N-P); 1066 (N-C). C, H, N microanalysis: found (%): C 76.53, H 6.19, N 3.19; calculated for $C_{28}H_{27}NP_2$: C 76.52, H 6.15, N 3.17.

3.4.3 *N,N*-Bis(diphenylphosphino)cyclopentanamine (3)

The title compound, PNP-*c*Pent, was prepared in a similar fashion as PNP-*c*Prop in §3.4.1 using cyclopentylamine (1.0 ml, 0.010 mol). Yield 1.010 g (22 %). δ_H (600 MHz CD_2Cl_2) 1.30-1.40 (2 H, m, CH_2); 1.50-1.56 (2 H, m, CH_2); 1.64-1.74 (2 H, m, CH_2); 1.79-1.90 (2 H, m, CH_2); 3.73-3.90 (1 H, m, CH); 7.15-7.51 (20 H, m, Ar). δ_C (151 MHz CD_2Cl_2) 24.4 (s, C-C); 34.4 (t, C-C); 63.0 (t, N-C); 128.4 (d, ArC); 128.9 (s, ArC); 133.2 (d, ArC); 140.5 (d, P-C). δ_P (121 MHz CD_2Cl_2) 51.6 (s). υ_{max}/cm^{-1} 1431-1500 (ArC); 1309 (N-P); 1050 (N-C). C, H, N microanalysis: found (%): C 76.81, H 6.45, N 3.09; calculated for $C_{29}H_{29}NP_2$: C 76.80, H 6.40, N 3.00.

3.4.4 *N,N*-Bis(diphenylphosphino)cyclohexanamine (4)

The title compound, PNP-*c*Hex, was prepared in a similar fashion as PNP-*c*Prop in §3.4.1 using cyclohexylamine (1.14 ml, 0.010 mol). Yield 2.500 mg (54 %). δ_H (600 MHz CD_2Cl_2) 1.15-0.98 (3 H, m, CH_2); 1.41 (2 H, d, CH_2); 1.47-1.55 (1 H, m, CH_2); 1.60 (2 H, d, CH_2); 1.87 (2 H, q, CH_2); 3.20-3.30 (1 H, m, CH) 7.17-7.56 (20 H, m, Ar). δ_C (151 MHz CD_2Cl_2) 26.5 (s, C-C); 27.0 (s, C-C); 35.5 (t, C-C); 60.8 (t, N-C); 128.4 (d, ArC); 128.9 (s, ArC); 133.2 (d, ArC); 140.7 (d, P-C). δ_P (121 MHz CD_2Cl_2) 51.0 (s). υ_{max}/cm^{-1} 1433-1502 (ArC); 1307 (N-P); 1056 (N-C). C, H, N microanalysis: found (%): C 77.07, H 6.68, N 3.00; calculated for $C_{30}H_{31}NP_2$: C 77.10, H 6.60, N 2.70.

3.5 Synthesis of Pt(II)-PNP complexes

3.5.1 Bis[*N,N*-bis(diphenylphosphanyl)cyclopropanamine-κ^2P,P']platinum(II) bis(trifluoromethanesulfonate)

[Pt(cod)Cl_2] (20.0 mg, 0.0535 mmol), dissolved in the minimum amount of dichloromethane, was added in a rapid drop-wise manner to a solution of PNP-*c*Prop (47.7 mg, 0.112 mmol) and AgTriflate (30.32 mg, 0.118 mmol), dissolved in the minimum volume of dichloromethane-methanol (1:1). After stirring for 20 min, the solvent was removed completely under reduced pressure. Dichloromethane was added until no further dissolution of solid was evident. The resulting heterogeneous mixture was filtered to remove the insoluble NaCl by-product. The colourless solid product was precipitated upon addition of methanol followed by a reduction in solvent volume under reduced pressure. The compound was isolated by filtration and washed with diethyl ether (10 ml). Layering of a dichloromethane solution of the product with methanol gave colourless crystals, suitable for X-ray diffraction. Yield 40.1 mg (56 %). δ_H (600 MHz CD_2Cl_2) 0.41-0.46 (4 H, m, CH_2); 0.49-0.54 (4 H, m, CH_2); 2.50-2.56 (2 H, m, CH); 7.34 (16 H, s, ArH); 7.51 (16 H, t, ArH); 7.77 (8 H, t, ArH). δ_C (151 MHz CD_2Cl_2) 6.6 (s, C-C); 33.9 (s, N-C); 124.5 (m, P-C); 131.0 (t, ArC); 133.3 (d, ArC); 135.4 (s, ArC). δ_P (243 MHz, CD_2Cl_2) 43.7 (t, J(Pt-P) = 1069 Hz). υ_{max}/cm^{-1} 1436-1520 (ArC); 1311 (N-P); 1068 (N-C); 1263 (C-F); 1031 (S-O). C, H, N microanalysis: found (%): C 51.05, H 4.21, N 2.02; calculated for $C_{59}H_{58}F_6N_2O_6P_4PtS_2$: C 51.00, H 4.19, N 2.00.

3.5.2 Bis[*N,N*-bis(diphenylphosphanyl)cyclobutanamine-κ^2P,P']platinum(II) bis(trifluoromethanesulfonate)

The title compound, [Pt(PNP-*c*But)$_2$], was prepared in good yield in a similar fashion as [Pt(PNP-*c*Prop)$_2$] in §3.5.1 using PNP-*c*But (49.3 mg, 0.112 mmol). Layering of a dichloromethane solution of the product with methanol gave colourless crystals, suitable for X-ray diffraction. Yield 68.8 mg (94 %). δ_H (600 MHz CD_2Cl_2) 1.27-1.41 (4 H, m, CH_2); 1.62-1.80 (8 H, m, CH_2); 3.61-3.70 (2 H, m, CH); 7.36 (16 H, s, ArH); 7.49 (16 H, t, ArH); 7.74 (8 H, t, ArH). δ_C (151 MHz CD_2Cl_2) 15.5 (s, C-C); 31.6 (s, C-C); 57.4 (s, N-C); 124.9 (m, P-C);

130.9 (t, ArC); 133.1 (t, ArC); 135.2 (s, ArC). δ_P (243 MHz, CD_2Cl_2) 39.2 (t, J(Pt-P) = 1064 Hz). υ_{max}/cm^{-1} 1436-1520 (ArC); 1307 (N-P); 1100 (N-C); 1263 (C-F); 1030 (S-O). C, H, N microanalysis: found (%): C 51.73, H 4.41, N 1.98; calculated for $C_{61}H_{62}F_6N_2O_6P_4PtS_2$: C 51.70, H 4.41, N 1.95.

3.5.3 Bis[*N*,*N*-bis(diphenylphosphanyl)cyclopentanamine-κ^2*P*,*P*']platinum(II) bis(trifluoromethanesulfonate)

The title compound, [Pt(PNP-*c*Pent)$_2$], was prepared in good yield in a similar fashion as [Pt(PNP-*c*Prop)$_2$] in §3.5.1 using PNP-*c*Pent (50.9 mg, 0.112 mmol). Layering of a dichloromethane solution of the product with methanol gave colourless crystals, suitable for X-ray diffraction. Yield 19.3 mg (26 %). δ_H (600 MHz CD_2Cl_2) 0.97-1.08(4 H, m, CH_2); 1.08-1.19 (4 H, m, CH_2); 1.18-1.31 (4 H, m, CH_2); 1.36-1.52 (4 H, m, CH_2); 3.41-3.56 (2 H, m, CH); 7.43 (16 H, s, ArH); 7.50 (16 H, t, ArH); 7.72 (8 H, t, ArH). δ_C (151 MHz CD_2Cl_2) 23.0 (s, C-C); 32.4 (s, C-C); 66.4 (s, N-C); 125.2 (m, P-C); 130.9 (t, ArC); 133.2 (t, ArC); 135.2 (s, ArC). δ_P (243 MHz, CD_2Cl_2) 39.7 (t, J(Pt-P) = 1064 Hz). υ_{max}/cm^{-1} 1437-1517 (ArC); 1312 (N-P); 1143 (N-C); 1264 (C-F); 1031 (S-O). C, H, N microanalysis: found (%): C 51.77, H 4.34, N 1.98; calculated for $C_{61}H_{61}F_6N_2O_6P_4PtS_2$: C 51.80, H 4.33, N 1.99.

3.5.4 Bis[*N*,*N*-bis(diphenylphosphanyl)cyclohexanamine-κ^2*P*,*P*']platinum(II) bis(hexafluoridophosphate)

The title compound, [Pt(PNP-*c*Hex)$_2$], was prepared in good yield in a similar fashion as [Pt(PNP-*c*Prop)$_2$] in §3.5.1 using PNP-*c*Hex (52.5 mg, 0.112 mmol) and $NaPF_6$ (20.0 mg, 0.118 mmol). Layering of a dichloromethane solution of the product with methanol gave colourless crystals, suitable for X-ray diffraction. Yield 44.0 mg (58 %). δ_H (600 MHz CD_2Cl_2) 0.62-0.72 (2 H, m, CH_2); 0.78-0.96 (8 H, m, CH_2); 1.31 (6 H, t, CH_2); 1.39 (4 H, d, CH_2); 3.00-3.15 (2 H, m, CH); 7.44 (16 H, s, ArH); 7.49 (16 H, t, ArH); 7.71 (8 H, t, ArH). δ_C (151 MHz CD_2Cl_2) 24.7 (s, C-C); 25.8 (s, C-C); 34.0 (s, C-C); 66.9 (s, N-C); 125.4 (m, P-C); 130.9 (s, ArC); 133.1 (t, ArC); 135.1 (s, ArC). δ_P (243 MHz, CD_2Cl_2) 39.9 (t, J(Pt-P) = 1062 Hz); -144.0 (m, PF_6).

υ_{max}/cm^{-1} 1438-1510 (ArC); 1308 (N-P); 1068 (N-C). C, H, N microanalysis: found (%): C 50.75, H 4.40, N 1.97; calculated for $C_{60}H_{62}F_{12}N_2P_6Pt$: C 50.77, H 4.40, N 1.90.

3.5.5 Bis[*N,N*-bis(diphenylphosphanyl)-*n*-pentylamine-κ^2P,P'] platinum(II) bis(hexafluoridophosphate)

The title compound, [Pt(PNP-*n*Pent)$_2$], was prepared in good yield in a similar fashion as [Pt(PNP-*c*Prop)$_2$] in §3.5.1 using PNP-*n*Pent2 (50.8 mg, 0.112 mmol) and $NaPF_6$ (20.0 mg, 0.118 mmol). Layering of a dichloromethane solution of the product with methanol gave colourless crystals, suitable for X-ray diffraction. Yield 51.2 mg (69 %). δ_H (600 MHz CD_2Cl_2) 0.6 (6 H, t, CH_3); 0.75-0.80 (4 H, m, CH_2); 0.87-0.91 (4 H, m, CH_2); 1.08-1.11 (2 H, m, CH_2); 2.84-2.90 (2 H, m, CH); 7.3 (16 H, s, ArH); 7.5 (16 H, t, ArH); 7.8 (8 H, t, ArH). δ_C (151 MHz CD_2Cl_2) 22.0 (s, C-C); 29.1 (s, C-C); 29.5 (s, C-C); 31.0 (s, C-C); 51.3 (s, N-C); 124.7 (m, P-C); 131.1 (s, ArC); 133.1 (t, ArC); 135.4 (s, ArC). δ_P (243 MHz, CD_2Cl_2) 40.6 (t, J(Pt-P) = 1064 Hz); -144.1 (m, PF_6). υ_{max}/cm^{-1} 1436-1512 (ArC); 1312 (N-P); 1059 (N-C). C, H, N microanalysis: found (%): C 49.87, H 4.45, N 2.00; calculated for $C_{58}H_{62}F_{12}N_2P_6Pt$: C 49.90, H 4.48, N 2.01.

3.6 Synthesis of Pd(II)-PNP complexes

3.6.1 Bis[*N,N*-bis(diphenylphosphanyl)cyclopropanamine-κ^2P,P']palladium(II) bis(hexafluoridophosphate)

[Pd(cod)Cl_2] (20.0 mg, 0.070 mmol), dissolved in the minimum amount of dichloromethane, was added in a rapid drop-wise manner to a solution of PNP-*c*Prop (62.9 mg, 0.148 mmol) and $NaPF_6$ (25.8 mg, 0.148 mmol), dissolved in the minimum volume of dichloromethane-methanol (1:1). After stirring for 20 min, the solvent was removed completely under reduced pressure. Dichloromethane was added until no further dissolution of solid was evident. The resulting heterogeneous mixture was filtered to remove the insoluble NaCl by-product. The colourless solid product was precipitated upon addition of methanol followed by a reduction in solvent volume under reduced pressure. The compound was isolated by filtration and washed with

diethyl ether (10 ml). Layering of a dichloromethane solution of the product with methanol gave yellow crystals, suitable for X-ray diffraction. Yield 45.2 mg (48 %). δ_H (300 MHz CD_2Cl_2) 0.44-0.52 (8 H, m, CH_2); 2.50-2.60 (2 H, m, CH); 7.33 (16 H, s, ArH); 7.50 (16 H, t, ArH); 7.76 (8 H, t, ArH). δ_C (151 MHz CD_2Cl_2) 7.1 (s, C-C); 30.1 (s, N-C); 124.8 (m, P-C); 131.2 (t, ArC); 133.2 (t, ArC); 135.2 (s, ArC). δ_P (121 MHz, CD_2Cl_2) 50.3 (s); -144 (m, PF_6). υ_{max}/cm^{-1} 1436-1502 (ArC); 1305 (N-P); 1065 (N-C). C, H, N microanalysis: found (%): C 52.00, H 4.04, N 2.25; calculated for $C_{54}H_{50}F_{12}N_2P_6Pd$: C 52.04, H 4.09, N 2.25.

3.6.2 Bis[*N*,*N*-bis(diphenylphosphanyl)cyclobutanamine-κ^2*P*,*P*']palladium(II) bis(hexafluoridophosphate)

The title compound, [Pd(PNP-*c*But)$_2$], was prepared in good yield in a similar fashion as [Pd(PNP-*c*Prop)$_2$] in §3.6.1 using PNP-*c*But (65.0 mg, 0.148 mmol). Layering of a dichloromethane solution of the product with methanol gave yellow crystals, suitable for X-ray diffraction. Yield 51.4 mg (54 %). δ_H (300 MHz CD_2Cl_2) 1.30-1.36 (4 H, m, CH_2); 1.64-1.73 (8 H, m, CH_2); 3.70-3.85 (2 H, m, CH); 7.33 (16 H, s, ArH); 7.47 (16 H, t, ArH); 7.73 (8 H, t, ArH). δ_C (151 MHz CD_2Cl_2) 15.6 (s, C-C); 31.9 (s, C-C); 56.5 (s, N-C); 125.0 (m, P-C); 131.1 (t, ArC); 133.0 (t, ArC); 135.1 (s, ArC). δ_P (121 MHz, CD_2Cl_2) 45.7 (s); -144 (m, PF_6). υ_{max}/cm^{-1} 1437-1522 (ArC); 1311 (N-P); 1069 (N-C). C, H, N microanalysis: found (%): C 53.71, H 4.74, N 2.12; calculated for $C_{59}H_{62}F_{12}N_2P_6Pd$: C 53.74, H 4.75, N 2.15.

3.6.3 Bis[*N*,*N*-bis(diphenylphosphanyl)cyclopentanamine-κ^2*P*,*P*']-palladium(II) bis(hexafluoridophosphate)

The title compound, [Pd(PNP-*c*Pent)$_2$], was prepared in good yield in a similar fashion as [Pd(PNP-*c*Prop)$_2$] in §3.6.1 using PNP-*c*Pent (67.0 mg, 0.148 mmol). Layering of a dichloromethane solution of the product with methanol gave yellow crystals, suitable for X-ray diffraction. Yield 28.0 mg (28 %). δ_H (300 MHz CD_2Cl_2) 0.95-1.00 (6 H, m, CH_3); 1.05-1.20 (12 H, m, CH_2); 1.30-1.38 (6 H, m, CH_2); 3.52-3.60 (2 H, m, CH); 7.45 (22 H, m, ArH); 7.66 (8 H, t, ArH). δ_C (151 MHz CD_2Cl_2) 23.1 (s, C-C); 32.4 (s, C-C); 65.4 (s, N-C); 126.4 (m, P-C);

130.6 (t, ArC); 133.2 (t, ArC); 134.5 (s, ArC). δ_P (121 MHz, CD_2Cl_2) 45.8 (s); -144 (m, PF_6). υ_{max}/cm^{-1} 1436-1511 (ArC); 1309 (N-P); 1060 (N-C). C, H, N microanalysis: found (%): C 54.38, H 4.94, N 2.08; calculated for $C_{61}H_{66}F_{12}N_2P_6Pd$: C 54.39, H 4.94, N 2.04.

3.6.4 Bis[*N,N*-bis(diphenylphosphanyl)cyclohexanamine-κ^2P,P']palladium(II) bis(hexafluorophosphate)

The title compound, [Pd(PNP-*c*Hex)$_2$], was prepared in good yield in a similar fashion as [Pd(PNP-*c*Prop)$_2$] in §3.6.1 using PNP-*c*Hex (69.1 mg, 0.148 mmol). Layering of a dichloromethane solution of the product with methanol gave yellow crystals, suitable for X-ray diffraction. Yield 74.5 mg (75 %). δ_H (600 MHz CD_2Cl_2) 0.63-0.69 (2 H, m, CH_2); 0.80-0.94 (8 H, m, CH_2); 1.15-1.40 (10 H, m, CH_2); 3.14-3.22 (2 H, m, CH); 7.43 (16 H, s, ArH); 7.49 (16 H, t, ArH); 7.71 (8 H, t, ArH). δ_C (151 MHz CD_2Cl_2) 24.7 (s, C-C); 25.8 (s, C-C); 34.3 (s, C-C); 66.1 (s, N-C); 125.6 (m, P-C); 131.0 (s, ArC); 133.0 (t, ArC); 134.9 (s, ArC). δ_P (121 MHz, CD_2Cl_2) 46.7 (s); -144 (m, PF_6). υ_{max}/cm^{-1} 1438-1530 (ArC); 1307 (N-P); 1066 (N-C). C, H, N microanalysis: found (%): C 50.75, H 4.40, N 1.97; calculated for $C_{60}H_{62}F_{12}N_2P_6Pd$: C 50.71, H 4.42, N 1.95.

3.7 Discussion

A range of PNP-ligands as well as [M(PNP-alkyl)$_2$] (M = Pt(II), Pd(II)) complexes were successfully synthesized and characterized. PNP-*c*Pent and the corresponding platinum and palladium complexes gave the least desirable yields of 20-30 % compared to the 45-94 % of all other synthesized products. Further investigation is needed to clarify the reason for the PNP-*c*Pent ligand and corresponding metal complexes to be the only outlier, in the range synthesized in this chapter (**Scheme 3.1**), which produce significantly lower yields. The ligands: PNP-*c*Prop, PNP-*c*But, PNP-*c*Pent and PNP-*c*Hex have been reported previously in literature in which they were used mainly with chromium for ethylene tetramerization.7 These were all re-synthesized to fully characterize in order to evaluate not only the electronic differences, but also structural divergence from solid state X-ray crystallography (Chapter 4). PNP-Dimprop1(5) and PNP-*n*Pent2(6) have also been synthesized before, but in this case the necessary characterization

was available and was thus not discussed in this Chapter. The crystal structures of these two ligands are also available and were therefore re-synthesized to be used in the hydroformylation of olefins discussed in Chapter 7. The platinum and palladium coordinated complexes are all novel and were synthesized specifically for this study.

The ^{31}P NMR data for the free PNP-ligands yielded singlet peaks with chemical shifts which range between 49.3 and 63.4 ppm (**Table 3.1**). The [Pt(PNP-alkyl)$_2$] complexes were easily identified by ^{31}P NMR consisting of a singlet flanked by ^{195}Pt satellites. The J(Pt-P) for the various platinum(II) complexes are very similar with values in a narrow range between 1062 and 1069 Hz. This indicates that the electronic properties of the PNP-ligands are similar and the varying substituents on the N-atom of this particular range do not alter the electronic properties significantly.

The chemical shifts of the singlet observed for the [Pd(PNP-alkyl)$_2$] complexes range between 45.7 and 50.3 ppm, indicating a considerable shift when compared to the values of the non-coordinated diphosphinoamine ligands (**Table 3.1**). The small ppm range for the various palladium complexes also signifies no major electronic differences between the various PNP-ligands. No ^{31}P-^{31}P coupling were observed for the platinum or palladium compounds revealing identical P-atom environments for each complex in solution.

The Pt-P coupling constant values for dichloro-platinum(II) complexes of the type, [Pt(PNP-alkyl)Cl$_2$]2 (**Table 3.1**) revealed that the electronic factors of ligands PNP-Ethyl, PNP-*c*Hex and PNP-Dimprop to be very similar due to J(Pt-P) values ranging between 3228 and 3231 Hz. PNP-*c*Hex was also used as ligand in the [Pt(PNP-alkyl)$_2$] complex range where it was mentioned earlier to be electronically equivalent to PNP-*c*Prop, PNP-*c*But and PNP-*c*Pent. Therefore, it can be assumed that the electronic properties for all the PNP-ligands (PNP-*c*Prop, PNP-*c*But, PNP-*c*Pent, PNP-Ethyl, PNP-*c*Hex and PNP-Dimprop) are similar.

Table 3.1: ^{31}P NMR data for non-coordinated and metal coordinated (metal = Pt(II), Pd(II)) PNP compounds.

Compound	δ_P (ppm)	J(Pt-P) (Hz)
PNP-*c*Prop	63.4	
PNP-*c*But	49.3	
PNP-*c*Pent	51.6	
PNP-*c*Hex	51.0	
PNP-*n*Pent[a]	62.1	
PNP-Dimprop[a]	53.0	
[Pt(PNP-*c*Prop)$_2$]	43.7	1069
[Pt(PNP-*c*But)$_2$]	39.2	1064
[Pt(PNP-*c*Pent)$_2$]	39.7	1064
[Pt(PNP-*c*Hex)$_2$]	39.9	1062
[Pt(PNP-*n*Pent)]	40.6	1064
[Pt(PNP-Ethyl)Cl$_2$][a]	16.3	3228
[Pt(PNP-*c*Hex)Cl$_2$][a]	14.4	3231
[Pt(PNP-Dimprop)Cl$_2$][a]	18.4	3228
[Pd(PNP-*c*Prop)$_2$]	50.3	
[Pd(PNP-*c*But)$_2$]	45.7	
[Pd(PNP-*c*Pent)$_2$]	45.8	
[Pd(PNP-*c*Hex)$_2$]	46.7	
[Pd(PNP-*n*Pent)$_2$]	-	

[a] See Ref 2.

^{31}P NMR data for these types of compounds provided a quick and easy method to determine if a free PNP-ligand is present or whether a metal-PNP complex was formed. The single crystal X-ray crystallographic studies of the crystals obtained from the procedures mentioned above are discussed in detail in the following Chapters 4 and 5.

4 Single crystal X-ray crystallographic study of bis(diphenylphosphino)amine ligands

In this chapter...

Crystal structures of a series of non-coordinated bis(diphenylphosphino)amine ligands (PNP-ligands) are presented. Various structural parameters are examined and compared to relevant compounds.

4.1 Introduction

A detailed literature search[1] revealed many structures for various diphosphinoamine (PNP) ligands with a variety of substituents on both the N and P atoms of the type $R_2PN(R_1)PR_2$, where R_2 = substituted aryl groups, phenoxy groups, chlorine atoms, methoxy groups *etc.* However, less than 30 structures of the diphenyl substituent on the P atoms, $(Ph_2P)N(R_1)(PPh_2)$, with varying N-coordinated group, exist in literature. In this study, three new (diphenylphosphino)-amine ligands (PNP-ligands) have been synthesized, stepwise manipulating the cyclic substituent on the N atom from cyclopropyl to cyclopentyl (**Figure 4.1**). The single crystal structures thereof are studied to evaluate any steric and electronic correlations. The crystallographic data of crystal structures (1)-(3) are summarized in **Table 4.2**.

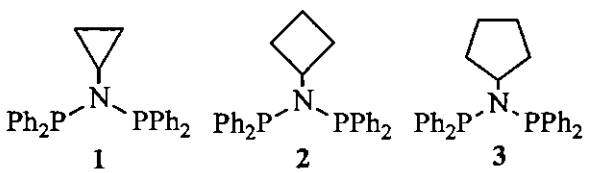


Figure 4.1: The diphosphinoamine ligands (PNP-ligands) discussed in this single crystal X-ray crystallographic study: (1) *N,N*-Bis(diphenylphosphanyl)cyclo-propylamine (PNP-*c*Prop); (2) *N,N*-Bis(diphenylphosphanyl)cyclobutanamine (PNP-*c*But); (3) *N,N*-Bis(diphenylphosphanyl)-cyclopentanamine (PNP-*c*Pent).

[1] *Cambridge Structural Database* (CSD), Version 5.33, Nov 2011 update. F.H. Allen, *Acta Cryst.*, B58 (2002) 380.

There are different possible conformations that non-coordinated disphosphinoamine ligands can adopt in the solid state.[2] The conformation of the type $C_{2V'}$ experiences the most steric interactions and is therefore not noteworthy of the conformation equilibrium (**Figure 4.2**). Conformations C_{2V} and C_S are thus expected for these type of compounds. It has been suggested that as the steric bulk of the R group increases, the C_S conformation is more likely in order to relieve major steric interaction.2 The ideal geometries of the conformers of the diphosphinoamine ligands were theoretically calculated for the ideal torsion angles of these conformers (**Table 4.1**).

The conformation adopted by of each of the free PNP-ligands in solid state will be further discussed in following paragraphs.

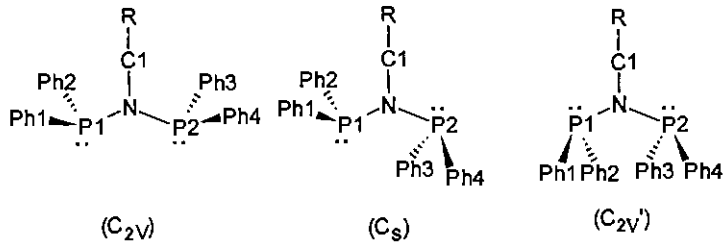


Figure 4.2: The possible principle conformations of diphosphinoamines (Ph = Phenyl, R = alkyl).

Table 4.1: The torsion angles (°) of the ideal principle conformations of diphosphinoamines (theoretically calculated).[a]

Torsion components	C_{2V}	C_S	$C_{2V'}$
C1 – N – P1 – C11[(b)]	-45	-50	-136
C1 – N – P1 – C21[(b)]	55	50	120
C1 – N – P2 – C31[(b)]	-55	-130	-151
C1 – N – P2 – C41[(b)]	45	130	106

a) Calculations were performed using the Gaussian 03 software suite and the B3LYP/LANL2DZ basis set. b) C11, C21, C31 and C41 are the phosphorous-coordinated carbon atoms of the phenyl groups: Ph1, Ph2, Ph3 and Ph4 (see **Figure 4.2**) respectively.

[2] R. Keat, L. Manojlovic-Muir, K.W. Muir, D.S. Rycroft, *J. Chem. Soc. Dalton Trans.*, (1981) 2192.

The Tolman cone angle[3] (described in detail in Chapter 2) is a measure of the steric demand induced by a ligand. Tertiary phosphines are commonly classified using this parameter, but the method can be applied to any ligand. In order to define a steric parameter for the alkyl group of the PNP-ligands, a modification of the Tolman cone angle is used, namely, the *Effective Tolman-based N-substituent steric effect* ($\theta_{N\text{-}sub}$). This parameter is constructed from the nitrogen atom with the sides' tangent to the Van der Waals radii of the outermost atoms on the substituents on the nitrogen-bonded carbon atom (C) (see **Figure 4.3**). The calculations of $\theta_{N\text{-}sub}$ were performed using **Equation 4.1**. This method was designed to systematically quantify the steric effect on the nitrogen atom into a justifiable parameter that could be used for further ligand design.

$$\boldsymbol{\theta} = \left(\frac{2}{3}\right)\sum_{i=1}^{3}\frac{\theta i}{2} \qquad \textbf{4.1}$$

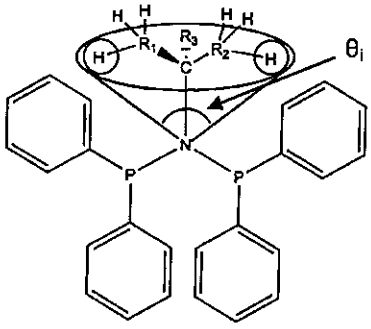


Figure 4.3: Effective Tolman-based $\theta_{N\text{-}sub}$ steric effect of bis(diphenylphosphino)-isopropylamine.

[3] C.A. Tolman, *Chem. Rev.*, 77 (1977) 313.

4.2 Experimental

The intensity data were collected on a Bruker X8 Apex II 4K Kappa CCD diffractometer equipped with graphite monochromated Mo *Kα* radiation, with a wavelength of 0.71073 Å, and with ω-and φ-scans at 100 K. All the cell refinements were performed with SAINT-Plus[4] while the data reduction was done with SAINT-Plus and XPREP4. The absorption corrections were obtained by the use of the multi-scan technique and the SADABS[5] software package. All the structures were solved with the use of the SIR-97[6] package, refinement was done with SHELXL-97[7] and WinGX[8] and the molecular graphics were completed with DIAMOND[9]. Unless otherwise stated, all the structures are shown with thermal ellipsoids drawn at a 50% probability level and all non-hydrogen atoms were anisotropically refined. Methyl, methylene, methine and aromatic hydrogen atoms were placed in geometrically idealized positions, C-H = 0.95 to 1.00 Å, and constrained to ride on their parent atoms, $U_{iso}(H) = 1.5\ U_{eq}(C)$ and $1.2\ U_{eq}(C)$ respectively. For the numbering of the phenyl rings, the first digit refers to the ring number while the second digit refers to the carbon atom in the ring

A summary of the general crystal data and refinement is given in **Table 4.2**, for all three PNP-ligands. All the atomic coordinates, anisotropic displacement parameters, bond distances, angles, torsion angles and hydrogen coordinates, of all the crystals reported in this Chapter, are given in the supplementary data (Appendix A).

[4] Bruker, *SAINT-Plus*, Version 7.12 (including XPREP), Bruker AXS Inc., Madison, Wisconsin, USA, 2004.
[5] Bruker, *SADABS*, Version 2004/1, Bruker AXS Inc., Madison, Wisconsin, USA, 1998.
[6] A. Altomare, M.C. Burla, M. Camalli, G.L. Cascarano, C. Giacovazzo, A. Guagliardi, A.G.G. Moliterni, G. Polidori, R. Spagna, *J. Appl. Cryst.*, 32 (1999) 837-838.
[7] Sheldrick, G.M., *SHELXL97*, Program for the refinement of crystal structures, University of Göttingen, Germany, 1997.
[8] L.J. Farrugia, *J. Appl. Cryst.*, 32 (1999) 837.
[9] K. Brandenburg, H. Putz, *DIAMOND*, Release 3.0c, Crystal Impact GbR, Bonn, Germany, 2006.

Table 4.2: Crystallographic data of PNP-*c*Prop (1), PNP-*c*But (2) and PNP-*c*Pent (3).

Crystallographic data	PNP-*c*Prop (1)	PNP-*c*But (2)	PNP-*c*Pent (3)
Empirical formula	$C_{27}H_{25}NP_2$	$C_{28}H_{27}NP_2$	$C_{29}H_{29}NP_2$
Formula weight (g mol^{-1})	425.42	439.45	453.47
Temperature (K)	100(2)	100(2)	100(2)
Crystal system	Monoclinic	Monoclinic	Triclinic
Space group	$P2_1/c$	$P2_1$	$P\bar{1}$
Unit cell dimensions			
a (Å)	14.460(4)	9.414(5)	8.803(5)
b (Å)	10.486(5)	9.664(5)	11.166(4)
c (Å)	17.053(5)	12.644(4)	12.685(5)
α (°)	90.000	90.000	97.144(4)
β (°)	119.358(5)	94.245(5)	101.261(5)
γ (°)	90.000	90.000	99.707(5)
Volume (Å^3)	2253.6(15)	1147.2(10)	1189.3(10)
Z	4	2	2
ρ_{calc} (g cm^{-3})	1.254	1.272	1.266
Crystal colour	Colourless	Colourless	Colourless
Crystal morphology	Cuboid	Cuboid	Cuboid
Crystal size (mm^3)	0.33 × 0.18 × 0.16	0.32 × 0.12 × 0.04	0.19 × 0.13 × 0.08
μ (mm^{-1})	0.21	0.21	0.2
F(000)	896	464	480
θ range (°)	2.5-27.5	2.7-28.3	2.7-28.0
Index ranges	$-18 \le h \le 19$ $-10 \le k \le 13$ $-22 \le l \le 22$	$-12 \le h \le 12$ $-12 \le k \le 12$ $-16 \le l \le 16$	$-11 \le h \le 11$ $-14 \le k \le 14$ $-16 \le l \le 16$
Reflections collected	33310	20748	12794
Unique reflections	5581	3035	5817
Reflections with $I > 2\sigma(I)$	4477	2930	4333
R_{int}	0.041	0.027	0.035
Completeness to theta (°, %)	28.4, 99.3	28.4, 99.9	28.3, 98.7
Data / restraints / parameters	5581 / 0 / 271	3035 / 1 / 281	5817 / 0 / 293
Goodness-of-fit on F^2	1.06	1.04	1.06
R [$I > 2\sigma(I)$]	$R_1 = 0.0392$ $wR_2 = 0.0959$	$R_1 = 0.0239$ $wR_2 = 0.0627$	$R_1 = 0.0445$ $wR_2 = 0.0943$
R (all data)	$R_1 = 0.0519$ $wR_2 = 0.1044$	$R_1 = 0.0254$ $wR_2 = 0.0637$	$R_1 = 0.0674$ $wR_2 = 0.1057$
ρ_{max}, ρ_{min} (e.Å^{-3})	0.33, -0.36	0.25, -0.18	0.34, -0.33

4.3 *N,N-Bis*(diphenylphosphanyl)cyclopropanamine (1)

The title ligand, PNP-*c*Prop (1), has been synthesized as described in Paragraph 3.4.1. The ligand crystallizes in a monoclinic crystal system in the $P2_1/c$ space group with four formula units per unit cell (Z = 4).[10] The asymmetric unit contains one complete molecule. The numbering scheme of the PNP-*c*Prop ligand is given in **Figure 4.4**.

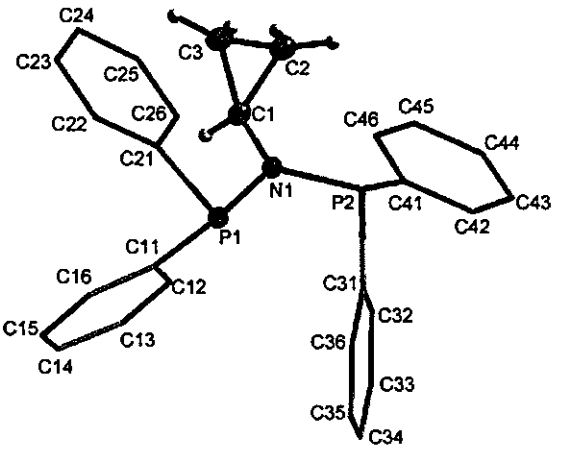


Figure 4.4: Molecular representation of PNP-*c*Prop (1). Hydrogen atoms of the phenyl rings have been omitted for clarity.

Table 4.3: Selected bond lengths (Å) and angles (°) for the crystal structure of PNP-*c*Prop (1).

Atoms	Bond length	Atoms	Bond angle
N1 – C1	1.452(2)	P1 – N1 – P2	122.6(1)
N1 – P1	1.730(1)	C1 – N1 – P1	120.3(1)
N1 – P2	1.721(1)	C1 – N1 – P2	116.0(1)
P1 – C11	1.834(2)	N1 – P1 – C11	103.6(1)
P1 – C21	1.843(2)	N1 – P1 – C21	102.4(1)
P2 – C31	1.835(2)	N1 – P2 – C31	105.3(1)
P2 – C41	1.828(2)	N1 – P2 – C41	103.5(1)
		C11 – P1 – C21	100.4(1)
		C31 – P2 – C41	102.3(1)

[10] I. Engelbrecht, H.G. Visser, A. Roodt, *Acta Cryst.*, E66 (2010) o2881.

The *Effective Tolman-based N-substituent steric effect* ($\theta_{N\text{-}sub}{}^{a}$) was calculated as 68.5 ° according to **Eq. 4.1** and **Figure 4.3**. Some of the important bond distances and angles were selected and are summarized in **Table 4.3**. All bond distances and angles are considered to be normal and fall within the range reported for similar complexes.[11,12,13,14,15] The N atom adapts an almost planar geometry with the two P atoms and the C atom attached to it in order to accommodate the steric bulk of the phenyl groups and the alkyl substituent (**Figure 4.5**).

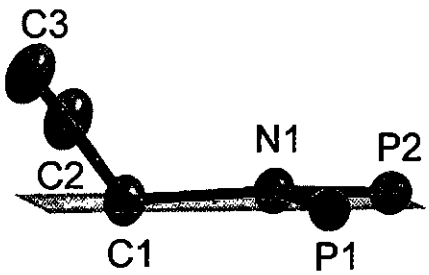


Figure 4.5: Partial structure view of PNP-*c*Prop (1) illustrating the plane constructed through C1/P1/P2.

The N atom is displaced by -0.098(2) Å from the C1/P1/P2 plane. Angles around the N atom range between 116.0(1) ° and 122.6(1) °, demonstrating the distorted tetrahedral geometry. The distorted tetrahedral geometry around the phosphorous atoms is illustrated by bond angles ranging between 100.4(1) ° and 105.3(1) °. This is due to the extra space needed by the lone electron pairs on the phosphorous atoms which force the three substituents, coordinated to the phosphorous atoms, to deviate from the ideal 109.5 ° tetrahedral angle by moving closer together.

Table 4.4: Selected torsion angles (°) for PNP-*c*Prop (1).

Atoms	Torsion angle
C1 – N1 – P1 – C11	58.6(1)
C1 – N1 – P1 – C21	−45.5(1)
C1 – N1 – P2 – C31	−121.2(1)
C1 – N1 – P2 – C41	131.8(1)

[11] F.A. Cotton, F.E. Kuhn, A. Yokochi, *Inorg. Chim. Acta,* 252 (1996) 251.
[12] Z. Fei, R. Scopeleti, P.J. Dyson, *J. Chem. Soc. Dalton Trans.*, (2003) 2772.
[13] N. Cloete, H.G. Visser, A. Roodt, J.T. Dixon, K. Blann, *Acta Cryst.*, E64 (2008) o480.
[14] N. Cloete, H.G. Visser, A. Roodt, W.F. Gabrielli, *Acta Cryst.*, E65 (2009) o3081.
[15] N. Cloete, H.G. Visser, A. Roodt, *Acta Cryst.*, E66 (2010) m51.

The C-N-P-C torsion angles (**Table 4.4**) indicate that the preferred conformation for this compound in the solid state is the C_S conformation (see **Figure 4.4** and **Table 4.1**).

There are no classical intermolecular hydrogen interactions. The crystal packing is stabilized by intermolecular C—H$\cdots\pi$ interactions resulting in a three-dimensional network as illustrated in **Figure 4.6** with distances, angles and symmetry operators summarized in **Table 4.5**.

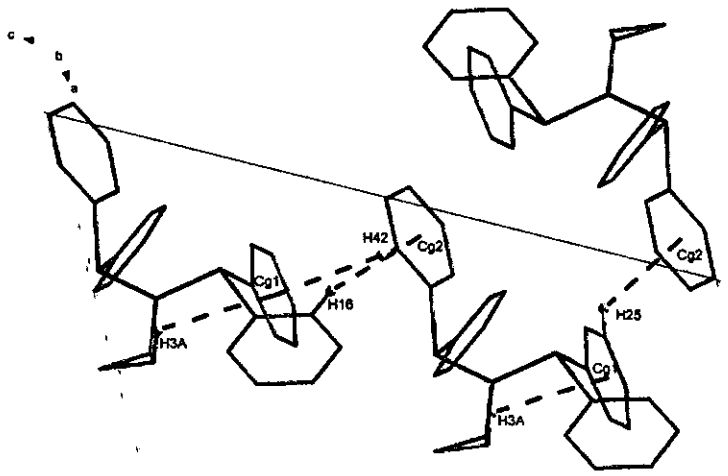


Figure 4.6: C—H$\cdots\pi$ interactions observed for PNP-*c*Prop (1), viewed along the b-axis. Hydrogen atoms, not taking part in the hydrogen interactions, are omitted for clarity. Cg1 and Cg2 are the centroids of the C21—C26 and C41—C46 rings, respectively.

Table 4.5: Hydrogen bonds for (PNP-*c*Prop) (Å and °). Cg1 and Cg2 are the centroids of the C21—C26 and C41—C46 rings, respectively.

D—H$\cdots$*A*	*D*—H	H$\cdots$*A*	*D*$\cdots$*A*	*D*—H$\cdots$*A*
C3—H3A$\cdots$Cg1	0.99	2.97	3.452(2)	111
C16—H16$\cdots$Cg2^{i}	0.95	2.77	3.664(2)	157
C25—H25$\cdots$Cg2^{ii}	0.95	2.98	3.750(2)	139
C42—H42$\cdots$Cg1^{iii}	0.95	2.85	3.466(2)	124

Symmetry codes: (i) x, $-y+1/2$, $z+1/2$; (ii) $-x+2$, $y+1/2$, $-z+3/2$; (iii) x, $-y+1/2$, $z-1/2$.

The molecules are packed in a head-to-tail fashion along the c-axis as illustrated in **Figure 4.7**.

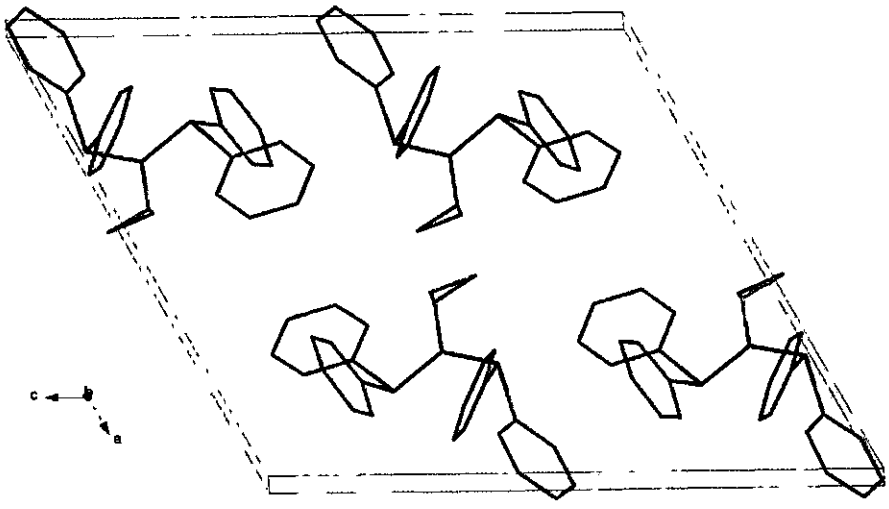


Figure 4.7: Crystal packing of PNP-*c*Prop (1) in the unit cell, viewed along the b-axis. Hydrogen atoms have been omitted for clarity.

4.4 *N,N-Bis*(diphenylphosphanyl)cyclobutanamine (2)

The title molecule, PNP-*c*But (2), has been synthesized as described in Paragraph 3.4.2. The compound crystallizes in a monoclinic crystal system in the $P2_1$ space group with two formula units per unit cell (Z = 2).[16] The asymmetric unit contains one complete molecule. The numbering scheme of the PNP-*c*But ligand is given in **Figure 4.8**.

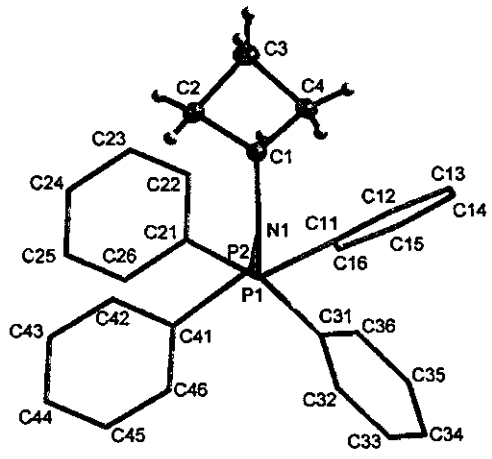


Figure 4.8: Molecular representation of PNP-*c*But (2). Hydrogen atoms of the phenyl rings have been omitted for clarity.

Table 4.6: Selected bond lengths (Å) and angles (°) for the crystal structure of PNP-*c*But (2).

Atoms	Bond length	Atoms	Bond angle
N1 – C1	1.478(2)	$\theta_{N\text{-}sub}$[a]	73.1
N1 – P1	1.714(2)	P1 – N1 – P2	123.5(1)
N1 – P2	1.719(2)	C1 – N1 – P1	120.8(1)
P1 – C11	1.837(2)	C1 – N1 – P2	115.2(1)
P1 – C21	1.840(2)	N1 – P1 – C11	102.2(1)
P2 – C31	1.838(2)	N1 – P1 – C21	105.3(1)
P2 – C41	1.827(2)	N1 – P2 – C31	108.1(1)
		N1 – P2 – C41	104.4(1)
		C11 – P1 – C21	100.0(1)
		C31 – P2 – C41	101.4(1)

[a] See **Eq. 4.1** and **Figure 4.3** for the calculation of $\theta_{N\text{-}sub}$.

[16] I. Engelbrecht, H.G. Visser, A. Roodt, *Acta Cryst.*, E67 (2011) o2041.

The *Effective Tolman-based N-substituent steric effect* ($\theta_{N\text{-}sub}$[a]) was calculated as 73.1 ° according to **Eq. 4.1** and **Figure 4.3**. Some of the important bond distances and angles were selected and are summarized in **Table 4.6** and all fall within the range reported for similar complexes.[11,12,13,14,15] The distance of the N atom from the C1/P1/P2 plane was calculated as -0.066(2) Å. The distorted tetrahedral around the N atom is further illustrated by bond angles ranging between 115.2(1) ° and 123.5(1) ° in order to accommodate the steric bulk of the substituents coordinated to this atom and the phenyl rings. The tetrahedral distortion of the phosphorous geometry is evident from the N-P-C and C-P-C angles that range between 102.2(1)-108.1(1) ° and 100.0(1) - 101.4(1) °, respectively.

Table 4.7: Selected torsion angles (°) for PNP-*c*But (2).

Atoms	Torsion Angle
C1 – N1 – P1 – C11	56.0(1)
C1 – N1 – P1 – C21	−48.1(2)
C1 – N1 – P2 – C31	−131.2(1)
C1 – N1 – P2 – C41	121.4(1)

The torsion angles (**Table 4.7**) indicate a C_S conformation for this molecule in the solid state (see **Figure 4.4** and **Table 4.1**).

The crystal packing is stabilized by a C—H···P intramolecular hydrogen bond (**Figure 4.9**) and intermolecular C—H···π interactions resulting in a three-dimensional network (**Figure 4.10**, **Table 4.8**).

UFS
BLOEMFONTEIN
BIBLIOTEEK - LIBRARY

1202 931 73

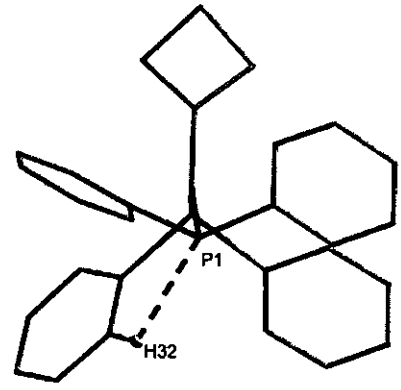


Figure 4.9: Hydrogen bond interaction for PNP-*c*But (2). Only the hydrogen atom with relevance to the hydrogen bond interaction is indicated.

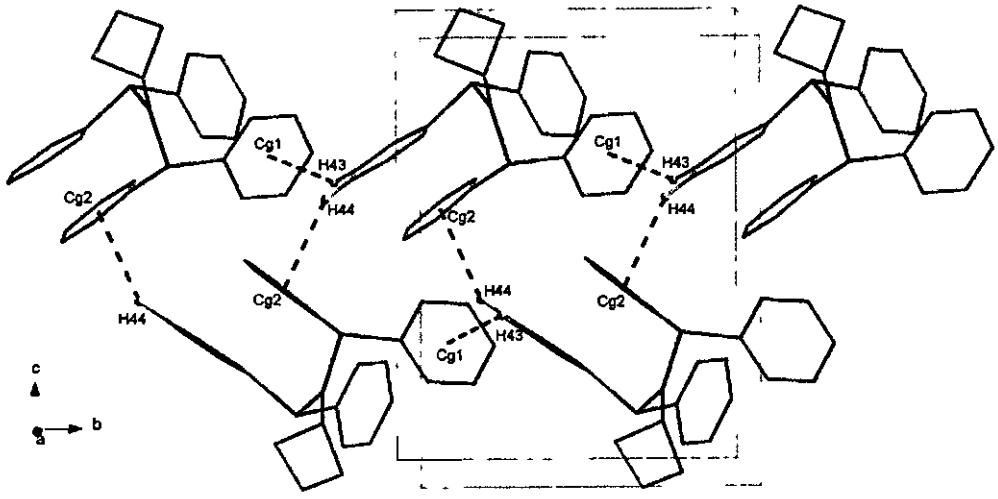


Figure 4.10: C—H···π interactions observed for PNP-*c*But (2), viewed along the a-axis forming a three-dimensional framework. Hydrogen atoms, not taking part in the hydrogen interactions, are omitted for clarity. Cg1 and Cg2 are the centroids of the C11—C16 and C21—C26 rings, respectively.

Table 4.8: Hydrogen bonds for PNP-*c*But (2) (Å and °). Cg1 and Cg2 are the centroids of the C11—C16 and C21—C26 rings, respectively.

D—H···*A*	*D*—H	H···*A*	*D*···*A*	*D*—H···*A*
C32—H32···P1	0.95	2.80	3.452 (2)	127
C43—H43···Cg1^{i}	0.95	2.87	3.686 (7)	144
C44—H44···Cg2^{ii}	0.95	2.81	3.614 (6)	143

Symmetry codes: (i) $x, y-1, z$; (ii) $-x+1, y-1/2, -z+1$.

The molecules are packed in a head-to-tail fashion along the b-axis (**Figure 4.11**).

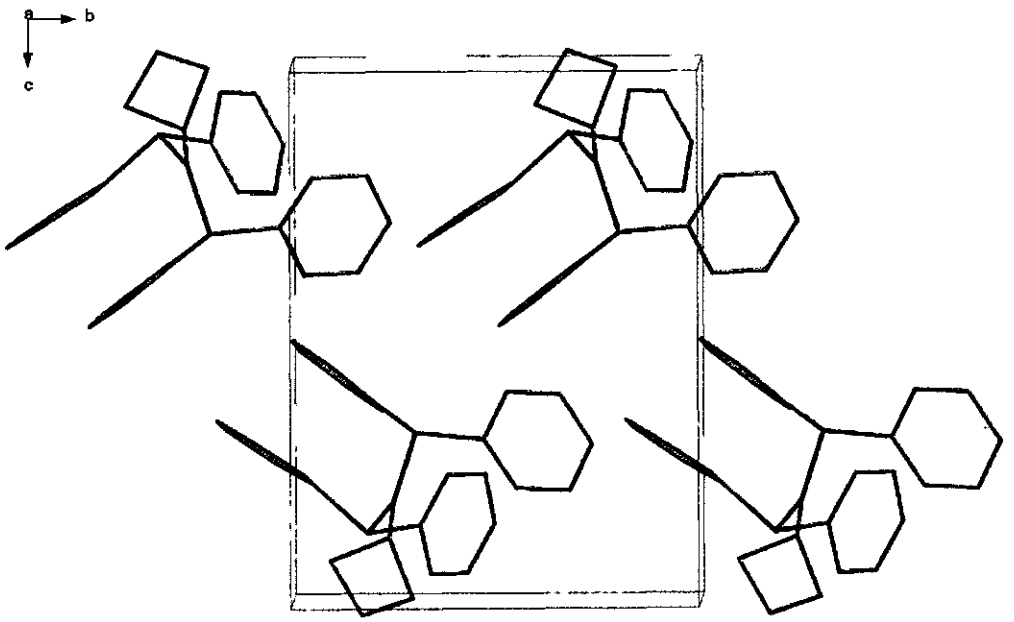


Figure 4.11: Crystal packing of PNP-*c*But (2) in the unit cell, viewed along the a-axis. Hydrogen atoms have been omitted for clarity.

4.5 *N,N-Bis*(diphenylphosphanyl)cyclopentylamine (3)

The title molecule, PNP-*c*Pent (3), has been synthesized as described in Paragraph 3.4.3. The compound crystallizes in a triclinic crystal system in the $P\bar{1}$ spacegroup with two formula units per unit cell (Z = 2). [17] The asymmetric unit contains one complete molecule. The numbering scheme of the PNP-*c*But ligand is given in **Figure 4.12**. One carbon atom (C4) in the cyclopentyl ring shows a 0.822(4):0.178(4) positional disorder.

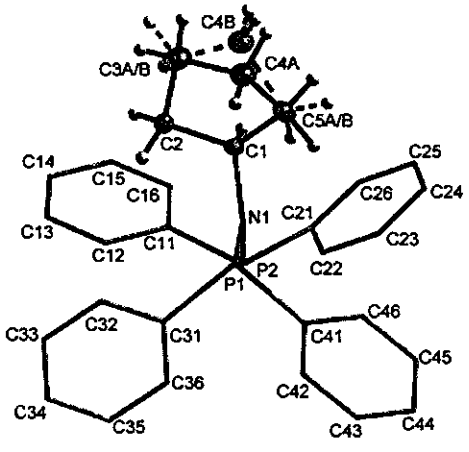


Figure 4.12: Molecular representation of PNP-*c*Pent (3). Major and minor disordered parts belonging together are numbered A and B respectively, with dashed lines denoting the minor disordered atoms. Hydrogen atoms of the phenyl rings have been omitted for clarity.

The major disordered component of the cyclopentane ring is in an envelope conformation [q_2 = 0.398(2) Å, φ = 78.5(3) °][18] with C3A as flap (**Figure 4.13 A**), which lies 0.590(2) Å from the plane of the remaining four atoms (C1/C2/C4A/C5A). The minor disordered component of the cyclopentane ring also has an envelope conformation [q_2= 0.379(6) Å, φ = 319.7(10) °] with C5B as flap (**Figure 4.13 B**), lying -0.528(2) Å from the plane of the other four atoms (C1/C2/C3B/C4B).

[17] I. Engelbrecht, H.G. Visser, A. Roodt, *Acta Cryst.*, E66 (2012) o3322.
[18] D. Cremer, J.A. Pople, *J. Am. Chem. Soc.*, 97 (1975) 1354.

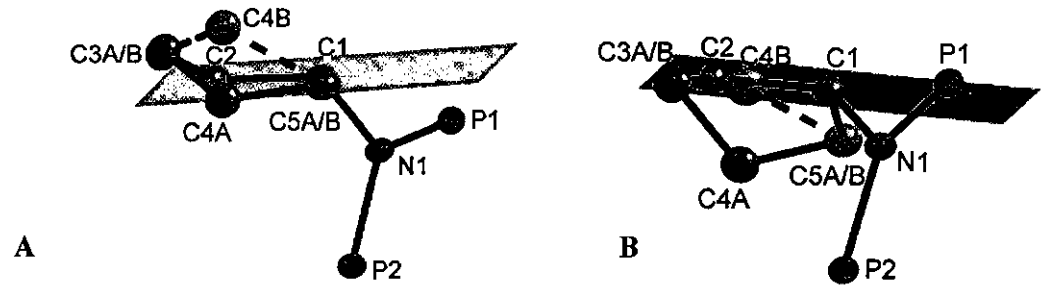


Figure 4.13: Partial structure views of PNP-*c*Pent (3) showing the envelope conformation of the cyclopentane ring with C3A as flap in **A**, representing the major disordered part of the cyclopentane ring and C5B as flap in **B**, for the minor disordered part. Planes are drawn through the remaining four atoms of the cyclopentane ring in each conformation.

Table 4.9: Selected bond lengths (Å) and angles (°) for the crystal structure of PNP-*c*Pent (3).

Atoms	Bond length	Atoms	Bond angle
N1 – C1	1.499(2)	P1 – N1 – P2	121.8(1)
N1 – P1	1.716(2)	C1 – N1 – P1	121.4(1)
N1 – P2	1.721(2)	C1 – N1 – P2	115.2(1)
P1 – C11	1.847(2)	N1 – P1 – C11	102.5(1)
P1 – C21	1.839(2)	N1 – P1 – C21	104.7(1)
P2 – C31	1.842(2)	N1 – P2 – C31	104.6(1)
P2 – C41	1.827(2)	N1 – P2 – C41	104.7(1)
		C11 – P1 – C21	101.7(1)
		C31 – P2 – C41	100.6(1)

[a] See **Eq. 4.1** and **Figure 4.3** for the calculation of $\theta_{N\text{-}sub}$. The $\theta_{N\text{-}sub}$ value was calculated as the average between the major and minor disordered cyclopentane ring.

The *Effective Tolman-based N-substituent steric effect* ($\theta_{N\text{-}sub}$) was calculated according to **Eq. 4.1** and **Figure 4.3**. The $\theta_{N\text{-}sub}$ value was calculated as the average between the major and minor disordered cyclopentane ring with a value of 79.3 °. Some of the important bond distances and angles were selected and are summarized in **Table 4.9**. All bond distances and angles are considered to be normal and fall within the range reported for similar complexes.[11,12,13,14,15] The central N atom is displaced by -0.120(2) Å from the plane defined by the remaining three atoms, C1/P1/P2. The distortion around the N atom is illustrated by angles between 115.2(1) ° and 121.8(1) °. Bond angles ranging from 100.6(1) ° to 104.7(1) ° shows the

distorted tetrahedral geometry around the phosphorous atoms with C-P-C angles being the most distorted.

Table 4.10: Selected torsion angles (°) for PNP-*c*Pent (3).

Atoms	Torsion Angle
C1 – N1 – P1 – C11	−45.8(2)
C1 – N1 – P1 – C21	60.0(2)
C1 – N1 – P2 – C31	119.3(1)
C1 – N1 – P2 – C41	−135.3(1)

Torsion angles (**Table 4.10**) indicate the molecule adopts a C_S conformation in the solid state (see **Figure 4.4** and **Table 4.1**).

Intramolecular C—H···P hydrogen bonds (**Figure 4.14**) exist as well as intra- and intermolecular C—H···π interactions which contribute to the supramolecular aggregation (**Figure 4.15**). The hydrogen bond interactions are summarized in **Table 4.11**.

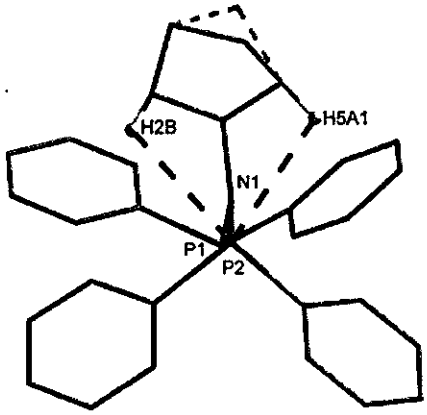


Figure 4.14: Hydrogen bond interactions for PNP-*c*Pent (3). Hydrogen atoms, not taking part in the hydrogen bonds, are omitted for clarity.

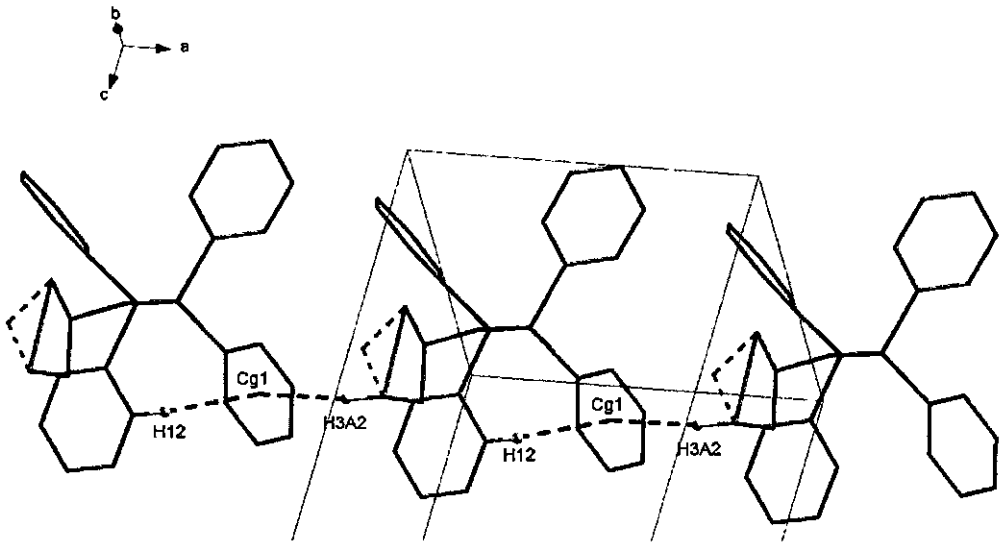


Figure 4.15: C—H···π interactions for PNP-*c*Pent (3), viewed along the b,c-plane showing the two-dimensional network. Hydrogen atoms, not taking part in the hydrogen interactions, are omitted for clarity. Cg1 is the centroid of the C11—C16 ring.

Table 4.11: Hydrogen bonds for (PNP-*c*Pent) (Å and °). Cg1 is the centroid of the C11—C16 ring.

D—H···*A*	*D*—H	H···*A*	*D*···*A*	*D*—H···*A*
C2—H2B···P2	0.99	2.82	3.269 (2)	108
C5A—H5A1···P2	0.99	2.82	3.202 (3)	104
C12—H12···Cg1	0.95	2.72	3.667 (2)	174
C3A—H3A2···Cg1^{i}	0.99	2.89	3.811 (2)	155

Symmetry codes: (i) $x+1, y, z$.

The molecules are packed in a head-to-tail fashion along the a-axis in **Figure 4.16**.

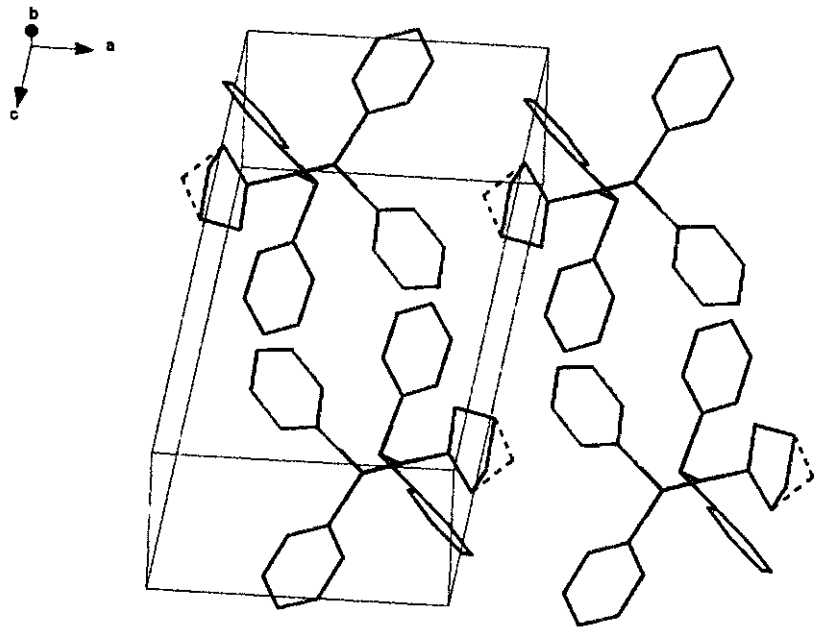


Figure 4.16: Crystal packing of PNP-*c*Pent (3) in the unit cell, viewed along the b-axis. Hydrogen atoms have been omitted for clarity.

4.6 Discussion

The crystal structures of three PNP-ligands containing various substituents bonded to the N atom were analyzed and discussed in this Chapter. The steric and electronic properties of these ligands were investigated to evaluate the effect induced when systematically changing the N-substituent from one ligand to another. Molecules **1**, **2** and **3** crystallize in a $P2_1/c$, $P2_1$ and $P\bar{1}$ spacegroup, respectively. Molecule **1** crystallizes with four independent molecules in the unit cell (Z = 4), while molecules **2** and **3** contains two molecules (Z = 2). The bond distances and angles for the three PNP-ligands are within normal range.[11,12,13,14,15] The crystal structure of all three ligands display molecular packing, stabilized by a variety of intramolecular hydrogen bonding and C—H$\cdots\pi$ interactions.

It was found that the largest effect in changing the substituents on the N atom from one ligand to another was the change in the P-N-P angle compared to the change in steric bulk of the N-substituent measured with the *Effective Tolman-based N-substituent steric parameter* ($\theta_{N\text{-}sub}$) (**Table 4.12**). The bulkiness of the N-substituent affects the P-N-P angle as well as the conformation of the ligand in the solid state. It is evident when comparing these PNP ligand structures that the P-N-P angle becomes smaller (PNP-Ethyl = 123.7(1) °, PNP-*i*Pent = 111.0 (1) °) with an increase in steric bulk ($\theta_{N\text{-}sub}$) (PNP-*i*Pent > PNP-Ethyl) of the substituent on the N atom. Therefore, the P-N-P bond angle is forced to close somewhat in order to accommodate the larger nitrogen-bound substituent.

Table 4.12: Comparison of P-N-P bond angles (°), $\theta_{N\text{-}sub}$ values and conformation adopted for various PNP-ligands.

Compound	P – N – P	$\theta_{N\text{-}sub}$	Conformation (See Figure 4.2)
PNP-Ethyl[a]	123.7(1)	62.9	C_S
PNP-*n*Pent[a]	123.4(1)	63.2	C_S
PNP-*c*Prop	122.6(1)	68.5	C_S
PNP-*c*But	123.5(1)	73.1	C_S
PNP-*c*Pent	121.8(1)	79.3	C_S
PNP-*i*Prop[b]	122.8(3)	80.3	C_S
PNP-*c*Hex[a]	119.0(1)	81.3	C_S
PNP-Dimprop[c]	117.9(1)	88.5	C_S
PNP-Phen[d]	113.2(2)	100.4	C_{2V}
PNP-*i*Pent[a]	111.0(1)	-	C_{2V}

[a] See Ref 19. [b] See Ref 2. [c] See Ref 13. [d] See Ref 12.

Within this ligand range, there also seems to be a definite switch in conformation, from C_S to C_{2V}, with substantially large $\theta_{N\text{-}sub}$, in effect causing a very small P-N-P bond angle. PNP-Phen and PNP-*i*Pent adopts a C_{2V} conformation and has significantly smaller P-N-P angles, 113.2(2) ° and 111.0(1) °, compared to the other PNP-ligands with a C_S conformation.

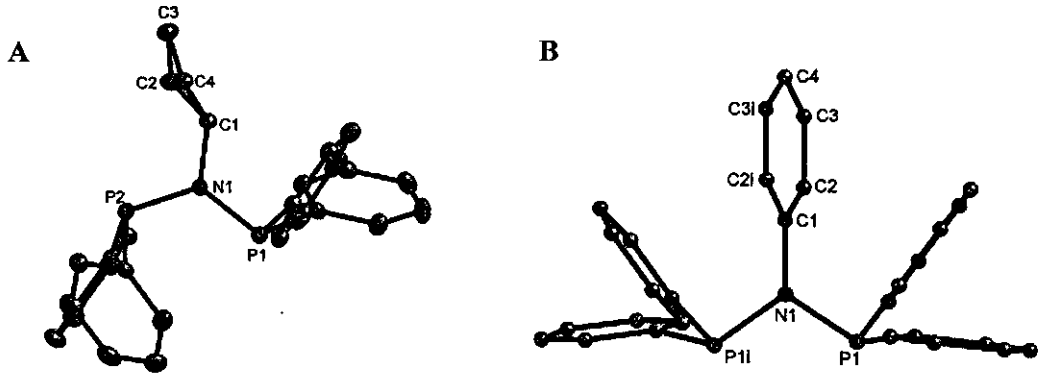


Figure 4.17: Graphical representation of the C_S conformer for PNP-*c*But (2) (**A**) and the C_{2V} conformer for PNP-Phen[12] (**B**).

[19] N.Cloete, PhD thesis, University of the Free State, 2009.

Selected bond lengths of the various C_S conformations of the non-coordinated PNP-ligands (see **Table 4.13**) indicate that the P-N bond lengths increase as the steric bulk of the alkyl moieties increase. This is evident when the P1-N1 and P2-N1 bonds lengths for PNP-Ethyl (1.712(1) ° and 1.713(1) °) and PNP-Dimprop (1.721(2) ° and 1.727(2) °) are compared. The same trend is observed for the C1-N1 bonds for the various free PNP-ligands. The bond lengths increases systematically in order to accommodate the larger alkyl groups and to prevent substantial steric crowding.

Table 4.13: Comparison of selected bond lengths (Å) for various PNP-ligands.

Compound	C1 – N1	P1 – N1	P2 – N1
PNP-Ethyl[a]	1.485(2)	1.712(1)	1.713(1)
PNP-*n*Pent[a]	1.482(1)	1.713(1)	1.712(1)
PNP-*c*Prop	1.452(2)	1.730(1)	1.721(1)
PNP-*c*But	1.478(2)	1.714(2)	1.719(2)
PNP-*c*Pent	1.499(2)	1.716(2)	1.721(2)
PNP-*i*Prop[b]	1.511(8)	1.706(4)	1.711(4)
PNP-*c*Hex[a]	1.502(6)	1.758(4)	1.686(5)
PNP-Dimprop[c]	1.515(2)	1.721(2)	1.727(2)

[a] See Ref 19. [b] See Ref 2. [c] See Ref 13.

It has been shown by this crystallographic study of the free bis(diphenylphosphino)amine ligands, that the P-N-P bond angle, selected bond lengths and the conformation of the PNP compounds are affected by the steric bulk of the nitrogen-coordinated substituent.

The synthetic procedure whereby the PNP-ligands were coordinated to Pt(II) and Pd(II) metal centers were discussed in Chapter 3. The various [M(PNP-alkyl)$_2$] (M = Pt, Pd) crystal structures obtained from the synthesis will be discussed in the following Chapter.

5 Single crystal X-ray crystallographic study of Pt(II)-PNP and Pd(II)-PNP complexes

In this chapter...

The crystallographic data of a series of [Pt(PNP-alkyl)$_2$] and [Pd(PNP-alkyl)$_2$] complexes were collected and are discussed in detail. Evaluation of different steric and electronic properties of the coordinated ligands can influence catalyst preparation during the hydroformylation of olefins.

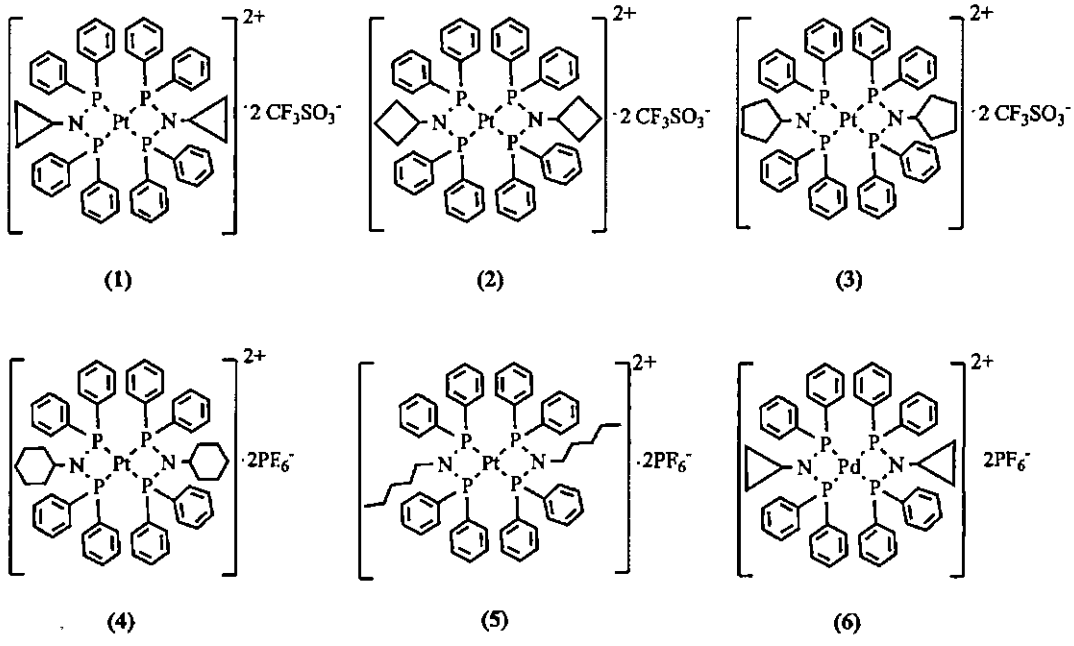
5.1 Introduction

A range of different PNP-ligands were synthesized and coordinated to Pt(II) and Pd(II) to serve as models for the real Rh(I) and Ir(I) pre-catalysts systems for use in olefin hydroformylation. The reason for using Pt(II) and Pd(II) is solely an instinctive one since these complexes are notoriously easy to synthesize and makes it possible to evaluate the solid state characteristics of the coordinated PNP-ligand, given the difficulty of isolating unstable Rh and Ir complexes. To date, less than 20 structures each for Rh- and Ir-PNP complexes have been reported in literature.[1]

The coordination chemistry of these PNP-ligands to the more stable metal centres of Pt(II) and Pd(II) is investigated to systematically evaluate the steric and electronic properties and the effects induced by the PNP-ligands when changing the N-substituent from one ligand to another. The structural behaviour of the free ligand as well as the coordinated complex can then be used to evaluate the structural factors that govern certain catalyst behaviour, such as activity and selectivity, during the hydroformylation process.

A number of square-planar complexes of Pt(II) and Pd(II) coordinated with various diphosphinoamine ligands have been synthesized and are represented in **Scheme 5.1**. The crystallographic data of the structures are summarized in **Table 5.1** and **Table 5.2**.

[1] *Cambridge Structural Database* (CSD), Version 5.33, Nov 2011 update. F.H. Allen, *Acta Cryst.*, B58 (2002) 380.



Scheme 5.1: Schematic representation of the crystal structures represented in this Chapter: (1) $[Pt(PNP\text{-}cProp)_2](CF_3SO_3)_2$; (2) $[Pt(PNP\text{-}cBut)_2](CF_3SO_3)_2$; (3) $[Pt(PNP\text{-}cPent)_2](CF_3SO_3)_2$; (4) $[Pt(PNP\text{-}cHex)_2](PF_6)_2$; (5) $[Pt(PNP\text{-}nPent)_2](PF_6)_2$; (6) $[Pd(PNP\text{-}cProp)_2](PF_6)_2$.

5.2 Experimental

The intensity data were collected on a Bruker X8 Apex II 4K Kappa CCD diffractometer equipped with graphite monochromated Mo *K*α radiation, with a wavelength of 0.71073 Å, and with ω-and φ-scans at 100 K. All the cell refinements were performed with SAINT-Plus[2] while the data reduction was done with SAINT-Plus and XPREP2. The absorption corrections were obtained by the use of the multi-scan technique and the SADABS[3] software package. All the structures were solved with the use of the SIR-97[4] package, refinement was done with SHELXL-97[5] and WinGX[6] and the molecular graphics were completed with DIAMOND[7]. Unless otherwise stated, all the structures are shown with thermal ellipsoids drawn at a 50% probability level and all non-hydrogen atoms were anisotropically refined. Methyl, methylene, methine and aromatic hydrogen atoms were placed in geometrically idealized positions, C-H = 0.95 to 1.00 Å, and constrained to ride on their parent atoms, $U_{iso}(H) = 1.5\ U_{eq}(C)$ and $1.2\ U_{eq}(C)$ respectively. For the numbering of the phenyl rings, the first digit refers to the ring number while the second digit refers to the carbon atom in the ring.

A summary of the general crystal data and refinement is given in **Table 5.1** and **Table 5.2**, for all $[M(PNP\text{-}alkyl)_2]$ (M = Pt, Pd) complexes. All the atomic coordinates, anisotropic displacement parameters, bond distances, angles, torsion angles and hydrogen coordinates, of all the crystal reported in this Chapter, are given in the supplementary data (Appendix A).

[2] Bruker, *SAINT-Plus*, Version 7.12 (including XPREP), Bruker AXS Inc., Madison, Wisconsin, USA, 2004.
[3] Bruker, *SADABS*, Version 2004/1, Bruker AXS Inc., Madison, Wisconsin, USA, 1998.
[4] A. Altomare, M.C. Burla, M. Camalli, G.L. Cascarano, C. Giacovazzo, A. Guagliardi, A.G.G. Moliterni, G. Polidori, R. Spagna, *J. Appl. Cryst.*, 32 (1999) 837.
[5] Sheldrick, G.M., *SHELXL97*, Program for the refinement of crystal structures, University of Göttingen, Germany, 1997.
[6] L.J. Farrugia, *J. Appl. Cryst.*, 32 (1999) 837.
[7] K. Brandenburg, H. Putz, *DIAMOND*, Release 3.0c, Crystal Impact GbR, Bonn, Germany, 2006.

Table 5.1: Crystallographic data of [Pt(PNP-*c*Prop)$_2$] (1), [Pt(PNP-*c*But)$_2$] (2) and [Pt(PNP-*c*Pent)$_2$] (3).

Crystallographic data	**[Pt(PNP-*c*Prop)$_2$] (1)**	**[Pt(PNP-*c*But)$_2$] (2)**	**[Pt(PNP-*c*Pent)$_2$] (3)**
Empirical formula	$C_{54}H_{50}N_2P_4Pt$ $\cdot 2(CF_3SO_3)$	$C_{56}H_{54}N_2P_4Pt$ $\cdot 2(CF_3SO_3)$	$C_{58}H_{58}N_2P_4Pt$ $\cdot 2(CF_3SO_3)$
Formula weight (g mol^{-1})	1368.10	1420.17	1400.18
Temperature (K)	100(2)	100(2)	100(2)
Crystal system	Monoclinic	Monoclinic	Monoclinic
Space group	$P2_1/n$	$P2_1/c$	$P2_1/c$
Unit cell dimensions			
a (Å)	11.828(4)	9.566(4)	10.041(5)
b (Å)	16.327(4)	14.347(5)	13.662(4)
c (Å)	14.380(5)	20.034(5)	20.928(5)
α (°)	90.000	90.000	90.000
β (°)	102.23(7)	91.109(5)	93.916(5)
γ (°)	90.000	90.000	90.000
Volume (Å^3)	2714(19)	2749.0(19)	2864.2(19)
Z	2	2	2
ρ_{calc} (g cm^{-3})	1.674	1.716	1.624
Crystal colour	Colourless	Colourless	Colourless
Crystal morphology	Cuboid	Cuboid	Cuboid
Crystal size (mm^3)	0.09 x 0.09 x 0.05	0.22 × 0.15 × 0.12	0.19 x 0.18 x 0.16
μ (mm^{-1})	2.855	2.82	2.707
F(000)	1368	1376	1408
θ range (°)	2.38-25.00	2.5-27.8	2.03-28.00
Index ranges	$-14 \le h \le 14$ $-19 \le k \le 19$ $-16 \le l \le 17$	$-12 \le h \le 12$ $-18 \le k \le 18$ $-26 \le l \le 26$	$-12 \le h \le 13$ $-18 \le k \le 18$ $-27 \le l \le 27$
Reflections collected	26503	34712	44370
Unique reflections	4773	6639	6894
Reflections with $I > 2\sigma(I)$	3209	5645	4869
R_{int}	0.0905	0.0446	0.101
Completeness to theta (°, %)	25.00, 99.9	28.00, 99.9	28.0, 99.8
Data / restraints / parameters	4773 / 5 / 343	6639 / 46 / 460	6894 / 7 / 398
Goodness-of-fit on F^2	1.054	1.287	1.023
R [$I > 2\sigma(I)$]	$R_1 = 0.0754$ $wR_2 = 0.1701$	$R_1 = 0.0634$ $wR_2 = 0.1217$	$R_1 = 0.0395$ $wR_2 = 0.0813$
R (all data)	$R_1 = 0.1156$ $wR_2 = 0.1942$	$R_1 = 0.0752$ $wR_2 = 0.1268$	$R_1 = 0.0695$ $wR_2 = 0.0929$
ρ_{max}, ρ_{min} (e.Å^{-3})	3.729, -1.484	1.756, -1.321	1.392, -1.417

Table 5.2: Crystallographic data of [Pt(PNP-*c*Hex)$_2$] (4) and [Pt(PNP-*n*Pent)$_2$] (5) and [Pd(PNP-cProp)$_2$] (6)

Crystallographic data	[Pt(PNP-*c*Hex)$_2$] (4)	[Pt(PNP-*n*Pent)$_2$] (5)	[Pd(PNP-*c*Prop)$_2$] (6)
Empirical formula	$C_{60}H_{62}N_2P_4Pt \cdot 2(PF_6) \cdot 2(CH_2Cl_2)$	$C_{58}H_{62}N_2P_4Pt \cdot 2(PF_6) \cdot 2(CH_2Cl_2)$	$C_{54}H_{50}N_2P_4Pd \cdot 2(PF_6)$
Formula weight (g mol^{-1})	1588.38	1565.85	1245.16
Temperature (K)	100(2)	100(2)	100(2)
Crystal system	Monoclinic	Monoclinic	Monoclinic
Space group	$P2_1/c$	Cc	$C2/m$
Unit cell dimensions			
a (Å)	13.350(5)	11.3876(10)	15.854(4)
b (Å)	18.764(4)	24.283(3)	21.798(5)
c (Å)	15.248(5)	23.102(2)	16.150(4)
α (°)	90.000	90.000	90.000
β (°)	123.333(5)	97.669(4)	90.115(5)
γ (°)	90.000	90.000	90.000
Volume (Å^3)	3191.3(18)	6331.1(11)	5581(3)
Z	2	4	2
ρ_{calc} (g cm^{-3})	1.653	1.643	1.482
Crystal colour	Colourless	Colourless	Yellow
Crystal morphology	Cuboid	Cuboid	Plate
Crystal size (mm^3)	0.32 × 0.29 × 0.14	0.26 x 0.19 x 0.13	0.19 x 0.12 x 0.05
μ (mm^{-1})	2.59	2.61	0.583
F(000)	1589	3136	2520.0
θ range (°)	2.8-28.2	4.16-28.00	1.87-28.18
Index ranges	$-13 \le h \le 17$ $-25 \le k \le 24$ $-20 \le l \le 20$	$-13 \le h \le 15$ $-32 \le k \le 32$ $-30 \le l \le 30$	$-21 \le h \le 21$ $-28 \le k \le 28$ $-21 \le l \le 21$
Reflections collected	57085	47664	44918
Unique reflections	7899	14210	6904
Reflections with $I > 2\sigma(I)$	6367	13180	4023
R_{int}	0.042	0.0300	0.1329
Completeness to theta (°, %)	28.4, 99.1	28.00, 99.1	28.18, 98.1
Data / restraints / parameters	7899 / 18 / 503	14210 / 2 / 767	6904 / 0 / 351
Goodness-of-fit on F^2	1.03	0.808	1.071
R [$I > 2\sigma(I)$]	$R_1 = 0.0271$ $wR_2 = 0.0646$	$R_1 = 0.0244$ $wR_2 = 0.0538$	$R_1 = 0.1016$ $wR_2 = 0.2550$
R (all data)	$R_1 = 0.0383$ $wR_2 = 0.0697$	$R_1 = 0.0285$ $wR_2 = 0.0557$	$R_1 = 0.1653$ $wR_2 = 0.3260$
ρ_{max}, ρ_{min} (e.Å^{-3})	0.72, -0.99	1.042, -1.115	5.325, -1.296

5.3 Bis[*N*,*N*-bis(diphenylphosphanyl)cyclopropanamine-κ^2P,P'] platinum(II) bis(trifluoromethanesulfonate)

The complex, [Pt(PNP-*c*Prop)$_2$] (**1**), has been synthesized as described in Paragraph 3.5.1. The complex crystallizes in a monoclinic crystal system in the $P2_1/n$ space group with two formula units per unit cell (Z = 2). The Pt(II) atom, situated on an inversion centre, is coordinated by two PNP-*c*Prop bidentate ligands. The asymmetric unit contains one half of the complex molecule and a trifluoromethanesulfonate anion. The other half of the complex molecule and the second anion are generated through symmetry. Unstable bond lengths and angles were restrained within the anion to stabilize the refinement. The numbering scheme of the title complex is given in **Figure 5.1**.

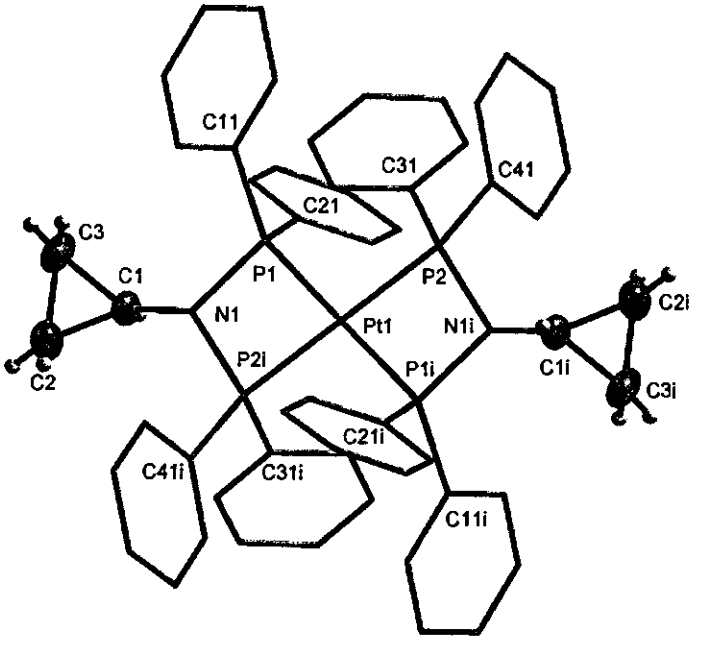


Figure 5.1: Molecular representation of [Pt(PNP-*c*Prop)$_2$] (1). Atoms generated through symmetry are represented by ending with 'i'. Hydrogen atoms of the phenyl rings and trifluoromethanesulfonate ions have been omitted for clarity. Symmetry transformations used to generate equivalent atoms: 1-x, -y, 1-z.

Table 5.3: Selected bond lengths (Å) and angles (°) for the crystal structure of [Pt(PNP-*c*Prop)$_2$] (1).

Atoms	Bond length	Atoms	Bond angle
Pt – P1	2.277(3)	P1 – Pt – P2	71.5(1)
Pt – P2	2.290(3)	P1 – N1 – P2	101.2(5)
N1 – C1	1.440(16)	C1 – N1 – P1	123.8(9)
N1 – P1	1.729(11)	C1 – N1 – P2	124.6(9)
N1 – P2	1.724(10)	N1 – P1 – C11	114.2(6)
P1 – C11	1.798(13)	N1 – P1 – C21	109.7(6)
P1 – C21	1.805(15)	N1 – P2 – C31	113.7(5)
P2 – C31	1.787(11)	N1 – P2 – C41	112.3(6)
P2 – C41	1.801(12)	C11 – P1 – C21	106.4(7)
		C31 – P2 – C41	107.7(5)

Some of the important bond distances and angles were selected and are summarized in **Table 5.3**. The bond distances and angles are all within range of similar complexes.[8,9,10,11,12] The *Effective Tolman-based N-substituent steric effect* ($\theta_{N\text{-}sub}{}^{a}$) was calculated as 69.5 ° (see Chapter 4, **Eq. 4.1** and **Figure 4.3**).

The P1-Pt-P2 angle of 71.5(1) ° illustrates the highly distorted square-planar geometry around the Pt(II) atom, deviating significantly from the ideal 90 °. The reported P1-Pt-P2 small bite angle forces the P1-N1-P2 angle to 101.2 (5) ° which illustrates the distorted tetrahedral geometry of the N atom. The N atom deviates with -0.30(1) Å from the C1/P1/P2i plane, showing that the N atom adopts an almost planar geometry with these atoms to accommodate the steric bulk of the phenyl groups and the alkyl group of the ligand (**Figure 5.2**). Bond angles ranging from 106.4(7) to 114.2(6) ° shows the distorted tetrahedral geometry around the phosphorous atoms.

[8] D.G. Farrar, C.S. Browning, *J. Chem. Soc. Dalton Trans.*, (1995) 521.
[9] P.J. Dyson, Z. Fei, R. Scopelliti, *Eur. J. Inorg. Chem.*, (2004) 530.
[10] N. Cloete, H.G. Visser, A. Roodt, *Acta Cryst.*, E66 (2010) m51.
[11] N. Cloete, H.G. Visser, A. Roodt, J.T. Dixon, K. Blann, K. *Acta Cryst.*, E64 (2008) o480.
[12] N. Cloete, H.G. Visser, A. Roodt, W.F. Gabrielli, *Acta Cryst.*, E65 (2009) o3081.

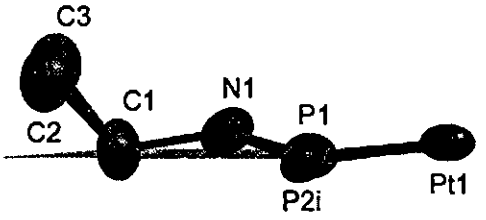


Figure 5.2: Partial structure view of [Pt(PNP-*c*Prop)$_2$] (1) illustrating the plane constructed through C1/P1/P2i.

Inter- and intramolecular C—H···F, C—H···π and C—H···O interactions contribute to the supramolecular aggregation illustrated in **Figure 5.3**. The hydrogen bond interactions are summarized in **Table 5.4**.

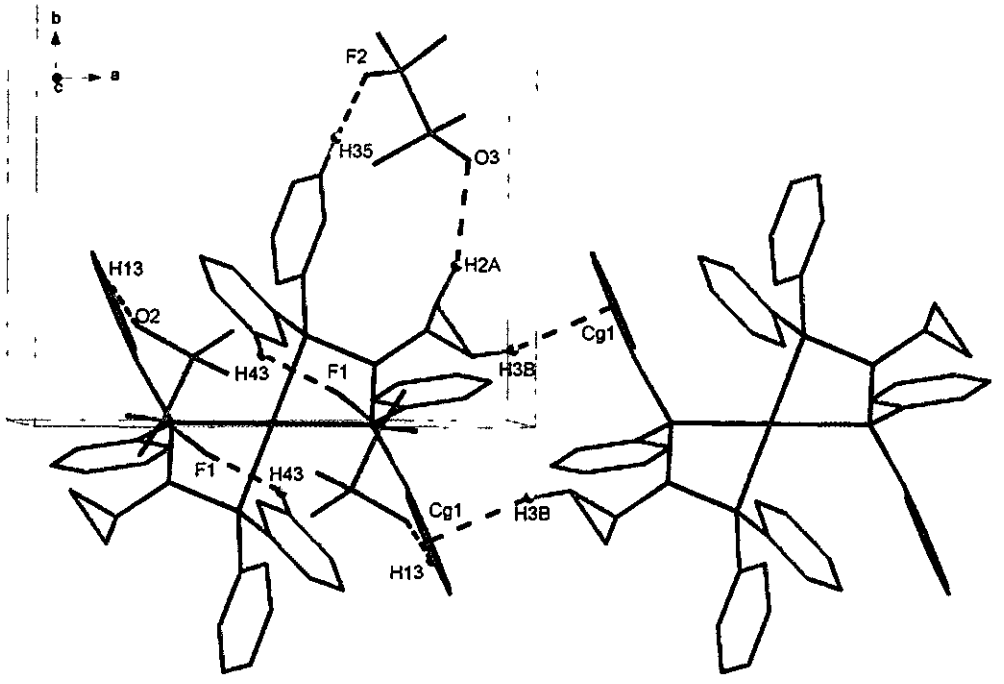


Figure 5.3: Hydrogen bonds observed for [Pt(PNP-*c*Prop)$_2$] (1), viewed along the c-axis. Hydrogen atoms, not taking part in the hydrogen bonds, are omitted for clarity. Cg1 is the centroid of the C11—C16 ring.

Table 5.4: Hydrogen bonds for [Pt(PNP-*c*Prop)$_2$] (1), (Å and °). Cg1 is the centroid of the C11—C16 ring.

D—H···*A*	*D*—H	H···*A*	*D*···*A*	*D*—H···*A*
C3—H3B···Cg1^{ii}	0.95	2.52	3.471(16)	160
C2—H2A···O3^{iii}	0.95	2.50	3.41(3)	152
C13—H13···O2	0.99	2.42	3.23(2)	142
C35—H35···F2^{iv}	0.99	2.48	3.293(19)	143
C43—H43···F1^{i}	0.99	2.37	3.197(18)	145

Symmetry codes: (ii) $-x, -y, -z+1$; (iii) $-x+1/2, y-1/2, -z+3/2$; (iv) $x+1/2, -y+1/2, z-1/2$; (i) $-x+1, -y, -z+1$.

The metal complex packs in a head-to-tail fashion along the a-axis, as illustrated in **Figure 5.4.**

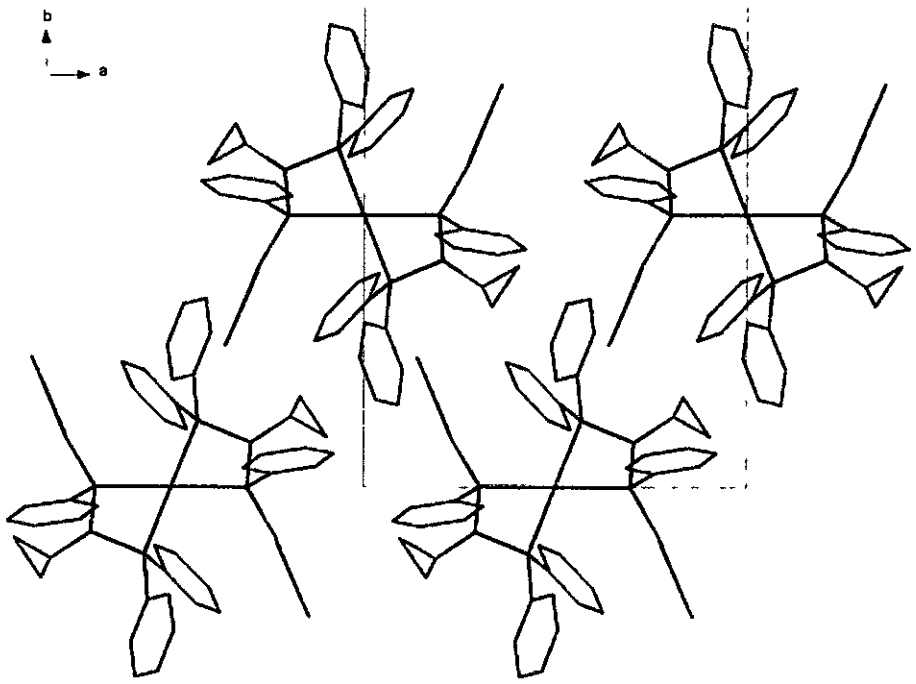


Figure 5.4: Crystal packing of [Pt(PNP-*c*Prop)$_2$] (1) in the unit cell, viewed along the c-axis. Hydrogen atoms and anion molecules omitted for clarity.

5.4 Bis[*N*,*N*-bis(diphenylphosphanyl)cyclobutanamine-κ^2P,P'] platinum(II) bis(trifluoromethanesulfonate)

The complex, [Pt(PNP-*c*But)$_2$] (**2**), has been synthesized as described in Paragraph 3.5.2. The platinum complex crystallizes in a monoclinic crystal system in the $P2_1/c$ space group with two formula units per unit cell ($Z = 2$). The asymmetric unit consists of one half of the platinum complex and a trifluoromethanesulfonate anion. The Pt(II) atom is situated on an inversion centre and coordinated by two PNP-*c*But bidentate ligands. The other half of the complex molecule and the second anion are generated through symmetry. The numbering scheme of the title complex is shown in **Figure 5.5**.

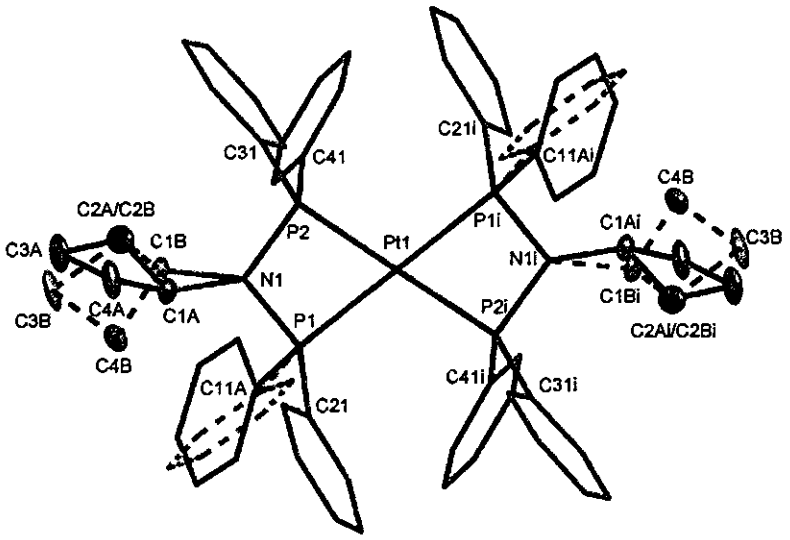


Figure 5.5: Molecular representation of [Pt(PNP-*c*But)$_2$] (2). Atoms generated through symmetry are represented by ending with 'i'. Major and minor disordered parts belonging together are numbered A and B respectively, with dashed lines denoting the minor disordered atoms. Hydrogen atoms and trifluoromethanesulfonate ions have been omitted for clarity. Symmetry transformations used to generate equivalent atoms: 2-x, -y, 2-z.

The cyclobutane ring, bonded to the nitrogen atom display a 0.631(15):0.369(15) conformational disorder and the C11—C16 phenyl ring, bonded to P1 a 0.824(7):0.176(7) positional disorder. The anion molecule displays a 0.596(10):0.404(10) positional disorder. The only way to secure a stable refinement with regards to the disordered anion was by adopting some atoms as isotropic. Also, a series of EADP constraints were applied in which the same isotropic or

anisotropic displacement parameters (Uij) are utilized for neighbouring atoms. Unstable bond lengths and angles were therefore also restrained within the disordered anion.

A typical bonding pattern is observed for the cyclobutane ring system bonded to N1, with average bond distances of 1.495 (9) Å for the major disordered part of the crystal structure and 1.624(2) Å for the minor disorder part. The cyclobutane ring adopts a CR-form (**Figure 5.6**) with average absolute torsion angles of 20.59 (6) Å and 31.11 (9) Å for the major- and minor disordered parts of the crystal structure, respectively.[13]

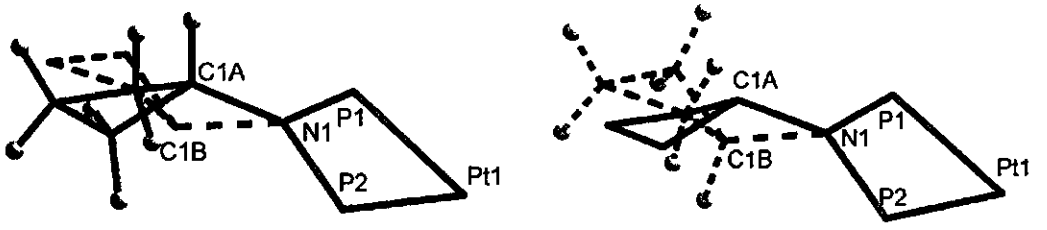


Figure 5.6: Partial structure view of [Pt(PNP-cBut)$_2$] (2) from different viewing angles indicating the conformation for the cyclobutane ring with hydrogen atom positions. Major and minor disordered parts belonging together are numbered A and B respectively, with dashed lines denoting the minor disordered atoms.

Some of the important bond distances and angles were selected and are summarized in **Table 5.5**. Bond distances and angles are all within range of similar complexes.[8,9,10,11,12] The *Effective Tolman-based N-substituent steric effect* ($\theta_{N\text{-}sub}{}^{a}$) was calculated as 71.1 ° (see Chapter 4, **Eq. 4.1** and **Figure 4.3**). The $\theta_{N\text{-}sub}$ value was calculated as the average between the major and minor disordered cyclobutane ring.

[13] D. Cremer, J.A. Pople, *J. Am. Chem. Soc.*, 97 (1975) 1354.

Table 5.5: Selected bond lengths (Å) and angles (°) for the crystal structure of [Pt(PNP-*c*But)$_2$] (2).

Atoms	Bond length	Atoms	Bond angle
Pt – P1	2.305(2)	P1 – Pt – P2	70.23(6)
Pt – P2	2.300(2)	P1 – N1 – P2	102.2(3)
N1 – C1A	1.456(13)	C11A – N1 – P1	122.3(6)
N1 – C1B	1.56(2)	C11B – N1 – P1	128.4(9)
N1 – P1	1.700(6)	C11A – N1 – P2	135.1(7)
N1 – P2	1.703(6)	C11B – N1 – P2	119.0(1)
P1 – C11A	1.824(8)	N1 – P1 – C11A	106.8(4)
P1 – C11B	1.632(18)	N1 – P1 – C11B	110.0(1)
P1 – C21	1.800(7)	N1 – P1 – C21	110.5(4)
P2 – C31	1.797(7)	N1 – P2 – C31	110.5(3)
P2 – C41	1.795(7)	N1 – P2 – C41	110.4(3)
		C11A – P1 – C21	109.1(4)
		C11B – P1 – C21	102.0(1)
		C31 – P2 – C41	107.1(3)

The distorted square-planar geometry around the Pt(II) atom is evident from the P1-Pt-P2 angle of 70.23(6) °, which deviates significantly from the ideal 90 °. The N atom adopts an almost planar geometry with the C atom attached to it and the two P-atoms to accommodate the steric bulk of the phenyl groups and the alkyl group of the ligand. The N atom is displaced by 0.056(5) and 0.313(5) Å from the C1A/P1/P2 and C1B/P1/P2 planes, respectively. The strain in the complex is further illustrated by angles around the N atom ranging between 102.2(3) and 135.1(7), showing the distorted tetrahedral geometry around the N atom. Bond angles ranging from 102.0(1) to 110.5(4) ° shows the distorted tetrahedral geometry around the phosphorous atoms.

The crystal packing is stabilized by intermolecular C—H$\cdots\pi$ interactions resulting in a three-dimensional network (**Figure 5.7**), summarized in **Table 5.6**.

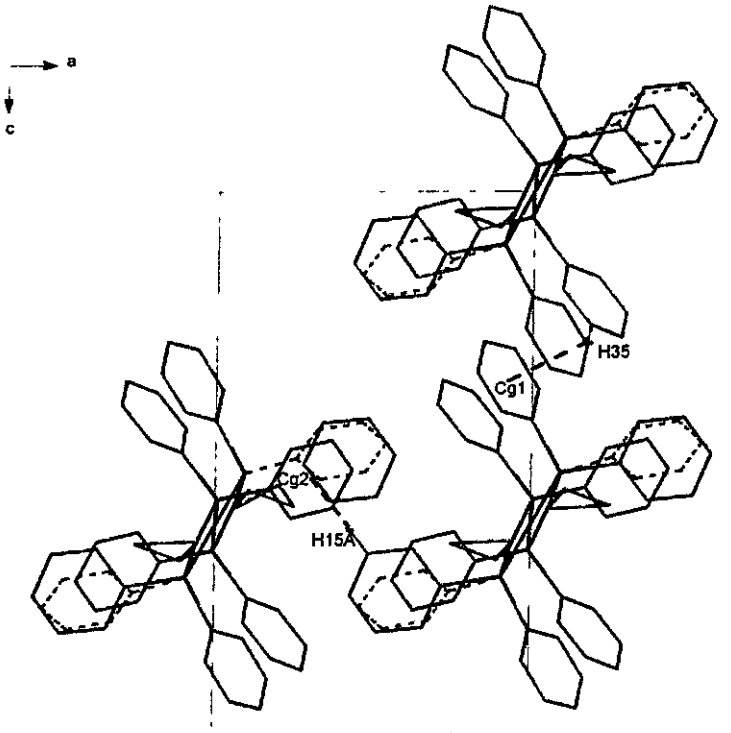


Figure 5.7: C—H···π interactions observed for [Pt(PNP-*c*But)$_2$] (2), viewed along the b-axis forming a three-dimensional framework. Hydrogen atoms, not taking part in the hydrogen interactions, are omitted for clarity. Cg1 and Cg2 are the centroids of the C21—C26 and C41—C46 rings, respectively.

Table 5.6: Hydrogen bonds for [Pt(PNP-*c*But)$_2$] (2) (Å and °). Cg1 and Cg2 are the centroids of the C21—C26 and C41—C46 rings, respectively.

D—H···*A*	*D*—H	H···*A*	*D*···*A*	*D*—H···*A*
C15*A*—H15*A*···Cg2^{ii}	0.93	2.72	3.444(9)	135
C35—H35···Cg1^{iii}	0.93	2.89	3.499(10)	124

Symmetry codes: (ii) $x+1, y, z$; (iii) $x, -y+1/2, z+1/2$.

The metal complex packs in a head-to-tail fashion along the a-axis and is illustrated in **Figure 5.8.**

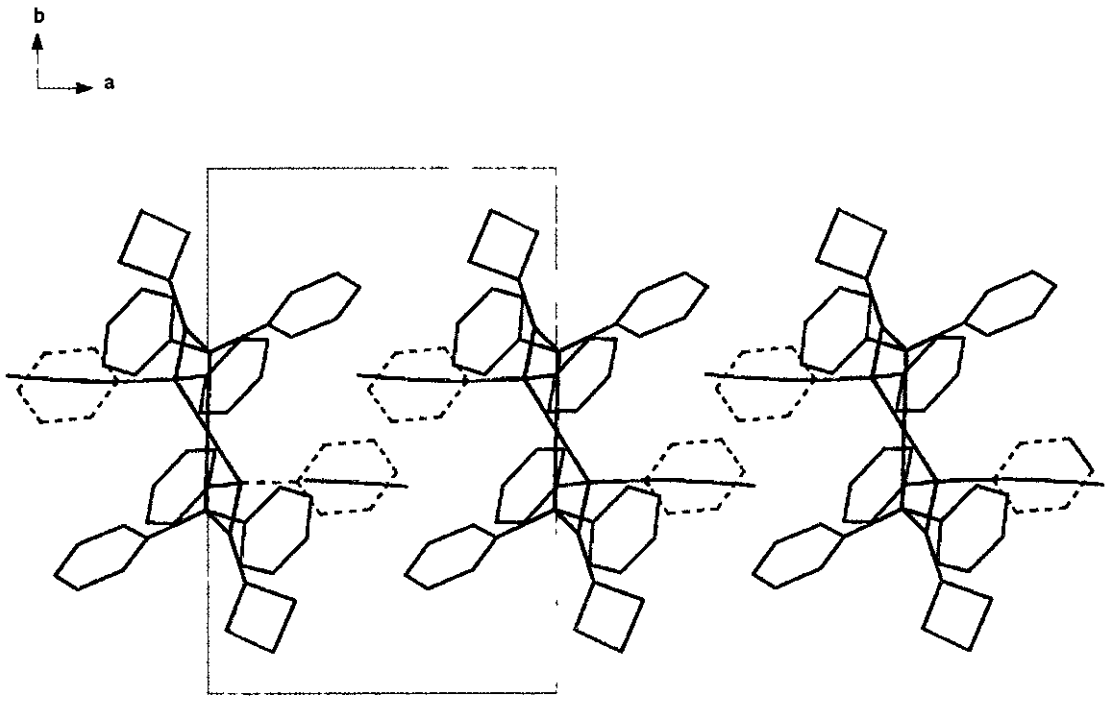


Figure 5.8: Crystal packing of [Pt(PNP-*c*But)$_2$] (2) along the c-axis. Hydrogen atoms and anion molecules omitted for clarity.

5.5 Bis[*N*,*N*-bis(diphenylphosphanyl)cyclopentanamine-κ^2P,P'] platinum(II) bis(trifluoromethanesulfonate)

The title complex, [Pt(PNP-*c*Pent)$_2$] (3), has been synthesized as described in Paragraph 3.5.3. The complex crystallizes in a monoclinic crystal system in the $P2_1/c$ space group with two formula units per unit cell (Z = 2). [14] The asymmetric unit consists of one half of the platinum complex and a trifluoromethanesulfonate anion. The Pt(II) atom is situated on an inversion centre and coordinated by two PNP-*c*Pent bidentate ligands. The other half of the complex molecule and the second anion are generated through symmetry. Unstable bond lengths and angles were restrained within the anion molecule. The numbering scheme of the title complex is shown in in **Figure 5.9**.

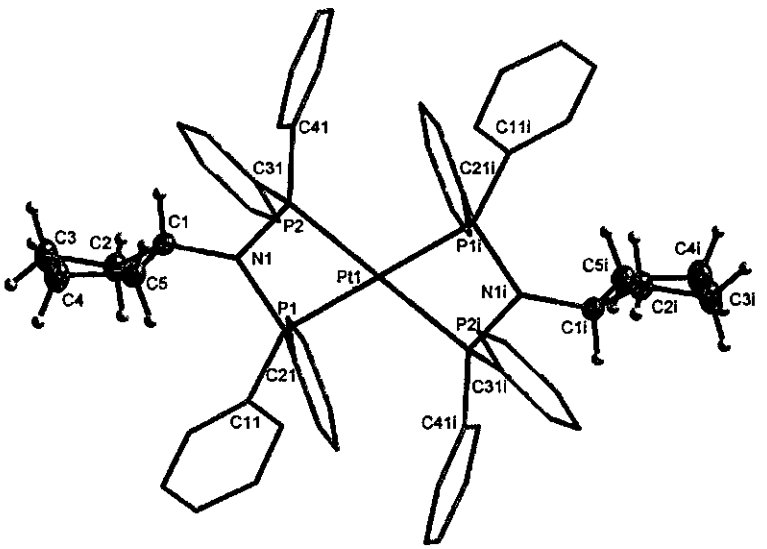


Figure 5.9: Molecular representation of the crystal structure of [Pt(PNP-*c*Pent)$_2$] (3). Atoms generated through symmetry are represented by ending with 'i'. Hydrogen atoms of the phenyl rings and trifluoromethanesulfonate ions have been omitted for clarity. Symmetry transformations used to generate equivalent atoms: $-x+2, -y, -z+2$.

[14] I. Engelbrecht, H.G. Visser, A. Roodt, *Acta Cryst.*, E68 (2012) m916.

The cyclopentane ring is twisted with an envelope conformation [q_2 = 0.420(5) Å, φ = 26.5(8) °][13] with atom C2 deviating 0.645(5) Å from the plane of the remaining four atoms (**Figure 5.10**). The trifluoromethanesulfonate anions are disordered over two positions with site occupancy factors of 0.511(11):0.489(11) (**Figure 5.9**).

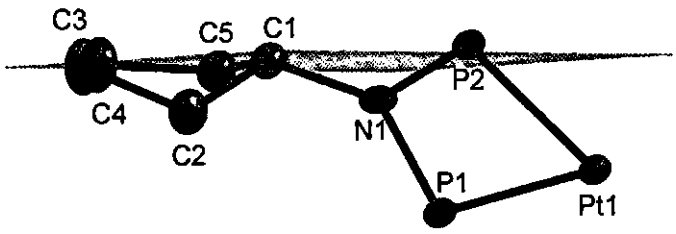


Figure 5.10: Partial structure view of [Pt(PNP-*c*Pent)$_2$] (3) showing the twisted cyclopentyl ring with C2 deviating away from the ring. The plane is constructed through the remaining four atoms (C1/C3/C4/C5).

Table 5.7: Selected bond lengths (Å) and angles (°) for the crystal structure of [Pt(PNP-*c*Pent)$_2$] (3).

Atoms	Bond length	Atoms	Bond angle
Pt – P1	2.314(1)	P1 – Pt – P2	70.31(4)
Pt – P2	2.294(1)	P1 – N1 – P2	102.3(2)
N1 – C1	1.484(6)	C1 – N1 – P1	133.6(3)
N1 – P1	1.704(4)	C1 – N1 – P2	122.5(3)
N1 – P2	1.703(4)	N1 – P1 – C11	113.3(2)
P1 – C11	1.805(4)	N1 – P1 – C21	112.1(2)
P1 – C21	1.806(4)	N1 – P2 – C31	110.5(2)
P2 – C31	1.794(4)	N1 – P2 – C41	108.0(2)
P2 – C41	1.805(4)	C11 – P1 – C21	105.1(2)
		C31 – P2 – C41	108.0(2)

Some of the important bond distances and angles were selected and are summarized in **Table 5.7**. Bond distances and angles are all within range of similar complexes.[8,9,10,11,12] The *Effective Tolman-based N-substituent steric effect* ($\theta_{N\text{-}sub}{}^{a}$) was calculated as 77.6 ° (see Chapter 4, **Eq. 4.1** and **Figure 4.3**).

The square-planar geometry of the complex is highly distorted with a P1-Pt-P2 bite angle of 70.31(4) °. Angles around the N atom ranging between 102.3(2) and 133.6(3) °, illustrates the severely distorted tetrahedral geometry around the N atom. The N atom is displaced by -0.1146(4) Å from the C1/P1/P2 plane showing that the N atom adopts an almost planar geometry with the two P-atoms and the C-atom attached to it to accommodate the steric bulk of the phenyl groups and the alkyl substituent of the ligand. The distorted tetrahedral geometry around the P-atoms is evident from N-P-C and C-P-C angles ranging between 105.1(2) and 113.3(2) °.

Intra- and intermolecular C—H···O interactions stabilize the crystal packing (**Figure 5.11**) and are reported in **Table 5.8**.

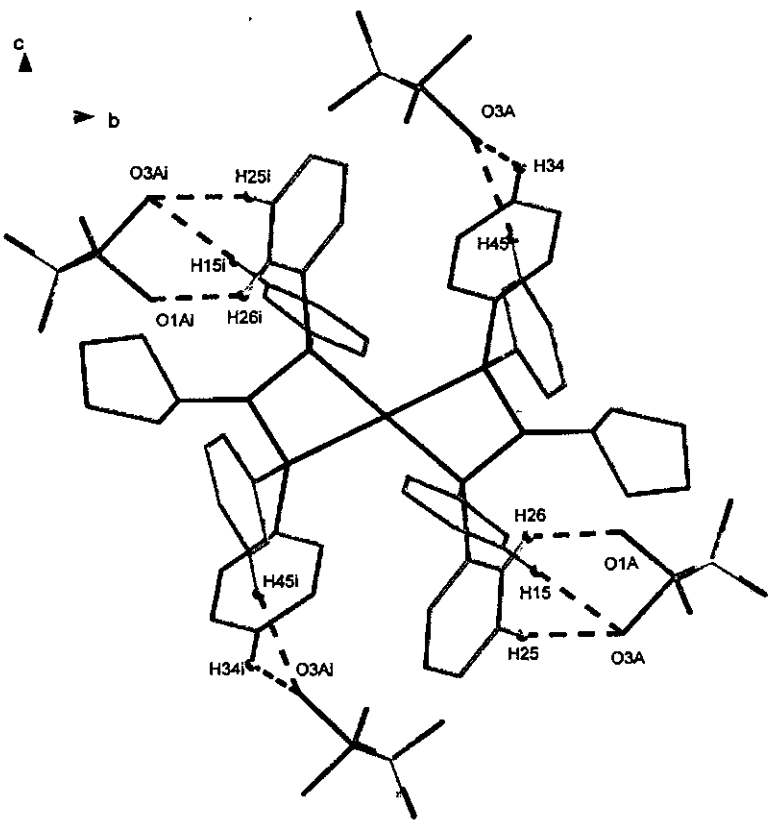


Figure 5.11: Hydrogen bond interaction observed for [Pt(PNP-cPent)$_2$] (3), viewed along the a-axis. Atoms generated through symmetry ends with "i". Only the hydrogen atom with relevance to the hydrogen bond interaction is indicated. Symmetry transformations used to generate equivalent atoms: $-x+2, -y, -z+2$.

Table 5.8: Hydrogen bonds for [Pt(PNP-*c*Pent)$_2$] (3) (Å and °).

D—H···*A*	*D*—H	H···*A*	*D*···*A*	*D*—H···*A*
C25—H25···O3A	0.95	2.52	3.398(9)	154
C26—H26···O1B	0.95	2.5	3.238(6)	135
C34—H34···O3A^{ii}	0.99	2.38	3.127(10)	135
C45—H45···O3A^{iii}	0.99	2.3	3.229(9)	165
C15—H15···O3A^{iv}	0.99	2.47	3.420(11)	178

Symmetry codes: (ii) x+1, −y+1/2, z+1/2; (iii) x, −y+1/2, z+1/2; (iv) x+1, y, z.

The metal complexes pack in a head-to-tail fashion along the b-axis as illustrated in **Figure 5.12.**

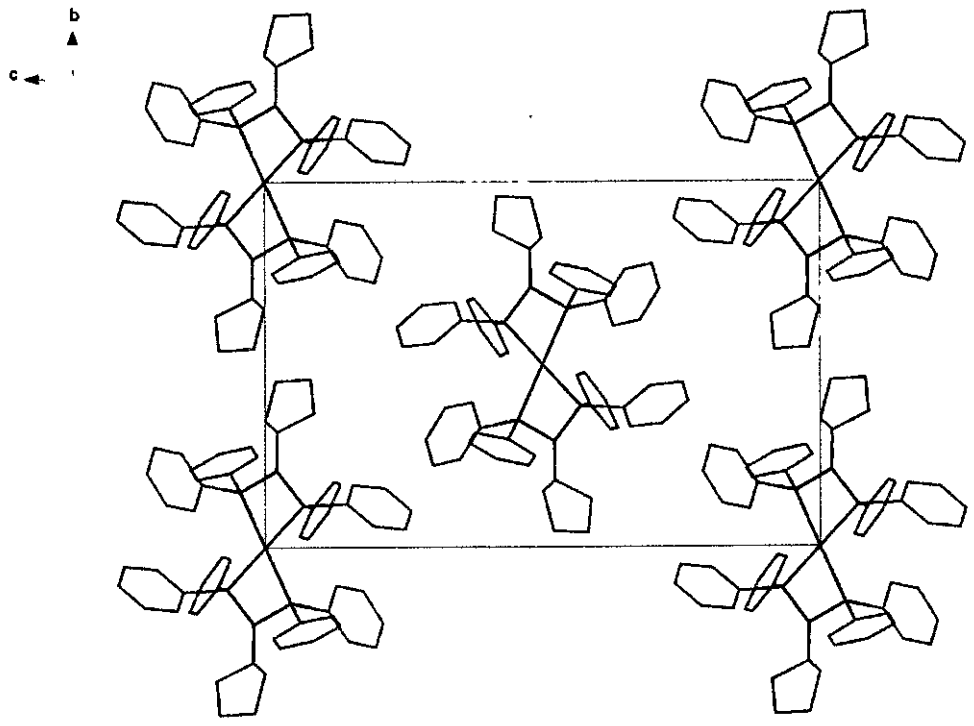


Figure 5.12: Crystal packing for [Pt(PNP-*c*Pent)$_2$] (3) as viewed along the a-axis. Hydrogen atoms and anion molecules omitted for clarity.

5.6 Bis[*N*,*N*-bis(diphenylphosphanyl)cyclohexylamine-κ^2P,P'] platinum(II) bis(hexafluoridophosphate) dichloromethane disolvate

The title complex, [Pt(PNP-*c*hex)$_2$] (4), has been synthesized as described in Paragraph 3.5.4. The complex crystallizes in a monoclinic crystal system in the $P2_1/c$ space group with two formula units per unit cell (Z = 2). [15] The Pt(II) atom, situated on an inversion centre, is coordinated by two PNP-*c*Hex bidentate ligands. The asymmetric unit contains one half of the complex molecule, a hexafluorophosphate anion and a dichloromethane solvent molecule. The other half of the complex molecule, the second anion and the second solvent molecule are generated through symmetry. The numbering scheme of the title complex is shown in **Figure 5.13**.

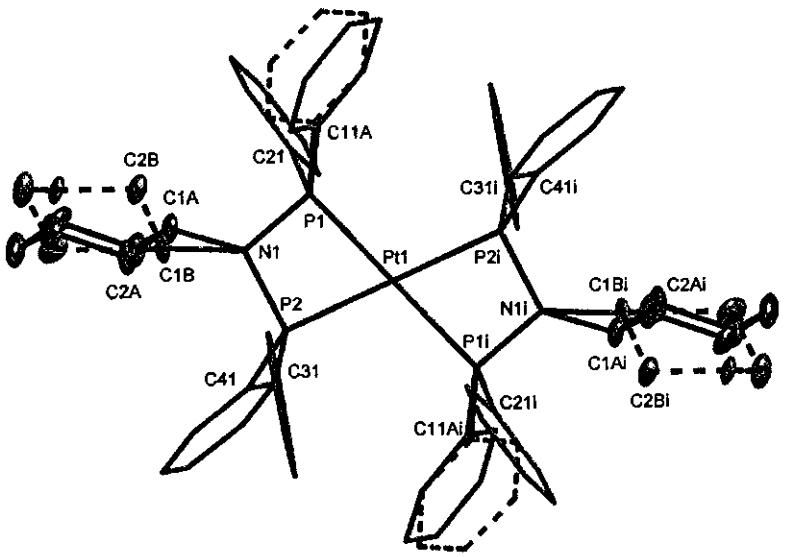


Figure 5.13: Molecular representation of the crystal structure of [Pt(PNP-*c*Hex)$_2$] (4). Atoms generated through symmetry are represented by ending with 'i'. Major and minor disordered parts belonging together are numbered A and B respectively, with dashed lines denoting the minor disordered atoms. Hydrogen atoms, solvent molecules and hexafluorophosphate ions have been omitted for clarity. Symmetry transformations used to generate equivalent atoms: 1-x, 1-y, 1-z. .

[15] I. Engelbrecht, H.G. Visser, A. Roodt, *Acta Cryst.*, E66 (2010) m994.

The cyclohexyl ring, bonded to the nitrogen atom, and the C11—C16 phenyl ring, bonded to P1, display a 0.630(7):0.370(7) and 0.60(2):0.40(2) positional disorder, respectively. The dichloromethane solvent molecules display a 0.526(4):0.474(4) positional disorder. EADP constraints (exact anisotropic displacement parameters (Uij)) were applied in some cases for neighbouring atoms in the disordered cyclohexyl ring as well as the disordered phenyl ring.

The cyclohexyl ring, bonded to N1, adopts a chair conformation in both the major- and minor disordered part of the crystal structure (typical Ring Flip) as can be seen in **Figure 5.14**. The puckering parameters for the major disordered cyclohexyl ring are Q = 0.565(14) Å, θ = 2.7(13) ° and φ = 35(114) ° with average C-C bond distances of 1.527(5) Å and average absolute torsion angle of 55.13(5) °. For the minor disordered cyclohexyl ring, the puckering parameters are as follows: Q = 0.56(3) Å, θ = 175(2) °and φ = 152(69) °. Average bond distances and average absolute torsion angle are 1.517(8) Å and 54.94(9) °, respectively for the minor disordered cyclohexyl ring.

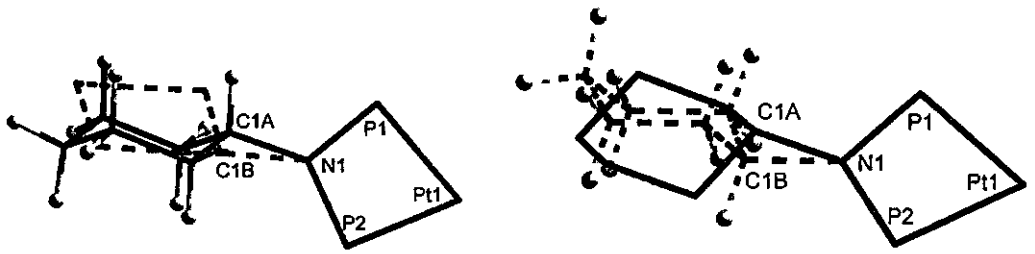


Figure 5.14: Partial structure view of [Pt(PNP-*c*Hex)$_2$] (4) from different viewing angles indicating the conformation for the cyclobutane ring with H-atom positions. Major and minor disordered parts belonging together are numbered A and B respectively, with dashed lines denoting the minor disordered atoms.

Table 5.9: Selected bond lengths (Å) and angles (°) for the crystal structure of [Pt(PNP-cHex)$_2$] (4).

Atoms	Bond length	Atoms	Bond angle
Pt – P1	2.292(1)	P1 – Pt – P2	70.76(3)
Pt – P2	2.300(1)	P1 – N1 – P2	102.6(1)
N1 – C1A	1.480(12)	C1A – N1 – P1	120.1(4)
N1 – C1B	1.56(2)	C1B – N1 – P1	137.3(6)
N1 – P1	1.701(3)	C1A – N1 – P2	134.0(4)
N1 – P2	1.706(2)	C1B – N1 – P2	119.3(7)
P1 – C11A	1.811(16)	N1 – P1 – C11A	110.5(11)
P1 – C11B	1.79(3)	N1 – P1 – C11B	110.8(17)
P1 – C21	1.799(3)	N1 – P1 – C21	111.3(1)
P2 – C31	1.804(3)	N1 – P2 – C31	110.9(1)
P2 – C41	1.794(3)	N1 – P2 – C41	111.0(1)
		C11A – P1 – C21	106.0(9)
		C11B – P1 – C21	102.4(13)
		C31 – P2 – C41	111.0(1)

Some of the important bond distances and angles were selected and are summarized in **Table 5.9**. Bond distances and angles are all within range of similar complexes.[8,9,10,11,12] The *Effective Tolman-based N-substituent steric effect* ($\theta_{N\text{-}sub}$) was calculated as 81.6 °. The $\theta_{N\text{-}sub}$ value was calculated as the average between the major and minor disordered cyclohexyl ring (see Chapter 4, **Eq. 4.1** and **Figure 4.3**). The P1-Pt-P2 angle of 70.76(3) ° indicates the distorted square-planar geometry around the Pt(II) atom. The reported P1-Pt-P2 small bite angle forces the P1-N1-P2 angle to 102.6(1) ° which demonstrates the deviation from the ideal tetrahedral geometry of the N atom. The N atom is displaced by 0.166(3) and -0.081(3) Å from the C1A/P1/P2 and C1B/P1/P2 planes, respectively showing that the N atom adopts an almost planar geometry with these atoms to accommodate the steric bulk of the phenyl groups and the alkyl group of the ligand. Bond angles ranging from 102.4(13) to 111.3(1) ° shows the distorted tetrahedral geometry around the phosphorous atoms.

Intramolecular hydrogen bonds together with intra- and intermolecular C—H···π interactions stabilize the crystal packing. These interactions are illustrated in **Figure 5.15** and summarized in **Table 5.10.**

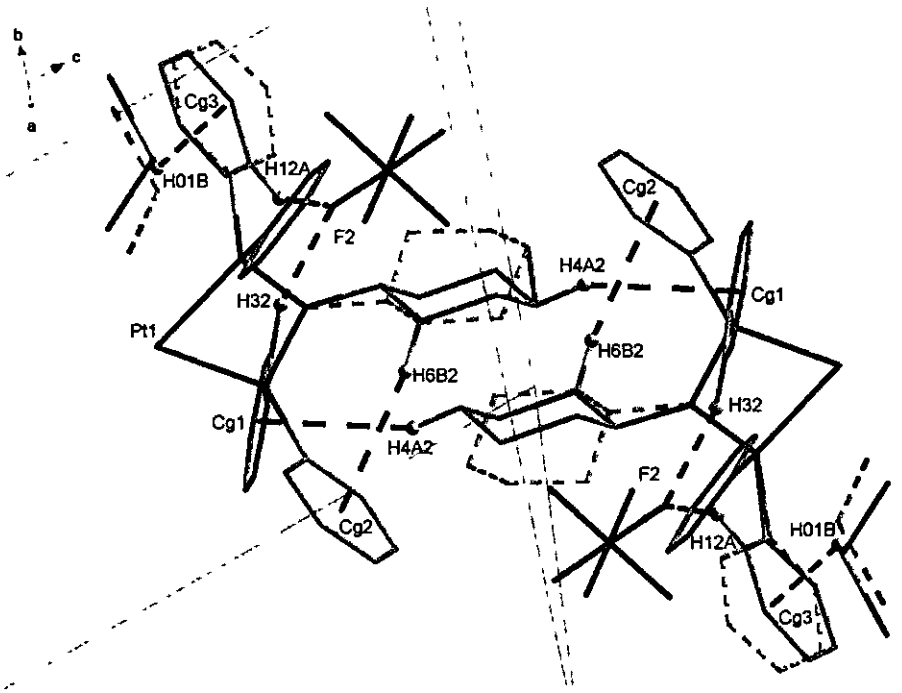


Figure 5.15: Hydrogen bond interactions observed for [Pt(PNP-*c*Hex)$_2$] (4), viewed along the a,b-plane. Hydrogen atoms, not taking part in the hydrogen interactions, are omitted for clarity. Cg1, Cg2 and Cg3 are the centroids of the C31—C36, C41—C46 and C11B—C16B rings, respectively.

Table 5.10: Hydrogen bonds for [Pt(PNP-*c*hex)$_2$] (Å and °). Cg1, Cg2 and Cg3 are the centroids of the C31—C36, C41—C46 and C11B—C16B rings, respectively.

D—H···*A*	*D*—H	H···*A*	*D*···*A*	*D*—H···*A*
C12A—H12A···F2	0.95	2.45	3.186(11)	134
C32—H32···F2	0.95	2.47	3.138(4)	127
C4A—H4A2···Cg1^{ii}	0.99	2.92	3.822(6)	152
C6B—H6B2···Cg2	0.99	2.87	3.82(4)	160
C01A—H01B···Cg3^{iii}	0.99	2.75	3.542(13)	138

Symmetry codes: (ii) $-x+2, -y+1, -z+2$; (iii) $-x+1, y-1/2, -z+3/2$.

The metal complexes pack in a head-to-tail fashion along the c-axis as illustrated in **Figure 5.16**.

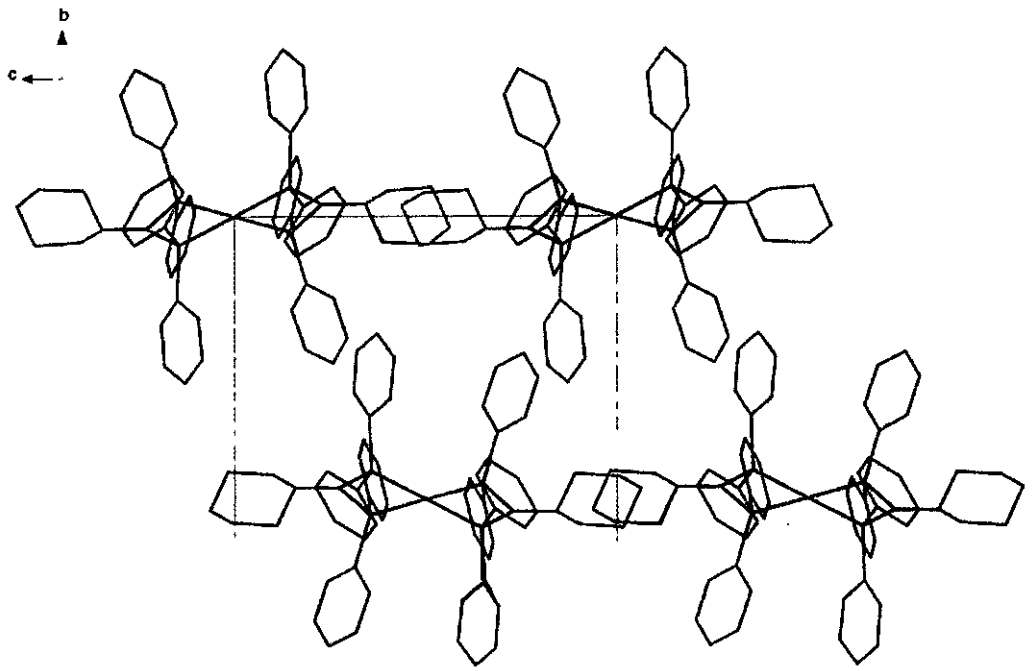


Figure 5.16: Crystal packing of for [Pt(PNP-*c*Hex)$_2$] (4), as viewed along the a-axis. Hydrogen atoms and anion molecules omitted for clarity.

5.7 Bis[*N*,*N*-bis(diphenylphosphanyl)-*n*-pentylamine-κ^2P,P'] platinum(II) bis(hexafluoridophosphate) dichloromethane disolvate

The title complex, [Pt(PNP-*n*Pent)$_2$] (5), has been synthesized as described in Paragraph 3.5.5. The complex crystallizes in a monoclinic crystal system in the *Cc* space group with four formula units per unit cell (Z = 4). The asymmetric unit contains one full complex molecule, two hexafluorophosphate molecules and two dichloromethane solvent molecules. The Pt(II) atom is coordinated by two PNP-*n*Pent bidentate ligands. The numbering scheme of the title complex is shown in **Figure 5.17**.

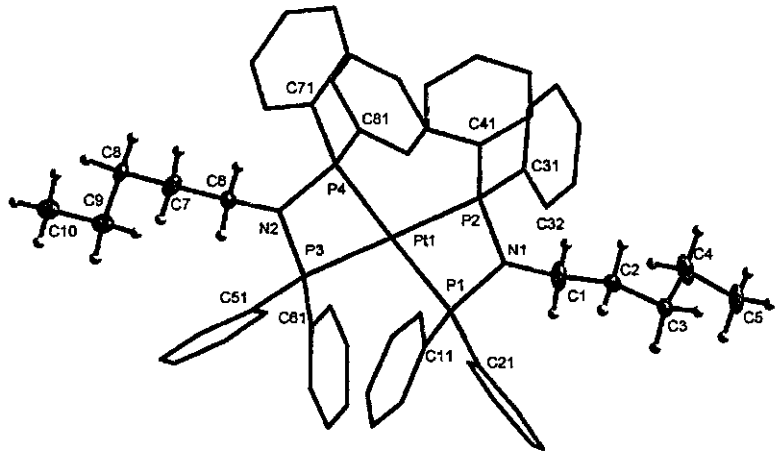


Figure 5.17: Molecular representation of the crystal structure of [Pt(PNP-*n*Pent)$_2$] (5). Hydrogen atoms of the phenyl rings, solvent molecules and hexafluorophosphate ions have been omitted for clarity.

One of the chlorine atoms of one of the dichloromethane solvent molecules display a 0.515(3):0.485(3) positional disorder. EADP constraints (exact anisotropic displacement parameters (Uij)) were applied in the disordered solvent molecule.

Table 5.11: Selected bond lengths (Å) and angles (°) for the crystal structure of [Pt(PNP-*n*Pent)$_2$] (5).

Atoms	Bond length	Atoms	Bond angle
Pt – P1	2.3063(8)	$\theta_{N\text{-}sub}$[a]	63.4
Pt – P2	2.2965(8)	P1 – Pt – P2	70.45(3)
Pt – P3	2.2994(8)	P1 – N1 – P2	103.4(1)
Pt – P4	2.2995(8)	P3 – Pt – P4	70.64(3)
N1 – C1	1.481(4)	P3 – N2 – P4	103.2(1)
N2 – C6	1.493(4)	C1 – N1 – P1	126.7(2)
N1 – P1	1.692(3)	C1 – N1 – P2	129.9(2)
N1 – P2	1.691(3)	C6 – N2 – P3	127.2(2)
N2 – P3	1.697(3)	C6 – N2 – P4	127.9(2)
N2 – P4	1.697(3)	N1 – P1 – C11	109.2(1)
P1 – C11	1.791(3)	N1 – P1 – C21	108.7(1)
P1 – C21	1.795(3)	N1 – P2 – C31	111.8(2)
P2 – C31	1.806(3)	N1 – P2 – C41	109.6(1)
P2 – C41	1.795(3)	N2 – P3 – C51	111.6(1)
P3 – C51	1.810(3)	N2 – P3 – C61	109.6(1)
P3 – C61	1.793(3)	N2 – P4 – C71	111.5(1)
P4 – C71	1.801(3)	N2 – P4 – C81	109.4(1)
P4 – C81	1.794(3)	C11 – P1 – C21	108.3(1)
		C31 – P2 – C41	107.1(2)
		C51 – P3 – C61	106.4(2)
		C71 – P4 – C81	105.5(1)

[a] See Chapter 4 for the calculation of $\theta_{N\text{-}sub}$. The $\theta_{N\text{-}sub}$ value was calculated as the average of the two non-symmetric PNP-*n*Pent ligands coordinated to the platinum.

Some of the important bond distances and angles were selected and are summarized in **Table 5.11**. Bond distances and angles are all within range of similar complexes.[8,9,10,11,12] The *Effective Tolman-based N-substituent steric effect* ($\theta_{N\text{-}sub}$) was calculated as 63.4 °. The $\theta_{N\text{-}sub}$ value was calculated as the average between the two non symmetrical PNP-*c*Pent ligands coordinated to the platinum (see Chapter 4, **Eq. 4.1** and **Figure 4.3**).

The distorted square-planar geometry around the Pt(II) atom is illustrated by P1-Pt-P2 and P3-Pt-P4 angles of 70.45(3) and 70.64(3) °, respectively. P1-N1-P2 and P3-N2-P4 angles of 103.4(1) and 103.2(1) °, respectively illustrate the deviation from the ideal tetrahedral geometry around the N-atoms. The N1 and N2 atoms are displaced by 0.019(3) and 0.118(3) Å from the C1/P1/P2 and C6/P3/P4 planes, respectively showing that the N atom adopts an almost planar geometry with these atoms to accommodate the steric bulk of the phenyl groups and the alkyl group of the ligand. Bond angles ranging from 105.5(1) to 111.8(2) ° shows the distorted tetrahedral geometry around the phosphorous atoms.

Intra- and intermolecular C—H···F interactions stabilize the crystal packing. These interactions are illustrated in **Figure 5.18** and summarized in **Table 5.12**.

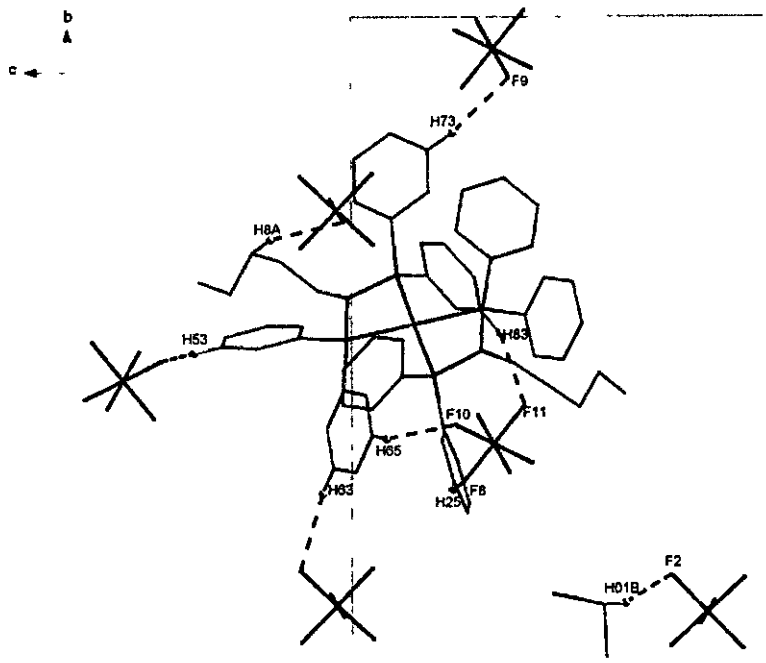


Figure 5.18: Hydrogen bond interactions observed for [Pt(PNP-*n*Pent)$_2$] (5), viewed along the a-axis. Hydrogen atoms, not taking part in the hydrogen interactions, are omitted for clarity.

Table 5.12: Hydrogen bonds for [Pt(PNP-*n*Pent)$_2$] (Å and °).

D—H···*A*	*D*—H	H···*A*	*D*···*A*	*D*—H···*A*
C25—H25···F8	0.95	2.53	3.437 (4)	160
C65—H65···F10	0.95	2.47	3.297 (4)	145
C83—H83···F11	0.95	2.37	3.267 (4)	158
C01—H01B···F2^{i}	0.99	2.29	3.244 (5)	161
C8—H8A···F3^{ii}	0.99	2.54	3.450 (4)	153
C53—H53···F7^{iii}	0.95	2.51	3.273 (4)	137
C63—H63···F4^{iv}	0.95	2.51	3.373 (4)	151
C73—H73···F9^{v}	0.95	2.53	3.426 (4)	156

Symmetry codes: (i) x+1/2, −y+3/2, z−1/2; (ii) x+1, y, z; (iii) x, −y+1, z+1/2; (iv) x+1/2, y−1/2, z; (v) x−1/2, y+1/2, z.

The molecules pack in a head-to-tail fashion along the b-axis as illustrated in **Figure 5.19**.

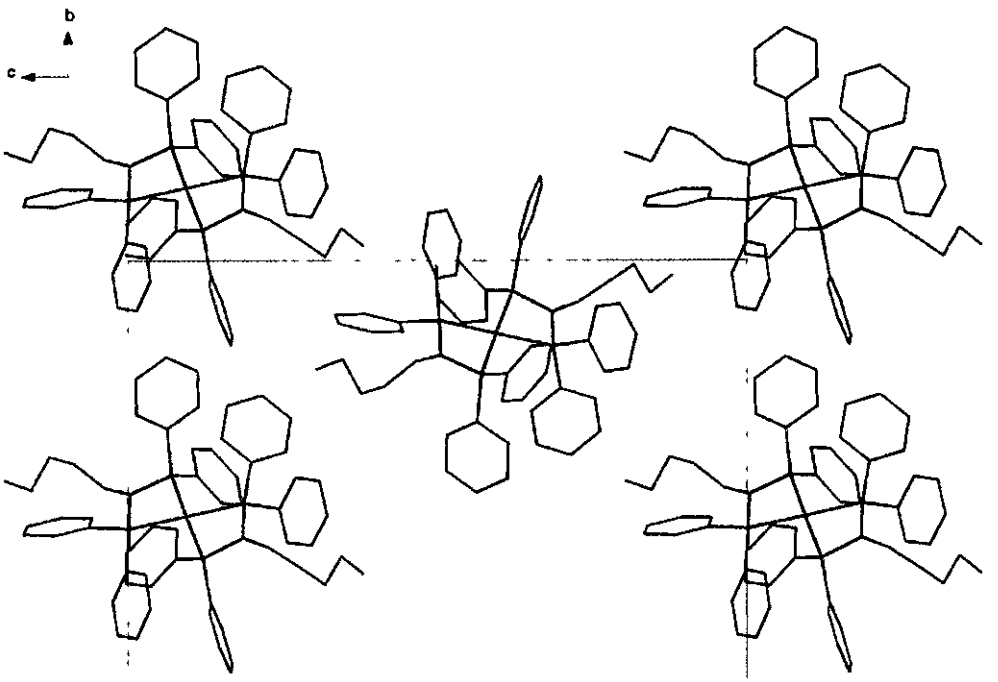


Figure 5.19: Crystal packing of for [Pt(PNP-*n*Pent)$_2$] (5), as viewed along the a-axis. Hydrogen atoms and anion molecules omitted for clarity.

5.8 Bis[*N*,*N*-bis(diphenylphosphanyl)cyclopropyl-κ^2*P*,*P*'] palladium(II) bis(hexafluoridophosphate)

The [Pd(PNP-alkyl)$_2$] complexes proved extremely difficult to crystallize and collect high-quality data for refining of the crystal due to very high symmetry and accompanying disorders. Therefore, only one worthy data collection of [Pd(PNP-*c*Prop)$_2$] (6) will be discussed. Even though this crystal is not fully refined, as can be seen from high R_{int} and wR values, (R_{int} = 0.133, wR = 0.326), due to solvent disorders, the main palladium component of the crystal is a clear representation of the correct complex. The palladium(II) complexes were synthesized to add on to the existing platinum compound information to further confirm results, as these complexes were expected to give similar outcomes.

The title complex, [Pd(PNP-*c*Prop)$_2$] (6), has been synthesized as described in Paragraph 3.6.1. The complex crystallizes in a monoclinic crystal system in the *C2/m* space group with two formula units per unit cell (Z = 2). The asymmetric unit consists of two independent [Pd(PNP-*c*Prop)$_2$] molecules and four hexafluorophosphate anions. The numbering scheme of the title complex is shown in **Figure 5.20**. The N atoms and carbon atom attached to it are situated on a mirror plane, whilst the Pd(II) atoms are situated both on a two-fold rotation axis and a mirror plane. The P atoms of the hexafluorophosphate ions are situated on two-fold rotation axis.

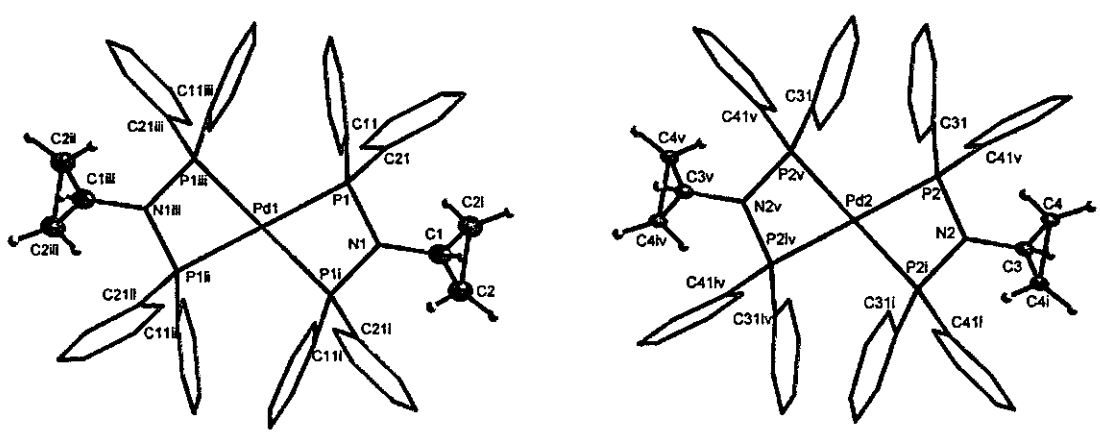


Figure 5.20: Molecular representation of the crystal structure of [Pd(PNP-*c*Prop)$_2$] (6). Atoms generated through symmetry are represented by atoms ending with 'i, ii, iii, iv, v'. Hydrogen atoms have been omitted for clarity. Symmetry transformations used to generate equivalent atoms: (i) x, 1-y, z; (ii) 1-x, 1-y, -z; (iii) 1-x, y, -z; (iv) –x, 1-y, 1-z; (v) –x, y, 1-z.

The two independent [Pd(PNP-*c*Prop)$_2$] molecules in the asymmetric unit have insignificant differences in bond lengths and angles as summarized in **Table 5.13**. The visual comparison between the two independent fractures also indicates a very good correlation (RMS = 0.120 Å) with slight differences in phenyl ring orientations (**Figure 5.21**).

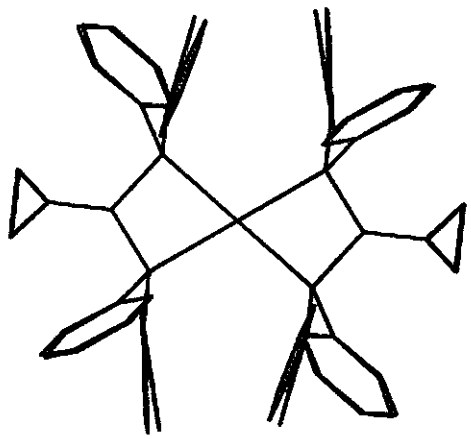


Figure 5.21: Graphical representation of an overlay of fragment 1 (red) and fragment 2 (black) of the crystal structure of [Pd(PNP-*c*Prop)$_2$] (RMS value = 0.120 Å). Overlay fit excluded all H-atoms.

Table 5.13: Selected bond lengths (Å) and angles (°) for the crystal structure of [Pd(PNP-*c*Prop)$_2$] (6).

Atoms	Bond length	Atoms	Bond angle
Pd1 – P1	2.304(2)	$\theta_{N\text{-}sub}$[a]	69.3
Pd2 – P2	2.301(2)	P1 – Pd1 – P1i	70.4(1)
N1 – C1	1.469(2)	P2 – Pd2 – P2i	70.8(1)
N2 – C3	1.431(16)	P1 – N1 – P1i	102.3(5)
N1 – P1	1.706(7)	P2 – N2 – P2i	102.0(6)
N2 – P2	1.714(7)	C1 – N1 – P1	125.8(4)
P1 – C11	1.785(9)	C3 – N2 – P2	125.5(4)
P1 – C21	1.786(9)	N1 – P1 – C11	109.7(4)
P2 – C31	1.796(9)	N1 – P1 – C21	111.8(4)
P2 – C41v	1.796(9)	N2 – P2 – C31	108.9(5)
		N2 – P2 – C41	111.3(4)
		C11 – P1 – C21	106.8(4)
		C31 – P2 – C41v	106.6(4)

[a] See Chapter 4 for the calculation of $\theta_{N\text{-}sub}$. The $\theta_{N\text{-}sub}$ value was calculated as the average of the two independent palladium complexes.

Some of the important bond distances and angles were selected and are summarized in **Table 5.13**. Bond distances and angles are all within range of similar complexes.[8,9,10,11,12] The *Effective Tolman-based N-substituent steric effect* ($\theta_{N\text{-}sub}$) was calculated as the average between the two independent [Pd(PNP-*c*Prop)$_2$] molecules in the asymmetric unit with a value of 69.3 ° (see Chapter 4, **Eq. 4.1** and **Figure 4.3**).

The P1-Pd1-P1i and P2-Pd2-P2i angles are 70.4(1) and 70.8(1) °, respectively illustrating the distorted square-planar geometry around the Pd(II) atom. The strain in the complex is further illustrated by the distorted tetrahedral geometry around the N atom with P1-N1-P1i and P2-N2-P2i angles of 102.3(5) and 102.0(6) °, respectively. The N1 atom is displaced by -0.227(1) Å from the plane constructed through the two P-atoms and C-atom attached to it (C1/P1/P1i) while the N2 atom is perfectly planar to the C2/P2/P2i plane showing that the N-atoms adopt an almost planar geometry with these atoms to accommodate the steric bulk of the phenyl groups and the alkyl group of the ligand. Bond angles ranging from 106.6(4) to 111.8(4) ° shows the distorted tetrahedral geometry around the phosphorous atoms with C-P-C angles being the most distorted.

Due to the incomplete nature of this crystal structure, detailed and accurate data for these atoms are not available and therefore, the crystal packing and hydrogen bonding will not be discussed in detail as for the previous platinum(II) complexes.

The palladium complexes were expected to give very similar results as the platinum compounds to prove that the PNP-ligands bind in similar fashion to various metal complexes. The palladium bond distances and angles fall perfectly within range with the platinum results. The P-M-P (M = metal) angles for both [Pt(PNP-*c*Prop)$_2$] and [Pd(PNP-*c*Prop)$_2$] complexes are between 70.4(1) and 71.5(1) ° and the P-N-P angles between 101.2(5) and 102.3(5)°. The [Pd(PNP-*c*Prop)$_2$] structure shows the same square-planar disorders around the metal centre as well as the distorted tetrahedral geometries around the N and P atoms. The N atom is also forced almost planar to the two P atoms and C atom attached to it to accommodate the steric bulk of the phenyl rings and the alkyl substituent on the N atom.

5.9 Discussion

The crystal structures of five platinum complexes, [Pt(PNP-*c*Prop)$_2$] (1), [Pt(PNP-*c*But)$_2$] (2), [Pt(PNP-*c*Pent)$_2$] (3), [Pt(PNP-*c*Hex)$_2$] (4) and [Pt(PNP-*n*Pent)$_2$] (5) as well as one palladium complex, [Pd(PNP-*c*Prop)$_2$] (6), were analyzed and discussed in this Chapter. A crystallographic investigation of the complexes in this study was considered important to fully understand the coordination mode, differences in steric and electronic properties and the effects induced by the PNP-ligands when changing the N-substituent from one ligand to another. All complexes crystallize in a monoclinic crystal system. Complex **1**, was refined in a non-standard $P2_1/n$ space group, the standard equivalent setting is $P2_1/c$, but caused unstable refinement. Thus, complexes **1**, **2**, **3** and **4** crystallize in the same space group, $P2_1/c$, with two formula units in the unit cell (Z = 2). Complex **5** crystallizes in a *Cc* space group with four formula units in the unit cell (Z = 4) and complex **6** crystallizes in a *C2/m* space group with two formula units in the unit cell (Z = 2). The crystal structure of all three ligands display molecular packing, stabilized by a variety of inter- and intramolecular hydrogen bonding and C—H$\cdots\pi$ interactions. The bond distances and angles for the [Pt(PNP-alkyl)$_2$] and [Pd(PNP-alkyl)$_2$] complexes are comparable to other structurally characterised Pt/Pd(II)diphosphinoamine complexes.[8,9,10,11,12]

It was noted that stable chelate complexes were formed despite the strain caused by the severely distorted square-planar geometry around the metal centres with P-M-P bond angles that range from 70.23(6) to 72.3(1) ° (**Table 5.14**), illustrating the rigidity of the P-N-P frame upon coordination. The P-N-P angles decrease from the much larger P-N-P angle observed for the non-coordinated PNP-ligands (Chapter 4), in order to accommodate coordination to the platinum centre. There is a tendency for the P-N-P angle to slightly decrease as the steric bulk of the nitrogen-coordinated alkyl moiety increases (**Table 5.14**). The P-N-P angles for the least bulky [Pt(PNP-Ethyl)$_2$] and [Pt(PNP-*n*Pent)$_2$] (103.4(1) and 100.0(2) °, respectively) are slightly larger than for the most bulky [Pt(PNP-Dimprop)$_2$] (98.6(4) °). This trend is as expected, as a bulkier alkyl substituent on the nitrogen atom forces the P-N-P angle to become smaller in order to accommodate the larger moiety.

Table 5.14: Comparison of selected bond angles (°) and $\theta_{N\text{-}sub}$ (°) values for [M(PNP-alkyl)$_2$] and [MCl$_2$(PNP-alkyl)] (M = Pt, Pd) complexes.

Complex	P1 – M – P2	P1 – N1 – P2	$\theta_{N\text{-}sub}$[a] (Free Ligand)	$\theta_{N\text{-}sub}$ (Pt/Pd Coordinated)
[PtCl$_2$(PNP-Ethyl)][b]	72.1(1)	100.0(2)	62.9	62.8
[Pt(PNP-*n*Pent)$_2$][c]	70.45(3)	103.4(1)	63.2	63.4
[Pt(PNP-*n*Pent)$_2$][c]	70.64(3)	103.2(1)	-	-
[Pt(PNP-*c*Prop)$_2$]	71.5(1)	101.2(5)	68.5	69.5
[Pd(PNP-*c*Prop)$_2$][d]	70.4(1)	102.3(5)	68.5	69.3
[Pd(PNP-*c*Prop)$_2$][d]	70.8(1)	102.0(6)	-	-
[Pt(PNP-*c*But)$_2$]	70.23(6)	102.2(3)	73.1	71.1
[Pt(PNP-*c*Pent)$_2$]	70.31(4)	102.3(2)	79.3	77.6
[Pt(PNP-*c*Hex)$_2$]	70.76(3)	102.6(11)	81.3	81.6
[PtCl$_2$(PNP-Dimprop)][e]	72.3(1)	98.6(4)	88.5	86.1

[a] Calculated from crystal data for the non-coordinated PNP-ligands in (**Table 4.12**) Chapter 4. [b] See Ref 16. [c] The P-Pt-P and P-N-P angles for [Pt(PNP-*n*Pent)$_2$] are as follows: P3-Pt-P4 and P3-N2-P4 due to non-symmetrical crystal. [d] The P-Pd-P and P-N-P angles for [Pd(PNP-*c*Prop)$_2$] are as follows: P1-Pd-P1i, P2-Pd-P2i, P1-N1-P1i and P2-N2-P2i due to the two independent Pd(II) complexes in the asymmetric unit of the crystal structure. [e] See Ref 11.

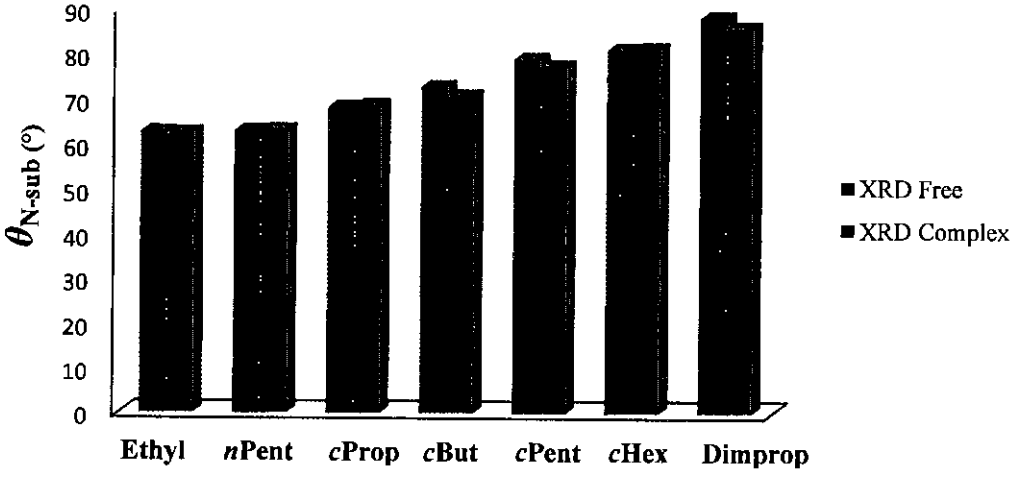


Figure 5.22: $\theta_{N\text{-}sub}$ (°) values for the crystallographic (**XRD**) structure data of various free PNP-ligands (**Free**) and Pt/Pd-PNP coordinated complexes (**Complex**).

[16] N.Cloete, PhD thesis, University of the Free State, 2009.

The $\theta_{N\text{-}sub}$ values for the non-coordinated PNP-ligands as well as the coordinated complexes of platinum(II) and palladium(II) are in very good correlation (**Table 5.14** and **Figure 5.22**). The $\theta_{N\text{-}sub}$ value increases systematically from PNP-Ethyl < PNP-*n*Pent < PNP-*c*Prop < PNP-*c*But < PNP-*c*Pent < PNP-*c*Hex < PNP-Dimprop. The $\theta_{N\text{-}sub}$ values also play an important role in the orientation of the phenyl rings of these [M(PNP-alkyl)$_2$] (M = Pt, Pd) complexes and will be discussed in detail in the following Chapter.

Theoretical calculations were consequently performed on all the [Pt(PNP-alkyl)$_2$] and [Pd(PNP-alkyl)$_2$] complexes discussed above. These optimized structures are presented, discussed and compared to the crystal structures of the corresponding complexes in Chapter 6.

6 Theoretical study of non-coordinated PNP-ligands and Pt(II)/Pd(II) PNP-coordinated complexes

In this chapter...

The theoretical calculations of the crystal structures of the non-coordinated PNP-ligands as well as the [M(PNP-alkyl)$_2$] (M = Pt(II), Pd(II)) complexes are presented. The calculated structures are compared with the crystallographic data of the corresponding complexes.

6.1 Introduction

Theoretical calculations are increasingly being used to gather information involving metal complexes in coordination and organometallic chemistry.[1,2,3] Computational software is used to determine amongst other, molecular geometry, transition states, energies of molecules and chemical reactivity. Several calculation methods exist and can be classified into the following broad classes starting from the simplest, molecular mechanics, to the advanced *ab initio* methods:[4,5]

- Molecular Mechanics (MM)
- Semi-empirical methods (SE)
- Density functional theory (DFT)
- *Ab initio* calculations

[1] T. Woo, E. Folga, T. Ziegler, *Organometallics*, 12 (1993) 1289.
[2] V. Branchadell, M. Moreno-Manas, F. Pajuelo, R. Pleixtas, *Organometallics*, 18 (1999) 4934.
[3] U. Burckhardt, G.L. Casty, T.D. Tilley, T. Woo, U. Rothlisberger, *Organometallics*, 19 (2000) 3830.
[4] E. Lewars, *Computation Chemistry: Introduction to the theory and applications of molecular and quantum mechanics*, Kluwer Academic, New York, USA, 2004.
[5] F.Jensen, *Introduction to Computational Chemistry*, 2nd Ed., John Wiley & Sons Ltd., England, UK, 2007.

The DFT calculations are based on electron density function rather than wave function and are known for its reasonable results, accuracy and reasonable computational requirements.

DFT optimized geometric structures for the [Pt(PNP-alkyl)$_2$] and [Pd(PNP-alkyl)$_2$] complexes in this PhD study have therefore been optimized, in the gas phase, and are compared with the X-ray crystallographic data in conjunction with the free PNP-ligands, in order to better understand the factors which determine the adopted structure in solid state.[6,7,8] This study was undertaken to determine from the differences and similarities the factors which influences the geometry of the square-planar complexes as the alkyl substituents of the coordinated diphosphinoamine ligands change from one complex to another (see **Scheme 3.1** and **Scheme 5.1**).

6.2 Experimental

The DFT molecular orbital calculations were carried out using the Gaussian 03[9] software suite. Becke's three parameter hybrid functional with the Lee-Yang-Parr correlation (B3LYP)[10,11] exchange correlation functional was used. The basis set employed in this study was 6-311++G(d,p)[12,13,14] for the main group elements and LanL2DZ[15] for the middle to late transition metals. Vibrational frequencies were calculated at 6-311++G(d,p) for the main group elements and LanL2DZ for the middle to late transition metals with minimum energies

[6] A. Magistrato, M. Merlin, P.S. Pregosin, U. Rothlisberger, *Organometallics*, 19 (2000) 3591.
[7] T.A. Atesin, S.S. Oster, K. Skugrud, W.D. Jones, *Inorg. Chim. Acta*, 359 (2006) 2798.
[8] X. Zhao, Q. Pan, M. Li, B. Xia, H. Zhang, *J. Mol. Struc.*, 822 (2007) 65.
[9] Gaussian 03, Revision C.01, M. J. Frisch, G. W. Trucks, H. B. Schlegel, G. E. Scuseria, M. A. Robb, J. R. Cheeseman, J. A. Montgomery, T. Vreven, K. N. Kudin, J. C. Burant, J. M. Millam, S. S. Iyengar, J. Tomasi, V. Barone, B. Mennucci, M. Cossi, G. Scalmani, N. Rega, G. A. Petersson, H. Nakatsuji, M. Hada, M. Ehara, K. Toyota, R. Fukuda, J. Hasegawa, M. Ishida, T. Nakajima, Y. Honda, O. Kitao, H. Nakai, M. Klene, X. Li, J. E. Knox, H. P. Hratchian, J. B. Cross, C. Adamo, J. Jaramillo, R. Gomperts, R. E. Stratmann, O. Yazyev, A. J. Austin, R. Cammi, C. Pomelli, J. W. Ochterski, P. Y. Ayala, K. Morokuma, G. A. Voth, P. Salvador, J. J. Dannenberg, V. G. Zakrzewski, S. Dapprich, A. D. Daniels, M. C. Strain, O. Farkas, D. K. Malick, A. D. Rabuck, K. Raghavachari, J. B. Foresman, J. V. Ortiz, Q. Cui, A. G. Baboul, S. Clifford, J. Cioslowski, B. B. Stefanov, G. Liu, A. Liashenko, P. Piskorz, I. Komaromi, R. L. Martin, D. J. Fox, T. Keith, M. A. Al-Laham, C. Y. Peng, N. Nanayakkara, M. Challacombe, P. M. W. Gill, B. Johnson, W. Chen, M. W. Wong, C. Gonzalez, J. A. Pople, Gaussian, Inc, Pittsburgh PA, 2003.
[10] A.D. Becke, *J. Chem. Phys.*, 98 (1993) 5648.
[11] C. Lee, W. Yang, R.G. Parr, *Phys. Rev.*, B37 (1988) 785.
[12] R. Ditchfield, W.J. Hehre, J.A. Pople, *J. Chem. Phys.*, 54 (1971) 724.
[13] M.S. Gordon, *Chem. Phys. Lett.*, 76 (1980) 163.
[14] V.A. Rassolov, M.A. Ratner, J.A. Pople, P.C. Redfern, L.A. Curiss, *J. Comp. Chem.*, 22 (2001) 976.
[15] P.J. Hay, W.R. Wadt, *J. Chem. Phys.*, 82 (1985) 299.

confirmed to have zero imaginary frequencies. The frequencies are unscaled and were used to compute the zero-point vibrational energies. These optimized structures were then compared to the solid state crystallographic data of the corresponding complexes. Molecular graphics were obtained using DIAMOND[16] and overlays of the calculated structures with the corresponding crystal structures were obtained using HyperChem 7.5[17]. Selected geometric parameters of the calculated structures and corresponding crystal structures are presented and discussed. Theoretical calculations were performed on the following complexes (see Chapters 4 and 5 for the abbreviations):

(1) PNP-*c*Prop
(2) PNP-*c*But
(3) PNP-*c*Pent
(4) [Pt(PNP-*c*Prop)$_2$]
(5) [Pt(PNP-*c*Pent)$_2$]
(6) [Pt(PNP-*c*Hex)$_2$]
(7) [Pd(PNP-*c*Prop)$_2$]
(8) [Pd(PNP-*c*But)$_2$]
(9) [Pd(PNP-*c*Pent)$_2$]

Each of the crystal structures are denoted with numerical values for example 1, 2 and 3, while the corresponding calculated structures at B3LYP/6-31++G(d,p) are indicated as 1*, 2*, 3* and so forth. Cartesian coordinates and Gibbs free energies for all the computed structures are given in the supplementary data (Appendix B).

[16] K. Brandenburg, H. Putz, *DIAMOND*, Release 3.0c, Crystal Impact GbR, Bonn, Germany, 2006.
[17] HyperChemTM Release 7.52, Windows Molecular Modeling System, HyperCube Inc., 2002.

6.3 Theoretical calculations of non-coordinated PNP-ligands

6.3.1 PNP-*c*Prop (1 *vs* 1*)

The PNP-*c*Prop (1) crystal structure, see §4.3 is visually compared to the corresponding calculated structure (1*) (**Figure 6.1**).

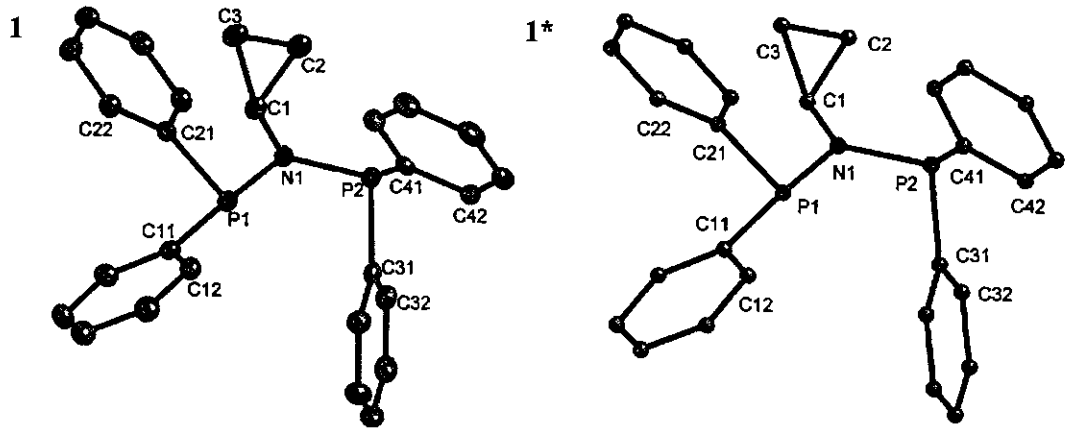


Figure 6.1: Graphical representation of the crystal structure (1) at 50 % probability and DFT optimized structure (1*) of PNP-*c*Prop. Hydrogen atoms were omitted for clarity.

Table 6.1: Comparison of selected geometrical parameters of crystal structure PNP-*c*Prop (1) with the theoretical structure (1*) (Å and °).

Bond length	$1_{Crystal}$	1^*_{DFT}	Bond angle	$1_{Crystal}$	1^*_{DFT}
P1 – N1	1.730(1)	1.756	P1 – N1 – P2	122.6(1)	120.8
P2 – N1	1.721(1)	1.758	C1 – N1 – P1	120.3(1)	121.1
N1 – C1	1.452(2)	1.459	C1 – N1 – P2	116.0(1)	116.8
P1 – C11	1.834(2)	1.857	C11 – P1 – C21	100.4(1)	101.5
P1 – C21	1.843(2)	1.859	C31 – P2 – C41	102.3(1)	102.3
P2 – C31	1.835(2)	1.859			
P2 – C41	1.828(2)	1.849			

The P-N bond lengths of the crystal structure are slightly shorter (1.730(1) and 1.721(1) Å) than that of the optimized structure (1.756 Å and 1.758 Å for bond lengths, P1-N1 and P2-N1 respectively). This is the same for the C-P bonds which are shorter for the crystal structure (1.828(2) -1.843(2) Å) than the calculated structure (1.849 - 1.859 Å).

The P-N-P bond angle for the calculated structure (120.8 °) is only 1.8 ° smaller than that of the solid state crystal structure (122.6(1) °). The rest of the bond angles as reported in **Table 6.1** are very similar within experimental error. Both structures adopt a C_S conformation (see Chapter 4, **Figure 4.2**) as can be seen by an overlay of the two structures given (**Figure 6.2**) with a RMS value of 0.201 Å.

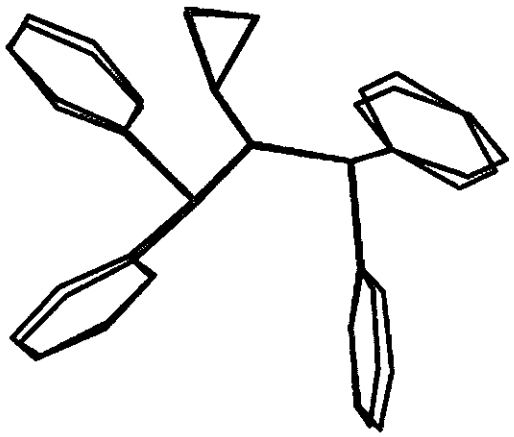


Figure 6.2: Graphical representation of an overlay of the crystal structure (red) and the DFT optimized structure (black) of PNP-*c*Prop (RMS value = 0.201 Å). Overlay fit excluded all hydrogen atoms.

6.3.2 PNP-*c*But (2 *vs* 2*)

The PNP-*c*But (2) crystal structure, see §4.4 is visually compared to the corresponding calculated structure (2*) in **Figure 6.3**.

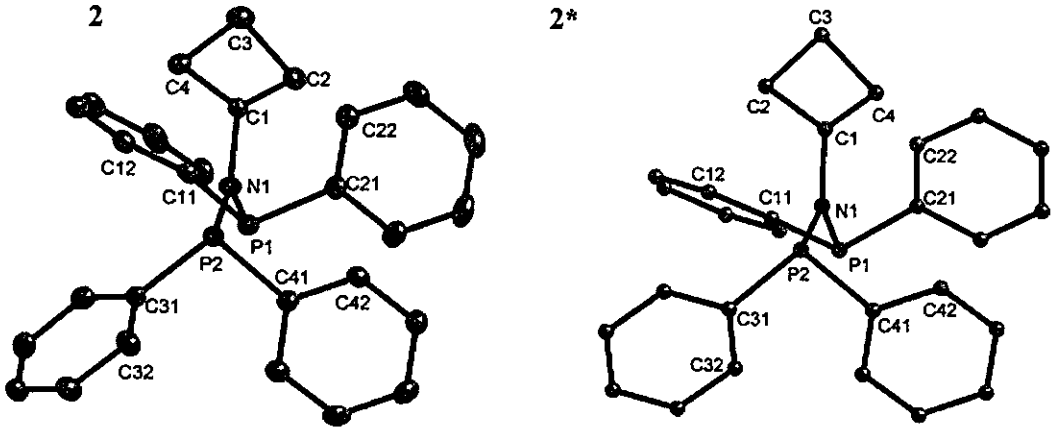


Figure 6.3: Graphical representation of the crystal structure (2) at 50 % probability and DFT optimized structure (2*) of PNP-*c*But. Hydrogen atoms were omitted for clarity.

Table 6.2: Comparison of selected geometrical parameters of crystal structure PNP-*c*But (2) with the theoretical structure (2*) (Å and °).

Bond length	$2_{Crystal}$	2^*_{DFT}	Bond angle	$2_{Crystal}$	2^*_{DFT}
P1 – N1	1.714(2)	1.744	P1 – N1 – P2	123.5(1)	121.6
P2 – N1	1.719(2)	1.747	C1 – N1 – P1	120.8(1)	122.0
N1 – C1	1.478(2)	1.476	C1 – N1 – P2	115.2(1)	116.4
P1 – C11	1.837(2)	1.854	C11 – P1 – C21	100.0(1)	101.3
P1 – C21	1.840(2)	1.864	C31 – P2 – C41	101.4(1)	102.8
P2 – C31	1.838(2)	1.856			
P2 – C41	1.827(2)	1.848			

The P-N bond lengths of the crystal structure are yet again shorter (1.714(2) and 1.719(2) Å) than that of the calculated structure (1.744 Å and 1.747 Å for bond lengths, P1-N1 and P2-N1 respectively). Also, the C-P bonds are shorter for the crystal structure (1.827(2) - 1.840(2) Å) than the calculated structure (1.848 - 1.864 Å). Similar trends were observed for PNP-*c*Prop.

The P-N-P bond angle of 121.6 ° for the calculated structure is slightly smaller than that of the solid state crystal structure (123.5(1) °). The C1-N1-P1 angle of 122.0 ° for the calculated

structure is also slightly larger than the 120.8 ° for the crystal structure. The rest of the bond angles as reported in **Table 6.2** are similar within experimental error. An overlay of the two structures (RMS = 0.418 Å) indicate that both structures adopt a C_S conformation (see Chapter 4, **Figure 4.2**) as can be seen in **Figure 6.4**.

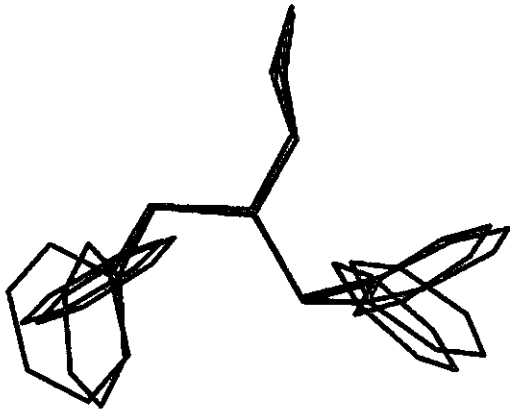


Figure 6.4: Graphical representation of an overlay of the crystal structure (red) and the DFT optimized structure (black) of PNP-*c*But (RMS value = 0.418 Å). Overlay fit excluded all hydrogen atoms.

6.3.3 PNP-*c*Pent (3 *vs* 3*)

The PNP-*c*Pent (3) crystal structure, see §4.5 is visually compared to the corresponding calculated structure (3*) (**Figure 6.5**).

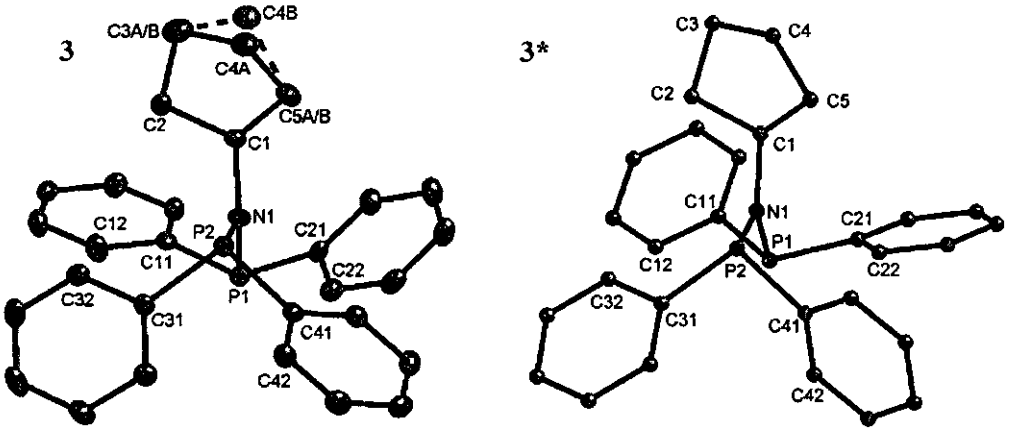


Figure 6.5: Graphical representation of the crystal structure (3) at 50 % probability and DFT optimized structure (3*) of PNP-*c*Pent. Hydrogen atoms were omitted for clarity.

Table 6.3: Comparison of selected geometrical parameters of crystal structure PNP-*c*Pent (3) with the theoretical structure (3*) (Å and °).

Bond length	$3_{Crystal}$	3^*_{DFT}	Bond angle	$3_{Crystal}$	3^*_{DFT}
P1 – N1	1.716(2)	1.746	P1 – N1 – P2	121.8(1)	121.8
P2 – N1	1.721(2)	1.751	C1 – N1 – P1	121.4(1)	122.1
N1 – C1	1.499(2)	1.491	C1 – N1 – P2	115.2(1)	116.1
P1 – C11	1.847(2)	1.864	C11 – P1 – C21	101.7(1)	101.5
P1 – C21	1.839(2)	1.855	C31 – P2 – C41	100.6(1)	102.6
P2 – C31	1.842(2)	1.849			
P2 – C41	1.827(2)	1.858			

The P-N and P-C bond lengths for the calculated structure is longer than for the crystal structure, with P-N bond lengths of 1.746 and 1.751 Å compared to 1.716(2) and 1.721(2) Å for the calculated and crystal structure respectively. The P-C bond lengths of 1.849 - 1.864 Å for the calculated structure are also slightly larger than for the solid state structure with values ranging between 1.827(2) and 1.847(2) Å.

The P-N-P angle for the crystal- and calculated structure are exactly the same (121.8 °), unlike the previously discussed compounds (PNP-*c*Prop and PNP-*c*But) in which the P-N-P angle of the calculated structure was smaller than for the crystal structure in both cases. The C1-N1-P1 angle of 122.1 ° for **3*** is slightly larger than the crystal data angle of 121.4(1) °. The rest of the bond angles as reported in **Table 6.3** are similar within experimental error.

One carbon atom (C4) in the cyclopentyl ring (**Figure 6.5**) shows a 0.822(4):0.178(4) positional disorder in the crystal structure (Chapter 4). Therefore, an overlay was done for both the major- and minor disordered crystal with the calculated structure.

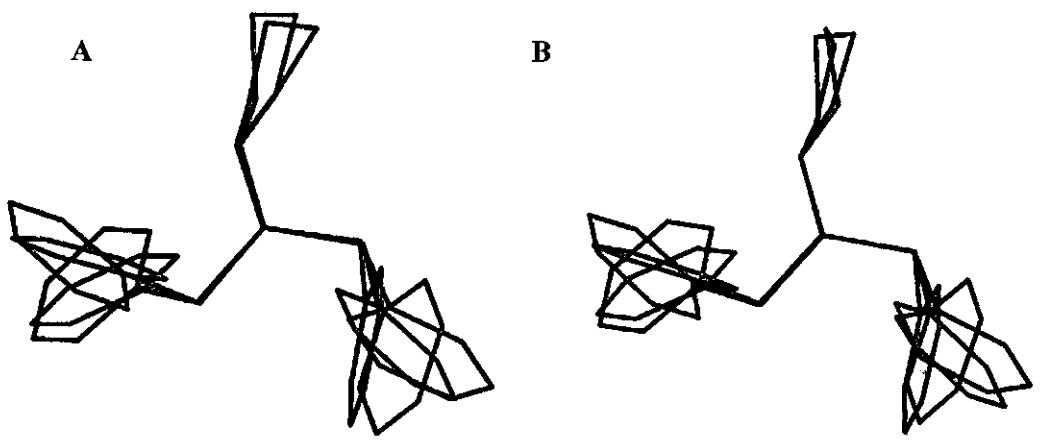


Figure 6.6: Graphical representation of an overlay of the major (**A**) and minor (**B**) distorted crystal structures (red) and the DFT optimized structures (black) of PNP-*c*Pent (RMS value = 0.892 and 0.894 Å for **A** and **B** respectively). Overlay fit excluded all hydrogen atoms.

Both the major- and minor disordered structures have reasonable overlays with the calculated structure with RMS values of 0.892 and 0.894 Å, respectively. Even though the phenyl rings do not match perfectly, it is clear from **Figure 6.5** that both the crystal- and calculated structures have the same C_S conformation (see Chapter 4, **Figure 4.2**).

It is clear that there are seemingly more spacial degrees of freedom in the optimized structures. The fact that there is a statistical disorder present in the solid state, is a manifestation of this.

6.4 Theoretical calculations of [Pt(PNP-alkyl)$_2$] complexes

6.4.1 [Pt(PNP-*c*Prop)$_2$] (4 *vs* 4*)

The [Pt(PNP-*c*Prop)$_2$] (4) crystal structure, see §5.3 is visually compared to the corresponding calculated structure (4*) (**Figure 6.7**).

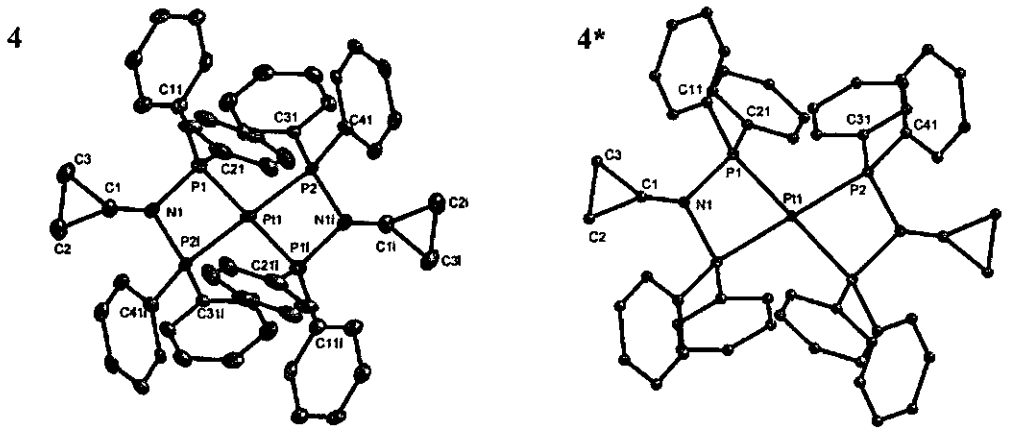


Figure 6.7: Graphical representation of the crystal structure (4) at 50 % probability and DFT optimized structure (4*) of [Pt(PNP-*c*Prop)$_2$]. Hydrogen atoms were omitted for clarity.

The optimized structure adopted a distorted square-planar geometry similar to the corresponding crystal structure with a P-Pt-P angle of 72.1 *vs* 71.5(1) °, deviating significantly from the ideal 90 ° (**Table 6.4**). The P-N-P angle for the solid state is less than for the optimized (101.2(5) *vs* 104.7 °). All C-P-C angles are very similar for both calculated and crystal structures.

Table 6.4: Comparison of selected bond angles (°) of crystal structure [Pt(PNP-*c*Prop)$_2$] (4) with the theoretical structure (4*).

Bond angles	$4_{Crystal}$	4^*_{DFT}
P1 – Pt – P2	71.5(1)	72.1
P1 – N1 – P2	101.2(5)	104.7
C11 – P1 – C21	106.4(7)	107.7
C31 – P2 – C41	107.7(5)	107.8

Table 6.5: Comparison of selected bond lengths (Å) of crystal structure [Pt(PNP-*c*Prop)$_2$] (4) with the theoretical structure (4*).

Bond Length	$4_{Crystal}$	4^*_{DFT}
Pt – P1	2.277(3)	2.425
Pt – P2	2.290(3)	2.425
P1 – N1	1.729(11)	1.801
P2 – N1	1.724(10)	1.803
N1 – C1	1.440(16)	1.456
P1 – C11	1.798(13)	1.861
P1 – C21	1.805(15)	1.856
P2 – C31	1.787(11)	1.856
P2 – C41	1.801(12)	1.860

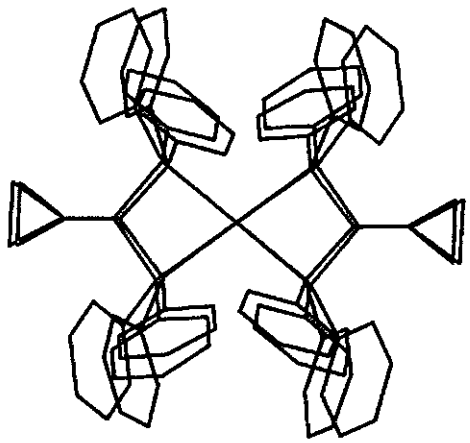


Figure 6.8: Graphical representation of an overlay of the crystal structure (red) and the DFT optimized structure (black) of [Pt(PNP-*c*Prop)$_2$]. (RMS value = 0.680 Å). Overlay fit excluded all hydrogen atoms.

Slightly longer bond lengths are predicted in the optimized structure in comparison to the corresponding bond lengths of the crystal structure (**Table 6.5**). The visual comparison of the two structures yields a reasonable overlay with a RMS value of 0.680 Å.

6.4.2 [Pt(PNP-*c*Pent)$_2$] (5 *vs* 5*)

The predicted structure for [Pt(PNP-*c*Pent] (5*) and the crystal structure (5) (see §5.5) to which it is compared is shown in **Figure 6.9**.

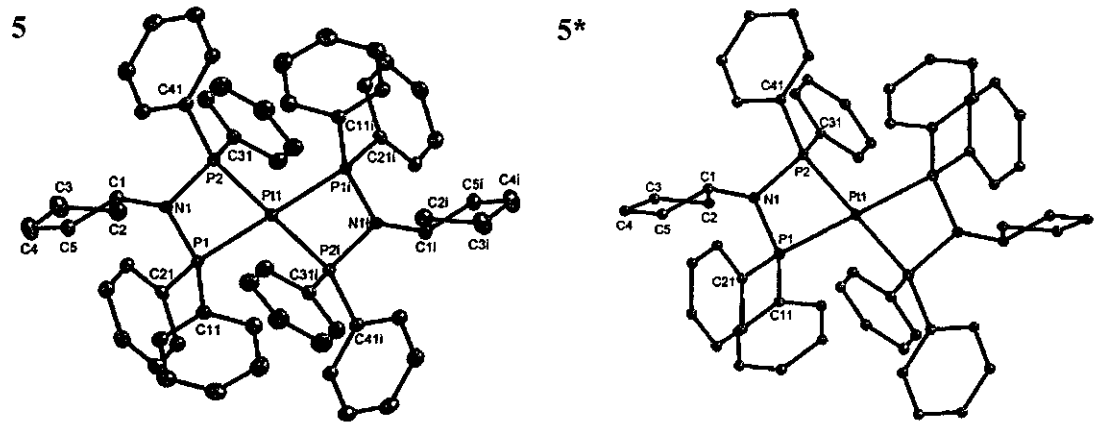


Figure 6.9: Graphical representation of the crystal structure (5) at 50 % probability and DFT optimized structure (5*) of [Pt(PNP-*c*Pent)$_2$]. Hydrogen atoms were omitted for clarity.

Table 6.6: Comparison of selected bond angles (°) of crystal structure [Pt(PNP-*c*Pent)$_2$] (5) with the theoretical structure (5*).

Bond angles	$5_{Crystal}$	5^*_{DFT}
P1 – Pt – P2	70.31(4)	72.0
P1 – N1 – P2	102.3(2)	105.3
C11 – P1 – C21	105.1(2)	108.1
C31 – P2 – C41	108.0(2)	106.6

The P-Pt-P bite angle for the calculated structure (72.0 °) is slightly larger than the corresponding angle found in the crystal structure (70.31(4) °) (**Table 6.6**). The difference between the P-N-P angle of the crystal and calculated structure is 2.93 °. The distortion of the square-planar geometry of the Pt-PNP complex is evident from the P-Pt-P bite angle which deviates from the ideal 90 ° geometry. The C-P-C (C11-P1-C21 and C31-P2-C41) angles are 105.1(2) and 108.0(2) °, respectively which are similar to the corresponding calculated angles of 108.1 and 106.6 °.

Table 6.7: Comparison of selected bond lengths (Å) of crystal structure [Pt(PNP-*c*Pent)$_2$] (5) with the theoretical structure (5*).

Bond Length	$5_{Crystal}$	5^*_{DFT}
Pt – P1	2.314(1)	2.427
Pt – P2	2.294(1)	2.420
P1 – N1	1.704(4)	1.795
P2 – N1	1.703(4)	1.790
N1 – C1	1.484(6)	1.496
P1 – C11	1.805(4)	1.861
P1 – C21	1.806(4)	1.864
P2 – C31	1.794(4)	1.860
P2 – C41	1.805(4)	1.862

The bond lengths in **Table 6.7** reveals longer bond lengths for the optimized complex (5*) in comparison with the corresponding lengths of the crystal structure (5).

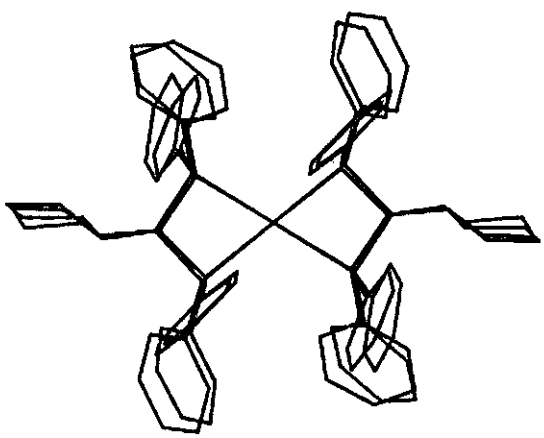


Figure 6.10: Graphical representation of an overlay of the crystal structure (red) and the DFT optimized structure (black) of [Pt(PNP-*c*Pent)$_2$]. (RMS value = 0.345 Å). Overlay fit excluded all hydrogen atoms.

The visual comparison between the crystal and optimized structure is given in **Figure 6.10**. A adequate overlay was obtained for the solid state structure compared to the optimized structure with a RMS values of 0.345 Å.

6.4.3 [Pt(PNP-*c*Hex)$_2$] (6 *vs* 6*)

The crystal structure of [Pt(PNP-*c*Hex] (6) (see §5.6) contains a 0.630(7):0.370(7) occupancy disorder of the cyclohexyl moiety, bonded to N, as well as a 0.60(2):0.40(2) positional disorder of the C11—C16 phenyl ring, bonded to P1 (see Chapter 5, **Figure 5.13**). Both the major- and minor disordered parts of the crystal structure are compared to the calculated structure (6*) (**Figure 6.11** and **Figure 6.12**, respectively).

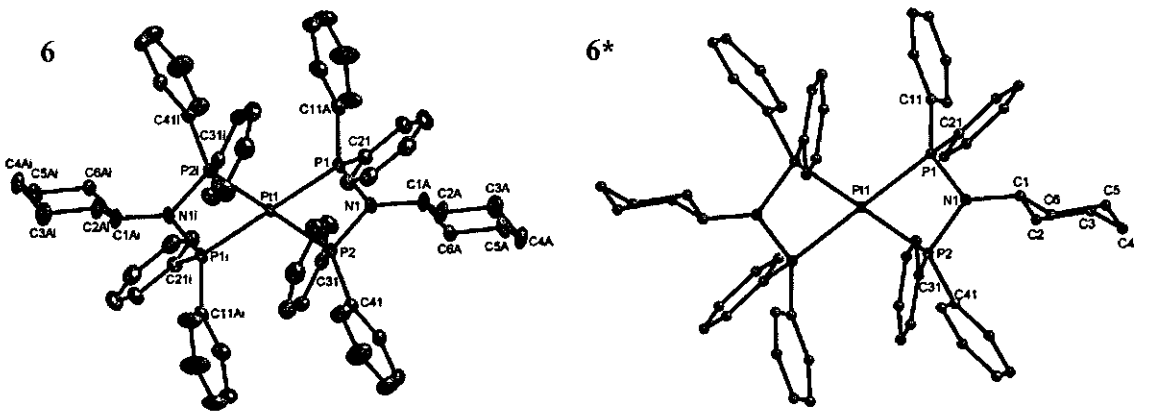


Figure 6.11: Graphical representation of the major disordered crystal structure (6) at 50 % probability and DFT optimized structure (6*) of [Pt(PNP-*c*Hex)$_2$]. Major disordered parts belonging together are numbered with an A. Hydrogen atoms were omitted for clarity.

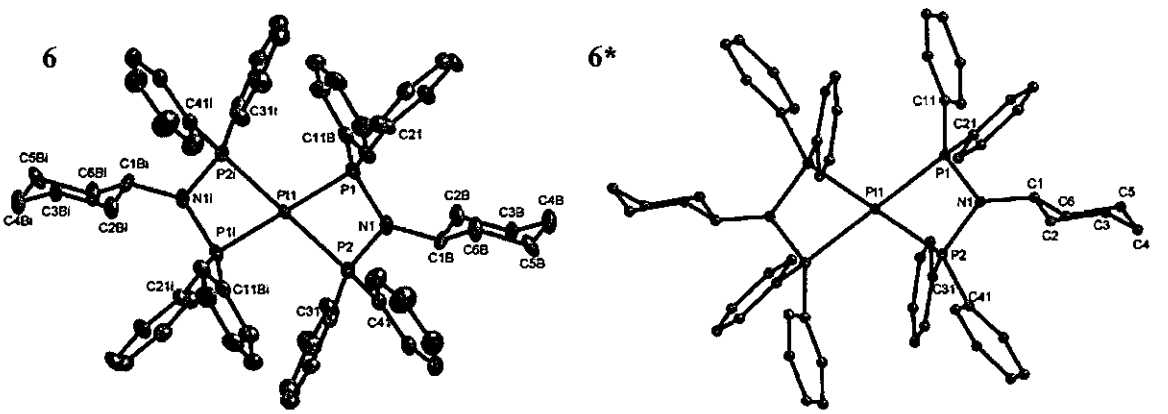


Figure 6.12: Graphical representation of the minor disordered crystal structure (6) at 50 % probability and DFT optimized structure (6*) of [Pt(PNP-*c*Hex)$_2$]. Minor disordered parts belonging together are numbered with a B. Hydrogen atoms were omitted for clarity.

Table 6.8: Comparison of selected bond angles (°) of crystal structure [Pt(PNP-*c*Hex)$_2$] (6) with the theoretical structure (6*).

Bond angles	$6_{Crystal}$	6^*_{DFT}
P1 – Pt – P2	70.76(3)	72.0
P1 – N1 – P2	102.6(1)	105.2
C11A – P1 – C21	106.0(9)	106.4
C11B – P1 – C21	102.4(13)	-
C31 – P2 – C41	111.0(1)	108.6

The P1-Pt-P2 bite angle for the calculated structure (72.0 °) is again slightly larger than that of the crystal structure (70.76(3) °), but both indicate a significant deviation from the 90 ° angle expected for a square-planar complex (**Table 6.8**). The C-P-C (C11A-P1-C21 and C31-P2-C41) angles for the major disordered part of the crystal structure are 106.0(9) and 111.0(1) °, respectively which are similar to the corresponding calculated angles of 106.4 and 108.6 °. These values however, differ slightly from the C11B-P1-P21 angle of 102.4(13) ° for the minor disordered crystal structure.

Table 6.9: Comparison of selected bond lengths (Å) of crystal structure [Pt(PNP-*c*Hex)$_2$] (6) with the theoretical structure (6*).

Bond Length	$6_{Crystal}$	6^*_{DFT}
Pt – P1	2.292(1)	2.421
Pt – P2	2.300(1)	2.425
P1 – N1	1.701(3)	1.789
P2 – N1	1.706(2)	1.795
N1 – C1A	1.480(12)	1.507
N1 – C1B	1.56(2)	-
P1 – C11A	1.811(16)	1.862
P1 – C11B	1.79(3)	-
P1 – C21	1.799(3)	1.861
P2 – C31	1.804(3)	1.864
P2 – C41	1.794(3)	1.860

The bond lengths compare well for the corresponding **6** and **6*** structures with the crystal structure containing slightly shorter bond lengths (**Table 6.9**).

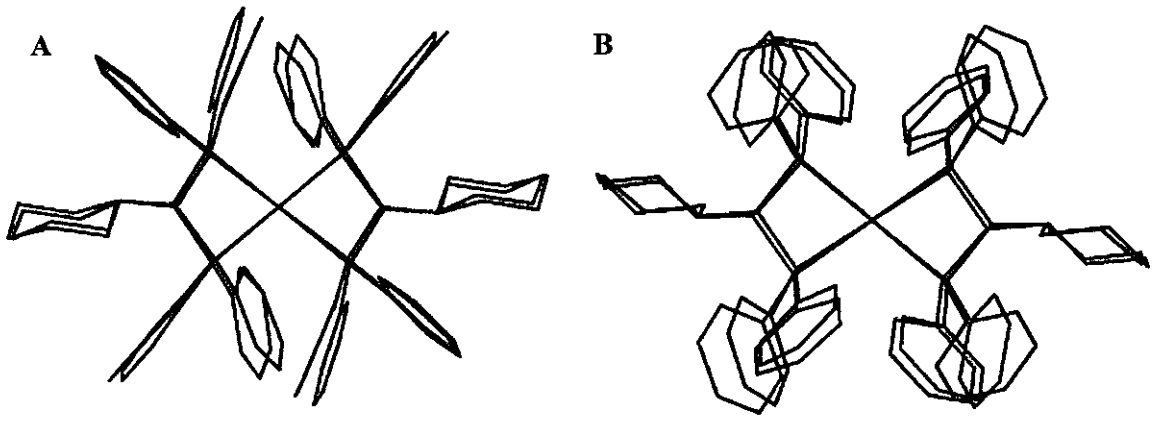


Figure 6.13: Graphical representation of an overlay of the major (**A**) and minor (**B**) distorted crystal structures (red) and the DFT optimized structures (black) of [Pt(PNP-*c*Hex)$_2$] (RMS value = 0.313 and 1.333 Å for **A** and **B** respectively). Overlay fit excluded all hydrogen atoms.

The visual comparison between the major- and minor disordered parts of the crystal structure compared to the optimized structure is seen in (**Figure 6.13 A** and **B**). The overlay of the major disordered solid state structure with the DFT structure gives a good RMS value of 0.313 Å, while the overlay between the minor disordered part of **6** with **6*** gives a less desirable RMS value of 1.333 Å. This is due to the phenyl ring orientation of the disordered C11—C16 phenyl ring of the crystal structure with C11B-P1-C21 angle of 102.4(13) ° compared to 106.4 ° for **6***. **Figure 6.14** shows the difference in the disordered phenyl ring orientation with the conformational switch of the cyclohexyl ring.

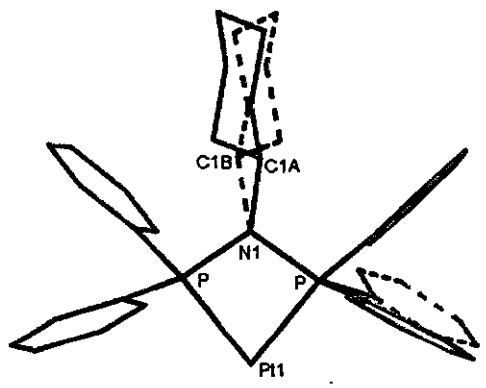


Figure 6.14: Partial structural view of the crystal structure of [Pt(PNP-*c*Hex)$_2$] (6). Disordered parts belonging together are numbered A and B respectively. Fragmented lines indicate the minor disordered crystal structure.

6.4.4 [Pd(PNP-*c*Prop)$_2$] (7 *vs* 7*)

There are two independent Pd(II) molecules in the asymmetric unit of the crystal structure (see §5.7). An overlay of these two independent molecules showed they are very similar with a RMS value of 0.120 Å. Therefore, the predicted structure for [Pd(PNP-*c*Prop] (7*) will only be compared to one of the independent molecules of the solid state structure (7) as given in **Figure 6.15**.

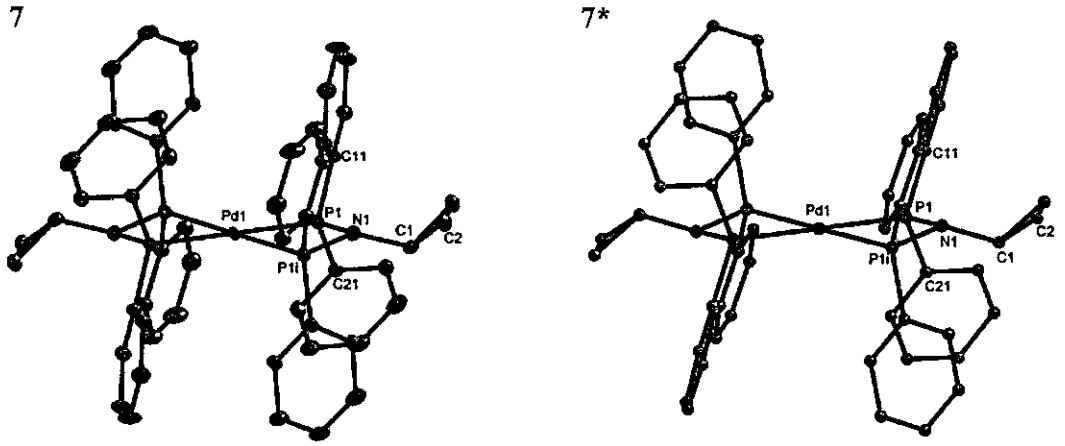


Figure 6.15: Graphical representation of the crystal structure (7) at 50 % probability and DFT optimized structure (7*) of [Pd(PNP-*c*Prop)$_2$]. Hydrogen atoms were omitted for clarity.

Table 6.10: Comparison of selected bond angles (°) of crystal structure [Pd(PNP-*c*Prop)$_2$] (7) with the theoretical structure (7*).

Bond angles	$7_{Crystal}$	7^*_{DFT}
P1 – Pd1 – P1i	70.4(1)	72.1
P1 – N1 – P1i	102.3(5)	105.3
C11 – P1 – C21	106.8(4)	107.5

The P-Pt-P angles for both the crystal structure (70.4(1) °) and DFT structure (72.1 °) indicate the distorted square-planar geometry around the Pt(II) with the DFT calculated angle slightly larger than the solid state structure (**Table 6.10**). The P-N-P angle for 7* (105.3 °) is somewhat larger than for 7 (102.3(5) °).

Table 6.11: Comparison of selected bond lengths (Å) of crystal structure [Pd(PNP-*c*Prop)$_2$] (7) with the theoretical structure (7*).

Bond Length (Å)	$7_{Crystal}$	7^*_{DFT}
Pd1 – P1	2.304(2)	2.435
P1 – N1	1.706(7)	1.802
N1 – C1	1.469(2)	1.457
P1 – C11	1.785(9)	1.861
P1 – C21	1.786(9)	1.859

All bond lengths **Table 6.11** are as expected all a bit longer for the optimized structure compared to the corresponding lengths of the crystal structure.

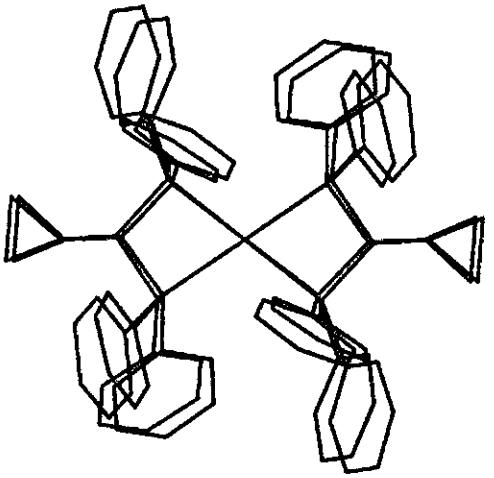


Figure 6.16: Graphical representation of an overlay of the crystal structure (red) and the DFT optimized structure (black) of [Pd(PNP-*c*Prop)$_2$] (RMS value = 0.409 Å). Overlay fit excluded all hydrogen atoms.

A RMS value of 0.409 Å was obtained for the overlay of the crystal structure with the DFT optimized structure of [Pd(PNP-*c*Prop)$_2$] and a visual representation of the overlay is given in **Figure 6.16.**

6.5 Discussion

6.5.1 Non-coordinated PNP-ligands

The theoretical structures for various PNP-ligands (PNP-*c*Prop, PNP-*c*But and PNP-*c*Pent) were successfully calculated and optimized. A trend was observed for the series of free PNP-alkyl ligand crystals (discussed in Chapter 4) in which the P-N-P angle became smaller as the steric bulk of the alkyl moiety increased. The same trend was observed for the calculated PNP-alkyl structures, although not as apparent compared to the crystal data, with the P-N-P angle of PNP-Ethyl (122.8 °) being 2.8 ° larger than for PNP-Dimprop (120.0 °) (**Table 6.12**).

Table 6.12: Comparison of selected bond angles (°) for optimized and crystallographic structures of non-coordinated PNP-alkyl ligands.

Ligand	P – N – P (Crystal)	P – N – P (DFT)	$\theta_{N\text{-}sub}$ (°) (Crystal)[a]	$\theta_{N\text{-}sub}$ (°)* (DFT)	$\theta_{N\text{-}sub}$ (°) (Average)	Conformation
PNP-Ethyl[b]	123.7(1)	122.8	62.9	63.8	63.4	C_S
PNP-*n*Pent[b]	123.4(1)	121.1	63.2	64.6	63.9	C_S
PNP-*c*Prop	122.6(1)	120.8	68.5	70.9	69.7	C_S
PNP-*c*But	123.5(1)	121.6	73.1	75.9	74.5	C_S
PNP-*c*Pent	121.8(1)	121.8	79.3	82.9	81.1	C_S
PNP-*i*Prop[c]	122.8(3)	-	80.3	-	80.3	C_S
PNP-*c*Hex[b]	119.0(1)	121.3	81.3	84.5	82.9	C_S
PNP-Dimprop[d]	117.9(1)	120.0	88.5	83.9	86.2	C_S

[a] $\theta_{N\text{-}Sub}$ determined from the crystallographic data, see Chapter 4. [b] See Ref 18. [c] See Ref 19. [d] See Ref 20.

All the optimized structures adopted the same Cs conformation (see Chapter 4, **Figure 4.2**) as their corresponding crystal structures as expected in order to accommodate the steric bulk of the substituent on the N-atom (**Table 6.12**). The $\theta_{N\text{-}sub}$ values calculated for the crystal structures are in good correlation with the corresponding DFT optimized structures.

[18] N.Cloete, PhD thesis, University of the Free State, 2009.
[19] R. Keat, L. Manojlovic-Muir, K.W. Muir, D.S. Rycroft, *J. Chem. Soc. Dalton Trans.*, (1981) 2192.
[20] N. Cloete, H.G. Visser, A. Roodt, J.T. Dixon, K. Blann, *Acta Cryst.*, E64 (2008) o480.

The N1-C1 bond lengths for the optimized and crystallographic structures are similar within experimental error (**Table 6.13**). All other bond lengths for the optimized structures were longer than the corresponding bond lengths of the related crystal structures. It is inherent of the technique, when performing theoretical calculations, to over-estimate the bond lengths for the structures calculated.[4,5]

Table 6.13: Selected bond lengths (Å) for optimized and crystallographic structures of non-coordinated PNP-alkyl ligands.

Ligand	P1 – N1 (Crystal)	P1 – N1 (DFT)	P2 – N1 (Crystal)	P2 – N1 (DFT)	N1 – C1 (Crystal)	N1 – C1 (DFT)
PNP-Ethyl[a]	1.712(1)	1.744	1.713(1)	1.749	1.485(2)	1.487
PNP-*n*Pent[a]	1.713(1)	1.736	1.712(1)	1.728	1.482(1)	1.488
PNP-*c*Prop	1.730(1)	1.756	1.721(1)	1.758	1.452(2)	1.459
PNP-*c*But	1.714(2)	1.744	1.719(2)	1.747	1.478(2)	1.476
PNP-*c*Pent	1.716(2)	1.746	1.721(2)	1.751	1.499(2)	1.491
PNP-*c*Hex[a]	1.758(4)	1.752	1.686(5)	1.749	1.502(6)	1.499
PNP-Dimprop[b]	1.721(2)	1.752	1.727(2)	1.753	1.515(2)	1.505

[a] See Ref 18. [b] See Ref 20.

It appears that selected bond lengths (P1-N1, P2-N1 and N1-C1) for the calculated and free PNP-ligands increase in length as the alkyl moiety of the PNP-ligands become more sterically bulky (**Table 6.13**). The above-mentioned bond lengths are for example slightly longer for PNP-Dimprop in comparison to the corresponding bond lengths of PNP-Ethyl. It is possible that the bonds are calculated to be longer in order to accommodate the sterically bulky alkyl substituent on the nitrogen atom. It is of interest to note that a similar trend with regards to the bond lengths were observed and discussed in the crystallographic study of the non-coordinated PNP-ligands in Chapter 4.

6.5.2 [Pt/Pd(PNP-alkyl)$_2$] complexes

The structures of various [Pt(PNP-alkyl)$_2$] and [Pd(PNP-alkyl)$_2$] compounds were successfully calculated and optimized. The bond angles for the various [Pt(PNP-alkyl)$_2$] calculated complexes compare well to the corresponding crystal structures and to [PtCl$_2$(PNP-alkyl)] complexes in literature (**Table 6.14**). The P-Pt-P bite angles for the optimized complexes range between 72.0 and 74.0 °, indicating a significantly distorted square-planar geometry at the platinum(II) centre.

The reported P-Pt-P small bite angle forces the P-N-P angle to 101.4 - 105.7 °, which is significantly smaller than the corresponding angles of the free PNP-alkyl ligand structures which were calculated to be between 120.0 and 122.8 ° (**Table 6.13**). This illustrates the deviation from the ideal tetrahedral geometry around the nitrogen atom. The P-N-P angles for the crystallized structures are slightly smaller than for the optimized structures. The distorted tetrahedral geometry at the phosphorous atoms is evident from the C-P-C angles of the calculated structures which ranging between 106.6 and 108.6 °. The distortions predicted for the calculated [Pt(PNP-alkyl)$_2$] complexes are similar to that of the corresponding crystal complexes as discussed in Chapter 5.

Table 6.14: Comparison of selected bond angles (°) for optimized and crystallographic structures of [Pt(PNP-alkyl)$_2$] and [PtCl$_2$(PNP-alkyl)] complexes.

Complex	P – Pt – P (Crystal)	P – Pt – P (DFT)	P – N – P (Crystal)	P – N – P (DFT)
[PtCl$_2$(PNP-Ethyl)][a]	72.1(1)	72.8	100.0(2)	101.4
[Pt(PNP-*n*Pent)$_2$][b]	70.45(3)	-	103.40(13)	-
[Pt(PNP-*n*Pent)$_2$][b]	70.64(3)	-	103.15(13)	-
[Pt(PNP-*c*Prop)$_2$]	71.5(1)	72.1	101.2(5)	104.7
[Pt(PNP-*c*But)$_2$]	70.23(6)	72.1	102.2(3)	105.7
[Pt(PNP-*c*Pent)$_2$]	70.31(4)	72.0	102.32(19)	105.3
[Pt(PNP-*c*Hex)$_2$]	70.76(3)	72.0	102.58(12)	105.2
[PtCl$_2$(PNP-Dimprop)][a]	72.3(1)	74.0	98.6(4)	102.5

[a] See Ref 18. [b] The P-Pt-P and P-N-P angles for [Pt(PNP-*n*Pent)$_2$] are as follows: P1-Pt-P2, P3-Pt-P4, P1-N1-P2 and P3-N2-P4 due to non symmetrical PNP-*n*Pent ligands in the crystal structure.

The bond angles for the predicted structures of the [Pd(PNP-alkyl)$_2$] complexes (**Table 6.15**) are comparable to the bond angles of the respective platinum complexes (**Table 6.14**). This was expected as Pt(II) and Pd(II) analogue complexes generally behave in the same manner. The Pd(II) complexes share the same distorted square-planar geometry around the metal centre with P-Pd-P angles ranging between 71.9 and 72.1 ° for the optimized structures. Only one crystal structure was obtained for the palladium complexes ([Pd(PNP-*c*Prop)$_2$]) which is also in good correlation with the DFT calculated structure. The P-N-P angles of 100.6 - 106.2 ° are also similar to those of the platinum analogues with P-N-P angles of the solid state structures being slightly smaller than the P-N-P angles for the optimized structures. The bond lengths for all the optimized structures are slightly longer than the corresponding bond lengths of the related crystal structures. It is inherent of the technique, when performing theoretical calculations, to over-estimate the bond lengths for the structures calculated.[4,5]

Table 6.15: Comparison of selected bond angles (°) for the calculated and crystal [Pd(PNP-alkyl)$_2$] and [PdCl$_2$(PNP-alkyl)] complexes.

Complex	P – Pt – P (Crystal)	P – Pd – P (DFT)	P – N – P (Crystal)	P – N – P (DFT)
[Pd(PNP-*c*Prop)$_2$][a]	70.4(1)	72.1	102.3(5)	105.3
[Pd(PNP-*c*Prop)$_2$][a]	70.8(1)	-	102.0(6)	-
[Pd(PNP-*c*But)$_2$]	-	72.0	-	106.2
[Pd(PNP-*c*Pent)$_2$]	-	71.9	-	105.6
[PdCl$_2$(PNP-Dimprop)][b]	71.6(1)	72.1	99.7(3)	100.6

[a] The P-Pd-P and P-N-P angles for [Pd(PNP-*c*Prop)$_2$] are as follows: P1-Pd-P1i, P2-Pd-P2i, P1-N1-P1i and P2-N2-P2i due to the two independent Pd(II) molecules in the asymmetric unit of the crystal structure. [b] See Ref 18.

6.5.3 Phenyl ring orientations for [Pt/Pd(PNP-alkyl)$_2$] complexes

There are two distinct conformations ("basket"-like and "fan"-like)[18] for the orientation of the phenyl rings for these square-planar complexes and these conformations are best described with the use of torsion angles. In the "basket"-like conformation, Ring 2 (ring containing R21) and Ring 3 (ring containing R31) are twisted towards each other (**Figure 6.17**) with torsion angles of ±175 ° for Ring 2 (M-P-R21-R22) and ±10 ° for Ring 3 (M-P-R31-R32) (**Table 6.16**). Ring 1 and 4 have approximately the same orientation.

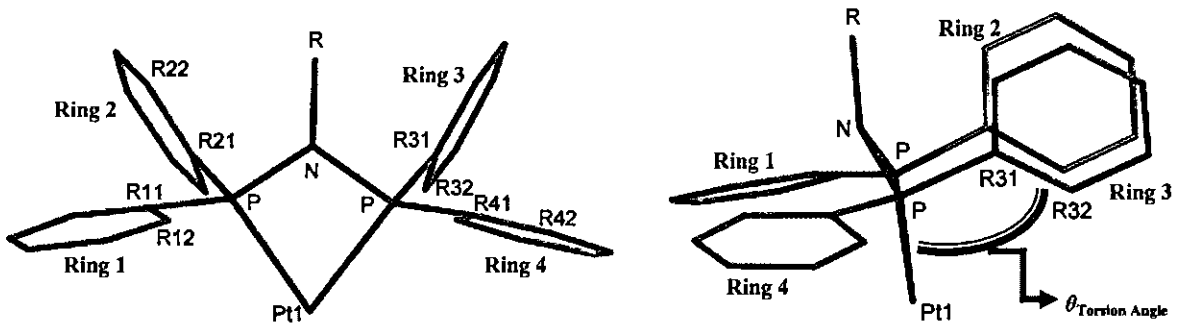


Figure 6.17: Graphical representation of part of the metal complex of different viewing angles of the "basket"-like conformation as adopted by selected platinum(II) and palladium(II) PNP-ligand coordinated complexes. (R = alkyl moiety).

The complexes that have the 'basket-like' conformation and slight variations thereof are: [Pt(PNP-*c*Prop)$_2$], [Pt(PNP-*c*Pent)$_2$], [Pt(PNP-*c*Hex)$_2$] (**Table 6.16**). The phenyl rings of [M(PNP-alkyl)$_2$] (M = Pt(II)/Pd(II)) complexes with alkyl moieties that are less sterically bulky have more degrees of freedom and the phenyl rings adopt a "fan"-like orientation (**Figure 6.18**). In this type of conformation, Rings I and 3 has a flatter orientation, as illustrated in **Figure 6.18**, whereas Rings 2 and 4 are twisted. Typical torsion angles for Rings 1 and 3 are ±80 ° and ±175 ° for Rings 2 and 4.

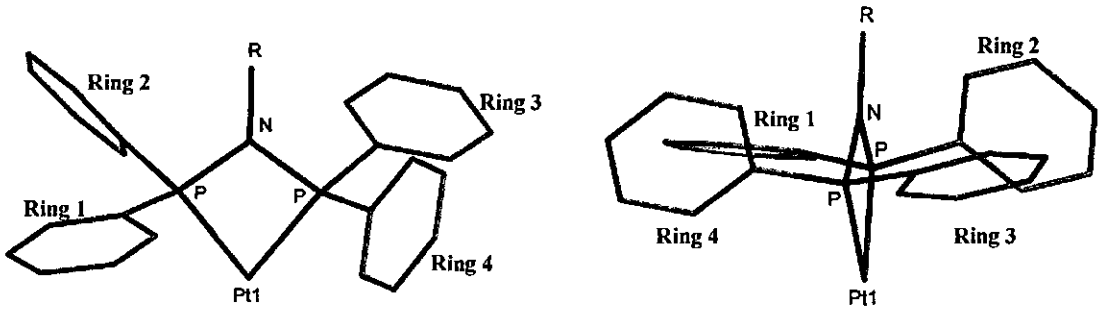


Figure 6.18: Graphical representation of part of the metal complex from different viewing angles of the "fan"-like conformation as adopted by selected platinum(II) and palladium(II) PNP-ligand coordinated complexes. (R = alkyl moiety).

Table 6.16: Comparison of selected torsion angles (°) of the crystal structures for [M(PNP-alkyl)$_2$] (M = Pt(II)/Pd(II)) with the theoretical structures.

Compounds	Ring 1 Crystal	Ring 1* DFT	Ring 2 Crystal	Ring 2* DFT	Ring 3 Crystal	Ring 3* DFT	Ring 4 Crystal	Ring 4* DFT
[PtCl$_2$(PNP-Ethyl)][a]	-63.6(4)	-63.9	175.2(3)	174.5	-80.8(4)	-67.5	-172.8(3)	173.1
[PtCl$_2$(PNP-*n*Prop)][a]	76.7(2)	68.1	176.6(2)	173.6	60.1(2)	-65.1	178.1(2)	-174.7
[Pt(PNP-*n*Pent)$_2$][b]	65.0(3)	-	-177.7(3)	-	64.0(4)	-	174.9(3)	-
[Pt(PNP-*n*Pent)$_2$][b]	65.8(3)	-	179.1(3)	-	79.5(3)	-	171.5(3)	-
[Pt(PNP-*c*Prop)$_2$]	65.0(1)	69.2	-176.9(8)	-174.5	-7.2(2)	0.4	98.3(1)	102.5
[Pd(PNP-*c*Prop)$_2$][c]	71.1(8)	70.4	-179.2(6)	-175.0	-2.9(9)	-2.4	97.2(7)	105.5
[Pd(PNP-*c*Prop)$_2$][c]	67.5(8)	-	-176.5(6)	-	-3.1(8)	-	102.4(7)	-
[Pt(PNP-*c*But)$_2$]	95.5(7)	-	135.7(7)	-	12.1(6)	-	78.0(6)	-
[Pt(PNP-*c*But)$_2$][d]	-	-	-175.2(2)	-	-	-	-	-
[Pd(PNP-*c*But)$_2$]	-	74.7	-	167.5	-	71.9	-	175.7
[Pt(PNP-*c*Pent)$_2$]	81.3(4)	72.6	-175.9(3)	170.6	10.6(4)	9.3	89.7(4)	90.5
[Pd(PNP-*c*Pent)$_2$]	-	88.1	-	173.3	-	12.5	-	101.3
[Pt(PNP-*c*Hex)$_2$]	77.9(3)	66.9	164.9(2)	171.4	9.4(3)	9.5	76.9(2)	88.8
[Pt(PNP-*c*Hex)$_2$][d]	-	-	-	-	-	-	53.7(6)	-
[PtCl$_2$(PNP-Dimprop)][e]	-78.2(2)	-66.0	-174.4(2)	-177.6	-11.8(3)	-5.5	-98.4(2)	139.4
[PdCl$_2$(PNP-Dimprop)][a]	-79.6(7)	-137.2	-174.6(6)	-170.7	-13.5(7)	-5.7	-95.7(6)	-101.3

[a] See Ref 18. [b] Values for [Pt(PNP-*n*Pent)$_2$] due to non symmetrical crystal structure. [c] The [Pd(PNP-*c*Prop)$_2$] Ring values are for each of the two independent Pd(II) molecules in the asymmetric unit of the crystal structure. [d] Minor disordered part of the crystal structure for [Pt(PNP-*c*But)$_2$] and [Pt(PNP-*c*Hex)$_2$]. e See Ref 20.

The orientations of Rings 1 and 2 typically stay the same for the "basket-" and "fan"-like conformations as can be seen in **Figure 6.17** and **Figure 6.18** and comparable values in **Table 6.16**. Rings 3 and 4 are the deciding factor for the specific type of conformations which is also where the obvious switch in torsion angle is witnessed, from ±80 ° for the "fan"-like to ±10 ° for the "basket"-like conformation when looking at Ring 3. Ring 4 switches from a ±175 ° to a ±80 ° torsion angle for the "fan-" and "basket"-like conformations, respectively.

Complexes that adopts the "fan"-like arrangement for the phenyl rings are: [PtCl$_2$(PNP-Ethyl)], [PtCl$_2$(PNP-*n*Prop)] and [Pt(PNP-*n*Pent)$_2$] (**Table 6.16**), i.e. the ones with the smaller steric impact from the R-substituent. For [Pt(PNP-*c*But)$_2$], Ring 2 shows a significant difference in torsion angles for the major- and minor disordered parts of the crystal structure, nevertheless still

having an overall "basket"-like orientation for both. The calculated structure for the palladium analogue, [Pd(PNP-*c*But)$_2$], however, indicates a "fan"-like orientation when looking at Ring 3 (71.9 °) and Ring 4 (175.7 °) (**Table 6.16**). It is visually clear from an overlay of the minor-disordered crystal structure (red) of [Pt(PNP-*c*But)$_2$] and the DFT optimized structure (black) of [Pd(PNP-*c*But)$_2$] that the conformation differs from a "basket"-like conformation for the platinum crystal complex to a "fan"-like orientation for the analogue DFT calculated palladium complex (**Figure 6.19**). The minor disordered crystal structure for [Pt(PNP-*c*But)$_2$] was used for visual purposes for the overlay due to Ring 2 having a more accurate torsion angle (-175.2(2) °) than the major- disordered part (135.7(2) °) for resembling a "basket"-like conformation, although proven that the major- and minor crystal disorders imitate the "basket"-like orientation.

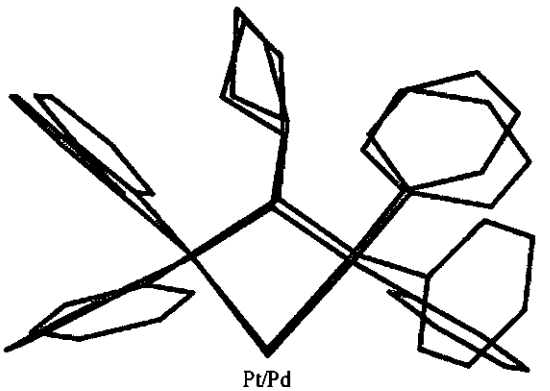


Figure 6.19: Graphical representation of part of the metal complex of an overlay of the minor- disordered crystal structure (red) of [Pt(PNP-*c*But)$_2$] and the DFT optimized structures (black) of [Pd(PNP-*c*But)$_2$]. Overlay fit excluded all hydrogen atoms.

The torsion angles in Ring 4 for the crystal structure and the calculated structure of [PtCl$_2$(PNP-Dimprop)] are substantially different, -98.4 and 139.4 °, respectively (**Table 6.16**). There are only small differences between the other torsion angles in when comparing the crystal and calculated structures. This indicates that the orientations of three of the four phenyl rings are similar and both structures adopted a "basket"-like orientation. Ring 2 for [PdCl$_2$(PNP-Dimprop)] is the only ring differing in orientation between the crystal structure and calculated structure (-79.6(7) and -137.2 °, respectively). A similar "basket-like" orientation for rings 3 and 4 are observed for both structures to accommodate the sterically bulky alkyl moiety (**Table 6.16**).

The reason for these two conformations ("basket"- and "fan"-like) can in part be attributed to the *Effective Tolman-based N-substituent steric effect* ($\theta_{N\text{-}sub}$) described in Chapter 4, **Figure 4.3**. The $\theta_{N\text{-}sub}$ values for the crystal data is in good agreement with the optimized structures as seen in **Table 6.17** and **Figure 6.20**. The following complexes: [$PtCl_2$(PNP-Ethyl)], [$PtCl_2$(PNP-*n*Butyl)], [$PtCl_2$(PNP-*n*Prop)] and [Pt(PNP-*n*Pent)$_2$] have $\theta_{N\text{-}Sub}$ values between 61.8 and 64.6 ° and adopt a "fan"-like conformation. The conformation switches to a "basket"-like orientation for the larger $\theta_{N\text{-}Sub}$ values between 69.3 and 86.5 ° for [Pt(PNP-*c*Prop)$_2$], [Pd(PNP-*c*Prop)$_2$], [Pt(PNP-*c*Pent)$_2$], [Pt(PNP-*c*Hex)$_2$] and [$PtCl_2$(PNP-Dimprop)].

Table 6.17: Calculated $\theta_{N\text{-}sub}$ (°) values for the crystal structures and theoretical structures of various [M(PNP-alkyl)$_2$] and [MCl_2(PNP-alky)] (M = Pt, Pd) complexes.

Complex	$\theta_{N\text{-}sub}$ (Crystal)[a]	$\theta_{N\text{-}sub}$ (DFT)	Phenyl ring orientation
[$PtCl_2$(PNP-Ethyl)][b]	62.8	61.8	Fan
[$PtCl_2$(PNP-*n*Prop)][b]	63.2	64.6	Fan
[Pt(PNP-*n*Pent)$_2$][c]	63.4		Fan
[Pt(PNP-*c*Prop)$_2$]	69.5	71.2	Basket
[Pd(PNP-*c*Prop)$_2$][d]	69.3	71.1	Basket
[Pt(PNP-*c*But)$_2$][e]	71.1	76.2	Basket
[Pd(PNP-*c*But)$_2$]	-	76.2	Basket
[Pt(PNP-*c*Pent)$_2$]	77.6	81.9	Basket
[Pd(PNP-*c*Pent)$_2$]	-	81.9	Basket
[Pt(PNP-*c*Hex)$_2$][e]	81.6	84.9	Basket
[$PtCl_2$(PNP-Dimprop)][f]	86.1	-	Basket
[$PdCl_2$(PNP-Dimprop)][b]	86.3	86.5	Basket

[a] $\theta_{N\text{-}Sub}$ determined from the crystallographic data, see Chapter 5. [b] See Ref 18. [c] Values for [Pt(PNP-*n*Pent)$_2$] due to non symmetrical crystal structure. [d] The [Pd(PNP-*c*Prop)$_2$] values are for each of the two independent Pd(II) molecules in the asymmetric unit of the crystal structure. [e] Major- and minor disordered parts of the crystal structures of [Pt(PNP-*c*But)$_2$] and [Pt(PNP-*c*Hex)$_2$]. [f] See Ref 20.

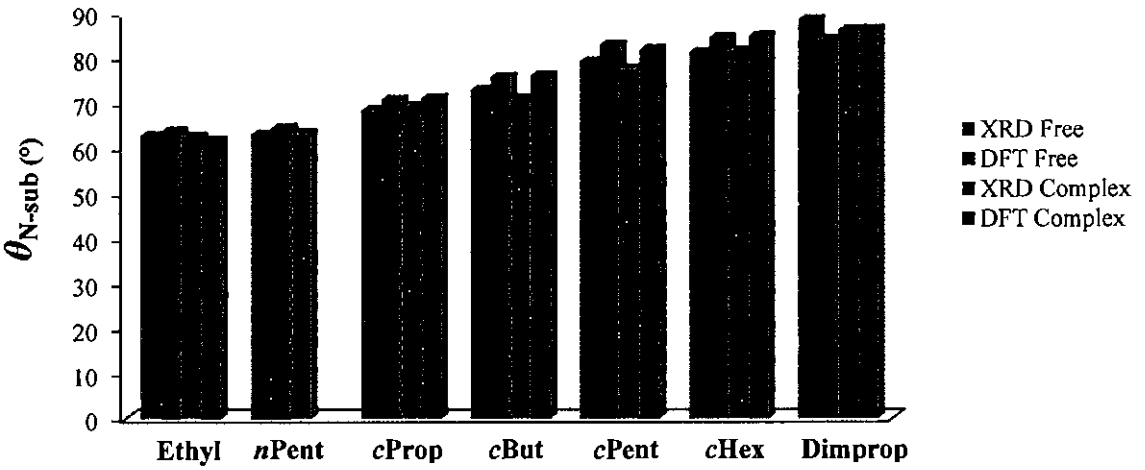


Figure 6.20: $\theta_{N\text{-}sub}$ (°) values for the crystallographic (**XRD**) and optimized (**DFT**) structure data of various free PNP-ligands (**Free**) and Pt/Pd-PNP coordinated complexes (**Complex**).

The change in $\theta_{N\text{-}Sub}$ is significant when branching is present in the alkyl substituent, at the nitrogen coordinated C-atom, as can be seen from the linear PNP-*n*Prop, [$PtCl_2$(PNP-*n*Prop)] (63.9 °), that is significantly smaller than the branched [Pt(PNP-*c*Prop)$_2$] (70.4 °) and [Pd(PNP-*c*Prop)$_2$] (70.2 °). This is also true for linear PNP-*n*Butyl, ([$PtCl_2$(PNP-*n*Butyl)]), *vs* branched PNP-*c*Butyl, ([Pt(PNP-*c*But)$_2$]), with $\theta_{N\text{-}Sub}$ values of 63.8 *vs* 73.7 °, respectively, as well as for [Pt(PNP-*n*Pent)$_2$] (63.5 °) and [Pt(PNP-*c*Pent)$_2$] (79.8 °) (**Table 6.17**).

6.6 Conclusion

This Chapter described the DFT optimized structures of the free PNP-ligands and various platinum(II)- and palladium(II) coordinated bis(diphenylphosphino)amine complexes, illustrating excellent correlation when compared to the corresponding crystal structures. Overlay diagrams of the theoretical molecules with their experimental solid state counterparts have provided a visual means to compare the structures. Reasonable overlay diagrams and RMS values were obtained for the PNP-ligands as well as for the Pt/Pd coordinated complexes. The DFT approximations are reasonable and can be utilized if the coordination mode of a specific complex is required, but which cannot be crystallized for some reason or other.

7 Catalytic Hydroformylation of 1-octene

In this chapter...

Correlations between the measured steric parameter of the various PNP-ligands and the catalytic activity and selectivity of rhodium and iridium PNP coordinated complexes as hydroformylation catalysts are presented and discussed.

7.1 Introduction

Preliminary catalytic experiments on the hydroformylation of 1-octene, which produces linear (nonanal) and branched aldehydes, is discussed in this Chapter. Bis(diphenylphosphine)amine (PNP) ligands, with various alkyl and cycloalkyl substituents attached to the N atom of the ligand backbone were tested together with rhodium and iridium as hydroformylation catalysts. The steric bulk and natural bite angle of ligands have been reported to have a decisive effect on activity, stability and selectivity achieved by catalysts in hydroformylation reactions.[1,2,3,4] Since these PNP-ligands have relatively small bite angles (70.23(6) - 72.3(1) °, see Chapter 5) it was decided to study the influence of the steric effect of the N-alkyl moiety in an effort to maximize overall selectivity and ultimately structurally fine-tune these PNP-ligands towards more efficient hydroformylation catalysts.

It has to be stated that detailed optimizations of all the effects which might affect the catalytic activity where not performed. This study merely provides a "proof of concept" of the influence of selected PNP-ligands to some key experiments. More complete optimizations and other variations will be the subject of a subsequent study.

---

[1] A. van Rooy, J.N.H. de Bruijn, C.F. Roobeek, P.C. Kamer, P.W.N.M. van Leeuwen, *J. Organomet. Chem.*, 507 (1996) 69.
[2] M. Kranenburg, P.C.J. Kamer, P.W.N.M. van Leeuwen, D. Vogtb, W. Keim, *J. Chem. Soc., Chem. Commun.*, (1995) 2177.
[3] T. Hayashi, T. Kawabata, T. Isoyama, I. Ogata, *Bull Chem. Soc. Jpn.*, 54 (1981) 3438.
[4] T. Kawabata, T. Hayashi, T. Isoyama, I. Ogata, *J. Chem. Soc. Chem. Commun.*, (1979) 462.

7.2 Experimental

7.2.1 General

All reactions were conducted under argon unless otherwise stated. Toluene was percolated through neutral alumina and distilled from sodium/benzophenone under N_2. See Chapter 3 for the synthesis and characterization of the PNP ligands and $[Rh(acac)(CO)_2]$ precursor. $[Ir(acac)(CO)_2]$ was obtained from Sigma-Aldrich and used without further purification. Samples from the hydroformylation reactions were analyzed on a Shimadzu GC-2010 gas chromatograph fitted with a Flame Ionisation Detector (FID) and a Agilent Technologies HP-1 30m column with a 0.25 mm internal diameter. Mass spectrometry of compounds and reaction mixtures were performed by means of electron impact (EI) ionization making use of a Shimadzu GC-MS QP-2010 gas chromatograph-mass spectrometer fitted with a DB-5 MS column (30 m, 0.32 mm i.d., 0.25 μm film thickness) utilizing helium as carrier gas.

7.2.2 Catalytic hydroformylation

The batch reactions were performed in a 100ml PARR model 4560 stainless hastelloy autoclave fitted with internal mechanical stirring, a temperature control unit and a sampling valve. Typically, 1 eq. PNP-ligand (0.05 mmol), 1000 eq. alkene, dodecane (2.00 g) as internal standard and toluene (40 ml) as solvent were loaded into the reactor. The system was purged three times with Ar and heated to the chosen reaction temperature with constant stirring at 250 rpm. Then 0.05 mmol catalyst precursor ($[M(acac)(CO)_2]$ (M = Rh, Ir)) in 10 ml of toluene was placed in the substrate vessel and injected into the autoclave by the required pressure with CO/H_2 (1:1). Samples (250 μl diluted to 1.00 ml with toluene) were taken periodically and analyzed by temperature-controlled GC and GC-MS.

7.2.3 High pressure FT-IR (HP IR) experiments

Infrared spectra were recorded on a Bruker Tensor 27 Standard System spectrophotometer with a laser range of 4000 - 370 cm^{-1}, equipped with a temperature cell regulator, accurate within 0.3 °C. The high-pressure experiments were carried out in a 50 ml autoclave equipped with a mechanical stirrer, a temperature and pressure control. The solution was pumped through a bypass, in which ZnS windows were embedded. The infrared windows are each 4.5 mm thick with a 20 mm diameter and an optical diameter of 10 mm. The autoclave was flushed with argon prior to use. In a typical experiment, the HP IR autoclave was charged with 1 eq. PNP-ligand (0.30 mmol), 100 eq. alkene, dodecane (2.00 g) and toluene (25 ml). The system was purged three times with Ar and heated to the chosen reaction temperature. The substrate vessel was then charged with 0.3 mmol catalyst precursor [Rh(acac)$(CO)_2$] in 5 ml of toluene and injected into the autoclave by the required pressure with CO/H_2 (1:1). Product formation was monitored with time by FT IR.

7.2.4 General hydroformylation results calculations

% Conversion = (n(1-octene)out/n(1-octene)in) x 100

% Isomerisation = n(2-octene)/n(1-octene converted) x 100

% Yield nonanal = n(nonanal)/n(1-octene converted) x 100

l:b = linear:branched ratio representing the linear:branched selectivity

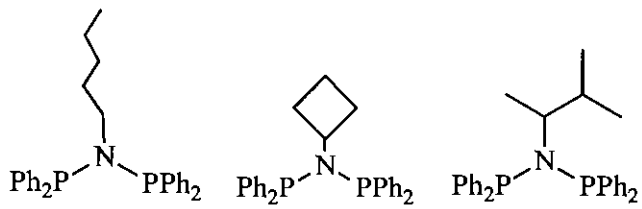
TON = (% conv / 100) x (n(1-octene) / n(catalyst))

TOF = TON / time(h)

7.3 Results and discussion

As stated previously, the aim of this study was to investigate the influence of the steric effect induced by the N-substituent of the PNP-ligand to achieve higher selectivity towards the most desired linear aldehydes at the expense of side-product formation. The range of PNP-ligands synthesized and discussed in Chapter 3, showed similar electronic properties. The largest difference within the range of PNP-ligands was in fact the steric bulk of the alkyl moiety attached to the N atom, measured by a modification of the *Effective Tolman Angle* ($\theta_{N\text{-}sub}$) as described in Chapter 4.

In order to provide more tangible evidence of this concept, catalytic runs were performed using the least sterically bulky PNP-*n*Pent ($\theta_{N\text{-}sub}$ = 64 °) (**1**), a moderately bulky PNP-*c*But ($\theta_{N\text{-}sub}$ = 74 °) (**2**) and the most bulky PNP-Dimprop ($\theta_{N\text{-}sub}$ = 86 °) (**3**) to study the effects towards selectivity and activity (**Scheme 7.1**).



1 **2** **3**

Scheme 7.1: Diphosphinoamine ligands (PNP-ligands): (1) *N,N*-Bis(diphenylphosphanyl)-*n*-pentylamine (PNP-*n*Pent); (2) *N,N*-Bis(diphenylphosphanyl)cyclobutanamine (PNP-*c*But); (3) *N,N*-Bis(diphenyl-phosphanyl)-1,2-dimethylpropylamine (PNP-Dimprop)

7.3.1 Rhodium catalyzed hydroformylation of 1-octene

The rhodium catalyzed hydroformylation of 1-octene was performed at 80 °C and 20 bar of 1:1 CO/H_2 using a 0.05 mmol of $[Rh(acac)(CO)_2]$ precursor catalyst and 1 eq. of PNP-ligand. The production of octene isomers, nonanal, and 2-methyloctanal was monitored by gas chromatography. The rhodium precursor, $[Rh(acac)(CO)_2]$, gave active catalysts with the PNP-*n*Pent (**1**), PNP-*c*But (**2**) and PNP-Dimprop (**3**) ligands. The activity of these complexes were compared to that of PPh_3 as ligand, since $[RhHCO(PPh_3)_3]$[5] is the current catalyst used for industrial scale hydroformylation, made *in situ* with the $[Rh(acac)(CO)_2]$ precursor, PPh_3 and syngas (CO/H_2). PPh_3 is however used in large excess in the industry, but for this project, only 2 eq. were used as a reference to enable more direct comparison (i.e. equivalent stoichiometric ratio of coordinating P-donor atoms) to the chelating diphosphine ligands.

Complexes **1-3** represent rhodium complexes containing a chelating, bidentate diphosphine small bite angle ligand, with the added effect of an amino group coordinated to both phosphorous atoms. The varying substituent on the N atom seems to have a significant effect on the activity and selectivity of the catalyst. The results of the experiments with Ligands **1-3** are shown in **Table 7.1**.

Table 7.1: Hydroformylation of 1-octene by $[Rh(acac)(CO)_2]$ precursor combined with Ligands **1-3** in toluene.

Entry	Ligand	M:L ratio[a]	Time (min)	Conversion (%)	Linear aldehyde (%)	l:b ratio[b]	Isomerisation[c] (%)	TOF (h^{-1})	$\theta_{N\text{-}sub}$[d] (°)
1	PPh_3	1:2	120	98	50.8	1.9:1	26.3	470	145[e]
2	**1**	1:1	190	98	23.9	1.9:1	63.7	310	64
3	**2**	1:1	160	97	30.7	1.9:1	53.0	359	74
4	**3**	1:1	90	98	50.9	2.3:1	27.3	635	86

Reaction conditions: [Rh] = 1.00 mM, 1-octene:Rh = 1000:1, 20 bar syngas ($CO:H_2$ = 1:1), 80 °C. [a] M:L = metal to PNP-ligand ratio. [b] l:b = linear-to-branched selectivity, branched products, generally > 98 % 2-methyloctanal. [c] Isomerised products, generally > 95 % 2-octene. [d] Calculated as an average of the crystal structures and DFT calculated structures for the free ligands and $[M(PNP\text{-}alkyl)_2]$ (M = Pt, Pd) complexes. See Chapters 4, 5 and 6. [e] See Ref 6.

[5] P.W.N.M van Leeuwen, C. Claver (Eds.), *Rhodium Catalyzed Hydroformylation*, Kluwer Academics Publishers, Dordrecht, 2000.
[6] C.A. Tolman, *Chem. Rev.*, 77 (1977) 313.

The selectivity for linear aldehyde formation increases at the cost of internal isomerisation with an increase in the steric bulk of the ligand from 23.9 % for **1** ($\theta_{N\text{-}sub}$ = 64 °) (Entry 2, **Table 7.1**) to 50.9 % for **3** ($\theta_{N\text{-}sub}$ = 86 °) (Entry 4, **Table 7.1**) as illustrated in **Figure 7.1**. A systematic increase in the $\theta_{N\text{-}sub}$ values also lead to higher catalyst activities. Substitution of the *n*Pent (**1**) group for a Dimprop (**3**) group, doubles the hydroformylation rate and decreases isomerisation by 50 % (**Figure 7.2**).

For Ligand **3**, almost the same yield for nonanal and the same extent of isomerisation is observed (Entry 4, **Table 7.1**) as for the hydroformylation experiments with PPh_3 as ligand (Entry 1, **Table 7.1**). The introduction of Ligand **3** also leads to a slight increase in l:b ratio and a higher hydroformylation rate, compared to PPh_3. All reactions eventually reach 100 % conversions (**Figure 7.2**) with isomerisation as the only side-product. The higher selectivity provides evidence to suggest that these ligands introduce a larger steric effect, resulting in more linear products.

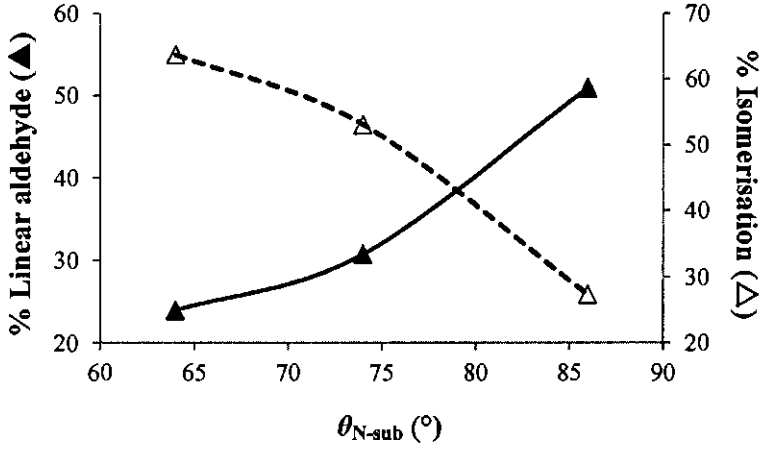


Figure 7.1: Results from hydroformylation of 1-octene by [Rh(acac)(CO)$_2$] and Ligands **1-3** as given in **Table 7.1.** Total increase in linear aldehyde formation (▲) and total isomerisation decrease (△) as a result of an increase in $\theta_{N\text{-}sub}$. [Rh] = 1.00 mM, 1-octene:Rh = 1000:1, 20 bar syngas (CO:H_2 = 1:1), 80 °C. M:PNP-ligand = 1:1

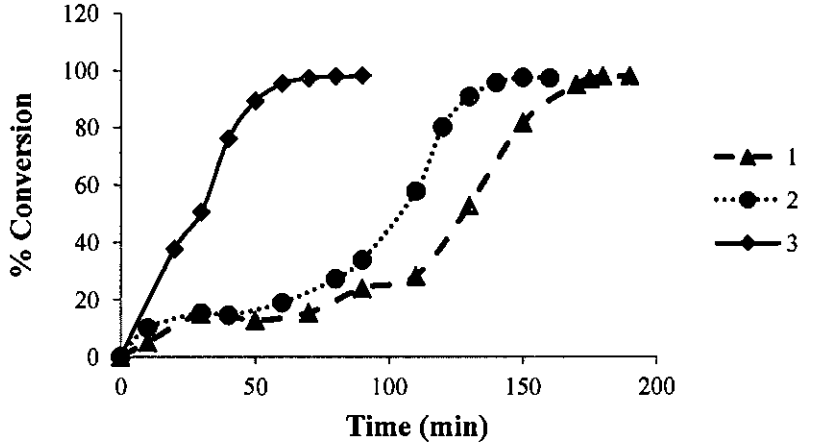


Figure 7.2: Conversion as a function of time for the hydroformylation of 1-octene by $[Rh(acac)(CO)_2]$ precursor combined with ligands **1-3** as given in **Table 7.1**. [Rh] = 1.00 mM, 1-octene:Rh = 1000:1, 20 bar syngas ($CO:H_2$ = 1:1), 80 °C. M:PNP-ligand = 1:1.

It was decided to introduce PPh_3 together with the PNP-ligands to investigate the possible influence of the combined ligand effects on hydroformylation selectivity (**Table 7.2**). The metal:PNP-ligand ratio was kept constant at 1:1 while PPh_3 was added in different ratio's. Addition of PPh_3 to the PNP-ligands proved advantageous across the board, increasing linear selectivity, activity and significantly suppressing the unwanted isomerisation (e.g. Entries 2-4, **Table 7.1** *vs* Entries 5-7, **Table 7.2**).

Table 7.2: Hydroformylation of 1-octene by $[Rh(acac)(CO)_2]$ precursor combined with Ligands **1-3** with added PPh_3 in various ratio's in toluene.

Entry	Ligand	M:L:PPh_3 ratio[a]	Time (min)	Conversion (%)	Linear aldebyde (%)	l:b ratio[b]	Isomerisation[c] (%)	TOF (h^{-1})
5	**1**	1:1:1	145	96	62.2	2.9:1	16.3	384
6	**2**	1:1:1	105	97	43.7	2.7:1	39.9	534
7	**3**	1:1:1	90	98	60.6	2.3:1	13.4	665
8	**3**	1:1:2	130	98	43.1	1.9:1	35.1	413
9	**3**	1:1:3	110	95	39.1	2.2:1	42.9	516
10	**3**	1:1:4	120	98	47.0	2.5:1	34.0	487

Reaction conditions: [Rh] = 1.00 mM, 1-octene:Rh = 1000:1, 20 bar syngas ($CO:H_2$ = 1:1), 80 °C. [a] M:L:PPh_3 = metal to PNP-ligand to PPh_3 ratio. [b] l:b = linear-to-branched selectivity, branched products, generally > 98 % 2-methyloctanal. [c] Isomerised products, generally > 95 % 2-octene.

- Ligand 1

The most striking difference was the three-fold increase in linear selectivity from 23.9 % (Entry 2, **Table 7.1**) to 62.2 % (Entry 5, **Table 7.2**), accompanied by a significant increase in l:b ratio (1.9 - 2.9) upon addition of 1 eq. PPh_3 in combination with the PNP-ligand. This is graphically illustrated in **Figure 7.3**. The corresponding isomerisation decreased four-fold from 63.7 to 16.3 %.

- Ligand 2

An increase in nonanal yield of 30.7 - 43.7 % (Entry 3, **Table 7.1** *vs* Entry 6, **Table 7.2**) is observed for Ligand **2** when combined with PPh_3 ligand. The significant difference between the linear aldehyde yield for Ligand **2** (43.7 %) (Entry 6, Table 7.2) opposed to the ± 60 % for Ligands **1** and **3** (Entries 5 and 7, **Table 7.2**) are unknown. A considerable increase in l:b ratio (1.9 - 2.7) along with a decrease in isomerisation products from 53.0 – 39.9 % is also observed for Ligand **2**.

- Ligand 3

Shows a good overall improvement with a 10 % increase in linear selectivity and a decrease in isomerisation (27.3 - 13.4 %) (Entry 4, **Table 7.1** *vs* Entry 7, **Table 7.2**).

Remarkably, the combination of the PNP-ligand with PPh_3 in a 1:1 ratio increases the hydroformylation activity, without losing the selectivity for linear aldehyde formation. In this case where PPh_3 is combined with the PNP-ligands, a definite trend in selectivity is not observed with an increase in $\theta_{N\text{-}sub}$ of the PNP-ligand (**Figure 7.3**). The addition of PPh_3 therefore resulted in an improved selectivity for each PNP-ligand at the cost of isomerisation. All reactions eventually reach 100 % conversions (**Figure 7.4**) with isomerisation as the only side-product.

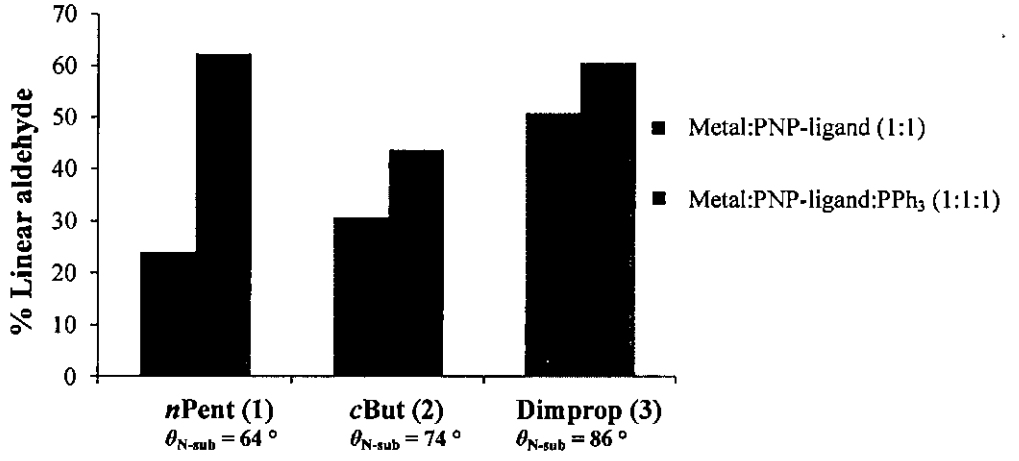


Figure 7.3: Combined results as given in **Table 7.1** and **Table 7.2** for the linear aldehyde selectivity for the hydroformylation of 1-octene with $[Rh(acac)(CO)_2]$ combined with various PNP-ligands in a M:PNP-ligand (metal to PNP-ligand) ratio of 1:1 and M:PNP-ligand:PPh_3 ratio of 1:1:1. [Rh] = 1.00 mM, 1-octene:Rh = 1000:1, 20 bar syngas ($CO:H_2$ = 1:1), 80 °C.

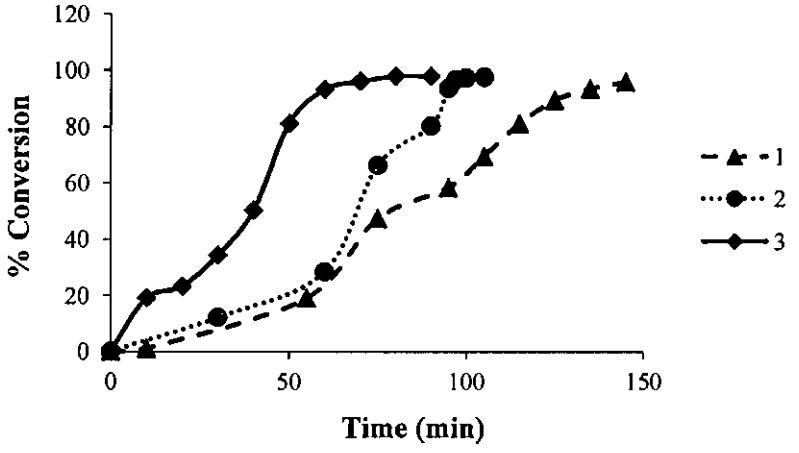


Figure 7.4: Conversion as a function of time for the hydroformylation of 1-octene with $[Rh(acac)(CO)_2]$ precursor combined with 1 eq. PPh_3 and 1 eq. of Ligands **1-3** as given in **Table 7.2**. [Rh] = 1.00 mM, 1-octene:Rh = 1000:1, 20 bar syngas ($CO:H_2$ = 1:1), 80 °C. M:PNP-ligand:PPh_3 = 1:1:1.

Since Ligand **3** showed the highest activity under the same conditions (Entry 4, **Table 7.1** and Entry 7, **Table 7.2**), it was therefore selected as the ligand to modify the catalyst used to investigate activity under different reaction conditions. Upon addition of more than 1 eq. of PPh_3 with ligand **3** (Entries 8-10, **Table 7.2**), the results are very similar with linear selectivity approximately 43 % and with 35 % isomerization observed. These results resemble that of the reference reaction (Entry 1, **Table 7.1**) using only 2 eq. of PPh_3. This suggests that an excess

amount of PPh_3 ligand in combination with the PNP-ligand might cause the dissociation of the PNP-ligand from the metal centre, therefore mimicking the reference reaction. Also, the time taken for the completion of the hydroformylation process when larger than 1 eq. of PPh_3 is added (Entries 8-10, **Table 7.2**) is approx. 120 min. This time is similar for the reference reaction (Entry 1, **Table 7.1**) which also suggests the possibility that the PNP-ligand dissociates when larger PPh_3 ratios are utilized.

7.3.1.1 Effect of the metal precursor and ligand ratio's on catalytic activity

During initial catalytic test runs, a series of precursor rhodium catalysts, $[Rh(cod)Cl]_2$, [Rh(acac)(cod)] and $[Rh(cod)(PPh_3)_2]PF_6$,[7] were combined with the moderate bulky PNP-*c*But, to establish optimum reaction conditions for the hydroformylation process. Experiments were conducted with a M:PNP-ligand ratio of 1:50 with no results after which the M:PNP-ligand ratio was scaled down to 1:5 in which only the $[Rh(cod)Cl]_2$ precursor showed a 10 % conversion over 20 hours. The M:PNP-ligand ratio was systematically reduced even further until it was found that $[Rh(acac)(CO)_2]$ was the only precursor to produce active catalysts in a 1:1 M:PNP-ligand ratio with the PNP-ligands. It can be argued that with higher M:PNP-ligand ratio's, the steric bulk around the metal centre becomes too large, therefore inhibiting the alkene from coordinating.

7.3.1.2 Effect of temperature and syngas ratio's on catalytic activity

As mentioned before, PNP-Dimprop (**3**) showed the highest activity of the three ligands and was thus used to investigate hydroformylation activity under different reaction conditions. The rhodium catalyzed hydroformylation was also done at 50, 60 and 70 °C (Entries 12-14, **Table 7.3**). The catalyst remained inactive for several hours at 50 and 60 °C, showing absolute no activity. At 70 °C (Entry 14, **Table 7.3**) hydroformylation occurred, but at a rate three times slower than identical conditions at 80 °C (Entry 4, **Table 7.3**). A slightly lower linear aldehyde formation from 50.9 to 44.0 % and a lower l:b ratio was also observed. Generally, an increase in temperature is expected to result in overall enhanced rate and therefore increased productivities. This is however only true once the catalyst becomes active, i.e. from 70 to 80 °C. The optimum

[7] R.R. Schrock, J.A. Osborn, J. Am. Chem. Soc., 93:10 (1971) 2397.

temperature for this study was chosen at 80 °C since conversion started instantly when using the most active Ligand **3**, and was completed within 90 min, allowing enough time for collecting efficient data.

Table 7.3: Hydroformylation of 1-octene by [Rh(acac)(CO)$_2$] precursor combined with Ligand **3** at various temperatures and syngas (CO/H$_2$) ratio's in toluene.

Entry	Ligand	Syngas (CO/H$_2$)	Time (h)	Conversion (%)	Linear aldehyde (%)	l:b ratio[a]	Isomerisation[b] (%)	TOF (h^{-1})	Temp (°C)
4[c]	3	1:1	1.5	98	50.9	2.3:1	27.3	635	80
12	3	1:1	16.0	-	-	-	-	-	50
13	3	1:1	16.0	-	-	-	-	-	60
14	3	1:1	4.5	97	44.0	1.7:1	29.4	210	70
15	3	1:2	1.5	93	32.5	2.2:1	52.9	617	80

Reaction conditions: [Rh] = 1.00 mM, 1-octene:Rh = 1000:1, 20 bar syngas (CO:H$_2$), [a] l:b = linear-to-branched selectivity, branched products, generally > 98 % 2-methyloctanal. [b] Isomerised products, generally > 95 % 2-octene. [c] As given in **Table 7.1**.

A 1:2 syngas (CO/H$_2$) ratio was utilized with Ligand **3** (Entry 15, **Table 7.3**) at 20 bar and 80 °C, in order to investigate possible hydrogenation of the aldehyde towards the alcohol. Similar activity was observed (Entry 4 *vs* Entry 15) however, accompanied by a two-fold increase of the % isomerisation from 27.3 to 52.9 %, thus promoting internal isomerisation and decreasing linear aldehyde formation (from 50.9 to 32.5 %), making the 1:1 syngas ratio the most favorable. This observation indicates that the isomerisation reaction is probably first-order in [H$_2$].

7.3.1.3 Effect of reaction variables on catalyst activity

The PNP-ligands has to coordinate to the rhodium metal centre competing with olefin, hydrogen and carbon monoxide. During initial catalytic test runs, PNP-cBut (**2**) was used as a model ligand due to its moderate bulkiness. At first, the [Rh(acac)(CO)$_2$] precursor and the PNP-ligand was introduced into the reactor. The system was allowed to reach reaction temperature (80 °C) and pressurized to the desired pressure (20 bar) with CO/H$_2$ (1:1). The reaction was allowed to stir at these conditions for an hour assuming it would result in the conversion to the active catalyst species, [RhH(CO)$_m$(ligand)$_n$]. Addition of the alkene substrate (octene after 1h, **Figure 7.5**) resulted in a proportional increase in conversion up to 40 % in the first 100 min. Over the next 60 min an exponential increase in conversion was observed, reaching 95 % conversion and then stabilized until complete conversion is achieved at 200 min (Entry 16, **Table 7.4**). In order

to determine whether or not the active species has been formed completely, the rhodium and ligand was stirred under syngas at 80 °C for 2 hours. The same trend was detected (octene after 2h, **Figure 7.5**, Entry 17, **Table 7.4**). It seems thus that an induction period is required during the first 90 min of the reaction, corresponding to the time required to attain thermal equilibration and in part also form the active species, $[RhH(CO)_m(ligand)_n(alkene)]$.

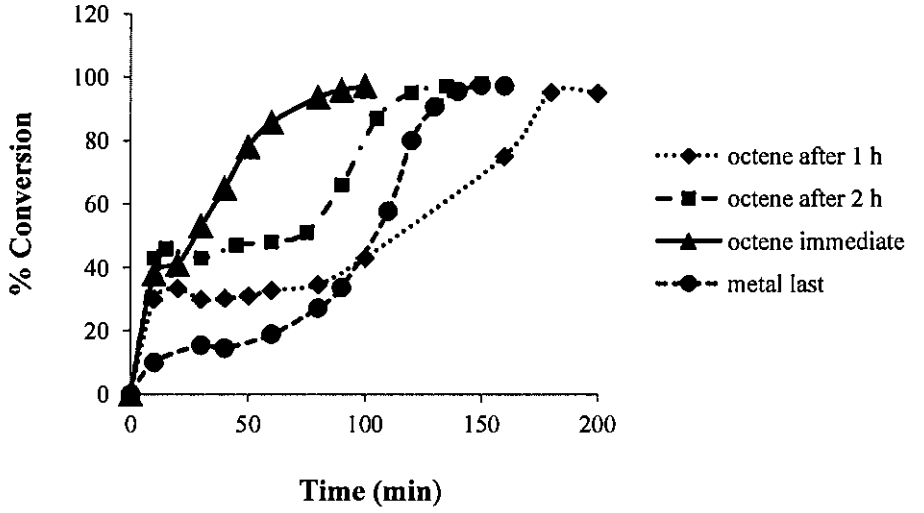


Figure 7.5: Conversion as a function of time for the hydroformylation of 1-octene with $[Rh(acac)(CO)_2]$ and PNP-*c*But (**2**) *via* different reaction variables. [Rh] = 1.00 mM, 1-octene:Rh = 1000:1, 20 bar syngas ($CO:H_2$ = 1:1), 80 °C. M:PNP-ligand = 1:1.

Table 7.4: Hydroformylation of 1-octene by $[Rh(acac)(CO)_2]$ precursor combined with Ligand **2** conducted *via* different reaction variables in toluene.

Entry	Ligand	M:L ratio[a]	Time (min)	Conversion (%)	Linear aldehyde (%)	l:b ratio[b]	Isomerisation[c] (%)	TOF (h^{-1})
3[d]	**2**	1:1	160	97	30.7	1.9:1	53.0	359
16	**2**	1:1	200	98	28.5	1.3:1	50.1	255
17	**2**	1:1	150	98	28.9	1.4:1	50.0	219
18	**2**	1:1	100	97	46.8	2.6:1	35.2	578

Reaction conditions: [Rh] = 1.00 mM, 1-octene:Rh = 1000:1, 20 bar syngas ($CO:H_2$ = 1:1), 80 °C. [a] M:L = metal to PNP-ligand. [b] l:b = linear-to-branched selectivity, branched products, generally > 98 % 2-methyloctanal. [c] Isomerised products, generally > 95 % 2-octene. [d] As given in **Table 7.1**.

To establish if the alkene is indeed required to form the active species, $[RhH(CO)_m(ligand)_n(alkene)]$, it was decided to introduce the $[Rh(acac)(CO)_2]$, PNP-ligand and alkene into the reactor all at once (octene immediate, **Figure 7.5**, Entry 18, **Table 7.4**). The mixture was allowed to reach the desired temperature and was pressurized with syngas. This time no induction period was observed and hydroformylation commenced systematically, indicating that alkene binding probably forms part of the generation of the active species. A higher yield is observed than for the other methods (Entries 3, 16 and 17, **Table 7.4**) with less isomerisation. This however is not necessarily an accurate representation with the current available results as hydroformylation starts while the reactor is still in the process of reaching the desired temperature. It was nevertheless then decided on the method used throughout the catalytic investigation (Entry 3, **Table 7.4**), i.e. to add the PNP-ligand and alkene to the reactor and allowing it to reach the desired temperature before adding the rhodium precursor and pressurizing with syngas (metal last, **Figure 7.5**). The gradually increasing conversion was followed *via* GC. These methodology changes gave insight as to the active species and catalyst behaviour.

7.3.1.4 HP IR study

To gain further insight into the reaction mechanism, ambient and high-pressure IR studies were performed in an attempt to better understand the catalyst performance. Again, only PNP-Dimprop (**3**), that showed the highest hydroformylation activity overall, was used for these preliminary studies. During IR studies, both carbonyl groups ($\upsilon_{(CO)}$ = 2080, 2012 cm^{-1}) of the rhodium precursor, $[Rh(acac)(CO)_2]$, are substituted by the bidentate PNP-ligand (**Figure 7.6**). Upon addition of 0.5 eq. of PNP-ligand to $[Rh(acac)(CO)_2]$, half of the starting metal reacts with the PNP-ligand, causing peaks, attributed to the starting complex, to decrease by 50 % in intensity, however no new CO vibration peak appeared. When 1 eq. of PNP-ligand is added, the initial carbonyl peaks of the rhodium disappear completely and again, no new peaks are observed in the CO region of the IR spectra. This is also the case for when 1 eq. of PNP-ligand is combined with 1 eq. of PPh_3 and added to $[Rh(acac)(CO)_2]$.

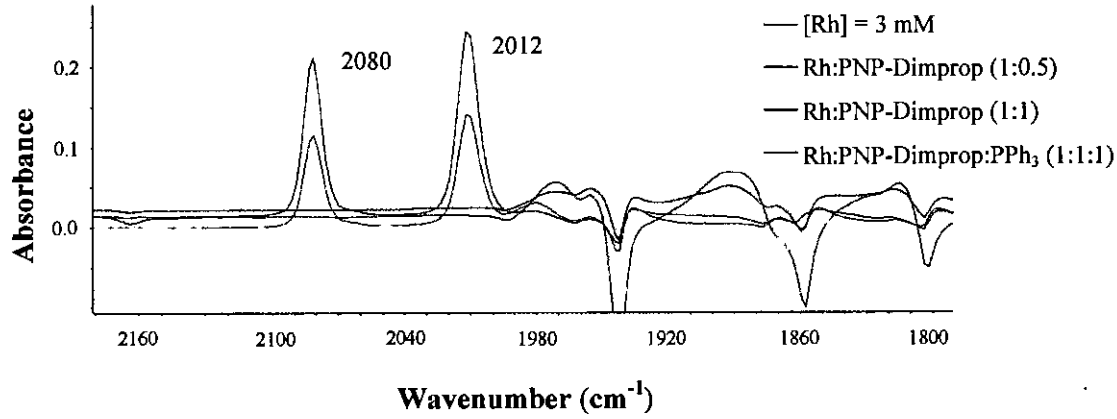


Figure 7.6: IR spectra of the CO region recorded for $[Rh(acac)(CO)_2]$ with various equivalents of PNP-Dimprop (**3**) and PPh_3. [Rh] = 3.00 mM, 25 °C, toluene.

HP IR was consequently also used to study the rhodium complexes that are formed at high pressures upon mixing the ligands and $[Rh(acac)(CO)_2]$ under an atmosphere of CO/H_2 (1:1) at 80 °C. The HP IR spectra obtained for the PNP-ligands, did not show the formation of the $[RhH(CO)_2(ligand)]$ complex, the catalyst's assumed resting state in rhodium-diphosphine catalyzed hydroformylation (**Figure 7.7**).[8,9] The two CO stretching vibrations for $[Rh(acac)(CO)_2]$ ($\upsilon_{(CO)}$ = 2080, 2012 cm^{-1}) disappear upon the addition of 1 eq. of PNP-ligand, indicating that the bidentate ligand displaces both CO groups, most probably forming the [Rh(acac)(PNP-ligand)] complex. Stirring of the rhodium precursor with the ligand under pressure for 3 hours, still does not lead to any signs of M-CO stretching frequencies. Immediately after addition of 1-octene (υ = 1640 cm^{-1}), the strong absorption band of the aldehyde (υ = 1730 cm^{-1}) appeared in the IR spectrum, providing evidence that the hydroformylation reaction has started (**Figure 7.7**). Absorbance values for the aldehyde product is larger than for 1-octene due to the higher IR activity of the carbonyl peak of the aldehyde *vs* the C=C bond of 1-octene. Due to the variation in the baseline, important peaks are integrated and plotted against time, rather than absorption, for more accurate results (**Figure 7.8**). No carbonyl stretching frequencies were observed for the duration of hydroformylation.

[8] L.A. van der Veen, M.D.K. Boele, F.R. Bregman, P.C.J. Kamer, P.W.N.M van Leeuwen, K. Goubitz, J. Fraanje, H. Schenk, C. Bo, *J. Am. Chem. Soc.*, 120 (1988) 11616.
[9] L.A. van der Veen, P.K. Keeven, P.C.J. Kamer, P.W.N.M van Leeuwen, *J. Chem. Soc., Dalton Trans.*, (2000) 2105.

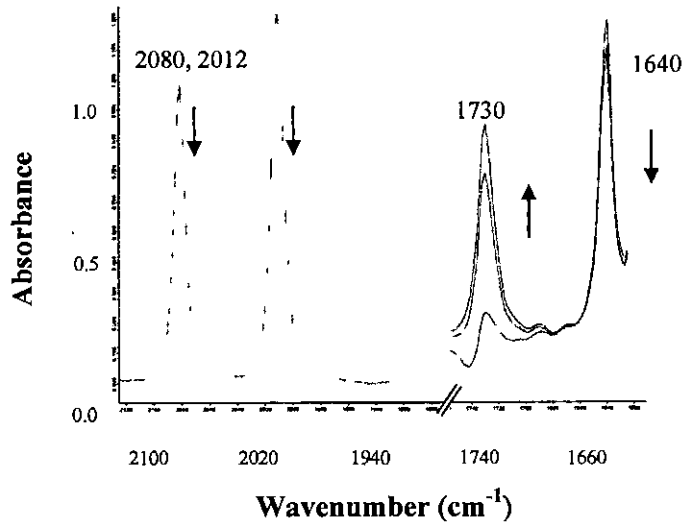


Figure 7.7: Difference IR spectra of the *in situ* HP IR experiment of the hydroformylation of 1-octene by [Rh(acac)$(CO)_2$] precursor combined with Ligand **3** in toluene. [Rh] = 10 mM, 1-octene:Rh = 100:1, 20 bar syngas ($CO:H_2$ = 1:1), 80 °C. M:PNP-ligand = 1:1.

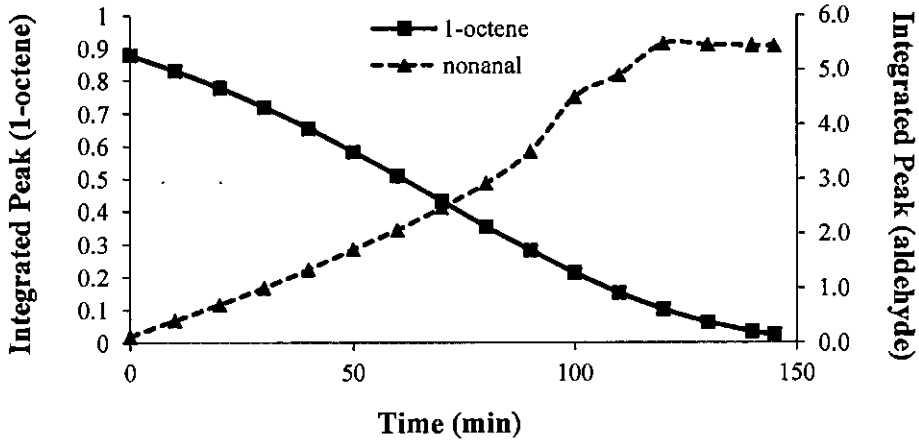


Figure 7.8: HP IR kinetic data for the decrease of 1-octene (υ = 1640 cm^{-1}) and the increase of aldehyde product (υ = 1730 cm^{-1}) *vs* time for the hydroformylation of 1-octene by [Rh(acac)$(CO)_2$] precursor combined with Ligand **3** in toluene. [Rh] = 10.00 mM, 1-octene:Rh = 100:1, 20 bar syngas ($CO:H_2$ = 1:1), 80 °C, M:PNP-ligand = 1:1.

Reaction conditions for the HP IR studies differ from those utilized in the PARR reactor (§ 7.2.2), due to the higher catalyst concentrations needed in order to monitor carbonyl peaks while keeping [1-octene] constant. An increase tendency in linear aldehyde yield, from 50.9 - 57.1 %, is observed for the HP IR results (Entry 19, **Table 7.5**) compared to PARR reactor studies (Entry 4). A significant increase in l:b ratio (2.3 - 3.3) is also seen with almost the same

amount of isomerisation. The HP IR reaction time is almost twice that of the PARR reactor. A number of variables can be the cause of these discrepancies due to the different reaction conditions. Further experiments are thus required before making any additional conclusions. At this stage, HP IR does not seem to be able to render any new information concerning catalyst intermediates and active species.

Table 7.5: Hydroformylation of 1-octene by [Rh(acac)(CO)$_2$] precursor combined with Ligand **3** followed by *in situ* HP IR in toluene.

Entry	Ligand	M:L ratio[a]	Time (min)	Conversion (%)	Linear aldehyde (%)	l:b ratio[b]	Isomerisation[c] (%)	TOF (h^{-1})
4[d]	3	1:1	90	98	50.9	2.3:1	27.3	635
19	3	1:1	160	100	57.1	3.3:1	25.6	-

Reaction conditions: [Rh] = 10.0 mM, 1-octene:Rh = 100:1, 20 bar syngas (CO:H_2 = 1:1), 80 °C. [a] M:L = metal to PNP-ligand ratio. [b] l:b = linear-to-branched selectivity, branched products, generally > 98 % 2-methyloctanal. [c] Isomerised products, generally > 95 % 2-octene. [d] As given in **Table 7.1**.

7.3.2 Iridium catalyzed hydroformylation of 1-octene

The iridium catalyzed hydroformylation of 1-octene was performed at 100 °C and 40 bar of 1:1 CO/H_2 using a 0.05 mmol of $[Ir(acac)(CO)_2]$ precursor catalyst and 1 eq. of PNP-ligand. The production of octene isomers, nonanal, and 2-methyloctanal was monitored by gas chromatography. The iridium reference reaction with 2 eq. PPh_3 showed no activity for the same period utilized for the Rh(I) analogue (Entry 1, **Table 7.1**) to reach complete conversion. The iridium precursor, $[Ir(acac)(CO)_2]$, gave active catalysts with ligands **1-3** (**Table 7.6**), all reaching 100 % conversion. No hydrogenation was observed for any of the reactions, only internal isomerisation. One of the major drawbacks of the Ir(I) catalyst systems is extensive isomerisation of the substrate alkene (± 80 %). The same trend of increasing linear aldehyde formation with an increase in steric bulk ($\theta_{N\text{-}sub}$) of the ligand was also not observed for the iridium catalyzed hydroformylation compared to the rhodium analogous reactions. All three ligands gave similar results regarding linear product yield (± 13 %) and isomerization (Entries 1-3, **Table 7.6**). Ligand **3** showed higher activity, but a lower l:b ratio than ligands **1** and **2**, with **2** producing the highest l:b ratio of 2.1 (**Figure 7.9**).

Table 7.6: Hydroformylation of 1-octene by $[Ir(acac)(CO)_2]$ precursor combined with Ligand **1-3** in toluene.

Entry	Ligand	M:L ratio[a]	Time (min)	Conversion (%)	Linear aldehyde (%)	l:b ratio[b]	Isomerisation[c] (%)	TOF (h^{-1})	$\theta_{N\text{-}sub}$[d] (°)
1	**1**	1:1	240	98	13.1	1.8:1	79.6	226	64
2	**2**	1:1	200	98	15.7	2.1:1	76.8	271	74
3	**3**	1:1	130	98	11.1	1.6:1	81.8	416	86

Reaction conditions: [Ir] = 1.00 mM, 1-octene:Ir = 1000:1, 40 bar syngas ($CO:H_2$ = 1:1), 100 °C. [a] M:L = metal to PNP-ligand ratio. [b] l:b = linear-to-branched selectivity, branched products, generally > 98 % 2-methyloctanal). [c] Isomerised products, generally > 95 % 2-octene. [d] Calculated as an average of the crystal structures and DFT calculated structures for the free ligands and $[M(PNP\text{-}alkyl)_2]$ (M = Pt, Pd) complexes. See Chapters 4, 5 and 6.

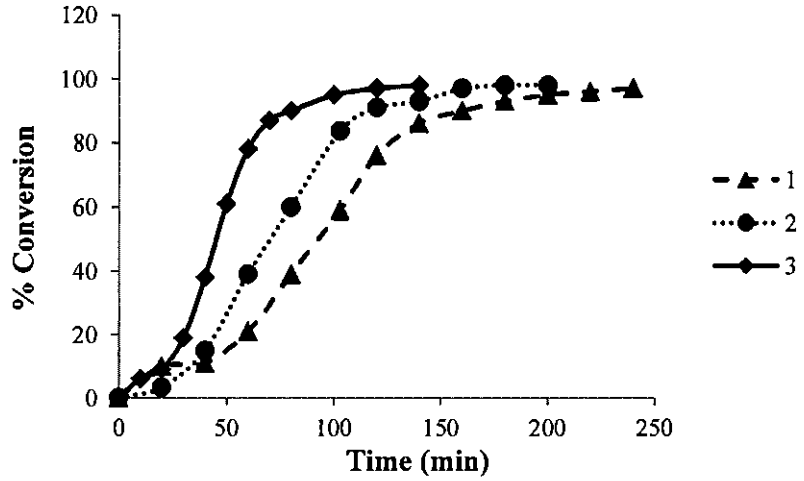


Figure 7.9: Conversion as a function of time for the hydroformylation of 1-octene with [Ir(acac)(CO)$_2$] precursor combined with 1 eq. of Ligands **1-3** as given in **Table 7.6**. [Ir] = 1.00 mM, 1-octene:Ir = 1000:1, 40 bar syngas (CO:H_2 = 1:1), 100 °C. M:PNP-ligand = 1:1.

Although not significant, additions of 1 eq. of PPh_3 to the PNP-ligands (Ligands **1-3**) lead to an increase in linear selectivity and a decrease in isomerisation (Entries 1-3, **Table 7.6** *vs* Entries 4-6, **Table 7.7**).

Table 7.7: Hydroformylation of 1-octene by [Ir(acac)(CO)$_2$] precursor combined with Ligands **1-3** with added PPh_3 in a M:PNP-ligand:PPh_3 ratio of 1:1:1.

Entry	Ligand	M:L:PPh_3 ratio[a]	Time (min)	Conversion (%)	Linear aldehyde (%)	l:b ratio[b]	Isomerisation[c] (%)	TOF (h^{-1})
4	**1**	1:1:1	210	98	20.3	2.1:1	70.3	279
5	**2**	1:1:1	210	98	9.6	1.7:1	84.8	265
6	**3**	1:1:1	210	98	18.6	2.3:1	73.2	267

Reaction conditions: [Ir] = 1.00 mM, 1-octene:Ir = 1000:1, 40 bar syngas (CO:H_2 = 1:1), 100 °C. [a] M:L:PPh_3 = metal to PNP-ligand to PPh_3 ratio. [b] l:b = linear-to-branched selectivity, branched products, generally > 98 % 2-methyloctanal. [c] Isomerised products, generally > 95 % 2-octene.

With the exception of **2**, Ligands **1** and **3** gave near identical results for nonanal selectivity (± 20 %) as well as isomerisation (± 70 %) when combined with PPh_3 (Entries 4 and 6, **Table 7.7**, **Figure 7.10**). These results are an improvement of the 13 % linear aldehyde yield and 80 % isomerisation found when only the PNP-ligands were used (Entries 1 and 3, **Table 7.6**). The opposite outcome for Ligand **2**, giving a lower nonanal yield (9.6 %) and a higher isomerisation yield (84.8 %) with added PPh_3 (Entry 5, **Table 7.7**), compared to 15.7 and 76.8 %, respectively for the PNP-ligand only (Entry 2, **Table 7.6**) cannot be explained with the current data in hand.

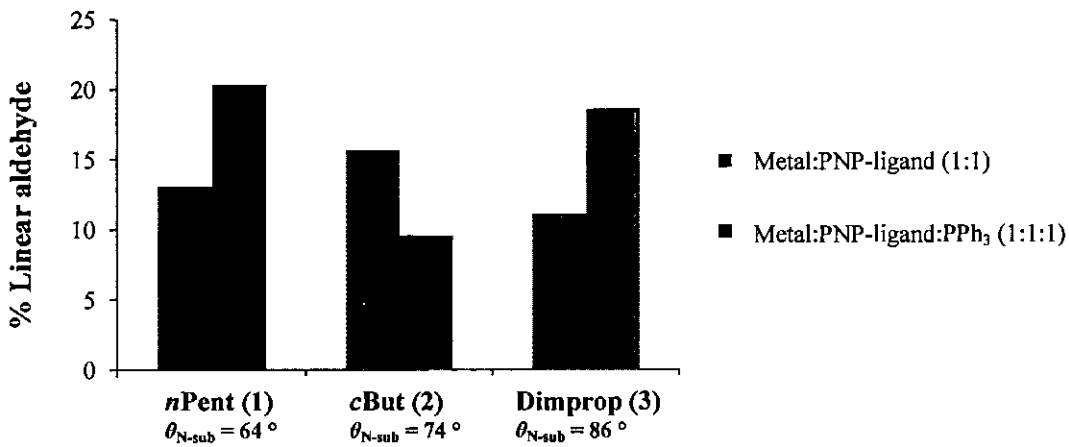


Figure 7.10: Combined results as given in **Table 7.6** and **Table 7.7**for the linear aldehyde selectivity for the hydroformylation of 1-octene with $[Ir(acac)(CO)_2]$ combined with various PNP-ligands in a M:PNP-ligand (metal to PNP-ligand) ratio of 1:1 and M:PNP-ligand:PPh_3 ratio of 1:1:1. [Ir] = 1.00 mM, 1-octene:Ir = 1000:1, 40 bar syngas ($CO:H_2$ = 1:1), 100 °C.

The changed behaviour of PNP-*c*But (**2**), was also observed for the rhodium analogue complexes with added PPh_3 (Entry 3, **Table 7.1** *vs* Entry 6, **Table 7.2**). Ligands **1** and **3** also gave near identical results with regards to selectivity and isomerization with **2** representing the outlier in the rhodium hydroformylation processes with added PPh_3. The activity of the iridium catalyzed process is similar for all three ligands (**Figure 7.11**).

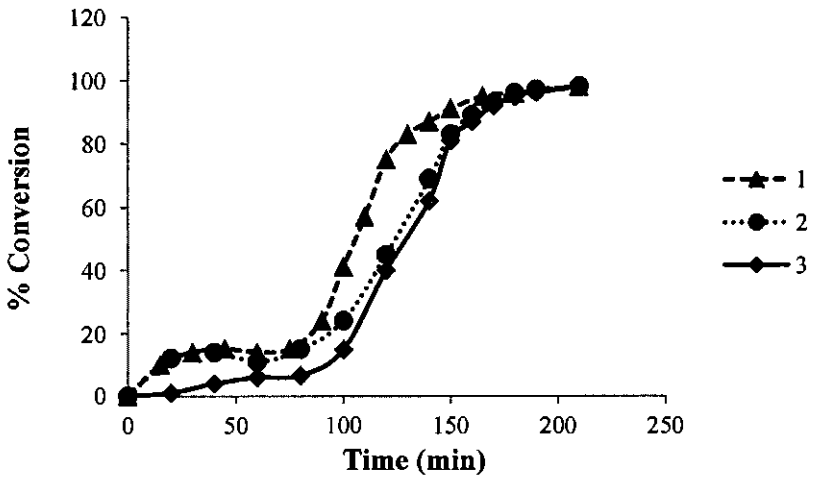


Figure 7.11: Conversion as a function of time for the hydroformylation of 1-octene with $[Ir(acac)(CO)_2]$ precursor combined with 1 eq. PPh_3 and 1 eq. of Ligands **1-3** as given in **Table 7.7**. [Ir] = 1.00 mM, 1-octene:Ir = 1000:1, 40 bar syngas ($CO:H_2$ = 1:1), 100 °C, M:PNP-ligand:PPh_3 = 1:1:1.

7.4 Conclusion

A range of PNP-ligands were prepared and evaluated with regards to their rhodium and iridium catalyzed hydroformylation performance using 1-octene as substrate. Catalytic parameters recorded were the selectivity towards the linear aldehyde product and the percentage of 1-octene isomerization.

The natural bite angle of bidentate ligands has been reported to have a decisive effect on activity, stability and selectivity achieved by catalysts in hydroformylation reactions. [10,11,12,13,14] The concept of the natural bite angle is a means to predict chelational preferences of bidentate ligands and is determined only by ligand backbone constraints and not by metal valance angles. These bite angles affect the selectivity towards linear aldehydes as regioselectivity is determined by relative stabilities of the transition states during alkene insertion. The bidentate ligand may be

[10] R.H. Crabtree, *The Organometallic Chemistry of the Transition Metals*, Wiley, New York, 2001.
[11] L. van der Veen, P. Keeven, G. Schoemaker, J. Reek, P. Kamer, P.W.N.M. van Leeuwen, M. Lutz, A. Spek, *Organometallics*, 19 (2000) 872.
[12] T.J. Devon, G.W. Phillips, T.A. Puckette, J.L. Stavinoha, J.J. van der Bilt, *Chem. Abstr.* 108 (1988) 7890.
[13] M. Kranenburg, Y.E.M. van der Burgt, P.C.J. Kamer, P.W.N.M. van Leeuwen, *Organometallics*, 14 (1995) 3081.
[14] A. van Rooy, P.C.J. Kamer, P.W.N.M. van Leeuwen, K. Goubitz, J. Fraanje, N. Veldman, A.K. Spek, *Organometallics*, 15 (1996) 835.

coordinated in either an equatorial-equatorial (ee) or an equatorial-axial (ea) fashion. An ee complex would typically require a bite angle of 120° and ea one of 90°. Bite angles influences the nature of the intermediates, which then influence the regioselectivity.[15,16,17] Large bite angles favour the ee intermediate, disfavouring the branched pathway. It was proposed by van Leeuwen *et al.* that a larger bite angle would increase the steric bulk around the area where the olefin adds, thus favouring the linear product.[18] Addition of electron withdrawing and –donating groups to the backbone of the diphosphine ligands can also contribute to the preferred equatorial or axial coordination of the ligand to the metal centre, thus influencing linear aldehyde selectivity.[19,20]

The PNP-ligands in this study have similar electronic properties (Chapter 3) and relatively small bite angles (70.23(6) - 72.3(1) °, see Chapter 5), thus the effectiveness of the bidentate diphosphines as catalyst ligands are considered to be dependent on steric effects. Three PNP-ligands were specifically selected for the study to ensure a satisfactory spread of steric properties of the ligands. The *Effective Tolman-based N-substituent steric effect* ($\theta_{N\text{-}sub}$), which is a modification of the popular Tolman angle6, was determined from previously discussed crystal structures of the free ligand as well as Pt(II) and Pd(III) PNP-coordinated complexes. Three ligands, namely, PNP-*n*Pent ($\theta_{N\text{-}Sub}$ = 64 °) (**1**), PNP-*c*But ($\theta_{N\text{-}Sub}$ = 74 °) (**2**) and PNP-Dimprop ($\theta_{N\text{-}Sub}$ = 86 °) (**3**) were selected from a range of PNP-ligands for the hydroformylation reactions. It was found that the activity and selectivity was significantly dependent on the steric bulk of the N-substituent of the PNP-ligand. For the rhodium catalyzed hydroformylation, an increase in linearity was found with a systematic increase in steric bulk of the ligand from 23.9 % for **1**, 30.7 % for **2** and 50.9 % for **3** (Entries 2-4, **Table 7.8**). The larger $\theta_{N\text{-}sub}$ value of **3** lead to a catalyst activity double that of ligand **1**. The % isomerisation decreased as the linear aldehyde selectivity and steric bulk of the ligands increased. The combination of these PNP-ligands with PPh_3 improved linear selectivity even more (**Table 7.9**). The combination of the PNP-ligand with PPh_3 in a 1:1 ratio increases the hydroformylation activity, without losing the selectivity for

[15] C. Casey, L. Petrovich, *J. Am. Chem. Soc.*, 117 (1995) 6007.
[16] J. Brown, A.G.J. Kent, *Perkin Trans.*, 2 (1987) 1597.
[17] P. Dierkes, P.W.N.M. van Leeuwen, *J. Chem. Soc. Dalton Trans.*, (1999) 1519.
[18] L.A. van der Veen, M.D.K. Boele, F.R. Bregman, P.C. Kamer, P.W.N.M. van Leeuwen, K. Goubitz, J. Fraanje, J. Schenk, C. Bo, *J. Am. Chem. Soc.*, 120 (1998) 11616.
[19] C. Casey, E. Paulsen, E. Beuttenmueller, B. Profit, B. Matter, D. Powell, *J. Am. Chem. Soc.*, 121 (1999) 1985.
[20] J.D. Unruh, J.R. Christenson, *J. Mol. Catal.*, 14 (1982) 19.

linear aldehyde formation. Linear selectivity increased significantly from 23.9 to 62.2 % for Ligand **1** accompanied by a higher l:b ratio of 2.9 *vs* 1.9. Isomerisation decreased from 63.7 to 16.3 %. Ligand **3** also showed good overall improvement with a 10 % increase in linear selectivity and a decrease in isomerisation (27.3 - 13.4 %). Ligand **2** showed the least improvement, nevertheless, an improvement of nonanal yield from 30.7 - 43.7 % and a decrease in isomerisation products from 53.0 - 39.9 %.

The same trend of increasing linear aldehyde formation with an increase in steric bulk ($\theta_{N\text{-}sub}$) of the ligand was not observed for the iridium catalyzed hydroformylation (**Table 7.8**). Ligands **1-3** gave similar results regarding linear product yield (± 13 %) and isomerisation (80 %). Ligand **3** showed higher activity, but a lower l:b ratio than ligands **1** and **2**. With added PPh_3, ligands **1** and **3** gave near identical results for nonanal selectivity (± 20 %) as well as isomerisation (± 70 %) which is an improvement of the 13 % linear aldehyde yield and 80 % isomerisation found with no added PPh_3 (**Table 7.9**). Ligand **2** was the outlier, producing lower linear selectivity and a higher % isomerisation.

Table 7.8: Comparison of the hydroformylation of 1-octene by $[M(acac)(CO)_2]$ (M = Rh, Ir) precursors combined with Ligands **1-3** in toluene. M:PNP-ligand ratio = 1:1.

Entry	Ligand	M:L ratio[a]	Time (min)	Conversion (%)	Linear aldehyde (%)	l:b ratio[b]	Isomerisation[c] (%)	TOF (h^{-1})	$\theta_{N\text{-}sub}$[d] (°)
Rhodium catalyzed hydroformylation									
2[e]	**1**	1:1	190	98	23.9	1.9:1	63.7	310	64
3[e]	**2**	1:1	160	97	30.7	1.9:1	53.0	359	74
4[e]	**3**	1:1	90	98	50.9	2.3:1	27.3	635	86
Iridium catalyzed hydroformylation									
1[f]	**1**	1:1	240	98	13.1	1.8:1	79.6	226	64
2[f]	**2**	1:1	200	98	15.7	2.1:1	76.8	271	74
3[f]	**3**	1:1	130	98	11.1	1.6:1	81.8	416	86

Reaction conditions: [M] = 1.00 mM (M = Rh, Ir), 1-octene:M = 1000:1, 20 bar syngas ($CO:H_2$ = 1:1), 80 °C. [a] M:PNP-ligand = metal to PNP-ligand ratio. [b] l:b = linear-to-branched selectivity, branched products, generally > 98 % 2-methyloctanal. [c] Isomerised products, generally > 95 % 2-octene. [d] Calculated as an average of the crystal structures and DFT calculated structures for the free ligands and $[M(PNP\text{-}alkyl)_2]$ (M = Pt, Pd) complexes. See Chapters 4, 5 and 6. [e] As given in **Table 7.1**. [f] As given in **Table 7.6**.

Table 7.9: Comparison of the hydroformylation of 1-octene by $[M(acac)(CO)_2]$ (M = Rh, Ir) precursors combined with Ligands **1-3** in toluene. M:PNP-ligand:PPh_3 ratio = 1:1:1.

Entry	Ligand	M:L: PPh_3 ratio[a]	Time (min)	Conversion (%)	Linear aldehyde (%)	l:b ratio[b]	Isomerisation[c] (%)	TOF (h^{-1})	$\theta_{N\text{-}sub}$[d] (°)
Rhodium catalyzed hydroformylation									
5[e]	1	1:1:1	145	96	62.2	2.9:1	16.3	384	64
6[e]	2	1:1:1	105	97	43.7	2.7:1	39.9	534	74
7[e]	3	1:1:1	90	98	60.6	2.3:1	13.4	665	86
Iridium catalyzed hydroformylation									
4[f]	1	1:1:1	210	98	20.3	2.1:1	70.3	279	64
5[f]	2	1:1:1	210	98	9.6	1.7:1	84.8	265	74
6[f]	3	1:1:1	210	98	18.6	2.3:1	73.2	267	86

Reaction conditions: [M] = 1.00 mM (M = Rh, Ir), 1-octene:M = 1000:1, 20 bar syngas ($CO:H_2$ = 1:1), 80 °C. [a] M:PNP-ligand:PPh_3 = metal to PNP-ligand to PPh_3 ratio. [b] l:b = linear-to-branched selectivity, branched products, generally > 98 % 2-methyloctanal. [c] Isomerised products, generally > 95 % 2-octene. [d] Calculated as an average of the crystal structures and DFT calculated structures for the free ligands and $[M(PNP\text{-}alkyl)_2]$ (M = Pt, Pd) complexes. See Chapters 4, 5 and 6. [e] As given in **Table 7.2**. [f] As given in **Table 7.7**.

Rhodium is clearly the more active hydroformylation catalyst, compared to iridium, when utilized with PNP-ligands and upon addition of PPh_3 in combination with the bidendate ligands (**Table 7.8** and **Table 7.9**). Iridium shares the same trend of increasing linear selectivity, when the PNP-ligand is combined with PPh_3, than its rhodium analogues. A distinct anomaly is observed for Ligand **2**, in both rhodium and iridium catalyzed hydroformylation, when PPh_3 is combined with the PNP-ligand. Similar results are however achieved for Ligands **1** and **3**, both showing improvement of linear selectivity, with the addition of PPh_3 compared to only using the PNP-ligand. This is true for both rhodium and iridium catalyzed reactions. Ligand **2** deviates from these results, showing an increase in selectivity for the rhodium catalyzed reactions, but a decrease in linear aldehyde formation during the iridium catalyzed reactions. This discrepancy cannot be explained at this stage. Iridium's overall slower catalyst activity, and tendency to be more stable,[21] may be useful in future studies as model catalysts for evaluating catalyst intermediates and active species for these PNP-systems.

[21] P.W.N.M. Van Leeuwen, *Homogeneous Catalysis: Understanding the Art*, Dordrecht: Kluwer Academic Publishers, 2004.

HP IR studies revealed that the reaction between [Rh(acac)$(CO)_2$] and the bidentate PNP-ligand gives [Rh(acac)(ligand)] in which both carbonyl groups are substituted with the chelating ligand. Reaction under syngas does not produce carbonyl frequencies that can be monitored. Therefore, not allowing catalyst intermediates and active species to be studied throughout the hydroformylation process *via* IR techniques. Samples taken directly from hydroformylation processes were insoluble at lower temperatures and extremely unstable, making NMR spectra of possible active species impractical at this stage. HP NMR studies have to be conducted in the future or perhaps a different solvent considered, helping with solubility, in order to further investigate catalyst behaviour during the hydroformylation process.

At temperatures of 50 and 60 ° no activity was observed over several hours for the rhodium catalyzed hydroformylation (Entries 12 and 13, **Table 7.3**). The catalyst only became active at 70 °C (Entry 14, **Table 7.3**), but gave less desirable results than the reactions when conducted at 80 °C (Entry 4, **Table 7.3**). An increase in temperature is expected to result in overall enhanced rate and therefore increased productivities. Higher concentrations of the PNP-ligands other than a 1:1 ratio with the metal resulted in zero activity (§ 7.3.1.1). This may be due to increased steric effects which might significantly inhibit alkene coordination.

The PNP-ligands produced active hydroformylation complexes with [M(acac)$(CO)_2$] (M = Rh, Ir) precursor catalysts. The catalytic study was conducted to provide evidence of the effectiveness of the PNP-ligands based mainly by a steric factor. This was proven for the rhodium catalyzed hydroformylation with various PNP-ligands of different steric bulkiness. This study has given valuable insight into the effects exhibited by the Rh-PNP complexes by varying the substituent on the N atom of the ligand. This information has to be extended in future, also utilizing computational techniques, to predict catalyst activity and optimize performance over a broader range of reaction conditions.

8 Evaluation of study

In this chapter...

The success, results obtained and scientific importance of this study as well as a discussion of future possibilities are discussed.

8.1 Introduction

One of the original motivations for this study (see paragraph 1.2, Chapter 1) was to gain further insight into the chemistry and properties of various PNP-ligands, used as part of the catalyst system in homogeneous catalysis, and evaluate any correlations between the solid state structural parameters and the hydroformylation selectivity of these ligands (when complexed to Rh(I) and Ir(I)). The findings of this investigation are discussed below.

8.2 Evaluation

8.2.1 Synthesis and single crystal X-ray crystallographic study

The study was focussed on the investigation of the structural effects when the nitrogen-coordinated alkyl substituents are systematically varied for a range of diphosphinoamine ligands, which in turn have varying and high-yield catalytic activity and selectivity (when complexed to Rh(I) and Ir(I)). This lead to successful synthesis and characterization of a range of PNP-ligands with varying nitrogen-coordinated moieties.

The solid state study of selected free ligands revealed that the P-N-P angle decreased with an increase in steric bulk of the substituent on the N-atom. A range of metal-PNP complexes (metal = Pt(II), Pd(II)) was also synthesized and characterized in order to investigate the coordination mode of these PNP-ligands. Pt(II) and Pd(II) were used as model complexes due to the significant difficulty of crystallizing Rh- and Ir-PNP complexes. The single crystal X-ray

crystallographic studies on these complexes revealed that bond lengths and angles of the coordination polyhedron are not significantly affected by the different nitrogen-coordinated alkyl moieties. The most noticeable differences for the various compounds were the orientations of the phenyl rings that seem to be affected by the steric bulk of the N-substituent. It appears that a "basket"-like arrangement (as defined in Chapter 5) is adopted for ligands with a relatively sterically bulky nitrogen substituent and a "fan-like" arrangement for the less bulky moieties.

8.2.2 Computational study

A computational study of a range of PNP-ligands as well as the corresponding [M(PNP-alkyl)$_2$] complexes was conducted. DFT calculations were performed using the B3LYP exchange correlation functional with LanL2DZ used as basis set for the transition metals and 6-311++G(d,p) as basis set for the main group elements. Optimized structures (indicated by no imaginary frequencies) with the lowest relative energy were obtained and compared to the crystal structures of the corresponding free ligands and coordinated Pt(II) and Pd(II) complexes. A good correlation was observed for the free ligands between the conformations adopted in solid state and the predicted conformations, with comparable bond lengths and angles. Slight variations in the orientation of the phenyl rings were however observed between the optimized structures and the crystal structure due to relatively large degrees of freedom of the phenyl rings of these free ligands. Comparison of the theoretical structures of the metal-coordinated PNP complexes (metal = Pt(II), Pd(II)) with the crystallographic data of the corresponding compounds revealed that the theoretically calculated structures had similar phenyl ring arrangements ("basket" or "fan-like" as defined in Chapter 5) than the corresponding solid state complexes, even though no intermolecular interactions were considered in the theoretical calculations. It was consequently concluded that the arrangement of the phenyl rings, is largely influenced by the steric bulk of the alkyl substituents.

8.2.3 Catalytic selectivity *vs.* crystallographic data

A steric parameter was successfully defined (*Effective Tolman-based N-substituent steric effect* ($\theta_{N\text{-}sub}$)) in which the steric bulk of the nitrogen-coordinated alkyl substituent was quantified. The $\theta_{N\text{-}sub}$* (from theoretically calculated structures) values correlated very well with the crystal structures of the Pt/Pd coordinated complexes as well as for the free ligands. A comparison between $\theta_{N\text{-}sub}$ for various diphosphinoamine ligands and the catalytic selectivity towards linear aldehydes during the hydroformylation of 1-octene revealed a relatively good correlation with the catalytic selectivity increasing as $\theta_{N\text{-}sub}$ for the varying ligands increased. Combining these PNP-ligands with PPh_3 increased linear aldehyde selectivity even more, although not systematically with the increasing steric bulk ($\theta_{N\text{-}sub}$) of the N-substituent.

8.3 Future work

Immediate future sub projects are defined below, which will serve to quantify and optimize aspects of importance to this project.

- Perform further detailed theoretical calculations for other variations of PNP-ligands and determine the $\theta_{N\text{-}sub}$*.
- Then, synthesize the corresponding ligands as determined from theoretical calculations.
- Additional hydroformylation catalysis, using these novel ligands (together with Rh(I) and Ir(I)), to determine to what extent the catalytic behaviour can be predicted.
- Investigate correlations between the catalytic selectivity (when complexed with Rh(I) and Ir(I)) and various other R-groups coordinated to the phosphorous atoms of the PNP-ligands.
- Consider introducing additional substituents on the auxiliary phenyl ring substituents on the P-donor atoms and evaluating the above aspect.

The opportunities surrounding the hydroformylation catalysis are vast since these are novel reactions with very little literature on the subject. In depth temperature, pressure, concentration and solvent studies can be performed in order to gain insight into the mechanism of the reaction.

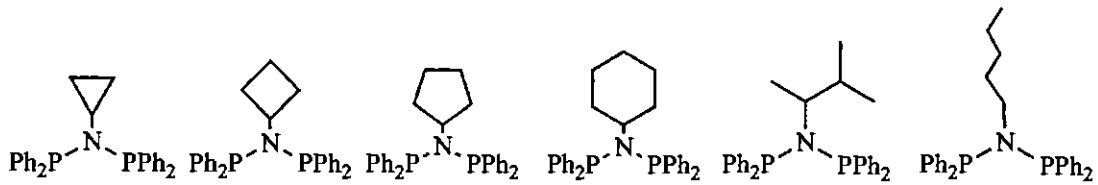
EVALUATION OF STUDY

HP NMR and HP IR studies can provide further information on intermediates in the catalytic cycle and general catalyst behaviour.

Summary

Hydroformylation for the production of aldehydes from alkenes, is a large and important homogeneously catalyzed industrial process. Most of these resulting aldehydes are hydrogenated to alcohols, having applications in plasticizer alcohols, detergents, wood preservatives and surfactants. Numerous phosphine ligands have been applied in these catalytic reactions signifying that changes in the ligand environment induce different steric and electronic properties into the catalyst system allowing to "tune" catalyst behaviour towards higher activity and selectivity.

A series of diphosphinoamine (PNP) ligands with various substituents on the N-atom, inducing different steric properties were synthesized and characterized (Scheme 1). Single crystal X-ray crystallographic studies of the PNP ligands revealed that the P-N-P bond angle decreases as the steric bulk of the alkyl moiety increases.



1 2 3 4 5 6

Scheme 1: Diphosphinoamine ligands (PNP-ligands) synthesized in this study. (1) *N,N*-Bis(diphenylphosphanyl)cyclopropylamine (PNP-*c*Prop); (2) *N,N*-Bis(diphenylphosphanyl)cyclobutanamine (PNP-*c*But); (3) *N,N*-Bis(diphenylphosphanyl)-cyclopentanamine (PNP-*c*Pent); (4) *N,N*-Bis(diphenylphosphanyl)cyclohexanamine (PNP-*c*Hex); (5) *N,N*-Bis(diphenylphosphanyl)-1,2-dimethylpropylamine (PNP-Dimprop); (6) *N,N*-Bis(diphenylphosphanyl)-*n*-pentylamine (PNP-*n*Pent).

The synthesis and coordination of the PNP-ligands to Pt(II) and Pd(II) served as models to quantify different effects which could then be rationalized for the Rh(I) and Ir(I) pre-catalysts systems for use in olefin hydroformylation. The reason for using Pt(II) and Pd(II) was therefore primarily to gain information on the coordination mode of these ligands, rather than the notoriously difficult to isolate and unstable Rh and Ir complexes. A total of three free PNP-ligands, four [Pt(PNP-alkyl)$_2$] and one [Pd(PNP-alkyl)$_2$] solid state crystal structures were

solved, which provided excellent structural fundamentals from which the catalysis could be pursued.

The study was also supplemented with theoretical chemistry. The comparison between the optimized structure and the crystal data revealed small differences, illustrating that predictions can be made in terms of ligand design in particular when solid state data is hard to obtain. The calculated structures indicated that the phenyl ring arrangement is affected by the steric bulk of the nitrogen-coordinated alkyl moiety which could ultimately affect the catalytic selectivity.

The steric demand of the ligands was defined by the *Effective Tolman-based N-substituent steric effect* ($\theta_{N\text{-}sub}$). The electron donating ability was evaluated through the first order Pt-P coupling constants as determined from the corresponding Pt-PNP complexes showing no significant difference between electronic properties of the ligands.

The hydroformylation of 1-octene was investigated utilizing Rh(I) and Ir(I) metal centres. The linearity of the aldehyde product increased with an increase in steric bulk of the ligand at the expense of side product formation during the rhodium catalyzed hydroformylation catalysis of 1-octene. A striking feature was that a 27 % improvement in the linear selectivity could be achieved by increasing the $\theta_{N\text{-}sub}$ angle of the N-substituent from 64 to 84 °. The parallel competing isomerisation of 1-octene varied from 63.7 % for a cone angle of 64 °, with a decrease to 27.3 % observed for PNP-Dimprop, with cone angle of 86 °. The N-alkyl moiety of the PNP-ligand can therefore be structurally fine-tuned towards efficient hydroformylation catalysts. Combining the PNP-ligands with PPh_3 gives rise to a more superior system with higher reactivity and lower alkene loss through isomerisation.

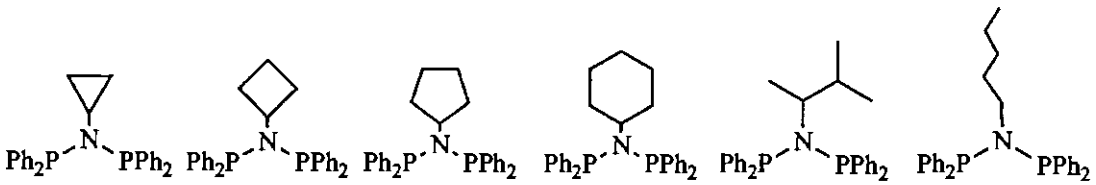
Iridium catalyzed hydroformylation did not yield the same trend of linear selectivity increase with an increase in $\theta_{N\text{-}sub}$ of the ligand, but did show similar behaviour to the Rh analogue when PPh_3 was combined with the PNP-ligands.

Keywords: Hydroformylation, Catalysis, 1-octene, Crystallographic study, Diphosphinoamine, Theoretical study, Steric parameter, Metal-PNP complexes.

Opsomming

Hidroformilering vir die produksie van aldehiede vanaf alkene is `n groot en belangrike homogene katalitiese nywerheidsproses. Die meeste van die gevolglike aldehiede word gehidrogeneer na alkohole en word gebruik as plastiseerder alkohole, skoonmaakmiddels, hout preserveermiddels en benatters. Veelvuldige fosfienligande is al gebruik in hierdie katalitiese reaksies, wat aandui dat veranderinge in die ligandomgewing verskillende steriese en elektroniese eienskappe in die katalitiese stelsel veroorsaak en dus hoër aktiwiteit en selektiwiteit tot gevolg het.

`n Reeks difosfienamien (PNP) ligande met verskeie substituente op die N-atoom, wat verskillende steriese eienskappe veroorsaak, is gesintetiseer en gekarakteriseer (Skema 1). Enkelkristal X-straal kristallografiese studies van die PNP ligande het onthul dat die P-N-P bindingshoek afneem wanneer die steriese massa van die alkielgroep toeneem.



1 2 3 4 5 6

Skema 1: Difosfienamien ligande (PNP-ligande) in hierdie studie vervaardig (1) *N,N*-Bis(difenielfosfaniel)siklopropielamien (PNP-*c*Prop); (2) *N,N*-Bis(difenielfosfaniel)siklobutanamien (PNP-*c*But); (3) *N,N*-Bis(difenielfosfaniel)-siklopentanamien (PNP-*c*Pent); (4) *N,N*-Bis(difenielfosfaniel)sikloheksanamien (PNP-*c*Heks); (5) *N,N*-Bis(difenielfosfaniel)-1,2-dimetielpropielamien (PNP-Dimprop); (6) *N,N*-Bis(difenielfosfaniel)-*n*-pentalamien (PNP-*n*Pent).

Die sintese en koördinasie van die PNP-ligande aan Pt(II) en Pd(II) dien as modelle om verskillende effekte te kwantifiseer, wat dan gebruik kan word in die Rh(I) en Ir(I) pre-katalitiese stelsel met toepassing in olefien hidroformilering. Die rede vir die gebruik van Pt(II) en Pd(II) is dus primêr die inwinning van inligting aangaande die koördinasiemodus van hierdie ligande, eerder as die aansienlik moeilike isolasie van onstabiele Rh and Ir komplekse. `n Totaal van drie vry PNP-ligande, vier [Pt(PNP-alkiel)$_2$] en een [Pd(PNP-alkiel)$_2$] vaste toestand kristalstrukture

is opgelos, wat uitstekende strukturele beginsels voorsien het waaruit die katalise opgevolg kon word.

Die studie word ook ondersteun deur teoretiese chemie. Die vergelyking van die geoptimaliseerde stukture en die kristaldata onthul klein verskille, wat illustreer dat voorspellings gemaak kan word in terme van ligand-ontwerp, veral wanneer vaste toestand data moeilik is om te verkry. Die berekende strukture toon aan dat die fenielringrangskikking beïnvloed word deur die steriese massa van die stikstof-gekoördineerde alkielgroep wat uiteindelik die katalitiese selektiwiteit sal beïnvloed.

Die steriese eise van die ligande word gedefinieer deur die *Effektiewe Tolman-gebaseerde N-substituent steriese effek* ($\theta_{N\text{-}sub}$). Die elektronskenkende vermoë is geëvalueer deur die eerste orde Pt-P koppelingskonstantes soos vasgestel uit die ooreenstemmende Pt-PNP komplekse, wat aandui dat elektroniese eienskappe tussen die ligande nie beduidend verskil nie.

Die hidroformilering van 1-okteen is ondersoek deur die gebruik van Rh(I) en Ir(I) metaalkerne. Die lineariteit van die aldehied produk neem toe met `n toename in steriese massa van die ligand, ten koste van neweprodukvorming gedrurende die rodium-gekataliseerde hidroformileringskatalise van 1-okteen. `n Treffende eienskap was dat `n 27 % verbetering in liniêre selektiwiteit bereik kon word deur die $\theta_{N\text{-}sub}$ hoek van die N-substituent van 64 na 84 ° te verhoog. Die parallel-kompeterende isomerisasie van 1-okteen wissel vanaf 63.7 % vir `n keëlhoek van 64 °, met `n afname na 27.3 % waargeneem vir PNP-Dimprop, met `n keëlhoek van 86 °. Die N-alkielgroep van die PNP-ligand kan dus struktureel verfyn word ten opsigte van effektiewe hidroformileringskataliste. Die kombinasie van PNP-ligande met PF_3 lei tot `n meer voortreflike stelsel met hoër reaktiwiteit en laer alkeenverlies as gevolg van isomerisasie.

Iridium gekataliseerde hidroformilering het nie dieselfde neiging van liniêre selektiwiteitstoename met `n toename in $\theta_{N\text{-}sub}$ van die ligand opgelewer nie, maar toon soortgelyke gedrag as die Rh analoog wanneer PPh_3 met die PNP-ligande gekombineer is.

Sleutelwoorde: Hidroformilering, Katalise, 1-okteen, Kristallografiese studie, Difosfienamien, Teoretiese studie, Steriese parameter, Metaal-PNP komplekse.

APPENDIX A

APPENDIX A

A1. Crystallographic data for PNP-*c*Prop

Table A 1: Fractional atomic coordinates and isotropic or equivalent isotropic displacement parameters (Å^2) for PNP-*c*Prop.

	x	*y*	*z*	U_{iso}*/U_{eq}
C1	0.59558 (12)	0.25225 (15)	0.55966 (10)	0.0209 (3)
H1	0.5473	0.1995	0.5729	0.025*
C2	0.54277 (14)	0.32353 (16)	0.47190 (11)	0.0267 (4)
H2A	0.4654	0.3121	0.4327	0.032*
H2B	0.5833	0.3354	0.4396	0.032*
C3	0.58012 (14)	0.39375 (16)	0.55920 (11)	0.0274 (4)
H3A	0.6436	0.4488	0.5804	0.033*
H3B	0.5256	0.4255	0.5735	0.033*
C11	0.71357 (12)	0.07960 (14)	0.74371 (10)	0.0184 (3)
C12	0.63529 (12)	−0.00544 (14)	0.68578 (11)	0.0211 (3)
H12	0.6151	−0.0062	0.6237	0.025*
C13	0.58661 (13)	−0.08882 (16)	0.71768 (11)	0.0248 (3)
H13	0.5327	−0.145	0.6773	0.03*
C14	0.61675 (14)	−0.08999 (16)	0.80836 (12)	0.0258 (4)
H14	0.5834	−0.1467	0.8303	0.031*
C15	0.69601 (13)	−0.00792 (15)	0.86719 (11)	0.0245 (3)
H15	0.7173	−0.0093	0.9295	0.029*
C16	0.74413 (13)	0.07601 (15)	0.83527 (11)	0.0213 (3)
H16	0.7984	0.1316	0.876	0.026*
C21	0.77084 (12)	0.33887 (14)	0.75153 (10)	0.0180 (3)
C22	0.68675 (13)	0.37085 (15)	0.76614 (10)	0.0205 (3)
H22	0.635	0.3084	0.7576	0.025*
C23	0.67822 (14)	0.49346 (15)	0.79308 (11)	0.0251 (3)
H23	0.6203	0.5145	0.8022	0.03*
C24	0.75390 (14)	0.58542 (16)	0.80678 (11)	0.0258 (4)
H24	0.7471	0.6694	0.8242	0.031*
C25	0.83918 (14)	0.55410 (15)	0.79498 (11)	0.0241 (3)
H25	0.8921	0.616	0.8057	0.029*
C26	0.84747 (13)	0.43169 (15)	0.76732 (10)	0.0207 (3)
H26	0.9061	0.4109	0.7591	0.025*
C31	0.76517 (12)	−0.03248 (14)	0.55113 (10)	0.0182 (3)
C32	0.68867 (13)	−0.12527 (15)	0.50250 (11)	0.0222 (3)
H32	0.6234	−0.1006	0.4519	0.027*
C33	0.70678 (14)	−0.25267 (15)	0.52714 (11)	0.0262 (4)
H33	0.654	−0.3147	0.4938	0.031*
C34	0.80162 (14)	−0.28923 (15)	0.60026 (12)	0.0272 (4)
H34	0.8142	−0.3766	0.6168	0.033*
C35	0.87866 (14)	−0.19906 (15)	0.64963 (12)	0.0269 (4)
H35	0.9436	−0.2245	0.7002	0.032*
C36	0.86059 (13)	−0.07105 (15)	0.62481 (11)	0.0223 (3)
H36	0.9137	−0.0095	0.6583	0.027*
C41	0.85308 (12)	0.20398 (14)	0.53650 (10)	0.0173 (3)
C42	0.91036 (12)	0.14796 (15)	0.49881 (10)	0.0201 (3)

H42	0.8889	0.0675	0.4699	0.024*
C43	0.99796 (13)	0.20875 (16)	0.50336 (11)	0.0239 (3)
H43	1.0358	0.1699	0.4772	0.029*
C44	1.03073 (13)	0.32609 (16)	0.54587 (12)	0.0267 (4)
H44	1.0911	0.3672	0.5492	0.032*
C45	0.97516 (14)	0.38290 (15)	0.58346 (12)	0.0266 (4)
H45	0.9978	0.4628	0.6131	0.032*
C46	0.88620 (13)	0.32314 (14)	0.57785 (11)	0.0222 (3)
H46	0.8474	0.3638	0.6024	0.027*
N1	0.70166 (10)	0.20116 (11)	0.59277 (8)	0.0171 (3)
P1	0.78650 (3)	0.18492 (4)	0.70717 (3)	0.01690 (10)
P2	0.72688 (3)	0.13260 (4)	0.51349 (3)	0.01718 (10)

Table A 2: Atomic displacement parameters (Å^2) for PNP-*c*Prop.

	U^{11}	U^{22}	U^{33}	U^{12}	U^{13}	U^{23}
C1	0.0195 (7)	0.0222 (8)	0.0204 (8)	0.0035 (6)	0.0094 (6)	−0.0003 (6)
C2	0.0286 (9)	0.0274 (8)	0.0215 (8)	0.0078 (7)	0.0101 (7)	0.0011 (7)
C3	0.0304 (9)	0.0247 (8)	0.0227 (8)	0.0083 (7)	0.0097 (7)	0.0006 (7)
C11	0.0196 (7)	0.0158 (7)	0.0213 (8)	0.0023 (6)	0.0112 (6)	0.0005 (6)
C12	0.0254 (8)	0.0202 (7)	0.0193 (8)	−0.0002 (6)	0.0124 (7)	−0.0017 (6)
C13	0.0272 (9)	0.0216 (8)	0.0261 (9)	−0.0058 (6)	0.0135 (7)	−0.0045 (7)
C14	0.0304 (9)	0.0222 (8)	0.0306 (9)	−0.0029 (7)	0.0194 (8)	0.0013 (7)
C15	0.0301 (9)	0.0257 (8)	0.0203 (8)	0.0007 (7)	0.0142 (7)	0.0019 (6)
C16	0.0227 (8)	0.0202 (7)	0.0196 (8)	−0.0014 (6)	0.0092 (6)	−0.0003 (6)
C21	0.0208 (8)	0.0186 (7)	0.0134 (7)	0.0010 (6)	0.0073 (6)	0.0002 (6)
C22	0.0220 (8)	0.0209 (7)	0.0187 (8)	−0.0005 (6)	0.0102 (6)	−0.0007 (6)
C23	0.0283 (9)	0.0251 (8)	0.0244 (8)	0.0051 (7)	0.0148 (7)	−0.0007 (7)
C24	0.0362 (9)	0.0186 (7)	0.0209 (8)	0.0025 (7)	0.0127 (7)	−0.0009 (6)
C25	0.0315 (9)	0.0206 (8)	0.0186 (8)	−0.0048 (7)	0.0112 (7)	−0.0011 (6)
C26	0.0227 (8)	0.0229 (8)	0.0165 (7)	−0.0022 (6)	0.0097 (6)	−0.0011 (6)
C31	0.0225 (8)	0.0173 (7)	0.0216 (8)	−0.0009 (6)	0.0161 (7)	−0.0015 (6)
C32	0.0253 (8)	0.0222 (8)	0.0232 (8)	−0.0029 (6)	0.0150 (7)	−0.0034 (6)
C33	0.0365 (10)	0.0211 (8)	0.0279 (9)	−0.0086 (7)	0.0210 (8)	−0.0066 (7)
C34	0.0413 (10)	0.0162 (7)	0.0311 (9)	−0.0017 (7)	0.0233 (8)	0.0003 (7)
C35	0.0289 (9)	0.0238 (8)	0.0286 (9)	0.0024 (7)	0.0146 (7)	0.0052 (7)
C36	0.0226 (8)	0.0192 (7)	0.0270 (8)	−0.0018 (6)	0.0136 (7)	−0.0008 (6)
C41	0.0200 (7)	0.0178 (7)	0.0147 (7)	0.0011 (6)	0.0088 (6)	0.0038 (6)
C42	0.0241 (8)	0.0178 (7)	0.0198 (8)	0.0027 (6)	0.0118 (7)	0.0018 (6)
C43	0.0246 (8)	0.0263 (8)	0.0264 (8)	0.0054 (6)	0.0169 (7)	0.0078 (7)
C44	0.0248 (8)	0.0280 (8)	0.0291 (9)	−0.0039 (7)	0.0147 (7)	0.0077 (7)
C45	0.0343 (9)	0.0196 (8)	0.0255 (9)	−0.0068 (7)	0.0143 (8)	0.0001 (6)
C46	0.0308 (9)	0.0178 (7)	0.0224 (8)	−0.0005 (6)	0.0164 (7)	0.0010 (6)
N1	0.0179 (6)	0.0186 (6)	0.0155 (6)	0.0020 (5)	0.0088 (5)	−0.0004 (5)
P1	0.0173 (2)	0.01718 (19)	0.0168 (2)	0.00046 (14)	0.00886 (16)	−0.00058 (14)
P2	0.0189 (2)	0.01685 (19)	0.0170 (2)	0.00047 (14)	0.00976 (16)	−0.00097 (14)

APPENDIX A

Table A 3: Bond lengths (Å) for PNP-*c*Prop.

Atoms	Bond length (Å)	Atoms	Bond length (Å)
C1—N1	1.452 (2)	C25—C26	1.393 (2)
C1—C3	1.500 (2)	C25—H25	0.95
C1—C2	1.504 (2)	C26—H26	0.95
C1—H1	1	C31—C36	1.395 (2)
C2—C3	1.504 (2)	C31—C32	1.399 (2)
C2—H2A	0.99	C31—P2	1.8349 (17)
C2—H2B	0.99	C32—C33	1.386 (2)
C3—H3A	0.99	C32—H32	0.95
C3—H3B	0.99	C33—C34	1.380 (3)
C11—C12	1.399 (2)	C33—H33	0.95
C11—C16	1.399 (2)	C34—C35	1.387 (2)
C11—P1	1.8342 (16)	C34—H34	0.95
C12—C13	1.390 (2)	C35—C36	1.393 (2)
C12—H12	0.95	C35—H35	0.95
C13—C14	1.386 (2)	C36—H36	0.95
C13—H13	0.95	C41—C46	1.399 (2)
C14—C15	1.390 (2)	C41—C42	1.402 (2)
C14—H14	0.95	C41—P2	1.8282 (16)
C15—C16	1.388 (2)	C42—C43	1.386 (2)
C15—H15	0.95	C42—H42	0.95
C16—H16	0.95	C43—C44	1.388 (2)
C21—C22	1.396 (2)	C43—H43	0.95
C21—C26	1.398 (2)	C44—C45	1.384 (2)
C21—P1	1.8433 (17)	C44—H44	0.95
C22—C23	1.391 (2)	C45—C46	1.391 (2)
C22—H22	0.95	C45—H45	0.95
C23—C24	1.390 (2)	C46—H46	0.95
C23—H23	0.95	N1—P2	1.7208 (13)
C24—C25	1.383 (2)	N1—P1	1.7301 (14)
C24—H24	0.95		

Table A 4: Bond angles (°) for PNP-*c*Prop.

Atoms	Bond angle (°)	Atoms	Bond angle (°)
N1—C1—C3	119.55 (14)	C26—C25—H25	120
N1—C1—C2	119.64 (14)	C25—C26—C21	121.00 (15)
C3—C1—C2	60.09 (11)	C25—C26—H26	119.5
N1—C1—H1	115.5	C21—C26—H26	119.5
C3—C1—H1	115.5	C36—C31—C32	118.53 (14)
C2—C1—H1	115.5	C36—C31—P2	125.74 (12)
C1—C2—C3	59.83 (11)	C32—C31—P2	115.68 (12)
C1—C2—H2A	117.8	C33—C32—C31	120.89 (16)
C3—C2—H2A	117.8	C33—C32—H32	119.6
C1—C2—H2B	117.8	C31—C32—H32	119.6
C3—C2—H2B	117.8	C34—C33—C32	119.85 (15)
H2A—C2—H2B	114.9	C34—C33—H33	120.1
C1—C3—C2	60.07 (11)	C32—C33—H33	120.1
C1—C3—H3A	117.8	C33—C34—C35	120.37 (15)

APPENDIX A

C2—C3—H3A	117.8	C33—C34—H34	119.8
C1—C3—H3B	117.8	C35—C34—H34	119.8
C2—C3—H3B	117.8	C34—C35—C36	119.81 (16)
H3A—C3—H3B	114.9	C34—C35—H35	120.1
C12—C11—C16	118.33 (14)	C36—C35—H35	120.1
C12—C11—P1	123.02 (12)	C35—C36—C31	120.55 (15)
C16—C11—P1	118.40 (12)	C35—C36—H36	119.7
C13—C12—C11	120.96 (15)	C31—C36—H36	119.7
C13—C12—H12	119.5	C46—C41—C42	118.17 (14)
C11—C12—H12	119.5	C46—C41—P2	122.20 (12)
C14—C13—C12	119.98 (15)	C42—C41—P2	118.81 (12)
C14—C13—H13	120	C43—C42—C41	120.72 (15)
C12—C13—H13	120	C43—C42—H42	119.6
C13—C14—C15	119.78 (15)	C41—C42—H42	119.6
C13—C14—H14	120.1	C42—C43—C44	120.36 (15)
C15—C14—H14	120.1	C42—C43—H43	119.8
C16—C15—C14	120.26 (15)	C44—C43—H43	119.8
C16—C15—H15	119.9	C45—C44—C43	119.75 (15)
C14—C15—H15	119.9	C45—C44—H44	120.1
C15—C16—C11	120.65 (15)	C43—C44—H44	120.1
C15—C16—H16	119.7	C44—C45—C46	120.09 (15)
C11—C16—H16	119.7	C44—C45—H45	120
C22—C21—C26	118.40 (14)	C46—C45—H45	120
C22—C21—P1	125.20 (12)	C45—C46—C41	120.89 (15)
C26—C21—P1	116.33 (12)	C45—C46—H46	119.6
C23—C22—C21	120.45 (15)	C41—C46—H46	119.6
C23—C22—H22	119.8	C1—N1—P2	116.03 (10)
C21—C22—H22	119.8	C1—N1—P1	120.30 (10)
C24—C23—C22	120.45 (16)	P2—N1—P1	122.58 (8)
C24—C23—H23	119.8	N1—P1—C11	103.56 (7)
C22—C23—H23	119.8	N1—P1—C21	102.40 (7)
C25—C24—C23	119.71 (15)	C11—P1—C21	100.43 (7)
C25—C24—H24	120.1	N1—P2—C41	103.54 (7)
C23—C24—H24	120.1	N1—P2—C31	105.26 (7)
C24—C25—C26	119.94 (15)	C41—P2—C31	102.29 (7)
C24—C25—H25	120		

A2. Crystallographic data for PNP-*c*But

Table A 5: Fractional atomic coordinates and isotropic or equivalent isotropic displacement parameters (Å^2) for PNP-*c*But.

	x	*y*	*z*	U_{iso}*/U_{eq}
C1	0.63564 (17)	0.73665 (19)	0.12318 (13)	0.0161 (3)
H1	0.7182	0.7791	0.1657	0.019*
C2	0.6829 (2)	0.5945 (2)	0.08102 (15)	0.0227 (4)
H2A	0.7631	0.5515	0.1244	0.027*
H2B	0.6039	0.528	0.0666	0.027*
C3	0.72812 (19)	0.6710 (2)	−0.01884 (14)	0.0243 (4)
H3A	0.8308	0.694	−0.016	0.029*
H3B	0.697	0.6245	−0.0864	0.029*
C4	0.63230 (18)	0.7937 (2)	0.00897 (13)	0.0202 (3)
H4A	0.6781	0.8854	0.0035	0.024*
H4B	0.5366	0.7926	−0.0291	0.024*
C11	0.61059 (17)	0.96900 (19)	0.30492 (14)	0.0170 (3)
C12	0.59621 (18)	1.04878 (19)	0.21255 (13)	0.0185 (3)
H12	0.5452	1.0127	0.151	0.022*
C13	0.65569 (17)	1.1803 (2)	0.20966 (14)	0.0207 (3)
H13	0.6468	1.2325	0.1458	0.025*
C14	0.72805 (19)	1.2358 (2)	0.29965 (16)	0.0238 (4)
H14	0.7687	1.3257	0.2977	0.029*
C15	0.7403 (2)	1.1586 (2)	0.39223 (15)	0.0259 (4)
H15	0.7887	1.1963	0.4542	0.031*
C16	0.68275 (19)	1.0269 (2)	0.39524 (14)	0.0223 (4)
H16	0.6923	0.9752	0.4593	0.027*
C21	0.67262 (18)	0.69892 (19)	0.37827 (13)	0.0177 (3)
C22	0.81721 (19)	0.7224 (2)	0.36534 (13)	0.0204 (3)
H22	0.845	0.7973	0.3228	0.024*
C23	0.9200 (2)	0.6362 (2)	0.41469 (14)	0.0249 (4)
H23	1.0179	0.6522	0.4053	0.03*
C24	0.8808 (2)	0.5268 (2)	0.47773 (14)	0.0283 (4)
H24	0.9515	0.4673	0.5103	0.034*
C25	0.7388 (2)	0.5049 (2)	0.49284 (14)	0.0270 (4)
H25	0.7118	0.431	0.5366	0.032*
C26	0.6354 (2)	0.5909 (2)	0.44406 (14)	0.0216 (4)
H26	0.5381	0.5759	0.4556	0.026*
C31	0.21248 (16)	0.8079 (2)	0.13397 (12)	0.0165 (3)
C32	0.17680 (19)	0.8748 (2)	0.22612 (14)	0.0227 (4)
H32	0.232	0.8584	0.2909	0.027*
C33	0.0619 (2)	0.9650 (2)	0.22457 (16)	0.0249 (4)
H33	0.0406	1.0117	0.2876	0.03*
C34	−0.02202 (19)	0.9870 (2)	0.13090 (16)	0.0241 (4)
H34	−0.1016	1.0474	0.13	0.029*
C35	0.0110 (2)	0.9203 (2)	0.03906 (15)	0.0251 (4)
H35	−0.0464	0.9348	−0.025	0.03*
C36	0.12781 (18)	0.8322 (2)	0.04019 (13)	0.0206 (4)
H36	0.1504	0.7879	−0.0235	0.025*

C41	0.30058 (17)	0.54508 (18)	0.21428 (12)	0.0156 (3)
C42	0.40188 (18)	0.45205 (19)	0.25833 (14)	0.0188 (3)
H42	0.4998	0.467	0.2484	0.023*
C43	0.3623 (2)	0.33809 (19)	0.31634 (14)	0.0219 (4)
H43	0.4331	0.2773	0.3472	0.026*
C44	0.2191 (2)	0.3130 (2)	0.32932 (14)	0.0244 (4)
H44	0.1914	0.2351	0.3687	0.029*
C45	0.11719 (19)	0.4034 (2)	0.28400 (15)	0.0250 (4)
H45	0.0191	0.3861	0.2915	0.03*
C46	0.15723 (19)	0.5188 (2)	0.22774 (14)	0.0208 (3)
H46	0.0864	0.5804	0.1982	0.025*
N1	0.50881 (15)	0.74590 (16)	0.18514 (11)	0.0153 (3)
P1	0.52394 (4)	0.79965 (6)	0.31465 (3)	0.01550 (9)
P2	0.35464 (4)	0.67934 (6)	0.12377 (3)	0.01489 (9)

Table A 6: Atomic displacement parameters (Å^2) for PNP-*c*But.

	U^{11}	U^{22}	U^{33}	U^{12}	U^{13}	U^{23}
C1	0.0156 (7)	0.0166 (7)	0.0163 (7)	0.0007 (6)	0.0022 (6)	−0.0001 (6)
C2	0.0231 (9)	0.0179 (8)	0.0279 (9)	0.0032 (7)	0.0082 (7)	−0.0003 (7)
C3	0.0249 (9)	0.0246 (9)	0.0245 (8)	−0.0014 (8)	0.0089 (7)	−0.0050 (8)
C4	0.0210 (8)	0.0228 (8)	0.0173 (7)	0.0008 (7)	0.0048 (6)	0.0025 (7)
C11	0.0123 (7)	0.0168 (8)	0.0217 (8)	0.0012 (6)	0.0006 (6)	−0.0022 (6)
C12	0.0183 (8)	0.0190 (8)	0.0181 (8)	0.0025 (6)	0.0006 (6)	−0.0033 (6)
C13	0.0183 (8)	0.0195 (8)	0.0247 (8)	0.0016 (7)	0.0034 (6)	0.0009 (7)
C14	0.0177 (8)	0.0173 (8)	0.0362 (10)	−0.0002 (7)	0.0007 (7)	−0.0030 (7)
C15	0.0217 (9)	0.0242 (10)	0.0301 (9)	0.0021 (7)	−0.0095 (7)	−0.0062 (8)
C16	0.0239 (9)	0.0222 (9)	0.0200 (8)	0.0037 (7)	−0.0037 (7)	−0.0016 (7)
C21	0.0202 (8)	0.0185 (8)	0.0142 (7)	0.0002 (7)	−0.0006 (6)	−0.0007 (6)
C22	0.0218 (8)	0.0218 (9)	0.0173 (8)	0.0007 (7)	−0.0007 (6)	−0.0004 (6)
C23	0.0221 (9)	0.0314 (10)	0.0206 (8)	0.0062 (7)	−0.0020 (7)	−0.0047 (7)
C24	0.0395 (11)	0.0248 (10)	0.0194 (8)	0.0130 (9)	−0.0074 (8)	−0.0038 (7)
C25	0.0448 (12)	0.0197 (9)	0.0156 (8)	0.0007 (8)	−0.0026 (7)	0.0019 (7)
C26	0.0278 (9)	0.0201 (8)	0.0166 (8)	−0.0038 (7)	−0.0006 (7)	−0.0003 (7)
C31	0.0139 (7)	0.0158 (7)	0.0197 (7)	−0.0015 (6)	0.0009 (6)	0.0011 (7)
C32	0.0213 (8)	0.0258 (9)	0.0206 (8)	0.0038 (7)	−0.0018 (7)	−0.0017 (7)
C33	0.0232 (9)	0.0237 (9)	0.0282 (9)	0.0033 (7)	0.0049 (7)	−0.0031 (7)
C34	0.0164 (8)	0.0206 (9)	0.0356 (10)	0.0017 (7)	0.0039 (7)	0.0055 (8)
C35	0.0207 (8)	0.0276 (10)	0.0262 (9)	−0.0003 (7)	−0.0038 (7)	0.0071 (8)
C36	0.0192 (8)	0.0239 (9)	0.0186 (8)	−0.0018 (6)	0.0001 (6)	0.0006 (6)
C41	0.0180 (8)	0.0145 (7)	0.0144 (7)	−0.0018 (6)	0.0017 (6)	−0.0027 (6)
C42	0.0164 (8)	0.0185 (8)	0.0216 (8)	0.0000 (6)	0.0025 (6)	−0.0016 (6)
C43	0.0242 (9)	0.0194 (9)	0.0223 (8)	0.0017 (7)	0.0026 (7)	0.0018 (7)
C44	0.0297 (9)	0.0185 (8)	0.0257 (8)	−0.0056 (8)	0.0074 (7)	0.0011 (7)
C45	0.0187 (8)	0.0247 (9)	0.0323 (10)	−0.0052 (7)	0.0073 (7)	−0.0018 (8)
C46	0.0181 (8)	0.0212 (8)	0.0231 (8)	−0.0006 (7)	0.0010 (6)	−0.0014 (7)
N1	0.0135 (6)	0.0178 (7)	0.0146 (6)	−0.0015 (5)	0.0012 (5)	−0.0021 (5)
P1	0.01451 (19)	0.0175 (2)	0.01444 (18)	−0.00069 (16)	0.00074 (14)	−0.00094 (16)
P2	0.01521 (19)	0.01517 (18)	0.01420 (18)	−0.00057 (16)	0.00048 (13)	−0.00147 (16)

APPENDIX A

Table A 7: Bond lengths (Å) for PNP-*c*But.

Atoms	Bond length (Å)	Atoms	Bond length (Å)
C1—N1	1.478 (2)	C24—C25	1.380 (3)
C1—C4	1.544 (2)	C24—H24	0.95
C1—C2	1.551 (2)	C25—C26	1.389 (3)
C1—H1	1	C25—H25	0.95
C2—C3	1.550 (3)	C26—H26	0.95
C2—H2A	0.99	C31—C32	1.395 (2)
C2—H2B	0.99	C31—C36	1.399 (2)
C3—C4	1.546 (3)	C31—P2	1.838 (2)
C3—H3A	0.99	C32—C33	1.388 (3)
C3—H3B	0.99	C32—H32	0.95
C4—H4A	0.99	C33—C34	1.390 (3)
C4—H4B	0.99	C33—H33	0.95
C11—C12	1.398 (2)	C34—C35	1.383 (3)
C11—C16	1.401 (2)	C34—H34	0.95
C11—P1	1.837 (2)	C35—C36	1.390 (3)
C12—C13	1.391 (3)	C35—H35	0.95
C12—H12	0.95	C36—H36	0.95
C13—C14	1.390 (3)	C41—C46	1.396 (2)
C13—H13	0.95	C41—C42	1.396 (2)
C14—C15	1.386 (3)	C41—P2	1.8271 (19)
C14—H14	0.95	C42—C43	1.389 (2)
C15—C16	1.384 (3)	C42—H42	0.95
C15—H15	0.95	C43—C44	1.391 (3)
C16—H16	0.95	C43—H43	0.95
C21—C26	1.396 (2)	C44—C45	1.389 (3)
C21—C22	1.401 (3)	C44—H44	0.95
C21—P1	1.8404 (19)	C45—C46	1.390 (3)
C22—C23	1.389 (3)	C45—H45	0.95
C22—H22	0.95	C46—H46	0.95
C23—C24	1.390 (3)	N1—P1	1.7138 (15)
C23—H23	0.95	N1—P2	1.7192 (16)

Table A 8: Bond angles (°) for PNP-*c*But.

Atoms	Bond angle (°)	Atoms	Bond angle (°)
N1—C1—C4	120.84 (14)	C23—C24—H24	120.1
N1—C1—C2	119.96 (14)	C24—C25—C26	120.05 (18)
C4—C1—C2	88.95 (13)	C24—C25—H25	120
N1—C1—H1	108.5	C26—C25—H25	120
C4—C1—H1	108.5	C25—C26—C21	120.91 (18)
C2—C1—H1	108.5	C25—C26—H26	119.5
C3—C2—C1	87.72 (14)	C21—C26—H26	119.5
C3—C2—H2A	114	C32—C31—C36	118.23 (16)
C1—C2—H2A	114	C32—C31—P2	126.41 (13)
C3—C2—H2B	114	C36—C31—P2	115.22 (13)
C1—C2—H2B	114	C33—C32—C31	120.98 (17)
H2A—C2—H2B	111.2	C33—C32—H32	119.5
C4—C3—C2	88.91 (13)	C31—C32—H32	119.5

APPENDIX A

C4—C3—H3A	113.8	C32—C33—C34	120.06 (18)
C2—C3—H3A	113.8	C32—C33—H33	120
C4—C3—H3B	113.8	C34—C33—H33	120
C2—C3—H3B	113.8	C35—C34—C33	119.69 (17)
H3A—C3—H3B	111.1	C35—C34—H34	120.2
C1—C4—C3	88.10 (13)	C33—C34—H34	120.2
C1—C4—H4A	114	C34—C35—C36	120.21 (17)
C3—C4—H4A	114	C34—C35—H35	119.9
C1—C4—H4B	114	C36—C35—H35	119.9
C3—C4—H4B	114	C35—C36—C31	120.80 (17)
H4A—C4—H4B	111.2	C35—C36—H36	119.6
C12—C11—C16	118.15 (17)	C31—C36—H36	119.6
C12—C11—P1	122.11 (13)	C46—C41—C42	118.17 (16)
C16—C11—P1	119.48 (14)	C46—C41—P2	121.48 (13)
C13—C12—C11	120.80 (16)	C42—C41—P2	119.57 (13)
C13—C12—H12	119.6	C43—C42—C41	121.28 (16)
C11—C12—H12	119.6	C43—C42—H42	119.4
C14—C13—C12	120.33 (17)	C41—C42—H42	119.4
C14—C13—H13	119.8	C42—C43—C44	120.01 (17)
C12—C13—H13	119.8	C42—C43—H43	120
C15—C14—C13	119.28 (18)	C44—C43—H43	120
C15—C14—H14	120.4	C45—C44—C43	119.19 (17)
C13—C14—H14	120.4	C45—C44—H44	120.4
C16—C15—C14	120.65 (17)	C43—C44—H44	120.4
C16—C15—H15	119.7	C44—C45—C46	120.68 (17)
C14—C15—H15	119.7	C44—C45—H45	119.7
C15—C16—C11	120.78 (18)	C46—C45—H45	119.7
C15—C16—H16	119.6	C45—C46—C41	120.65 (17)
C11—C16—H16	119.6	C45—C46—H46	119.7
C26—C21—C22	118.63 (16)	C41—C46—H46	119.7
C26—C21—P1	116.11 (14)	C1—N1—P1	120.76 (11)
C22—C21—P1	125.26 (13)	C1—N1—P2	115.22 (11)
C23—C22—C21	120.07 (17)	P1—N1—P2	123.53 (8)
C23—C22—H22	120	N1—P1—C11	102.24 (8)
C21—C22—H22	120	N1—P1—C21	105.31 (8)
C22—C23—C24	120.50 (18)	C11—P1—C21	99.99 (9)
C22—C23—H23	119.7	N1—P2—C41	104.36 (7)
C24—C23—H23	119.8	N1—P2—C31	108.07 (9)
C25—C24—C23	119.79 (17)	C41—P2—C31	101.44 (8)
C25—C24—H24	120.1		

A3. Crystallographic data for PNP-*c*Pent

Table A 9: Fractional atomic coordinates and isotropic or equivalent isotropic displacement parameters (Å^2) for PNP-*c*Pent.

	x	*y*	*z*	U_{iso}*/U_{eq}	Occ. (<1)
C1	0.91678 (19)	0.34252 (17)	0.75151 (15)	0.0160 (4)	
H1	0.9698	0.278	0.7211	0.019*	
C2	0.9126 (2)	0.44037 (18)	0.67528 (16)	0.0198 (4)	
H2A	0.9168	0.4043	0.6008	0.024*	
H2B	0.8154	0.4746	0.6716	0.024*	
C3A	1.0595 (2)	0.5401 (2)	0.72654 (18)	0.0283 (5)	0.822 (4)
H3A1	1.0467	0.6203	0.7042	0.034*	0.822 (4)
H3A2	1.1549	0.5173	0.706	0.034*	0.822 (4)
C4A	1.0695 (3)	0.5448 (2)	0.8501 (2)	0.0252 (6)	0.822 (4)
H4A1	1.1775	0.5823	0.8926	0.03*	0.822 (4)
H4A2	0.9939	0.5922	0.8748	0.03*	0.822 (4)
C5A	1.0262 (2)	0.41072 (18)	0.86124 (16)	0.0222 (4)	0.822 (4)
H5A1	0.9707	0.4024	0.9215	0.027*	0.822 (4)
H5A2	1.1226	0.3755	0.8771	0.027*	0.822 (4)
C3B	1.0595 (2)	0.5401 (2)	0.72654 (18)	0.0283 (5)	0.178 (4)
H3B1	1.1228	0.5556	0.6714	0.034*	0.178 (4)
H3B2	1.0268	0.6177	0.7509	0.034*	0.178 (4)
C4B	1.1460 (13)	0.5064 (11)	0.8099 (10)	0.0252 (6)	0.178 (4)
H4B1	1.1998	0.5793	0.8655	0.03*	0.178 (4)
H4B2	1.2274	0.4649	0.7861	0.03*	0.178 (4)
C5B	1.0262 (2)	0.41072 (18)	0.86124 (16)	0.0222 (4)	0.178 (4)
H5B1	1.0822	0.3549	0.9018	0.027*	0.178 (4)
H5B2	0.9686	0.4545	0.9082	0.027*	0.178 (4)
C11	0.7060 (2)	0.13812 (17)	0.55819 (15)	0.0155 (4)	
C12	0.6196 (2)	0.20991 (19)	0.49657 (16)	0.0222 (4)	
H12	0.5488	0.2514	0.5273	0.027*	
C13	0.6355 (2)	0.22151 (19)	0.39194 (16)	0.0222 (4)	
H13	0.5776	0.2722	0.3521	0.027*	
C14	0.7355 (2)	0.15971 (18)	0.34479 (16)	0.0193 (4)	
H14	0.7461	0.1676	0.2727	0.023*	
C15	0.8197 (2)	0.08648 (19)	0.40339 (16)	0.0228 (4)	
H15	0.8877	0.0431	0.3713	0.027*	
C16	0.8051 (2)	0.07612 (18)	0.50916 (16)	0.0191 (4)	
H16	0.8639	0.0258	0.5487	0.023*	
C21	0.8152 (2)	0.03788 (17)	0.74897 (15)	0.0164 (4)	
C22	0.7770 (2)	−0.08818 (18)	0.70735 (16)	0.0199 (4)	
H22	0.688	−0.1188	0.6487	0.024*	
C23	0.8659 (2)	−0.16896 (18)	0.74967 (16)	0.0218 (4)	
H23	0.8371	−0.2543	0.7205	0.026*	
C24	0.9970 (2)	−0.12568 (19)	0.83469 (16)	0.0227 (4)	
H24	1.058	−0.1811	0.8642	0.027*	
C25	1.0383 (2)	−0.00127 (19)	0.87619 (17)	0.0239 (4)	
H25	1.1293	0.029	0.9334	0.029*	
C26	0.9474 (2)	0.08001 (18)	0.83467 (16)	0.0206 (4)	

H26	0.9757	0.165	0.865	0.025*
C31	0.4685 (2)	0.35868 (17)	0.71326 (15)	0.0157 (4)
C32	0.4624 (2)	0.45295 (19)	0.65030 (16)	0.0204 (4)
H32	0.5452	0.5236	0.6677	0.024*
C33	0.3364 (2)	0.4442 (2)	0.56256 (17)	0.0253 (5)
H33	0.3344	0.5081	0.5197	0.03*
C34	0.2143 (2)	0.3431 (2)	0.53752 (16)	0.0246 (5)
H34	0.1288	0.337	0.4771	0.03*
C35	0.2165 (2)	0.24971 (19)	0.60091 (16)	0.0227 (4)
H35	0.1317	0.1805	0.5843	0.027*
C36	0.3429 (2)	0.25774 (18)	0.68856 (16)	0.0191 (4)
H36	0.3436	0.1941	0.7318	0.023*
C41	0.5704 (2)	0.29021 (17)	0.91837 (15)	0.0163 (4)
C42	0.4502 (2)	0.33272 (19)	0.96094 (16)	0.0207 (4)
H42	0.4064	0.3973	0.9326	0.025*
C43	0.3941 (2)	0.2821 (2)	1.04375 (17)	0.0257 (5)
H43	0.312	0.3116	1.0713	0.031*
C44	0.4581 (2)	0.1883 (2)	1.08629 (16)	0.0246 (4)
H44	0.4195	0.1529	1.1427	0.03*
C45	0.5785 (2)	0.14650 (19)	1.04613 (16)	0.0220 (4)
H45	0.6231	0.0828	1.0756	0.026*
C46	0.6347 (2)	0.19717 (18)	0.96279 (15)	0.0184 (4)
H46	0.7175	0.168	0.9361	0.022*
N1	0.75799 (16)	0.27932 (14)	0.76314 (12)	0.0155 (3)
P1	0.67417 (5)	0.13242 (5)	0.69726 (4)	0.01549 (12)
P2	0.64933 (5)	0.37383 (5)	0.81951 (4)	0.01544 (12)

Table A 10: Atomic displacement parameters (Å^2) for PNP-*c*Pent.

	U^{11}	U^{22}	U^{33}	U^{12}	U^{13}	U^{23}
C1	0.0132 (8)	0.0182 (10)	0.0159 (10)	0.0018 (7)	0.0040 (7)	0.0010 (8)
C2	0.0180 (8)	0.0241 (11)	0.0195 (10)	0.0056 (8)	0.0058 (8)	0.0071 (8)
C3A	0.0296 (11)	0.0227 (12)	0.0311 (13)	−0.0010 (9)	0.0105 (9)	0.0010 (10)
C4A	0.0254 (12)	0.0214 (14)	0.0251 (14)	−0.0007 (10)	0.0044 (10)	−0.0016 (11)
C5A	0.0175 (9)	0.0259 (12)	0.0199 (11)	0.0022 (8)	0.0009 (8)	−0.0006 (9)
C3B	0.0296 (11)	0.0227 (12)	0.0311 (13)	−0.0010 (9)	0.0105 (9)	0.0010 (10)
C4B	0.0254 (12)	0.0214 (14)	0.0251 (14)	−0.0007 (10)	0.0044 (10)	−0.0016 (11)
C5B	0.0175 (9)	0.0259 (12)	0.0199 (11)	0.0022 (8)	0.0009 (8)	−0.0006 (9)
C11	0.0151 (8)	0.0143 (9)	0.0138 (9)	−0.0017 (7)	0.0014 (7)	−0.0009 (7)
C12	0.0241 (9)	0.0267 (12)	0.0176 (11)	0.0114 (8)	0.0041 (8)	0.0019 (9)
C13	0.0274 (10)	0.0220 (11)	0.0167 (10)	0.0080 (8)	0.0000 (8)	0.0045 (8)
C14	0.0207 (9)	0.0220 (11)	0.0127 (10)	−0.0017 (8)	0.0026 (7)	0.0034 (8)
C15	0.0233 (9)	0.0285 (12)	0.0206 (11)	0.0085 (9)	0.0095 (8)	0.0067 (9)
C16	0.0193 (9)	0.0230 (11)	0.0166 (10)	0.0066 (8)	0.0042 (8)	0.0058 (8)
C21	0.0194 (8)	0.0189 (10)	0.0141 (10)	0.0055 (8)	0.0078 (7)	0.0055 (8)
C22	0.0227 (9)	0.0192 (10)	0.0173 (10)	0.0018 (8)	0.0060 (8)	0.0022 (8)
C23	0.0304 (10)	0.0160 (10)	0.0224 (11)	0.0056 (8)	0.0124 (9)	0.0036 (8)
C24	0.0295 (10)	0.0242 (11)	0.0202 (11)	0.0129 (9)	0.0101 (9)	0.0082 (9)
C25	0.0279 (10)	0.0267 (12)	0.0170 (10)	0.0101 (9)	0.0011 (8)	0.0024 (9)
C26	0.0274 (10)	0.0179 (10)	0.0169 (10)	0.0068 (8)	0.0043 (8)	0.0017 (8)

C31	0.0157 (8)	0.0190 (10)	0.0141 (9)	0.0065 (7)	0.0051 (7)	0.0016 (8)
C32	0.0181 (9)	0.0226 (11)	0.0224 (11)	0.0051 (8)	0.0074 (8)	0.0049 (9)
C33	0.0265 (10)	0.0344 (13)	0.0210 (11)	0.0153 (9)	0.0079 (9)	0.0103 (9)
C34	0.0226 (9)	0.0375 (13)	0.0143 (10)	0.0151 (9)	0.0010 (8)	−0.0008 (9)
C35	0.0185 (9)	0.0248 (11)	0.0214 (11)	0.0041 (8)	0.0009 (8)	−0.0039 (9)
C36	0.0199 (9)	0.0191 (10)	0.0188 (10)	0.0049 (8)	0.0053 (8)	0.0017 (8)
C41	0.0150 (8)	0.0184 (10)	0.0131 (9)	0.0008 (7)	0.0018 (7)	−0.0005 (8)
C42	0.0193 (9)	0.0260 (11)	0.0183 (10)	0.0073 (8)	0.0053 (8)	0.0041 (9)
C43	0.0213 (9)	0.0368 (13)	0.0204 (11)	0.0066 (9)	0.0085 (8)	0.0026 (9)
C44	0.0259 (10)	0.0309 (12)	0.0150 (10)	−0.0019 (9)	0.0065 (8)	0.0032 (9)
C45	0.0274 (10)	0.0204 (11)	0.0155 (10)	0.0024 (8)	0.0008 (8)	0.0024 (8)
C46	0.0189 (9)	0.0198 (10)	0.0146 (10)	0.0027 (8)	0.0024 (7)	−0.0007 (8)
N1	0.0127 (7)	0.0162 (8)	0.0166 (8)	0.0007 (6)	0.0042 (6)	−0.0002 (7)
P1	0.0157 (2)	0.0163 (3)	0.0142 (3)	0.00285 (19)	0.00334 (18)	0.0017 (2)
P2	0.0146 (2)	0.0171 (3)	0.0149 (3)	0.00371 (19)	0.00380 (18)	0.0017 (2)

Table A 11: Bond lengths (Å) for PNP-cPent.

Atoms	Bond length (Å)	Atoms	Bond length (Å)
C1—N1	1.499 (2)	C23—C24	1.388 (3)
C1—C2	1.547 (3)	C23—H23	0.95
C1—C5A	1.553 (3)	C24—C25	1.383 (3)
C1—H1	1	C24—H24	0.95
C2—C3A	1.530 (3)	C25—C26	1.393 (3)
C2—H2A	0.99	C25—H25	0.95
C2—H2B	0.99	C26—H26	0.95
C3A—C4A	1.546 (3)	C31—C36	1.396 (3)
C3A—H3A1	0.99	C31—C32	1.400 (3)
C3A—H3A2	0.99	C31—P2	1.842 (2)
C4A—C5A	1.512 (3)	C32—C33	1.390 (3)
C4A—H4A1	0.99	C32—H32	0.95
C4A—H4A2	0.99	C33—C34	1.378 (3)
C5A—H5A1	0.99	C33—H33	0.95
C5A—H5A2	0.99	C34—C35	1.394 (3)
C4B—H4B1	0.99	C34—H34	0.95
C4B—H4B2	0.99	C35—C36	1.393 (3)
C11—C16	1.392 (2)	C35—H35	0.95
C11—C12	1.400 (3)	C36—H36	0.95
C11—P1	1.847 (2)	C41—C46	1.391 (3)
C12—C13	1.381 (3)	C41—C42	1.403 (2)
C12—H12	0.95	C41—P2	1.8274 (19)
C13—C14	1.384 (3)	C42—C43	1.387 (3)
C13—H13	0.95	C42—H42	0.95
C14—C15	1.382 (3)	C43—C44	1.388 (3)
C14—H14	0.95	C43—H43	0.95
C15—C16	1.389 (3)	C44—C45	1.386 (3)
C15—H15	0.95	C44—H44	0.95
C16—H16	0.95	C45—C46	1.393 (3)
C21—C26	1.397 (3)	C45—H45	0.95
C21—C22	1.400 (3)	C46—H46	0.95

APPENDIX A

C21—P1	1.8388 (19)	N1—P1	1.7157 (17)
C22—C23	1.381 (3)	N1—P2	1.7205 (16)
C22—H22	0.95		

Table A 12: Bond angles (°) for PNP-*c*Pent.

Atoms	Bond angle (°)	Atoms	Bond angle (°)
N1—C1—C2	114.93 (14)	C22—C23—H23	120
N1—C1—C5A	113.39 (15)	C24—C23—H23	120
C2—C1—C5A	105.15 (16)	C25—C24—C23	119.51 (18)
N1—C1—H1	107.7	C25—C24—H24	120.2
C2—C1—H1	107.7	C23—C24—H24	120.2
C5A—C1—H1	107.7	C24—C25—C26	120.43 (19)
C3A—C2—C1	104.78 (16)	C24—C25—H25	119.8
C3A—C2—H2A	110.8	C26—C25—H25	119.8
C1—C2—H2A	110.8	C25—C26—C21	120.72 (19)
C3A—C2—H2B	110.8	C25—C26—H26	119.6
C1—C2—H2B	110.8	C21—C26—H26	119.6
H2A—C2—H2B	108.9	C36—C31—C32	118.66 (17)
C2—C3A—C4A	103.07 (17)	C36—C31—P2	124.46 (14)
C2—C3A—H3A1	111.1	C32—C31—P2	116.80 (14)
C4A—C3A—H3A1	111.1	C33—C32—C31	120.67 (19)
C2—C3A—H3A2	111.1	C33—C32—H32	119.7
C4A—C3A—H3A2	111.1	C31—C32—H32	119.7
H3A1—C3A—H3A2	109.1	C34—C33—C32	120.24 (19)
C5A—C4A—C3A	103.38 (19)	C34—C33—H33	119.9
C5A—C4A—H4A1	111.1	C32—C33—H33	119.9
C3A—C4A—H4A1	111.1	C33—C34—C35	119.90 (18)
C5A—C4A—H4A2	111.1	C33—C34—H34	120.1
C3A—C4A—H4A2	111.1	C35—C34—H34	120
H4A1—C4A—H4A2	109.1	C36—C35—C34	120.09 (19)
C4A—C5A—C1	107.22 (17)	C36—C35—H35	120
C4A—C5A—H5A1	110.3	C34—C35—H35	120
C1—C5A—H5A1	110.3	C35—C36—C31	120.40 (18)
C4A—C5A—H5A2	110.3	C35—C36—H36	119.8
C1—C5A—H5A2	110.3	C31—C36—H36	119.8
H5A1—C5A—H5A2	108.5	C46—C41—C42	118.29 (17)
H4B1—C4B—H4B2	108.5	C46—C41—P2	123.86 (13)
C16—C11—C12	117.63 (17)	C42—C41—P2	117.40 (14)
C16—C11—P1	125.95 (14)	C43—C42—C41	121.13 (18)
C12—C11—P1	116.41 (13)	C43—C42—H42	119.4
C13—C12—C11	121.19 (17)	C41—C42—H42	119.4
C13—C12—H12	119.4	C42—C43—C44	119.87 (18)
C11—C12—H12	119.4	C42—C43—H43	120.1
C12—C13—C14	120.32 (18)	C44—C43—H43	120.1
C12—C13—H13	119.8	C45—C44—C43	119.67 (18)
C14—C13—H13	119.8	C45—C44—H44	120.2
C15—C14—C13	119.47 (18)	C43—C44—H44	120.2
C15—C14—H14	120.3	C44—C45—C46	120.47 (18)
C13—C14—H14	120.3	C44—C45—H45	119.8

C14—C15—C16	120.17 (17)	C46—C45—H45	119.8
C14—C15—H15	119.9	C41—C46—C45	120.55 (17)
C16—C15—H15	119.9	C41—C46—H46	119.7
C15—C16—C11	121.20 (17)	C45—C46—H46	119.7
C15—C16—H16	119.4	C1—N1—P1	121.43 (12)
C11—C16—H16	119.4	C1—N1—P2	115.22 (12)
C26—C21—C22	117.78 (17)	P1—N1—P2	121.76 (9)
C26—C21—P1	124.69 (15)	N1—P1—C21	104.70 (9)
C22—C21—P1	117.13 (14)	N1—P1—C11	102.52 (8)
C23—C22—C21	121.44 (19)	C21—P1—C11	101.65 (8)
C23—C22—H22	119.3	N1—P2—C41	104.71 (8)
C21—C22—H22	119.3	N1—P2—C31	104.59 (8)
C22—C23—C24	120.10 (19)	C41—P2—C31	100.62 (9)

A4. Crystallographic data for [Pt(PNP-*c*Prop)$_2$]

Table A 13: Fractional atomic coordinates and isotropic or equivalent isotropic displacement parameters (Å^2) for [Pt(PNP-*c*Prop)$_2$].

	x	y	z	U_{iso}*/U_{eq}
C1	0.1902 (11)	−0.1303 (9)	0.5211 (11)	0.056 (4)
H1	0.1631	−0.1625	0.4614	0.067*
C01	0.2612 (17)	0.0086 (10)	0.8895 (13)	0.0965 (16)
C2	0.1653 (14)	−0.1664 (11)	0.6122 (12)	0.075 (5)
H2A	0.1255	−0.2200	0.6078	0.090*
H2B	0.2234	−0.1574	0.6719	0.090*
C3	0.0963 (14)	−0.0936 (10)	0.5680 (13)	0.074 (5)
H3A	0.1124	−0.0400	0.6004	0.089*
H3B	0.0145	−0.1027	0.5362	0.089*
C11	0.2287 (12)	0.0906 (8)	0.4818 (10)	0.050 (3)
C12	0.2212 (12)	0.1074 (9)	0.5755 (11)	0.060 (4)
H12	0.2467	0.0687	0.6248	0.072*
C13	0.1761 (13)	0.1815 (9)	0.5944 (11)	0.061 (4)
H13	0.1696	0.1938	0.6576	0.073*
C14	0.1401 (13)	0.2385 (9)	0.5235 (12)	0.064 (4)
H14	0.1081	0.2889	0.5384	0.076*
C15	0.1499 (12)	0.2231 (9)	0.4315 (11)	0.058 (4)
H15	0.1265	0.2628	0.3828	0.070*
C16	0.1944 (11)	0.1490 (8)	0.4119 (10)	0.053 (4)
H16	0.2018	0.1375	0.3487	0.064*
C21	0.2410 (15)	−0.0249 (9)	0.3326 (11)	0.068 (3)
C22	0.1237 (13)	−0.0380 (8)	0.3019 (10)	0.062 (4)
H22	0.0737	−0.0302	0.3449	0.074*
C23	0.0784 (15)	−0.0621 (9)	0.2099 (11)	0.068 (3)
H23	−0.0023	−0.0718	0.1896	0.082*
C24	0.1497 (15)	−0.0719 (9)	0.1488 (11)	0.068 (3)

H24	0.1170	−0.0887	0.0855	0.082*
C25	0.2664 (16)	−0.0591 (9)	0.1729 (11)	0.072 (5)
H25	0.3144	−0.0659	0.1282	0.086*
C26	0.3126 (14)	−0.0350 (9)	0.2687 (10)	0.061 (4)
H26	0.3934	−0.0258	0.2889	0.074*
C31	0.5582 (9)	0.2073 (7)	0.5332 (8)	0.033 (3)
C32	0.5032 (11)	0.1972 (7)	0.6092 (8)	0.042 (3)
H32	0.4747	0.1448	0.6217	0.050*
C33	0.4902 (13)	0.2627 (9)	0.6662 (10)	0.060 (4)
H33	0.4522	0.2556	0.7175	0.072*
C34	0.5321 (13)	0.3383 (9)	0.6488 (11)	0.061 (4)
H34	0.5213	0.3839	0.6869	0.073*
C35	0.5901 (12)	0.3478 (9)	0.5754 (10)	0.056 (4)
H35	0.6222	0.3996	0.5655	0.067*
C36	0.6019 (11)	0.2841 (8)	0.5174 (8)	0.044 (3)
H36	0.6398	0.2920	0.4661	0.053*
C41	0.5131 (11)	0.1547 (8)	0.3365 (8)	0.043 (3)
C42	0.5404 (11)	0.1068 (9)	0.2628 (9)	0.050 (3)
H42	0.5963	0.0644	0.2764	0.060*
C43	0.4839 (11)	0.1230 (9)	0.1701 (9)	0.050 (3)
H43	0.5021	0.0924	0.1190	0.060*
C44	0.4004 (11)	0.1844 (9)	0.1521 (9)	0.051 (3)
H44	0.3616	0.1949	0.0884	0.061*
C45	0.3727 (12)	0.2302 (8)	0.2247 (9)	0.048 (3)
H45	0.3143	0.2711	0.2115	0.057*
C46	0.4325 (10)	0.2152 (7)	0.3185 (8)	0.035 (3)
H46	0.4167	0.2474	0.3693	0.042*
N1	0.2936 (9)	−0.0823 (7)	0.5271 (7)	0.046 (3)
O1	0.3927 (12)	0.0728 (8)	0.7900 (9)	0.093 (4)
O2	0.2122 (12)	0.1392 (11)	0.8178 (10)	0.139 (7)
O3	0.394 (2)	0.1325 (11)	0.9396 (11)	0.192 (10)
F1	0.3451 (15)	−0.0387 (10)	0.9464 (12)	0.171 (7)
F2	0.1871 (15)	0.0147 (10)	0.9441 (10)	0.173 (8)
F3	0.2185 (17)	−0.0415 (14)	0.8172 (15)	0.225 (11)
P1	0.3035 (3)	0.0008 (2)	0.4547 (2)	0.0421 (7)
P2	0.5688 (3)	0.12237 (19)	0.4572 (2)	0.0337 (7)
S1	0.3214 (5)	0.0961 (3)	0.8544 (3)	0.0965 (16)
Pt1	0.5000	0.0000	0.5000	0.0363 (2)

Table A 14: Atomic displacement parameters (Å^2) for [Pt(PNP-*c*Prop)$_2$].

	U^{11}	U^{22}	U^{33}	U^{12}	U^{13}	U^{23}
C1	0.038 (8)	0.064 (9)	0.064 (9)	−0.011 (7)	0.010 (7)	0.002 (8)
C01	0.141 (5)	0.085 (3)	0.066 (3)	0.022 (3)	0.026 (3)	−0.008 (2)
C2	0.062 (11)	0.092 (13)	0.073 (11)	−0.009 (9)	0.018 (9)	0.013 (10)
C3	0.056 (10)	0.069 (11)	0.106 (13)	−0.005 (8)	0.036 (9)	−0.019 (10)
C11	0.048 (8)	0.048 (8)	0.055 (9)	0.001 (6)	0.014 (7)	−0.010 (7)
C12	0.057 (9)	0.052 (9)	0.070 (10)	0.007 (7)	0.013 (8)	−0.010 (8)
C13	0.065 (10)	0.064 (10)	0.061 (9)	0.004 (8)	0.028 (8)	−0.015 (8)
C14	0.069 (10)	0.046 (8)	0.081 (11)	0.021 (7)	0.027 (8)	−0.011 (8)
C15	0.059 (9)	0.047 (8)	0.072 (10)	0.006 (7)	0.022 (8)	−0.003 (7)

C16	0.052 (8)	0.051 (8)	0.066 (9)	−0.015 (7)	0.034 (7)	−0.018 (7)
C21	0.091 (8)	0.043 (5)	0.057 (6)	−0.003 (5)	−0.018 (5)	0.004 (4)
C22	0.071 (10)	0.039 (7)	0.061 (9)	0.010 (7)	−0.019 (8)	−0.004 (7)
C23	0.091 (8)	0.043 (5)	0.057 (6)	−0.003 (5)	−0.018 (5)	0.004 (4)
C24	0.091 (8)	0.043 (5)	0.057 (6)	−0.003 (5)	−0.018 (5)	0.004 (4)
C25	0.107 (14)	0.060 (10)	0.050 (9)	−0.014 (9)	0.020 (9)	0.004 (8)
C26	0.085 (11)	0.056 (8)	0.039 (8)	−0.014 (8)	0.004 (7)	0.004 (7)
C31	0.033 (6)	0.029 (6)	0.033 (6)	−0.001 (5)	0.001 (5)	−0.001 (5)
C32	0.049 (8)	0.040 (7)	0.042 (7)	−0.009 (6)	0.020 (6)	−0.006 (6)
C33	0.064 (10)	0.070 (10)	0.050 (8)	0.006 (8)	0.019 (7)	−0.023 (7)
C34	0.071 (10)	0.041 (8)	0.065 (10)	0.007 (7)	0.003 (8)	−0.022 (7)
C35	0.067 (10)	0.044 (8)	0.052 (8)	−0.006 (7)	0.004 (7)	0.006 (7)
C36	0.058 (8)	0.041 (7)	0.032 (6)	−0.007 (6)	0.006 (6)	−0.002 (6)
C41	0.049 (8)	0.044 (7)	0.034 (7)	−0.001 (6)	0.003 (6)	0.001 (6)
C42	0.047 (8)	0.067 (9)	0.037 (7)	0.009 (7)	0.014 (6)	−0.003 (6)
C43	0.046 (8)	0.062 (9)	0.046 (8)	−0.007 (7)	0.017 (6)	−0.010 (7)
C44	0.049 (8)	0.070 (9)	0.031 (7)	−0.013 (7)	0.004 (6)	0.013 (6)
C45	0.061 (9)	0.044 (7)	0.039 (7)	0.002 (6)	0.012 (6)	0.008 (6)
C46	0.038 (7)	0.037 (6)	0.029 (6)	−0.009 (5)	0.008 (5)	0.007 (5)
N1	0.042 (6)	0.055 (7)	0.043 (6)	0.009 (5)	0.016 (5)	−0.002 (5)
O1	0.127 (11)	0.084 (8)	0.088 (8)	0.018 (8)	0.066 (8)	0.008 (7)
O2	0.136 (13)	0.185 (16)	0.099 (10)	0.102 (12)	0.031 (9)	0.041 (11)
O3	0.31 (3)	0.119 (14)	0.095 (11)	−0.002 (15)	−0.079 (14)	−0.039 (10)
F1	0.234 (17)	0.141 (12)	0.181 (15)	0.091 (13)	0.138 (14)	0.083 (12)
F2	0.244 (17)	0.202 (15)	0.110 (10)	0.115 (14)	0.123 (11)	0.050 (10)
F3	0.197 (17)	0.30 (2)	0.23 (2)	−0.123 (17)	0.162 (16)	−0.150 (19)
P1	0.0492 (18)	0.0398 (16)	0.0357 (15)	0.0065 (18)	0.0058 (13)	−0.0018 (17)
P2	0.0298 (16)	0.0416 (17)	0.0309 (15)	0.0061 (13)	0.0089 (12)	−0.0019 (13)
S1	0.141 (5)	0.085 (3)	0.066 (3)	0.022 (3)	0.026 (3)	−0.008 (2)
Pt1	0.0501 (4)	0.0305 (3)	0.0275 (3)	0.0107 (4)	0.0062 (2)	−0.0034 (3)

Table A 15: Bond lengths (Å) for [Pt(PNP-*c*Prop)$_2$].

Atoms	Bond length (Å)	Atoms	Bong length (Å)
C1—N1	1.440 (16)	C31—C36	1.394 (16)
C1—C2	1.52 (2)	C31—C32	1.395 (16)
C1—C3	1.54 (2)	C31—P2	1.787 (11)
C1—H1	1.0000	C32—C33	1.375 (17)
C01—F2	1.30 (2)	C32—H32	0.9500
C01—F3	1.34 (2)	C33—C34	1.37 (2)
C01—F1	1.380 (16)	C33—H33	0.9500
C01—S1	1.719 (15)	C34—C35	1.38 (2)
C2—C3	1.50 (2)	C34—H34	0.9500
C2—H2A	0.9900	C35—C36	1.358 (18)
C2—H2B	0.9900	C35—H35	0.9500
C3—H3A	0.9900	C36—H36	0.9500
C3—H3B	0.9900	C41—C46	1.360 (17)
C11—C16	1.382 (19)	C41—C42	1.407 (17)
C11—C12	1.397 (19)	C41—P2	1.801 (12)
C11—P1	1.798 (13)	C42—C43	1.384 (17)

C12—C13	1.372 (19)	C42—H42	0.9500
C12—H12	0.9500	C43—C44	1.392 (19)
C13—C14	1.38 (2)	C43—H43	0.9500
C13—H13	0.9500	C44—C45	1.379 (18)
C14—C15	1.38 (2)	C44—H44	0.9500
C14—H14	0.9500	C45—C46	1.407 (16)
C15—C16	1.373 (18)	C45—H45	0.9500
C15—H15	0.9500	C46—H46	0.9500
C16—H16	0.9500	N1—P2^{i}	1.724 (10)
C21—C26	1.39 (2)	N1—P1	1.729 (11)
C21—C22	1.38 (2)	O1—S1	1.430 (12)
C21—P1	1.805 (15)	O2—S1	1.467 (9)
C22—C23	1.376 (19)	O3—S1	1.463 (14)
C22—H22	0.9500	P1—Pt1	2.277 (3)
C23—C24	1.35 (2)	P1—P2^{i}	2.668 (4)
C23—H23	0.9500	P2—N1^{i}	1.724 (10)
C24—C25	1.37 (2)	P2—Pt1	2.290 (3)
C24—H24	0.9500	P2—P1^{i}	2.668 (4)
C25—C26	1.42 (2)	Pt1—P1^{i}	2.277 (3)
C25—H25	0.9500	Pt1—P2^{i}	2.290 (3)
C26—H26	0.9500		

Symmetry codes: (i) $-x+1, -y, -z+1$.

Table A 16: Bond angles (°)for [Pt(PNP-*c*Prop)$_2$].

Atoms	Bond angle (°)	Atoms	Bond angle (°)
N1—C1—C2	118.4 (12)	C34—C33—C32	120.0 (13)
N1—C1—C3	116.4 (12)	C34—C33—H33	120.0
C2—C1—C3	58.9 (10)	C32—C33—H33	120.0
N1—C1—H1	116.8	C33—C34—C35	119.8 (13)
C2—C1—H1	116.8	C33—C34—H34	120.1
C3—C1—H1	116.8	C35—C34—H34	120.1
F2—C01—F3	109.0 (17)	C36—C35—C34	121.0 (13)
F2—C01—F1	100.2 (14)	C36—C35—H35	119.5
F3—C01—F1	103.0 (19)	C34—C35—H35	119.5
F2—C01—S1	119.2 (14)	C35—C36—C31	119.9 (12)
F3—C01—S1	113.1 (14)	C35—C36—H36	120.1
F1—C01—S1	110.4 (14)	C31—C36—H36	120.1
C3—C2—C1	61.1 (10)	C46—C41—C42	121.6 (11)
C3—C2—H2A	117.7	C46—C41—P2	119.6 (9)
C1—C2—H2A	117.7	C42—C41—P2	117.9 (10)
C3—C2—H2B	117.7	C43—C42—C41	118.6 (12)
C1—C2—H2B	117.7	C43—C42—H42	120.7
H2A—C2—H2B	114.8	C41—C42—H42	120.7
C2—C3—C1	60.0 (10)	C42—C43—C44	119.6 (12)
C2—C3—H3A	117.8	C42—C43—H43	120.2
C1—C3—H3A	117.8	C44—C43—H43	120.2
C2—C3—H3B	117.8	C45—C44—C43	121.6 (12)
C1—C3—H3B	117.8	C45—C44—H44	119.2
H3A—C3—H3B	114.9	C43—C44—H44	119.2

C16—C11—C12	119.8 (13)	C44—C45—C46	118.6 (12)
C16—C11—P1	119.1 (10)	C44—C45—H45	120.7
C12—C11—P1	120.3 (11)	C46—C45—H45	120.7
C13—C12—C11	118.1 (15)	C41—C46—C45	119.9 (12)
C13—C12—H12	121.0	C41—C46—H46	120.0
C11—C12—H12	120.9	C45—C46—H46	120.0
C12—C13—C14	121.4 (14)	C1—N1—P2^{i}	124.6 (9)
C12—C13—H13	119.3	C1—N1—P1	123.8 (9)
C14—C13—H13	119.3	P2^{i}—N1—P1	101.2 (5)
C13—C14—C15	120.9 (13)	N1—P1—C11	114.2 (6)
C13—C14—H14	119.6	N1—P1—C21	109.7 (6)
C15—C14—H14	119.6	C11—P1—C21	106.4 (7)
C16—C15—C14	118.1 (14)	N1—P1—Pt1	91.1 (4)
C16—C15—H15	120.9	C11—P1—Pt1	117.5 (5)
C14—C15—H15	120.9	C21—P1—Pt1	117.4 (6)
C15—C16—C11	121.7 (13)	N1—P1—P2^{i}	39.3 (3)
C15—C16—H16	119.2	C11—P1—P2^{i}	140.1 (5)
C11—C16—H16	119.2	C21—P1—P2^{i}	111.2 (5)
C26—C21—C22	119.0 (14)	Pt1—P1—P2^{i}	54.49 (9)
C26—C21—P1	119.4 (12)	N1^{i}—P2—C31	113.7 (5)
C22—C21—P1	121.6 (14)	N1^{i}—P2—C41	112.3 (6)
C23—C22—C21	120.8 (17)	C31—P2—C41	107.7 (5)
C23—C22—H22	119.6	N1^{i}—P2—Pt1	90.8 (4)
C21—C22—H22	119.7	C31—P2—Pt1	116.0 (4)
C24—C23—C22	119.4 (16)	C41—P2—Pt1	115.9 (4)
C24—C23—H23	120.3	N1^{i}—P2—P1^{i}	39.5 (4)
C22—C23—H23	120.4	C31—P2—P1^{i}	113.6 (4)
C25—C24—C23	123.6 (15)	C41—P2—P1^{i}	137.2 (4)
C25—C24—H24	118.2	Pt1—P2—P1^{i}	54.03 (10)
C23—C24—H24	118.3	O1—S1—O3	109.3 (13)
C24—C25—C26	116.6 (16)	O1—S1—O2	119.3 (9)
C24—C25—H25	121.7	O3—S1—O2	114.8 (12)
C26—C25—H25	121.7	O1—S1—C01	107.9 (9)
C21—C26—C25	120.7 (15)	O3—S1—C01	107.3 (11)
C21—C26—H26	119.6	O2—S1—C01	96.7 (11)
C25—C26—H26	119.7	P1^{i}—Pt1—P1	180.0
C36—C31—C32	119.0 (11)	P1^{i}—Pt1—P2^{i}	108.52 (12)
C36—C31—P2	121.5 (9)	P1—Pt1—P2^{i}	71.48 (12)
C32—C31—P2	119.5 (9)	P1^{i}—Pt1—P2	71.48 (12)
C33—C32—C31	120.3 (12)	P1—Pt1—P2	108.52 (12)
C33—C32—H32	119.9	P2^{i}—Pt1—P2	180.00 (8)
C31—C32—H32	119.9		

Symmetry codes: (i) $-x+1, -y, -z+1$.

A5. Crystallographic data for [Pt(PNP-*c*But)$_2$]

Table A 17: Fractional atomic coordinates and isotropic or equivalent isotropic displacement parameters (Å^2) for [Pt(PNP-*c*But)$_2$].

	x	*y*	*z*	U_{iso}*/U_{eq}	Occ. (<1)
C11A	1.2805 (8)	0.0946 (6)	0.9081 (4)	0.0221 (14)	0.824 (7)
C12A	1.3390 (9)	0.0951 (7)	0.8460 (4)	0.037 (2)	0.824 (7)
H12A	1.2817	0.0915	0.8080	0.044*	0.824 (7)
C13A	1.4841 (10)	0.1011 (10)	0.8395 (5)	0.057 (3)	0.824 (7)
H13A	1.5227	0.1014	0.7972	0.068*	0.824 (7)
C14A	1.5686 (10)	0.1066 (8)	0.8942 (5)	0.039 (2)	0.824 (7)
H14A	1.6646	0.1131	0.8894	0.047*	0.824 (7)
C15A	1.5126 (9)	0.1025 (6)	0.9570 (4)	0.0294 (18)	0.824 (7)
H15A	1.5713	0.1034	0.9945	0.035*	0.824 (7)
C16A	1.3702 (8)	0.0973 (6)	0.9642 (4)	0.0308 (19)	0.824 (7)
H16A	1.3331	0.0954	1.0067	0.037*	0.824 (7)
C12B	1.321 (3)	0.1580 (16)	0.8565 (13)	0.0221 (14)	0.176 (7)
H12B	1.2699	0.2049	0.8354	0.026*	0.176 (7)
C13B	1.464 (3)	0.1493 (15)	0.8450 (12)	0.0221 (14)	0.176 (7)
H13B	1.5073	0.1903	0.8161	0.026*	0.176 (7)
C14B	1.540 (2)	0.0792 (17)	0.8765 (14)	0.0221 (14)	0.176 (7)
H14B	1.6354	0.0733	0.8688	0.026*	0.176 (7)
C15B	1.475 (2)	0.0179 (14)	0.9197 (12)	0.0221 (14)	0.176 (7)
H15B	1.5263	−0.0290	0.9408	0.026*	0.176 (7)
C16B	1.333 (2)	0.0266 (16)	0.9312 (12)	0.0221 (14)	0.176 (7)
H16B	1.2889	−0.0144	0.9600	0.026*	0.176 (7)
C11B	1.2559 (19)	0.0967 (19)	0.8996 (15)	0.0221 (14)	0.176 (7)
C21	1.0021 (8)	0.1063 (6)	0.8424 (3)	0.0393 (18)	
C22	1.0214 (10)	0.0361 (7)	0.7952 (4)	0.055 (2)	
H22	1.0863	−0.0110	0.8035	0.066*	
C23	0.9433 (11)	0.0365 (8)	0.7354 (4)	0.067 (3)	
H23	0.9573	−0.0097	0.7037	0.080*	
C24	0.8465 (10)	0.1048 (10)	0.7238 (5)	0.078 (4)	
H24	0.7933	0.1043	0.6844	0.093*	
C25	0.8273 (10)	0.1742 (11)	0.7699 (4)	0.083 (4)	
H25	0.7617	0.2208	0.7614	0.100*	
C26	0.9053 (9)	0.1757 (9)	0.8296 (4)	0.066 (3)	
H26	0.8920	0.2230	0.8605	0.079*	
C31	1.1061 (7)	0.1742 (5)	1.1096 (3)	0.0287 (15)	
C32	1.2069 (7)	0.1077 (6)	1.1281 (4)	0.0395 (19)	
H32	1.2135	0.0521	1.1045	0.047*	
C33	1.2962 (8)	0.1255 (7)	1.1814 (4)	0.047 (2)	
H33	1.3664	0.0829	1.1923	0.056*	
C34	1.2826 (10)	0.2053 (8)	1.2184 (5)	0.063 (3)	
H34	1.3396	0.2149	1.2559	0.076*	
C35	1.1847 (11)	0.2709 (9)	1.2001 (6)	0.083 (4)	
H35	1.1788	0.3263	1.2239	0.100*	
C36	1.0949 (10)	0.2550 (7)	1.1465 (5)	0.057 (3)	

H36	1.0269	0.2988	1.1352	0.068*		
C41	0.8277 (7)	0.2037 (5)	1.0551 (3)	0.0303 (15)		
C42	0.7612 (8)	0.1798 (5)	1.1142 (4)	0.0360 (17)		
H42	0.8051	0.1399	1.1446	0.043*		
C43	0.6309 (8)	0.2151 (6)	1.1275 (4)	0.0391 (18)		
H43	0.5868	0.1982	1.1667	0.047*		
C44	0.5658 (8)	0.2746 (7)	1.0837 (5)	0.050 (2)		
H44	0.4776	0.2976	1.0932	0.060*		
C45	0.6297 (9)	0.3010 (8)	1.0252 (5)	0.069 (3)		
H45	0.5860	0.3429	0.9962	0.083*		
C46	0.7596 (8)	0.2642 (7)	1.0105 (5)	0.056 (3)		
H46	0.8018	0.2800	0.9706	0.067*		
N1	1.0626 (5)	0.1962 (4)	0.9680 (3)	0.0259 (12)		
P1	1.09269 (18)	0.09909 (12)	0.92181 (8)	0.0255 (4)		
P2	0.99356 (18)	0.15085 (12)	1.03867 (8)	0.0261 (4)		
Pt1	1.0000	0.0000	1.0000	0.02569 (11)		
C1A	1.1076 (13)	0.2885 (9)	0.9470 (7)	0.030 (3)	0.631	(15)
H1A	1.1027	0.2921	0.8982	0.036*	0.631	(15)
C2A	1.0537 (9)	0.3788 (6)	0.9760 (4)	0.048 (2)	0.631	(15)
H2A1	0.9844	0.4094	0.9476	0.057*	0.631	(15)
H2A2	1.0198	0.3722	1.0211	0.057*	0.631	(15)
C3A	1.187 (2)	0.4203 (15)	0.9734 (11)	0.050 (5)	0.631	(15)
H3A1	1.2129	0.4555	1.0130	0.060*	0.631	(15)
H3A2	1.2020	0.4566	0.9332	0.060*	0.631	(15)
C4A	1.2500 (12)	0.3231 (8)	0.9713 (9)	0.048 (4)	0.631	(15)
H4A1	1.2788	0.2991	1.0147	0.057*	0.631	(15)
H4A2	1.3235	0.3159	0.9390	0.057*	0.631	(15)
C4B	1.222 (3)	0.3188 (16)	0.9117 (13)	0.048 (7)	0.369	(15)
H4B1	1.1690	0.3053	0.8710	0.057*	0.369	(15)
H4B2	1.3187	0.2999	0.9082	0.057*	0.369	(15)
C1B	1.154 (2)	0.2867 (16)	0.9738 (13)	0.030 (3)	0.369	(15)
H1B	1.2193	0.2842	1.0119	0.036*	0.369	(15)
C3B	1.202 (4)	0.421 (3)	0.939 (2)	0.055 (10)	0.369	(15)
H3B1	1.1835	0.4675	0.9046	0.066*	0.369	(15)
H3B2	1.2740	0.4417	0.9702	0.066*	0.369	(15)
C2B	1.0537 (9)	0.3788 (6)	0.9760 (4)	0.048 (2)	0.369	(15)
H2B1	1.0353	0.4031	1.0202	0.057*	0.369	(15)
H2B2	0.9704	0.3766	0.9476	0.057*	0.369	(15)
C01A	0.5736 (15)	0.4962 (11)	0.8501 (6)	0.063 (5)	0.596	(10)
F1A	0.5474 (17)	0.4988 (13)	0.9126 (5)	0.078 (6)	0.596	(10)
F2A	0.4536 (19)	0.5071 (15)	0.8209 (8)	0.31 (3)	0.596	(10)
F3A	0.641 (2)	0.5697 (8)	0.8322 (6)	0.163 (10)	0.596	(10)
S01A	0.6696 (4)	0.3968 (4)	0.8201 (2)	0.0388 (12)	0.596	(10)
O1A	0.5574 (18)	0.3261 (11)	0.8425 (8)	0.111 (7)	0.596	(10)
O2A	0.7895 (10)	0.4047 (10)	0.8665 (6)	0.069 (4)	0.596	(10)
O3A	0.6800 (17)	0.4097 (12)	0.7535 (6)	0.058 (5)	0.596	(10)
C01B	0.5280 (17)	0.4516 (14)	0.8572 (10)	0.084 (13)	0.404	(10)
F1B	0.468 (3)	0.3686 (16)	0.8546 (17)	0.45 (6)	0.404	(10)
F2B	0.4444 (13)	0.500 (2)	0.8205 (8)	0.158 (19)	0.404	(10)
F3B	0.5090 (18)	0.4764 (13)	0.9180 (8)	0.040 (4)	0.404	(10)
S01B	0.7079 (9)	0.4451 (9)	0.8359 (3)	0.071 (3)	0.404	(10)

O1B	0.713 (2)	0.3379 (9)	0.8671 (7)	0.061 (6)	0.404 (10)
O2B	0.762 (3)	0.5132 (16)	0.8824 (12)	0.24 (3)	0.404 (10)
O3B	0.737 (3)	0.4319 (18)	0.7714 (8)	0.093 (13)	0.404 (10)

Table A 18: Atomic displacement parameters (Å^2) for [Pt(PNP-*c*But)$_2$].

	U^{11}	U^{22}	U^{33}	U^{12}	U^{13}	U^{23}
C11A	0.027 (4)	0.017 (3)	0.023 (3)	0.000 (3)	0.003 (3)	−0.001 (2)
C12A	0.035 (5)	0.059 (6)	0.016 (4)	0.007 (4)	−0.001 (3)	−0.008 (4)
C13A	0.035 (5)	0.114 (11)	0.022 (4)	0.021 (6)	0.002 (4)	−0.008 (6)
C14A	0.030 (5)	0.055 (6)	0.032 (5)	0.005 (4)	0.008 (4)	−0.003 (4)
C15A	0.032 (4)	0.032 (4)	0.024 (4)	0.008 (4)	−0.001 (3)	0.003 (3)
C16A	0.027 (4)	0.043 (5)	0.023 (4)	0.000 (4)	0.008 (3)	0.007 (4)
C12B	0.027 (4)	0.017 (3)	0.023 (3)	0.000 (3)	0.003 (3)	−0.001 (2)
C13B	0.027 (4)	0.017 (3)	0.023 (3)	0.000 (3)	0.003 (3)	−0.001 (2)
C14B	0.027 (4)	0.017 (3)	0.023 (3)	0.000 (3)	0.003 (3)	−0.001 (2)
C15B	0.027 (4)	0.017 (3)	0.023 (3)	0.000 (3)	0.003 (3)	−0.001 (2)
C16B	0.027 (4)	0.017 (3)	0.023 (3)	0.000 (3)	0.003 (3)	−0.001 (2)
C11B	0.027 (4)	0.017 (3)	0.023 (3)	0.000 (3)	0.003 (3)	−0.001 (2)
C21	0.031 (4)	0.062 (5)	0.025 (3)	−0.015 (4)	0.005 (3)	0.007 (3)
C22	0.068 (6)	0.064 (6)	0.033 (4)	−0.031 (5)	−0.010 (4)	−0.004 (4)
C23	0.073 (7)	0.098 (8)	0.029 (4)	−0.049 (6)	−0.008 (4)	0.005 (5)
C24	0.033 (5)	0.167 (13)	0.033 (5)	−0.024 (6)	0.002 (4)	0.026 (7)
C25	0.039 (5)	0.182 (14)	0.029 (4)	0.023 (7)	0.010 (4)	0.031 (6)
C26	0.045 (5)	0.128 (10)	0.025 (4)	0.025 (6)	0.018 (4)	0.017 (5)
C31	0.026 (3)	0.035 (4)	0.025 (3)	−0.011 (3)	0.008 (3)	−0.014 (3)
C32	0.024 (4)	0.052 (5)	0.043 (4)	−0.010 (3)	0.008 (3)	−0.023 (4)
C33	0.022 (4)	0.071 (6)	0.049 (5)	−0.007 (4)	0.005 (3)	−0.018 (4)
C34	0.047 (5)	0.101 (8)	0.041 (5)	−0.005 (5)	−0.011 (4)	−0.025 (5)
C35	0.072 (7)	0.099 (9)	0.078 (7)	0.028 (7)	−0.032 (6)	−0.066 (7)
C36	0.055 (5)	0.057 (6)	0.058 (6)	0.009 (4)	−0.012 (4)	−0.039 (5)
C41	0.027 (3)	0.032 (4)	0.032 (4)	−0.012 (3)	0.006 (3)	−0.010 (3)
C42	0.041 (4)	0.033 (4)	0.035 (4)	−0.004 (3)	0.017 (3)	−0.006 (3)
C43	0.039 (4)	0.044 (5)	0.035 (4)	−0.009 (4)	0.013 (3)	−0.012 (3)
C44	0.024 (4)	0.065 (6)	0.061 (6)	−0.007 (4)	0.014 (4)	−0.011 (5)
C45	0.035 (5)	0.101 (9)	0.072 (7)	0.008 (5)	0.022 (5)	0.021 (6)
C46	0.027 (4)	0.086 (7)	0.055 (5)	−0.009 (4)	0.021 (4)	0.007 (5)
N1	0.021 (3)	0.024 (3)	0.034 (3)	−0.008 (2)	0.007 (2)	−0.005 (2)
P1	0.0288 (9)	0.0298 (9)	0.0181 (7)	−0.0110 (7)	0.0045 (6)	−0.0002 (7)
P2	0.0261 (8)	0.0269 (9)	0.0255 (8)	−0.0113 (7)	0.0079 (7)	−0.0104 (7)
Pt1	0.0378 (2)	0.02526 (18)	0.01432 (15)	−0.01615 (17)	0.00896 (12)	−0.00824 (15)
C1A	0.018 (7)	0.026 (4)	0.046 (9)	−0.005 (5)	−0.001 (5)	−0.005 (6)
C2A	0.059 (5)	0.032 (4)	0.053 (5)	0.014 (4)	0.007 (4)	0.006 (4)
C3A	0.041 (10)	0.027 (8)	0.082 (14)	−0.004 (6)	−0.008 (11)	0.022 (10)
C4A	0.018 (6)	0.029 (7)	0.096 (13)	−0.003 (5)	0.001 (6)	0.018 (7)
C4B	0.057 (15)	0.039 (13)	0.047 (14)	−0.007 (11)	0.014 (12)	0.008 (10)
C1B	0.018 (7)	0.026 (4)	0.046 (9)	−0.005 (5)	−0.001 (5)	−0.005 (6)
C3B	0.027 (12)	0.042 (16)	0.10 (3)	−0.016 (10)	0.003 (19)	0.03 (2)
C2B	0.059 (5)	0.032 (4)	0.053 (5)	0.014 (4)	0.007 (4)	0.006 (4)
C01A	0.055 (10)	0.095 (15)	0.039 (8)	−0.024 (11)	0.020 (7)	−0.034 (10)

F1A	0.070 (11)	0.120 (14)	0.043 (7)	−0.011 (9)	0.002 (6)	−0.027 (7)
F2A	0.46 (5)	0.41 (5)	0.051 (12)	0.41 (5)	−0.026 (17)	−0.021 (17)
F3A	0.39 (3)	0.040 (6)	0.060 (8)	0.004 (11)	0.083 (13)	0.017 (6)
S01A	0.035 (2)	0.055 (3)	0.0265 (19)	0.0099 (17)	−0.0041 (15)	0.0196 (17)
O1A	0.111 (13)	0.118 (13)	0.101 (12)	−0.066 (11)	−0.053 (10)	0.056 (10)
O2A	0.025 (5)	0.101 (11)	0.080 (8)	0.010 (6)	−0.016 (5)	0.033 (8)
O3A	0.074 (9)	0.064 (12)	0.036 (7)	0.023 (7)	0.003 (6)	0.013 (6)
C01B	0.030 (13)	0.046 (17)	0.17 (4)	0.002 (11)	−0.041 (18)	−0.044 (19)
F1B	0.13 (3)	0.57 (9)	0.66 (10)	−0.19 (4)	0.22 (4)	−0.53 (9)
F2B	0.015 (7)	0.41 (6)	0.044 (13)	0.038 (17)	−0.021 (7)	−0.06 (2)
F3B	0.026 (8)	0.045 (9)	0.050 (9)	0.009 (7)	0.014 (6)	0.000 (6)
S01B	0.063 (5)	0.122 (8)	0.028 (3)	0.005 (5)	0.017 (3)	0.001 (4)
O1B	0.117 (16)	0.036 (9)	0.030 (7)	0.019 (9)	0.003 (8)	0.018 (6)
O2B	0.31 (4)	0.15 (3)	0.26 (4)	−0.20 (3)	−0.23 (4)	0.14 (3)
O3B	0.22 (4)	0.038 (11)	0.026 (10)	0.025 (18)	0.056 (16)	0.011 (9)

Table A 19: Bond lengths (Å) for [Pt(PNP-*c*But)$_2$].

Atoms	Bond length (Å)	Atoms	Bond length (Å)
C11A—C12A	1.375 (11)	C42—C43	1.376 (10)
C11A—C16A	1.401 (12)	C42—H42	0.9300
C11A—P1	1.824 (8)	C43—C44	1.366 (12)
C12A—C13A	1.399 (13)	C43—H43	0.9300
C12A—H12A	0.9300	C44—C45	1.384 (12)
C13A—C14A	1.351 (13)	C44—H44	0.9300
C13A—H13A	0.9300	C45—C46	1.388 (12)
C14A—C15A	1.378 (11)	C45—H45	0.9300
C14A—H14A	0.9300	C46—H46	0.9300
C15A—C16A	1.375 (11)	N1—C1A	1.456 (13)
C15A—H15A	0.9300	N1—C1B	1.56 (2)
C16A—H16A	0.9300	N1—P1	1.700 (6)
C12B—C13B	1.3900	N1—P2	1.703 (6)
C12B—C11B	1.3900	P1—Pt1	2.3053 (16)
C12B—H12B	0.9300	P1—P2	2.649 (2)
C13B—C14B	1.3900	P2—Pt1	2.2999 (18)
C13B—H13B	0.9300	Pt1—P2^{i}	2.2999 (18)
C14B—C15B	1.3900	Pt1—P1^{i}	2.3053 (16)
C14B—H14B	0.9300	C1A—C2A	1.514 (14)
C15B—C16B	1.3900	C1A—C4A	1.521 (18)
C15B—H15B	0.9300	C1A—H1A	0.9800
C16B—C11B	1.3900	C2A—C3A	1.41 (2)
C16B—H16B	0.9300	C2A—H2A1	0.9700
C11B—P1	1.632 (18)	C2A—H2A2	0.9700
C21—C26	1.380 (12)	C3A—C4A	1.52 (2)
C21—C22	1.397 (12)	C3A—H3A1	0.9700
C21—P1	1.800 (7)	C3A—H3A2	0.9700
C22—C23	1.399 (11)	C4A—H4A1	0.9700
C22—H22	0.9300	C4A—H4A2	0.9700
C23—C24	1.365 (16)	C4B—C1B	1.49 (3)
C23—H23	0.9300	C4B—C3B	1.58 (5)

C24—C25	1.374 (17)	C4B—H4B1	0.9700
C24—H24	0.9300	C4B—H4B2	0.9700
C25—C26	1.397 (12)	C1B—H1B	0.9800
C25—H25	0.9300	C3B—H3B1	0.9700
C26—H26	0.9300	C3B—H3B2	0.9700
C31—C36	1.380 (10)	C01A—F1A	1.283 (12)
C31—C32	1.400 (11)	C01A—F2A	1.288 (14)
C31—P2	1.797 (7)	C01A—F3A	1.289 (13)
C32—C33	1.379 (11)	C01A—S01A	1.805 (15)
C32—H32	0.9300	S01A—O3A	1.353 (11)
C33—C34	1.372 (13)	S01A—O2A	1.466 (11)
C33—H33	0.9300	S01A—O1A	1.550 (13)
C34—C35	1.373 (15)	C01B—F2B	1.284 (14)
C34—H34	0.9300	C01B—F3B	1.286 (15)
C35—C36	1.381 (12)	C01B—F1B	1.321 (15)
C35—H35	0.9300	C01B—S01B	1.784 (17)
C36—H36	0.9300	S01B—O3B	1.341 (14)
C41—C42	1.398 (9)	S01B—O2B	1.438 (18)
C41—C46	1.398 (12)	S01B—O1B	1.661 (16)
C41—P2	1.795 (7)		

Symmetry codes: (i) $-x+2, -y, -z+2$

Table A 20: Bond angles (°) for [Pt(PNP-*c*But)$_2$].

Atoms	Bond angle (°)	Atoms	Bond angle (°)
C12A—C11A—C16A	118.2 (8)	C1B—N1—P2	118.6 (10)
C12A—C11A—P1	123.8 (7)	P1—N1—P2	102.2 (3)
C16A—C11A—P1	117.9 (6)	C11B—P1—N1	109.8 (12)
C11A—C12A—C13A	120.5 (8)	C11B—P1—C21	102.0 (11)
C11A—C12A—H12A	119.8	N1—P1—C21	110.5 (4)
C13A—C12A—H12A	119.8	C11B—P1—C11A	7.2 (12)
C14A—C13A—C12A	120.4 (8)	N1—P1—C11A	106.8 (4)
C14A—C13A—H13A	119.8	C21—P1—C11A	109.1 (4)
C12A—C13A—H13A	119.8	C11B—P1—Pt1	123.7 (9)
C13A—C14A—C15A	120.1 (9)	N1—P1—Pt1	93.70 (19)
C13A—C14A—H14A	119.9	C21—P1—Pt1	116.8 (2)
C15A—C14A—H14A	119.9	C11A—P1—Pt1	118.3 (3)
C16A—C15A—C14A	120.1 (8)	C11B—P1—P2	127.4 (11)
C16A—C15A—H15A	119.9	N1—P1—P2	38.94 (19)
C14A—C15A—H15A	119.9	C21—P1—P2	126.2 (3)
C15A—C16A—C11A	120.7 (7)	C11A—P1—P2	120.9 (3)
C15A—C16A—H16A	119.7	Pt1—P1—P2	54.79 (5)
C11A—C16A—H16A	119.7	N1—P2—C41	110.4 (3)
C13B—C12B—C11B	120.0	N1—P2—C31	110.5 (3)
C13B—C12B—H12B	120.0	C41—P2—C31	107.1 (3)
C11B—C12B—H12B	120.0	N1—P2—Pt1	93.80 (19)
C12B—C13B—C14B	120.0	C41—P2—Pt1	119.3 (2)
C12B—C13B—H13B	120.0	C31—P2—Pt1	115.0 (2)
C14B—C13B—H13B	120.0	N1—P2—P1	38.85 (19)
C13B—C14B—C15B	120.0	C41—P2—P1	127.8 (2)

C13B—C14B—H14B	120.0		C31—P2—P1	122.1	(2)
C15B—C14B—H14B	120.0		Pt1—P2—P1	54.98	(5)
C16B—C15B—C14B	120.0		$P2^{i}$—Pt1—P2	180.000	(1)
C16B—C15B—H15B	120.0		$P2^{i}$—Pt1—P1	109.77	(6)
C14B—C15B—H15B	120.0		P2—Pt1—P1	70.23	(6)
C15B—C16B—C11B	120.0		$P2^{i}$—Pt1—$P1^{i}$	70.23	(6)
C15B—C16B—H16B	120.0		P2—Pt1—$P1^{i}$	109.77	(6)
C11B—C16B—H16B	120.0		P1—Pt1—$P1^{i}$	180.000	(1)
C16B—C11B—C12B	120.0		N1—C1A—C2A	124.3	(10)
C16B—C11B—P1	113.0	(14)	N1—C1A—C4A	118.2	(11)
C12B—C11B—P1	126.9	(14)	C2A—C1A—C4A	84.7	(9)
C26—C21—C22	119.4	(8)	N1—C1A—H1A	109.1	
C26—C21—P1	121.0	(7)	C2A—C1A—H1A	109.1	
C22—C21—P1	119.3	(7)	C4A—C1A—H1A	109.1	
C21—C22—C23	120.1	(10)	C3A—C2A—C1A	91.8	(12)
C21—C22—H22	120.0		C3A—C2A—H2A1	113.3	
C23—C22—H22	120.0		C1A—C2A—H2A1	113.3	
C24—C23—C22	119.9	(11)	C3A—C2A—H2A2	113.3	
C24—C23—H23	120.0		C1A—C2A—H2A2	113.3	
C22—C23—H23	120.0		H2A1—C2A—H2A2	110.6	
C23—C24—C25	120.3	(9)	C2A—C3A—C4A	88.4	(13)
C23—C24—H24	119.9		C2A—C3A—H3A1	113.9	
C25—C24—H24	119.9		C4A—C3A—H3A1	113.9	
C24—C25—C26	120.7	(11)	C2A—C3A—H3A2	113.9	
C24—C25—H25	119.6		C4A—C3A—H3A2	113.9	
C26—C25—H25	119.6		H3A1—C3A—H3A2	111.1	
C21—C26—C25	119.6	(10)	C3A—C4A—C1A	87.4	(12)
C21—C26—H26	120.2		C3A—C4A—H4A1	114.1	
C25—C26—H26	120.2		C1A—C4A—H4A1	114.1	
C36—C31—C32	119.4	(7)	C3A—C4A—H4A2	114.1	
C36—C31—P2	121.9	(6)	C1A—C4A—H4A2	114.1	
C32—C31—P2	118.7	(5)	H4A1—C4A—H4A2	111.3	
C33—C32—C31	119.5	(7)	C1B—C4B—C3B	86.6	(18)
C33—C32—H32	120.3		C1B—C4B—H4B1	114.2	
C31—C32—H32	120.3		C3B—C4B—H4B1	114.2	
C34—C33—C32	120.6	(9)	C1B—C4B—H4B2	114.2	
C34—C33—H33	119.7		C3B—C4B—H4B2	114.2	
C32—C33—H33	119.7		H4B1—C4B—H4B2	111.4	
C33—C34—C35	119.9	(8)	C4B—C1B—N1	117	(2)
C33—C34—H34	120.0		C4B—C1B—H1B	112.1	
C35—C34—H34	120.0		N1—C1B—H1B	112.1	
C34—C35—C36	120.4	(9)	C4B—C3B—H3B1	114.4	
C34—C35—H35	119.8		C4B—C3B—H3B2	114.4	
C36—C35—H35	119.8		H3B1—C3B—H3B2	111.5	
C31—C36—C35	120.1	(9)	F1A—C01A—F2A	104.5	(11)
C31—C36—H36	119.9		F1A—C01A—F3A	110.8	(12)
C35—C36—H36	119.9		F2A—C01A—F3A	102.6	(13)
C42—C41—C46	118.7	(7)	F1A—C01A—S01A	117.3	(13)
C42—C41—P2	118.0	(6)	F2A—C01A—S01A	113.5	(11)
C46—C41—P2	123.2	(5)	F3A—C01A—S01A	107.2	(10)
C43—C42—C41	120.2	(8)	O3A—S01A—O2A	122.9	(9)

C43—C42—H42	119.9	O3A—S01A—O1A	116.1 (9)
C41—C42—H42	119.9	O2A—S01A—O1A	113.8 (7)
C44—C43—C42	120.6 (7)	O3A—S01A—C01A	105.5 (8)
C44—C43—H43	119.7	O2A—S01A—C01A	97.2 (8)
C42—C43—H43	119.7	O1A—S01A—C01A	93.5 (9)
C43—C44—C45	120.8 (8)	F2B—C01B—F3B	107.1 (13)
C43—C44—H44	119.6	F2B—C01B—F1B	101.9 (13)
C45—C44—H44	119.6	F3B—C01B—F1B	102.6 (14)
C44—C45—C46	119.2 (10)	F2B—C01B—S01B	119.0 (14)
C44—C45—H45	120.4	F3B—C01B—S01B	113.3 (12)
C46—C45—H45	120.4	F1B—C01B—S01B	111.2 (16)
C45—C46—C41	120.5 (8)	O3B—S01B—O2B	129.9 (17)
C45—C46—H46	119.7	O3B—S01B—O1B	103.1 (13)
C41—C46—H46	119.7	O2B—S01B—O1B	112.2 (11)
C1A—N1—C1B	26.0 (9)	O3B—S01B—C01B	117.3 (15)
C1A—N1—P1	122.3 (6)	O2B—S01B—C01B	98.3 (15)
C1B—N1—P1	128.4 (9)	O1B—S01B—C01B	88.7 (11)
C1A—N1—P2	135.1 (7)		

Symmetry codes: (i) $-x+2, -y, -z+2$

A6. Crystallographic data for [Pt(PNP-*c*Pent)$_2$]

Table A 21: Fractional atomic coordinates and isotropic or equivalent isotropic displacement parameters (Å^2) for [Pt(PNP-*c*Pent)$_2$].

	x	y	z	U_{iso}*/U_{eq}	Occ. (<1)
C1	1.0762 (4)	0.3164 (3)	0.9779 (2)	0.0230 (10)	
H1	1.0169	0.3487	1.0081	0.028*	
C2	1.2188 (5)	0.3463 (3)	0.9988 (2)	0.0306 (11)	
H2A	1.2846	0.309	0.9754	0.037*	
H2B	1.238	0.3371	1.0455	0.037*	
C3	1.2184 (6)	0.4555 (4)	0.9805 (2)	0.0382 (12)	
H3A	1.1792	0.4957	1.0138	0.046*	
H3B	1.3102	0.4789	0.9748	0.046*	
C4	1.1334 (6)	0.4606 (4)	0.9179 (3)	0.0395 (13)	
H4A	1.1909	0.4654	0.8814	0.047*	
H4B	1.0748	0.5189	0.9174	0.047*	
C5	1.0489 (5)	0.3669 (3)	0.9123 (2)	0.0261 (10)	
H5A	1.0769	0.3247	0.8772	0.031*	
H5B	0.953	0.3827	0.9044	0.031*	
C11	1.2563 (4)	0.1091 (3)	0.91477 (19)	0.0207 (9)	
C12	1.3335 (5)	0.0312 (3)	0.9382 (2)	0.0264 (10)	
H12	1.2961	−0.017	0.9644	0.032*	
C13	1.4666 (5)	0.0238 (4)	0.9232 (2)	0.0330 (12)	
H13	1.5186	−0.0311	0.9374	0.04*	
C14	1.5222 (5)	0.0964 (4)	0.8878 (2)	0.0297 (11)	
H14	1.6139	0.0925	0.8795	0.036*	
C15	1.4480 (5)	0.1736 (4)	0.8645 (2)	0.0316 (11)	

H15	1.4876	0.2229	0.8401	0.038*	
C16	1.3142 (5)	0.1796 (3)	0.8768 (2)	0.0264 (10)	
H16	1.2613	0.232	0.8593	0.032*	
C21	0.9925 (4)	0.1201 (3)	0.85355 (19)	0.0201 (9)	
C22	1.0380 (4)	0.0582 (3)	0.8056 (2)	0.0236 (10)	
H22	1.1194	0.0232	0.8127	0.028*	
C23	0.9622 (5)	0.0492 (4)	0.7479 (2)	0.0272 (10)	
H23	0.9911	0.0073	0.7153	0.033*	
C24	0.8444 (5)	0.1013 (3)	0.7378 (2)	0.0265 (10)	
H24	0.7926	0.0946	0.6983	0.032*	
C25	0.8016 (5)	0.1625 (3)	0.7842 (2)	0.0263 (10)	
H25	0.7215	0.1989	0.7763	0.032*	
C26	0.8746 (4)	0.1713 (3)	0.8424 (2)	0.0222 (10)	
H26	0.8436	0.2127	0.8747	0.027*	
C31	1.1077 (4)	0.1741 (3)	1.11284 (19)	0.0208 (9)	
C32	1.2084 (5)	0.1038 (3)	1.1270 (2)	0.0263 (10)	
H32	1.2098	0.0452	1.1026	0.032*	
C33	1.3044 (5)	0.1194 (4)	1.1758 (2)	0.0317 (11)	
H33	1.3713	0.0716	1.1857	0.038*	
C34	1.3027 (5)	0.2060 (4)	1.2107 (2)	0.0346 (12)	
H34	1.37	0.2173	1.244	0.042*	
C35	1.2052 (5)	0.2756 (4)	1.1978 (2)	0.0364 (12)	
H35	1.2053	0.3344	1.2221	0.044*	
C36	1.1069 (5)	0.2591 (4)	1.1491 (2)	0.0302 (11)	
H36	1.0386	0.3063	1.1405	0.036*	
C41	0.8337 (4)	0.2049 (3)	1.0621 (2)	0.0209 (9)	
C42	0.7533 (5)	0.2500 (3)	1.0139 (2)	0.0267 (10)	
H42	0.7872	0.2625	0.9734	0.032*	
C43	0.6244 (5)	0.2764 (4)	1.0250 (2)	0.0324 (11)	
H43	0.57	0.3077	0.9922	0.039*	
C44	0.5735 (5)	0.2576 (4)	1.0840 (2)	0.0326 (12)	
H44	0.4837	0.2742	1.0909	0.039*	
C45	0.6538 (5)	0.2148 (4)	1.1327 (2)	0.0306 (11)	
H45	0.6198	0.2039	1.1733	0.037*	
C46	0.7842 (5)	0.1876 (3)	1.1222 (2)	0.0262 (10)	
H46	0.8392	0.1577	1.1554	0.031*	
N1	1.0451 (3)	0.2102 (3)	0.97884 (16)	0.0190 (8)	
P1	1.08226 (11)	0.11427 (8)	0.93121 (5)	0.01603 (7)	
P2	0.99258 (11)	0.15296 (8)	1.04487 (5)	0.01603 (7)	
Pt1	1	0	1	0.01603 (7)	
O1A	0.6874 (3)	0.3547 (3)	0.87585 (18)	0.0410 (9)	0.511 (11)
S1A	0.6839 (7)	0.4342 (5)	0.8293 (4)	0.0353 (13)	0.511 (11)
O2A	0.7720 (9)	0.4555 (9)	0.7931 (7)	0.080 (5)	0.511 (11)
O3A	0.5823 (9)	0.3523 (6)	0.7743 (3)	0.045 (3)	0.511 (11)
C01A	0.5385 (9)	0.4916 (7)	0.8440 (3)	0.0353 (13)	0.511 (11)
F3A	0.5273 (8)	0.5233 (6)	0.9030 (4)	0.048 (2)	0.511 (11)
F2A	0.4267 (8)	0.4383 (6)	0.8272 (6)	0.070 (3)	0.511 (11)
F1A	0.5064 (7)	0.5707 (5)	0.8087 (4)	0.042 (2)*	0.511 (11)
O1B	0.6874 (3)	0.3547 (3)	0.87585 (18)	0.0410 (9)	0.489 (11)
F3B	0.6075 (16)	0.5606 (9)	0.8840 (7)	0.129 (7)	0.489 (11)
O2B	0.7866 (7)	0.5037 (6)	0.8490 (5)	0.047 (3)	0.489 (11)

C01B	0.5446 (10)	0.5042 (8)	0.8351 (5)	0.0308 (12)	0.489 (11)
O3B	0.6795 (15)	0.4142 (10)	0.7618 (4)	0.082 (5)	0.489 (11)
S1B	0.6660 (6)	0.4067 (5)	0.8193 (4)	0.0308 (12)	0.489 (11)
F2B	0.4419 (11)	0.4684 (10)	0.8634 (6)	0.100 (5)	0.489 (11)
F1B	0.5215 (9)	0.5642 (6)	0.7862 (5)	0.058 (3)*	0.489 (11)

Table A 22: Atomic displacement parameters (Å^2) for [Pt(PNP-*c*Pent)$_2$].

	U^{11}	U^{22}	U^{33}	U^{12}	U^{13}	U^{23}
C1	0.027 (2)	0.019 (2)	0.023 (2)	0.0027 (19)	0.0023 (19)	0.0019 (19)
C2	0.034 (3)	0.028 (3)	0.029 (2)	−0.005 (2)	−0.002 (2)	−0.002 (2)
C3	0.047 (3)	0.032 (3)	0.036 (3)	−0.013 (3)	0.000 (2)	0.003 (2)
C4	0.050 (3)	0.028 (3)	0.039 (3)	−0.006 (3)	0.001 (3)	0.008 (2)
C5	0.031 (3)	0.023 (3)	0.024 (2)	0.003 (2)	0.000 (2)	0.0031 (19)
C11	0.024 (2)	0.021 (2)	0.017 (2)	0.0018 (18)	0.0011 (18)	−0.0008 (18)
C12	0.024 (2)	0.028 (3)	0.028 (2)	−0.0023 (19)	−0.001 (2)	0.000 (2)
C13	0.022 (2)	0.038 (3)	0.038 (3)	0.008 (2)	−0.003 (2)	0.002 (2)
C14	0.016 (2)	0.039 (3)	0.034 (3)	−0.002 (2)	0.004 (2)	−0.003 (2)
C15	0.027 (3)	0.038 (3)	0.029 (3)	0.000 (2)	0.004 (2)	0.002 (2)
C16	0.027 (3)	0.026 (3)	0.026 (2)	0.006 (2)	0.002 (2)	−0.001 (2)
C21	0.025 (2)	0.019 (2)	0.016 (2)	−0.0026 (18)	0.0029 (18)	0.0013 (17)
C22	0.024 (2)	0.024 (3)	0.023 (2)	0.0024 (19)	0.0018 (19)	−0.0010 (19)
C23	0.032 (3)	0.028 (3)	0.022 (2)	−0.002 (2)	0.002 (2)	−0.003 (2)
C24	0.028 (3)	0.030 (3)	0.021 (2)	−0.002 (2)	−0.0043 (19)	0.001 (2)
C25	0.023 (2)	0.026 (3)	0.030 (2)	0.003 (2)	0.001 (2)	0.002 (2)
C26	0.024 (2)	0.019 (2)	0.023 (2)	0.0034 (19)	0.0017 (19)	−0.0007 (18)
C31	0.026 (2)	0.019 (2)	0.017 (2)	0.0012 (18)	0.0005 (18)	0.0003 (18)
C32	0.029 (3)	0.025 (3)	0.024 (2)	0.000 (2)	0.000 (2)	−0.006 (2)
C33	0.027 (3)	0.041 (3)	0.026 (2)	0.005 (2)	−0.003 (2)	−0.002 (2)
C34	0.036 (3)	0.038 (3)	0.029 (3)	−0.001 (2)	−0.007 (2)	−0.007 (2)
C35	0.047 (3)	0.034 (3)	0.027 (3)	−0.004 (3)	−0.003 (2)	−0.012 (2)
C36	0.038 (3)	0.028 (3)	0.025 (2)	0.003 (2)	−0.001 (2)	-0.003 (2)
C41	0.023 (2)	0.019 (2)	0.021 (2)	0.0018 (18)	0.0023 (18)	−0.0035 (18)
C42	0.030 (3)	0.026 (3)	0.025 (2)	0.004 (2)	0.006 (2)	0.000 (2)
C43	0.033 (3)	0.032 (3)	0.032 (3)	0.009 (2)	0.001 (2)	0.004 (2)
C44	0.025 (3)	0.034 (3)	0.039 (3)	0.007 (2)	0.008 (2)	−0.005 (2)
C45	0.034 (3)	0.029 (3)	0.029 (2)	0.001 (2)	0.008 (2)	−0.004 (2)
C46	0.032 (3)	0.022 (2)	0.025 (2)	0.007 (2)	0.006 (2)	−0.001 (2)
N1	0.0225 (19)	0.020 (2)	0.0147 (16)	0.0061 (15)	0.0041 (15)	0.0005 (15)
P1	0.01943 (12)	0.01522 (12)	0.01339 (11)	0.00270 (10)	0.00077 (7)	0.00016 (10)
P2	0.01943 (12)	0.01522 (12)	0.01339 (11)	0.00270 (10)	0.00077 (7)	0.00016 (10)
Pt1	0.01943 (12)	0.01522 (12)	0.01339 (11)	0.00270 (10)	0.00077 (7)	0.00016 (10)
O1A	0.037 (2)	0.035 (2)	0.051 (2)	0.0101 (17)	0.0047 (18)	0.0085 (18)
S1A	0.049 (3)	0.025 (3)	0.032 (2)	0.023 (2)	0.0062 (19)	0.0012 (18)
O2A	0.039 (5)	0.096 (9)	0.106 (12)	−0.009 (6)	0.023 (6)	0.052 (8)
O3A	0.060 (6)	0.042 (5)	0.032 (4)	0.011 (4)	−0.010 (4)	−0.024 (4)
C01A	0.049 (3)	0.025 (3)	0.032 (2)	0.023 (2)	0.0062 (19)	0.0012 (18)
F3A	0.044 (5)	0.051 (5)	0.050 (4)	0.015 (3)	0.018 (4)	−0.008 (4)
F2A	0.028 (4)	0.051 (5)	0.127 (9)	−0.004 (3)	−0.032 (5)	−0.003 (6)
O1B	0.037 (2)	0.035 (2)	0.051 (2)	0.0101 (17)	0.0047 (18)	0.0085 (18)
F3B	0.169 (15)	0.075 (9)	0.129 (11)	0.060 (9)	−0.091 (11)	−0.077 (8)

O2B	0.020 (4)	0.042 (5)	0.080 (7)	0.001 (4)	0.011 (4)	0.018 (5)
C01B	0.0310 (18)	0.029 (3)	0.033 (3)	0.0079 (18)	0.0072 (15)	0.0028 (19)
O3B	0.115 (13)	0.099 (10)	0.031 (5)	0.050 (10)	−0.002 (6)	−0.028 (6)
S1B	0.0310 (18)	0.029 (3)	0.033 (3)	0.0079 (18)	0.0072 (15)	0.0028 (19)
F2B	0.077 (9)	0.161 (14)	0.064 (7)	0.058 (9)	0.026 (7)	0.002 (7)

Table A 23: Bond lengths (Å) for [Pt(PNP-*c*Pent)$_2$].

Atoms	Bond length (Å)	Atoms	Bond length (Å)
C1—N1	1.484 (6)	C32—C33	1.372 (6)
C1—C2	1.524 (6)	C32—H32	0.95
C1—C5	1.543 (6)	C33—C34	1.390 (7)
C1—H1	1	C33—H33	0.95
C2—C3	1.540 (7)	C34—C35	1.378 (7)
C2—H2A	0.99	C34—H34	0.95
C2—H2B	0.99	C35—C36	1.389 (6)
C3—C4	1.516 (7)	C35—H35	0.95
C3—H3A	0.99	C36—H36	0.95
C3—H3B	0.99	C41—C42	1.391 (6)
C4—C5	1.535 (7)	C41—C46	1.403 (6)
C4—H4A	0.99	C41—P2	1.805 (4)
C4—H4B	0.99	C42—C43	1.379 (6)
C5—H5A	0.99	C42—H42	0.95
C5—H5B	0.99	C43—C44	1.391 (7)
C11—C12	1.387 (6)	C43—H43	0.95
C11—C16	1.400 (6)	C44—C45	1.385 (7)
C11—P1	1.805 (4)	C44—H44	0.95
C12—C13	1.397 (7)	C45—C46	1.393 (6)
C12—H12	0.95	C45—H45	0.95
C13—C14	1.379 (7)	C46—H46	0.95
C13—H13	0.95	N1—P2	1.703 (4)
C14—C15	1.362 (7)	N1—P1	1.704 (4)
C14—H14	0.95	P1—Pt1	2.3139 (12)
C15—C16	1.388 (6)	P1—P2	2.6534 (15)
C15—H15	0.95	P2—Pt1	2.2943 (13)
C16—H16	0.95	Pt1—P2^{i}	2.2943 (13)
C21—C26	1.381 (6)	Pt1—P1^{i}	2.3139 (12)
C21—C22	1.413 (6)	O1A—S1A	1.458 (9)
C21—P1	1.806 (4)	S1A—O2A	1.237 (12)
C22—C23	1.388 (6)	S1A—C01A	1.704 (2)
C22—H22	0.95	S1A—O3A	1.859 (11)
C23—C24	1.384 (6)	C01A—F3A	1.320 (2)
C23—H23	0.95	C01A—F1A	1.336 (5)
C24—C25	1.373 (6)	C01A—F2A	1.364 (13)
C24—H24	0.95	F3B—C01B	1.398 (15)
C25—C26	1.384 (6)	O2B—S1B	1.873 (12)
C25—H25	0.95	C01B—F2B	1.318 (2)
C26—H26	0.95	C01B—F1B	1.320 (5)
C31—C36	1.387 (6)	C01B—S1B	1.850 (12)
C31—C32	1.412 (6)	O3B—S1B	1.226 (12)

C31—P2	1.794	(4)

Symmetry codes: (i) $-x+2, -y, -z+2$.

Table A 24: Bond angles (°) for [Pt(PNP-*c*Pent)$_2$].

Atoms	Bond angle (°)	Atoms	Bond angle (°)
N1—C1—C2	116.9 (4)	C35—C34—C33	121.2 (5)
N1—C1—C5	115.1 (3)	C35—C34—H34	119.4
C2—C1—C5	104.0 (4)	C33—C34—H34	119.4
N1—C1—H1	106.7	C34—C35—C36	119.4 (5)
C2—C1—H1	106.7	C34—C35—H35	120.3
C5—C1—H1	106.7	C36—C35—H35	120.3
C1—C2—C3	101.6 (4)	C31—C36—C35	120.5 (5)
C1—C2—H2A	111.4	C31—C36—H36	119.8
C3—C2—H2A	111.4	C35—C36—H36	119.8
C1—C2—H2B	111.4	C42—C41—C46	120.0 (4)
C3—C2—H2B	111.4	C42—C41—P2	120.4 (3)
H2A—C2—H2B	109.3	C46—C41—P2	119.0 (3)
C4—C3—C2	104.6 (4)	C43—C42—C41	119.9 (4)
C4—C3—H3A	110.8	C43—C42—H42	120
C2—C3—H3A	110.8	C41—C42—H42	120
C4—C3—H3B	110.8	C42—C43—C44	120.5 (4)
C2—C3—H3B	110.8	C42—C43—H43	119.8
H3A—C3—H3B	108.9	C44—C43—H43	119.8
C3—C4—C5	107.6 (4)	C45—C44—C43	120.0 (4)
C3—C4—H4A	110.2	C45—C44—H44	120
C5—C4—H4A	110.2	C43—C44—H44	120
C3—C4—H4B	110.2	C44—C45—C46	120.2 (5)
C5—C4—H4B	110.2	C44—C45—H45	119.9
H4A—C4—H4B	108.5	C46—C45—H45	119.9
C4—C5—C1	104.0 (4)	C45—C46—C41	119.4 (4)
C4—C5—H5A	111	C45—C46—H46	120.3
C1—C5—H5A	111	C41—C46—H46	120.3
C4—C5—H5B	111	C1—N1—P2	122.5 (3)
C1—C5—H5B	111	C1—N1—P1	133.6 (3)
H5A—C5—H5B	109	P2—N1—P1	102.32 (19)
C12—C11—C16	119.0 (4)	N1—P1—C11	113.27 (19)
C12—C11—P1	119.2 (3)	N1—P1—C21	112.14 (19)
C16—C11—P1	121.7 (3)	C11—P1—C21	105.09 (19)
C11—C12—C13	119.7 (5)	N1—P1—Pt1	93.07 (13)
C11—C12—H12	120.1	C11—P1—Pt1	118.91 (14)
C13—C12—H12	120.1	C21—P1—Pt1	114.36 (14)
C14—C13—C12	119.9 (5)	C11—P1—P2	124.81 (14)
C14—C13—H13	120.1	C21—P1—P2	128.24 (15)
C12—C13—H13	120.1	Pt1—P1—P2	54.50 (4)
C15—C14—C13	121.1 (4)	N1—P2—C31	110.5 (2)
C15—C14—H14	119.4	N1—P2—C41	107.96 (19)
C13—C14—H14	119.4	C31—P2—C41	108.0 (2)
C14—C15—C16	119.5 (5)	N1—P2—Pt1	93.78 (13)
C14—C15—H15	120.2	C31—P2—Pt1	115.73 (15)

C16—C15—H15	120.2	C41—P2—Pt1	119.61 (15)
C15—C16—C11	120.6 (4)	C31—P2—P1	120.20 (15)
C15—C16—H16	119.7	C41—P2—P1	128.04 (14)
C11—C16—H16	119.7	Pt1—P2—P1	55.19 (3)
C26—C21—C22	119.9 (4)	$P2^{i}$—Pt1—P2	180.0000 (10)
C26—C21—P1	123.0 (3)	$P2^{i}$—Pt1—$P1^{i}$	70.31 (4)
C22—C21—P1	116.6 (3)	P2—Pt1—$P1^{i}$	109.69 (4)
C23—C22—C21	119.2 (4)	$P2^{i}$—Pt1—P1	109.69 (4)
C23—C22—H22	120.4	P2—Pt1—P1	70.31 (4)
C21—C22—H22	120.4	$P1^{i}$—Pt1—P1	180.0000 (10)
C24—C23—C22	119.9 (4)	O2A—S1A—O1A	126.8 (7)
C24—C23—H23	120	O2A—S1A—C01A	131.2 (9)
C22—C23—H23	120	O1A—S1A—C01A	101.7 (5)
C25—C24—C23	120.7 (4)	O2A—S1A—O3A	98.5 (9)
C25—C24—H24	119.6	O1A—S1A—O3A	87.3 (5)
C23—C24—H24	119.6	C01A—S1A—O3A	87.0 (5)
C24—C25—C26	120.2 (4)	F3A—C01A—F1A	102.7 (8)
C24—C25—H25	119.9	F3A—C01A—F2A	107.2 (8)
C26—C25—H25	119.9	F1A—C01A—F2A	97.2 (7)
C21—C26—C25	120.1 (4)	F3A—C01A—S1A	116.7 (6)
C21—C26—H26	120	F1A—C01A—S1A	116.7 (7)
C25—C26—H26	120	F2A—C01A—S1A	114.1 (7)
C36—C31—C32	119.1 (4)	F2B—C01B—F1B	118.6 (10)
C36—C31—P2	122.7 (3)	F2B—C01B—F3B	101.7 (10)
C32—C31—P2	118.1 (3)	F1B—C01B—F3B	105.8 (11)
C33—C32—C31	120.5 (4)	F2B—C01B—S1B	111.0 (9)
C33—C32—H32	119.8	F1B—C01B—S1B	113.1 (7)
C31—C32—H32	119.8	F3B—C01B—S1B	104.9 (7)
C32—C33—C34	119.4 (5)	O3B—S1B—C01B	103.5 (7)
C32—C33—H33	120.3	O3B—S1B—O2B	98.8 (9)
C34—C33—H33	120.3	C01B—S1B—O2B	81.4 (6)

Symmetry codes: (i) $-x+2, -y, -z+2$.

A7. Crystallographic data for [Pt(PNP-*c*Hex)$_2$]

Table A 25: Fractional atomic coordinates and isotropic or equivalent isotropic displacement parameters (Å^2) for [Pt(PNP-*c*Hex)$_2$].

	x	*y*	*z*	U_{iso}*/U_{eq}	Occ. (<1)
C1A	0.7123 (8)	0.5220 (6)	0.8424 (9)	0.0219 (18)	0.630 (7)
H1A	0.6699	0.5599	0.8562	0.026*	0.630 (7)
C2A	0.8441 (5)	0.5445 (3)	0.8991 (3)	0.0299 (14)	0.630 (7)
H2A1	0.8889	0.509	0.8856	0.036*	0.630 (7)
H2A2	0.8497	0.5911	0.8715	0.036*	0.630 (7)
C3A	0.8998 (7)	0.5504 (4)	1.0172 (5)	0.0391 (16)	0.630 (7)
H3A1	0.861	0.59	1.0308	0.047*	0.630 (7)
H3A2	0.9861	0.5618	1.0529	0.047*	0.630 (7)

C4A	0.8855 (6)	0.4809 (3)	1.0631 (4)	0.0405 (17)	0.630 (7)
H4A1	0.9324	0.4426	1.0572	0.049*	0.630 (7)
H4A2	0.9178	0.4879	1.1385	0.049*	0.630 (7)
C5A	0.7558 (9)	0.4589 (5)	1.0064 (8)	0.036 (2)	0.630 (7)
H5A1	0.7105	0.494	1.02	0.043*	0.630 (7)
H5A2	0.7496	0.4119	1.0327	0.043*	0.630 (7)
C6A	0.7028 (19)	0.4544 (9)	0.8898 (17)	0.0228 (17)	0.630 (7)
H6A1	0.7439	0.4159	0.877	0.027*	0.630 (7)
H6A2	0.6172	0.4412	0.8536	0.027*	0.630 (7)
C1B	0.7520 (13)	0.5190 (12)	0.8490 (17)	0.024 (3)	0.370 (7)
H1B	0.831	0.5048	0.8615	0.029*	0.370 (7)
C2B	0.7677 (8)	0.5875 (5)	0.9006 (6)	0.028 (2)	0.370 (7)
H2B1	0.6897	0.6044	0.8862	0.034*	0.370 (7)
H2B2	0.798	0.6234	0.873	0.034*	0.370 (7)
C3B	0.8569 (9)	0.5787 (6)	1.0188 (7)	0.029 (2)	0.370 (7)
H3B1	0.9367	0.5673	1.0325	0.035*	0.370 (7)
H3B2	0.8637	0.6245	1.0539	0.035*	0.370 (7)
C4B	0.8217 (10)	0.5209 (6)	1.0662 (7)	0.040 (3)	0.370 (7)
C5B	0.7999 (16)	0.4511 (10)	1.0077 (15)	0.038 (4)	0.370 (7)
H5B1	0.773	0.4151	1.0379	0.045*	0.370 (7)
H5B2	0.8771	0.4344	1.0202	0.045*	0.370 (7)
C6B	0.705 (4)	0.455 (2)	0.886 (3)	0.040 (3)	0.370 (7)
H6B1	0.624	0.4643	0.8699	0.048*	0.370 (7)
H6B2	0.7037	0.4094	0.8515	0.048*	0.370 (7)
C11A	0.509 (3)	0.6467 (9)	0.648 (2)	0.0207 (12)	0.60 (2)
C16A	0.3952 (15)	0.6778 (12)	0.594 (2)	0.0273 (8)	0.60 (2)
H16A	0.3261	0.6484	0.5653	0.033*	0.60 (2)
C15A	0.3821 (12)	0.7511 (12)	0.5829 (14)	0.030 (3)	0.60 (2)
H15A	0.3045	0.7719	0.5443	0.035*	0.60 (2)
C14A	0.4835 (9)	0.7935 (5)	0.6283 (11)	0.040 (2)	0.60 (2)
H14A	0.4757	0.8439	0.6231	0.048*	0.60 (2)
C13A	0.5958 (7)	0.7629 (4)	0.6811 (13)	0.048 (4)	0.60 (2)
H13A	0.6649	0.7925	0.7121	0.058*	0.60 (2)
C12A	0.6090 (9)	0.6895 (5)	0.6894 (11)	0.036 (2)	0.60 (2)
H12A	0.6866	0.6687	0.7234	0.044*	0.60 (2)
C11B	0.506 (5)	0.6450 (13)	0.655 (3)	0.0207 (12)	0.40 (2)
C12B	0.6086 (14)	0.6845 (7)	0.7260 (12)	0.022 (2)	0.40 (2)
H12B	0.6837	0.6611	0.7682	0.027*	0.40 (2)
C13B	0.6009 (9)	0.7572 (5)	0.7357 (13)	0.030 (3)	0.40 (2)
H13B	0.67	0.7839	0.7849	0.036*	0.40 (2)
C14B	0.4914 (12)	0.7906 (6)	0.6728 (14)	0.028 (3)	0.40 (2)
H14B	0.4861	0.8408	0.6766	0.034*	0.40 (2)
C15B	0.390 (2)	0.7519 (18)	0.604 (2)	0.030 (3)	0.40 (2)
H15B	0.3142	0.7751	0.5647	0.035*	0.40 (2)
C16B	0.398 (2)	0.6792 (19)	0.594 (3)	0.0273 (8)	0.40 (2)
H16B	0.3287	0.653	0.5445	0.033*	0.40 (2)
C21	0.4170 (3)	0.51739 (15)	0.6806 (2)	0.0222 (6)	
C22	0.4104 (3)	0.55086 (17)	0.7594 (2)	0.0279 (7)	
H22	0.4558	0.5927	0.7923	0.034*	
C23	0.3373 (3)	0.52266 (19)	0.7891 (3)	0.0335 (7)	
H23	0.3336	0.5449	0.8432	0.04*	

C24	0.2697 (3)	0.46216 (18)	0.7400 (2)	0.0312 (7)		
H24	0.2199	0.443	0.7608	0.037*		
C25	0.2743 (3)	0.42946 (17)	0.6607 (2)	0.0276 (7)		
H25	0.2265	0.3886	0.6263	0.033*		
C26	0.3486 (3)	0.45657 (16)	0.6320 (2)	0.0241 (6)		
H26	0.3532	0.4335	0.5788	0.029*		
C31	0.8129 (3)	0.50637 (15)	0.6510 (2)	0.0208 (6)		
C32	0.8465 (3)	0.57719 (16)	0.6751 (2)	0.0286 (7)		
H32	0.8087	0.6067	0.6993	0.034*		
C33	0.9353 (3)	0.60518 (18)	0.6641 (3)	0.0377 (8)		
H33	0.9593	0.6535	0.6821	0.045*		
C34	0.9887 (3)	0.56276 (18)	0.6270 (3)	0.0333 (7)		
H34	1.0486	0.5821	0.6184	0.04*		
C35	0.9553 (3)	0.49219 (17)	0.6021 (3)	0.0300 (7)		
H35	0.9919	0.4633	0.5762	0.036*		
C36	0.8685 (3)	0.46349 (16)	0.6149 (2)	0.0234 (6)		
H36	0.8469	0.4147	0.5992	0.028*		
C41	0.7127 (3)	0.38095 (14)	0.6872 (2)	0.0215 (6)		
C42	0.8280 (3)	0.35531 (16)	0.7592 (2)	0.0255 (6)		
H42	0.8952	0.3859	0.7847	0.031*		
C43	0.8445 (3)	0.28564 (17)	0.7933 (2)	0.0317 (7)		
H43	0.923	0.2683	0.8424	0.038*		
C44	0.7477 (4)	0.24134 (18)	0.7563 (3)	0.0406 (9)		
H44	0.7593	0.1935	0.7805	0.049*		
C45	0.6336 (4)	0.26580 (19)	0.6842 (3)	0.0455 (9)		
H45	0.567	0.2346	0.6585	0.055*		
C46	0.6156 (3)	0.33545 (16)	0.6491 (3)	0.0321 (7)		
H46	0.5369	0.3521	0.599	0.039*		
N1	0.6583 (2)	0.52111 (12)	0.72778 (17)	0.0206 (5)		
F1	1.0498 (2)	0.69802 (10)	0.96793 (16)	0.0490 (6)		
F2	0.8895 (2)	0.71702 (11)	0.80417 (17)	0.0544 (6)		
F3	0.9056 (2)	0.77212 (16)	0.9418 (2)	0.0720 (8)		
F4	0.9237 (2)	0.83448 (11)	0.82524 (17)	0.0555 (6)		
F5	1.0843 (2)	0.81596 (12)	0.98976 (18)	0.0632 (7)		
F6	1.0704 (2)	0.76089 (16)	0.8535 (2)	0.0741 (8)		
P1	0.51549 (7)	0.55043 (4)	0.64387 (5)	0.01807 (14)		
P2	0.68416 (6)	0.47263 (4)	0.64749 (5)	0.01702 (14)		
P3	0.98835 (7)	0.76603 (4)	0.89695 (6)	0.02531 (17)		
Pt1	0.5	0.5	0.5	0.01390 (5)		
Cl1A	0.2941 (3)	0.24968 (16)	1.0253 (3)	0.0898 (11)	0.526	(4)
Cl2A	0.4137 (3)	0.36092 (12)	0.98377 (18)	0.0645 (8)	0.526	(4)
C01A	0.3384 (12)	0.2783 (6)	0.9426 (8)	0.088 (4)	0.526	(4)
H01A	0.2669	0.283	0.8701	0.105*	0.526	(4)
H01B	0.3921	0.2422	0.9419	0.105*	0.526	(4)
Cl1B	0.3117 (2)	0.20374 (13)	1.00257 (18)	0.0514 (8)*	0.474	(4)
Cl2B	0.3438 (3)	0.35456 (12)	0.9852 (2)	0.0534 (7)	0.474	(4)
C01B	0.2399 (8)	0.2844 (4)	0.9415 (7)	0.049 (2)	0.474	(4)
H01C	0.1982	0.2794	0.8644	0.058*	0.474	(4)
H01D	0.179	0.2956	0.9574	0.058*	0.474	(4)

Table A 26: Atomic displacement parameters (Å^2) for [Pt(PNP-*c*Hex)$_2$].

	U^{11}	U^{22}	U^{33}	U^{12}	U^{13}	U^{23}
C1A	0.023 (5)	0.024 (3)	0.010 (3)	−0.008 (4)	0.004 (4)	−0.001 (2)
C2A	0.028 (3)	0.033 (3)	0.014 (2)	−0.007 (2)	0.002 (2)	0.0017 (19)
C3A	0.040 (4)	0.041 (4)	0.020 (3)	−0.004 (3)	0.006 (3)	−0.005 (3)
C4A	0.054 (4)	0.040 (3)	0.015 (2)	0.007 (3)	0.011 (3)	0.005 (2)
C5A	0.065 (7)	0.030 (4)	0.024 (3)	0.000 (4)	0.032 (5)	0.002 (2)
C6A	0.036 (4)	0.021 (3)	0.019 (4)	0.001 (3)	0.019 (3)	0.003 (2)
C1B	0.012 (8)	0.039 (6)	0.012 (5)	−0.002 (7)	0.000 (7)	0.003 (4)
C2B	0.031 (5)	0.035 (5)	0.014 (4)	−0.005 (4)	0.010 (4)	−0.003 (3)
C3B	0.027 (5)	0.044 (6)	0.008 (4)	0.002 (4)	0.005 (4)	−0.004 (4)
C4B	0.043 (6)	0.056 (6)	0.017 (4)	0.002 (5)	0.014 (4)	0.004 (4)
C5B	0.057 (11)	0.042 (7)	0.033 (6)	0.008 (7)	0.037 (8)	0.008 (5)
C6B	0.043 (6)	0.056 (6)	0.017 (4)	0.002 (5)	0.014 (4)	0.004 (4)
C11A	0.027 (2)	0.0199 (15)	0.019 (3)	−0.0022 (14)	0.0149 (19)	−0.0038 (15)
C16A	0.0252 (17)	0.0286 (17)	0.0296 (16)	−0.0017 (14)	0.0161 (15)	−0.0051 (14)
C15A	0.031 (2)	0.0288 (18)	0.030 (7)	0.0092 (19)	0.018 (3)	0.002 (4)
C14A	0.049 (4)	0.022 (3)	0.052 (6)	0.007 (3)	0.029 (5)	−0.001 (4)
C13A	0.034 (4)	0.025 (3)	0.070 (9)	−0.006 (3)	0.018 (4)	−0.012 (4)
C12A	0.025 (3)	0.025 (3)	0.046 (6)	0.000 (3)	0.011 (4)	−0.010 (4)
C11B	0.027 (2)	0.0199 (15)	0.019 (3)	−0.0022 (14)	0.0149 (19)	−0.0038 (15)
C12B	0.032 (5)	0.017 (4)	0.024 (6)	−0.001 (3)	0.019 (5)	−0.003 (4)
C13B	0.035 (5)	0.023 (4)	0.030 (7)	−0.006 (4)	0.017 (5)	−0.012 (4)
C14B	0.038 (6)	0.016 (4)	0.039 (8)	−0.001 (4)	0.027 (6)	−0.006 (5)
C15B	0.031 (2)	0.0288 (18)	0.030 (7)	0.0092 (19)	0.018 (3)	0.002 (4)
C16B	0.0252 (17)	0.0286 (17)	0.0296 (16)	−0.0017 (14)	0.0161 (15)	−0.0051 (14)
C21	0.0253 (15)	0.0255 (14)	0.0212 (14)	0.0019 (12)	0.0163 (13)	0.0016 (11)
C22	0.0345 (18)	0.0308 (16)	0.0248 (15)	−0.0004 (14)	0.0203 (14)	−0.0038 (12)
C23	0.039 (2)	0.0436 (18)	0.0294 (17)	0.0050 (16)	0.0266 (16)	0.0002 (14)
C24	0.0257 (17)	0.042 (2)	0.0318 (17)	0.0063 (14)	0.0198 (15)	0.0111 (14)
C25	0.0208 (15)	0.0318 (16)	0.0275 (15)	−0.0008 (13)	0.0116 (13)	0.0047 (13)
C26	0.0255 (16)	0.0252 (15)	0.0227 (14)	0.0006 (12)	0.0140 (13)	0.0008 (11)
C31	0.0173 (13)	0.0249 (14)	0.0163 (12)	−0.0023 (11)	0.0067 (11)	0.0010 (11)
C32	0.0370 (18)	0.0249 (15)	0.0320 (16)	−0.0060 (13)	0.0241 (15)	−0.0056 (13)
C33	0.044 (2)	0.0319 (17)	0.045 (2)	−0.0157 (16)	0.0294 (18)	−0.0077 (15)
C34	0.0286 (17)	0.0397 (19)	0.0355 (18)	−0.0063 (14)	0.0201 (15)	0.0035 (14)
C35	0.0228 (15)	0.0404 (19)	0.0280 (16)	0.0037 (14)	0.0147 (14)	0.0039 (13)
C36	0.0191 (14)	0.0239 (15)	0.0234 (14)	0.0027 (12)	0.0092 (12)	0.0015 (12)
C41	0.0284 (15)	0.0186 (13)	0.0186 (13)	0.0023 (12)	0.0137 (12)	0.0007 (10)
C42	0.0322 (17)	0.0258 (15)	0.0198 (14)	0.0026 (13)	0.0152 (13)	0.0017 (11)
C43	0.0397 (19)	0.0331 (17)	0.0240 (15)	0.0123 (15)	0.0186 (15)	0.0094 (13)
C44	0.055 (2)	0.0254 (17)	0.045 (2)	0.0091 (16)	0.0297 (19)	0.0127 (15)
C45	0.047 (2)	0.0271 (18)	0.056 (2)	−0.0065 (16)	0.024 (2)	0.0057 (16)
C46	0.0327 (18)	0.0223 (15)	0.0345 (17)	−0.0024 (13)	0.0142 (15)	0.0014 (13)
N1	0.0277 (13)	0.0195 (11)	0.0122 (11)	−0.0019 (10)	0.0094 (10)	−0.0025 (9)
F1	0.0658 (15)	0.0295 (10)	0.0423 (12)	0.0081 (10)	0.0237 (11)	0.0069 (9)
F2	0.0586 (15)	0.0359 (11)	0.0416 (12)	−0.0169 (10)	0.0104 (11)	−0.0100 (9)
F3	0.0660 (17)	0.098 (2)	0.0795 (18)	0.0130 (15)	0.0571 (16)	−0.0007 (16)
F4	0.0587 (15)	0.0308 (11)	0.0434 (12)	0.0029 (10)	0.0068 (11)	0.0053 (9)
F5	0.0654 (16)	0.0408 (13)	0.0424 (13)	−0.0176 (11)	0.0036 (12)	−0.0055 (10)

F6	0.0680 (17)	0.105 (2)	0.0836 (19)	0.0132 (16)	0.0631 (16)	0.0188 (16)
P1	0.0247 (4)	0.0178 (3)	0.0151 (3)	−0.0015 (3)	0.0131 (3)	−0.0026 (3)
P2	0.0191 (4)	0.0164 (3)	0.0139 (3)	−0.0011 (3)	0.0079 (3)	−0.0012 (3)
P3	0.0242 (4)	0.0221 (4)	0.0284 (4)	−0.0023 (3)	0.0136 (3)	−0.0016 (3)
Pt1	0.01666 (8)	0.01500 (7)	0.01119 (7)	−0.00172 (6)	0.00838 (6)	−0.00207 (5)
Cl1A	0.129 (3)	0.073 (2)	0.105 (2)	−0.0276 (17)	0.087 (2)	−0.0308 (16)
Cl2A	0.087 (2)	0.0546 (13)	0.0543 (13)	0.0015 (13)	0.0400 (14)	0.0013 (10)
C01A	0.122 (10)	0.081 (7)	0.066 (6)	−0.027 (7)	0.055 (7)	−0.025 (5)
Cl2B	0.0664 (18)	0.0422 (12)	0.0650 (15)	−0.0022 (11)	0.0447 (14)	−0.0095 (10)
C01B	0.048 (5)	0.041 (5)	0.041 (5)	0.007 (4)	0.014 (4)	0.010 (4)

Table A 27: Bond lengths (Å) for [Pt(PNP-*c*Hex)$_2$].

Atoms	Bond length (Å)	Atoms	Bond length (Å)
C1A—N1	1.480 (12)	C16B—H16B	0.95
C1A—C6A	1.50 (2)	C21—C26	1.393 (4)
C1A—C2A	1.533 (10)	C21—C22	1.400 (4)
C1A—H1A	1	C21—P1	1.799 (3)
C2A—C3A	1.529 (7)	C22—C23	1.387 (4)
C2A—H2A1	0.99	C22—H22	0.95
C2A—H2A2	0.99	C23—C24	1.386 (5)
C3A—C4A	1.540 (9)	C23—H23	0.95
C3A—H3A1	0.99	C24—C25	1.386 (4)
C3A—H3A2	0.99	C24—H24	0.95
C4A—C5A	1.508 (12)	C25—C26	1.384 (4)
C4A—H4A1	0.99	C25—H25	0.95
C4A—H4A2	0.99	C26—H26	0.95
C5A—C6A	1.51 (2)	C31—C32	1.386 (4)
C5A—H5A1	0.99	C31—C36	1.398 (4)
C5A—H5A2	0.99	C31—P2	1.804 (3)
C6A—H6A1	0.99	C32—C33	1.389 (4)
C6A—H6A2	0.99	C32—H32	0.95
C1B—C2B	1.46 (2)	C33—C34	1.381 (5)
C1B—N1	1.56 (2)	C33—H33	0.95
C1B—C6B	1.60 (5)	C34—C35	1.382 (4)
C1B—H1B	1	C34—H34	0.95
C2B—C3B	1.528 (11)	C35—C36	1.385 (4)
C2B—H2B1	0.99	C35—H35	0.95
C2B—H2B2	0.99	C36—H36	0.95
C3B—C4B	1.514 (15)	C41—C46	1.385 (4)
C3B—H3B1	0.99	C41—C42	1.396 (4)
C3B—H3B2	0.99	C41—P2	1.794 (3)
C4B—C5B	1.52 (2)	C42—C43	1.379 (4)
C5B—C6B	1.57 (5)	C42—H42	0.95
C5B—H5B1	0.99	C43—C44	1.370 (5)
C5B—H5B2	0.99	C43—H43	0.95
C6B—H6B1	0.99	C44—C45	1.378 (5)
C6B—H6B2	0.99	C44—H44	0.95
C11A—C12A	1.38 (3)	C45—C46	1.382 (5)
C11A—C16A	1.40 (3)	C45—H45	0.95
C11A—P1	1.811 (16)	C46—H46	0.95

C16A—C15A	1.385 (15)	N1—P1	1.701 (3)
C16A—H16A	0.95	N1—P2	1.706 (2)
C15A—C14A	1.384 (15)	F1—P3	1.580 (2)
C15A—H15A	0.95	F2—P3	1.593 (2)
C14A—C13A	1.378 (12)	F3—P3	1.591 (2)
C14A—H14A	0.95	F4—P3	1.598 (2)
C13A—C12A	1.387 (12)	F5—P3	1.590 (2)
C13A—H13A	0.95	F6—P3	1.564 (2)
C12A—H12A	0.95	P1—Pt1	2.2918 (9)
C11B—C16B	1.37 (4)	P2—Pt1	2.2999 (9)
C11B—C12B	1.40 (4)	Pt1—P1^{i}	2.2918 (9)
C11B—P1	1.79 (3)	Pt1—P2^{i}	2.2999 (9)
C12B—C13B	1.383 (15)	Cl1A—C01A	1.747 (11)
C12B—H12B	0.95	Cl2A—C01A	1.765 (11)
C13B—C14B	1.381 (15)	C01A—H01A	0.99
C13B—H13B	0.95	C01A—H01B	0.99
C14B—C15B	1.38 (2)	Cl1B—C01B	1.760 (8)
C14B—H14B	0.95	Cl2B—C01B	1.757 (9)
C15B—C16B	1.39 (2)	C01B—H01C	0.99
C15B—H15B	0.95	C01B—H01D	0.99

Symmetry codes: (i) $-x+1, -y+1, -z+1$.

Table A 28: Bond angles (°) for [Pt(PNP-*c*Hex)$_2$].

Atoms	Bond angle (°)	Atoms	Bond angle (°)
N1—C1A—C6A	116.4 (11)	C22—C21—P1	120.9 (2)
N1—C1A—C2A	109.4 (7)	C23—C22—C21	119.7 (3)
C6A—C1A—C2A	109.6 (11)	C23—C22—H22	120.1
N1—C1A—H1A	107	C21—C22—H22	120.1
C6A—C1A—H1A	107	C24—C23—C22	120.2 (3)
C2A—C1A—H1A	107	C24—C23—H23	119.9
C3A—C2A—C1A	110.4 (6)	C22—C23—H23	119.9
C3A—C2A—H2A1	109.6	C23—C24—C25	120.4 (3)
C1A—C2A—H2A1	109.6	C23—C24—H24	119.8
C3A—C2A—H2A2	109.6	C25—C24—H24	119.8
C1A—C2A—H2A2	109.6	C26—C25—C24	119.7 (3)
H2A1—C2A—H2A2	108.1	C26—C25—H25	120.1
C2A—C3A—C4A	111.9 (5)	C24—C25—H25	120.1
C2A—C3A—H3A1	109.2	C25—C26—C21	120.5 (3)
C4A—C3A—H3A1	109.2	C25—C26—H26	119.8
C2A—C3A—H3A2	109.2	C21—C26—H26	119.8
C4A—C3A—H3A2	109.2	C32—C31—C36	119.4 (3)
H3A1—C3A—H3A2	107.9	C32—C31—P2	120.6 (2)
C5A—C4A—C3A	111.2 (6)	C36—C31—P2	119.4 (2)
C5A—C4A—H4A1	109.4	C31—C32—C33	120.3 (3)
C3A—C4A—H4A1	109.4	C31—C32—H32	119.8
C5A—C4A—H4A2	109.4	C33—C32—H32	119.8
C3A—C4A—H4A2	109.4	C34—C33—C32	119.9 (3)
H4A1—C4A—H4A2	108	C34—C33—H33	120
C4A—C5A—C6A	109.7 (9)	C32—C33—H33	120

C4A—C5A—H5A1	109.7	C33—C34—C35	120.2 (3)
C6A—C5A—H5A1	109.7	C33—C34—H34	119.9
C4A—C5A—H5A2	109.7	C35—C34—H34	119.9
C6A—C5A—H5A2	109.7	C34—C35—C36	120.2 (3)
H5A1—C5A—H5A2	108.2	C34—C35—H35	119.9
C1A—C6A—C5A	114.3 (14)	C36—C35—H35	119.9
C1A—C6A—H6A1	108.7	C35—C36—C31	119.9 (3)
C5A—C6A—H6A1	108.7	C35—C36—H36	120
C1A—C6A—H6A2	108.7	C31—C36—H36	120
C5A—C6A—H6A2	108.7	C46—C41—C42	119.4 (3)
H6A1—C6A—H6A2	107.6	C46—C41—P2	118.3 (2)
C2B—C1B—N1	113.5 (14)	C42—C41—P2	122.2 (2)
C2B—C1B—C6B	116 (2)	C43—C42—C41	120.1 (3)
N1—C1B—C6B	103 (2)	C43—C42—H42	119.9
C2B—C1B—H1B	107.9	C41—C42—H42	119.9
N1—C1B—H1B	107.9	C44—C43—C42	120.0 (3)
C6B—C1B—H1B	107.9	C44—C43—H43	120
C1B—C2B—C3B	109.1 (11)	C42—C43—H43	120
C1B—C2B—H2B1	109.9	C43—C44—C45	120.3 (3)
C3B—C2B—H2B1	109.9	C43—C44—H44	119.8
C1B—C2B—H2B2	109.9	C45—C44—H44	119.8
C3B—C2B—H2B2	109.9	C44—C45—C46	120.3 (3)
H2B1—C2B—H2B2	108.3	C44—C45—H45	119.8
C4B—C3B—C2B	113.4 (8)	C46—C45—H45	119.8
C4B—C3B—H3B1	108.9	C45—C46—C41	119.8 (3)
C2B—C3B—H3B1	108.9	C45—C46—H46	120.1
C4B—C3B—H3B2	108.9	C41—C46—H46	120.1
C2B—C3B—H3B2	108.9	C1A—N1—P1	120.1 (4)
H3B1—C3B—H3B2	107.7	C1B—N1—P1	137.3 (6)
C3B—C4B—C5B	110.2 (9)	C1A—N1—P2	134.0 (4)
C4B—C5B—C6B	115.4 (19)	C1B—N1—P2	119.3 (7)
C4B—C5B—H5B1	108.4	P1—N1—P2	102.58 (12)
C6B—C5B—H5B1	108.4	N1—P1—C11B	110.8 (17)
C4B—C5B—H5B2	108.4	N1—P1—C21	111.32 (13)
C6B—C5B—H5B2	108.4	C11B—P1—C21	102.4 (13)
H5B1—C5B—H5B2	107.5	N1—P1—C11A	110.5 (11)
C5B—C6B—C1B	103 (3)	C21—P1—C11A	106.0 (9)
C5B—C6B—H6B1	111.1	N1—P1—Pt1	93.47 (8)
C1B—C6B—H6B1	111.1	C11B—P1—Pt1	121.4 (10)
C5B—C6B—H6B2	111.1	C21—P1—Pt1	117.31 (10)
C1B—C6B—H6B2	111.1	C11A—P1—Pt1	117.7 (6)
H6B1—C6B—H6B2	109	N1—P2—C41	110.98 (12)
C12A—C11A—C16A	119.5 (11)	N1—P2—C31	110.86 (13)
C12A—C11A—P1	123 (2)	C41—P2—C31	107.74 (14)
C16A—C11A—P1	116.8 (19)	N1—P2—Pt1	93.08 (9)
C15A—C16A—C11A	120.6 (15)	C41—P2—Pt1	117.31 (10)
C15A—C16A—H16A	119.7	C31—P2—Pt1	116.09 (10)
C11A—C16A—H16A	119.7	F6—P3—F1	91.14 (14)
C14A—C15A—C16A	119.1 (13)	F6—P3—F5	90.24 (16)
C14A—C15A—H15A	120.4	F1—P3—F5	90.30 (12)
C16A—C15A—H15A	120.4	F6—P3—F3	179.34 (18)

C13A—C14A—C15A	120.3 (9)	F1—P3—F3	89.15 (14)
C13A—C14A—H14A	119.9	F5—P3—F3	89.16 (16)
C15A—C14A—H14A	119.9	F6—P3—F2	91.09 (16)
C14A—C13A—C12A	120.7 (8)	F1—P3—F2	90.39 (12)
C14A—C13A—H13A	119.7	F5—P3—F2	178.49 (15)
C12A—C13A—H13A	119.7	F3—P3—F2	89.51 (15)
C11A—C12A—C13A	119.7 (12)	F6—P3—F4	90.00 (15)
C11A—C12A—H12A	120.2	F1—P3—F4	178.76 (14)
C13A—C12A—H12A	120.2	F5—P3—F4	90.20 (12)
C16B—C11B—C12B	119.3 (16)	F3—P3—F4	89.72 (15)
C16B—C11B—P1	120 (3)	F2—P3—F4	89.08 (12)
C12B—C11B—P1	121 (3)	$P1^{i}$—Pt1—P1	180.0000 (10)
C13B—C12B—C11B	120.5 (18)	$P1^{i}$—Pt1—$P2^{i}$	70.76 (3)
C13B—C12B—H12B	119.7	P1—Pt1—$P2^{i}$	109.24 (3)
C11B—C12B—H12B	119.7	$P1^{i}$—Pt1—P2	109.24 (3)
C14B—C13B—C12B	119.0 (10)	P1—Pt1—P2	70.76 (3)
C14B—C13B—H13B	120.5	$P2^{i}$—Pt1—P2	180
C12B—C13B—H13B	120.5	Cl1A—C01A—Cl2A	111.5 (5)
C15B—C14B—C13B	120.9 (14)	Cl1A—C01A—H01A	109.3
C15B—C14B—H14B	119.5	Cl2A—C01A—H01A	109.3
C13B—C14B—H14B	119.5	Cl1A—C01A—H01B	109.3
C14B—C15B—C16B	120 (2)	Cl2A—C01A—H01B	109.3
C14B—C15B—H15B	120.1	H01A—C01A—H01B	108
C16B—C15B—H15B	120.1	Cl2B—C01B—Cl1B	110.9 (5)
C11B—C16B—C15B	120 (2)	Cl2B—C01B—H01C	109.5
C11B—C16B—H16B	119.8	Cl1B—C01B—H01C	109.5
C15B—C16B—H16B	119.8	Cl2B—C01B—H01D	109.5
C26—C21—C22	119.5 (3)	Cl1B—C01B—H01D	109.5
C26—C21—P1	119.6 (2)	H01C—C01B—H01D	108.1

Symmetry codes: (i) $-x+1, -y+1, -z+1$.

A8. Crystallographic data for [Pt(PNP-*n*Pent)$_2$]

Table A 29: Fractional atomic coordinates and isotropic or equivalent isotropic displacement parameters (Å^2) for [Pt(PNP-*n*Pent)$_2$].

	x	*y*	*z*	U_{iso}*/U_{eq}	Occ. (<1)
C1	0.1482 (3)	0.56240 (17)	0.77193 (14)	0.0287 (6)	
H1A	0.1064	0.5965	0.7575	0.034*	
H1B	0.0927	0.5402	0.7919	0.034*	
C01	0.8626 (5)	0.75498 (18)	0.64979 (17)	0.0559 (14)	
H01A	0.9186	0.7833	0.6393	0.067*	
H01B	0.79	0.7569	0.621	0.067*	
C2	0.1807 (3)	0.52966 (14)	0.71951 (14)	0.0255 (7)	
H2A	0.2232	0.5541	0.695	0.031*	
H2B	0.2349	0.4992	0.7338	0.031*	
C3	0.0724 (3)	0.50600 (16)	0.68260 (15)	0.0308 (8)	
H3A	0.0323	0.4804	0.707	0.037*	

H3B	0.0986	0.4843	0.6504	0.037*
C4	−0.0175 (3)	0.54921 (16)	0.65640 (14)	0.0289 (9)
H4A	0.0207	0.5737	0.6302	0.035*
H4B	−0.0417	0.5721	0.6883	0.035*
C5	−0.1280 (3)	0.52310 (16)	0.62195 (15)	0.0287 (6)
H5A	−0.1046	0.5004	0.5904	0.043*
H5B	−0.182	0.5522	0.6054	0.043*
H5C	−0.1681	0.5001	0.6481	0.043*
C6	0.7473 (3)	0.65347 (13)	1.03600 (13)	0.0153 (7)
H6A	0.8068	0.6693	1.0132	0.018*
H6B	0.7777	0.6174	1.0514	0.018*
C7	0.7345 (3)	0.69112 (14)	1.08671 (14)	0.0229 (8)
H7A	0.6786	0.6745	1.111	0.027*
H7B	0.7008	0.7267	1.0717	0.027*
C8	0.8540 (3)	0.70150 (14)	1.12475 (14)	0.0210 (7)
H8A	0.9092	0.7181	1.1	0.025*
H8B	0.8418	0.7286	1.1554	0.025*
C9	0.9120 (3)	0.65016 (16)	1.15412 (16)	0.0335 (9)
H9A	0.9334	0.6246	1.1238	0.04*
H9B	0.8547	0.6312	1.1759	0.04*
C10	1.0234 (3)	0.66455 (16)	1.19610 (15)	0.0301 (9)
H10A	1.0794	0.6843	1.1748	0.045*
H10B	1.0604	0.6306	1.2128	0.045*
H10C	1.0018	0.6879	1.2276	0.045*
C11	0.1754 (3)	0.54547 (12)	0.92209 (13)	0.0124 (6)
C12	0.1015 (3)	0.59109 (13)	0.92072 (14)	0.0173 (7)
H12	0.1063	0.6193	0.8926	0.021*
C13	0.0210 (3)	0.59546 (14)	0.96012 (14)	0.0214 (7)
H13	−0.0299	0.6266	0.9591	0.026*
C14	0.0144 (3)	0.55456 (14)	1.00112 (14)	0.0223 (8)
H14	−0.0404	0.5579	1.0285	0.027*
C15	0.0874 (3)	0.50870 (14)	1.00257 (14)	0.0219 (7)
H15	0.0821	0.4807	1.0308	0.026*
C16	0.1678 (3)	0.50367 (14)	0.96310 (14)	0.0181 (8)
H16	0.2174	0.4721	0.9638	0.022*
C21	0.3353 (3)	0.47632 (12)	0.86595 (12)	0.0124 (6)
C22	0.2482 (3)	0.43718 (13)	0.84764 (13)	0.0158 (7)
H22	0.1667	0.4462	0.846	0.019*
C23	0.2824 (3)	0.38498 (13)	0.83188 (14)	0.0201 (7)
H23	0.2238	0.3581	0.8194	0.024*
C24	0.4007 (3)	0.37181 (13)	0.83429 (14)	0.0202 (7)
H24	0.423	0.3359	0.8235	0.024*
C25	0.4881 (3)	0.41069 (13)	0.85241 (14)	0.0198 (7)
H25	0.5695	0.4015	0.854	0.024*
C26	0.4549 (3)	0.46288 (13)	0.86811 (12)	0.0159 (7)
H26	0.5138	0.4896	0.8804	0.019*
C31	0.4393 (3)	0.62230 (14)	0.75582 (14)	0.0138 (7)
C32	0.4829 (3)	0.57081 (13)	0.74347 (13)	0.0179 (7)
H32	0.4564	0.5389	0.7617	0.021*
C33	0.5654 (3)	0.56589 (15)	0.70451 (14)	0.0237 (8)
H33	0.5944	0.5306	0.6957	0.028*

C34	0.6049 (3)	0.61239 (15)	0.67874 (16)	0.0231 (9)
H34	0.661	0.6089	0.652	0.028*
C35	0.5639 (3)	0.66405 (14)	0.69120 (13)	0.0199 (7)
H35	0.5919	0.6957	0.6732	0.024*
C36	0.4817 (3)	0.66947 (13)	0.73026 (13)	0.0162 (6)
H36	0.4543	0.7049	0.7396	0.019*
C41	0.2697 (3)	0.69369 (13)	0.80151 (13)	0.0139 (6)
C42	0.2631 (3)	0.72902 (13)	0.84867 (14)	0.0170 (7)
H42	0.2964	0.7182	0.8869	0.02*
C43	0.2080 (3)	0.77987 (14)	0.83976 (15)	0.0238 (8)
H43	0.2029	0.8037	0.8719	0.029*
C44	0.1608 (3)	0.79582 (14)	0.78425 (15)	0.0245 (8)
H44	0.1262	0.8313	0.7779	0.029*
C45	0.1638 (3)	0.76030 (14)	0.73776 (15)	0.0236 (8)
H45	0.1278	0.7708	0.6999	0.028*
C46	0.2187 (3)	0.70949 (14)	0.74582 (14)	0.0206 (7)
H46	0.2216	0.6855	0.7135	0.025*
C51	0.4639 (3)	0.59396 (14)	1.06229 (14)	0.0128 (7)
C52	0.5255 (3)	0.58111 (13)	1.11684 (13)	0.0175 (7)
H52	0.6068	0.571	1.1202	0.021*
C53	0.4689 (3)	0.58301 (14)	1.16598 (13)	0.0210 (7)
H53	0.5116	0.5756	1.2034	0.025*
C54	0.3483 (3)	0.59587 (13)	1.16053 (15)	0.0215 (7)
H54	0.3083	0.5958	1.1941	0.026*
C55	0.2871 (3)	0.60865 (13)	1.10647 (15)	0.0201 (8)
H55	0.2054	0.6178	1.103	0.024*
C56	0.3451 (3)	0.60810 (12)	1.05696 (14)	0.0164 (7)
H56	0.3034	0.6174	1.0198	0.02*
C61	0.6169 (2)	0.52730 (12)	1.00093 (12)	0.0113 (6)
C62	0.5670 (3)	0.48035 (13)	1.02358 (13)	0.0168 (7)
H62	0.5011	0.4839	1.0446	0.02*
C63	0.6140 (3)	0.42899 (13)	1.01521 (14)	0.0194 (7)
H63	0.58	0.3972	1.0302	0.023*
C64	0.7105 (3)	0.42374 (14)	0.98505 (14)	0.0206 (7)
H64	0.7423	0.3883	0.9793	0.025*
C65	0.7610 (3)	0.46978 (13)	0.96313 (13)	0.0189 (7)
H65	0.8281	0.4659	0.9431	0.023*
C66	0.7136 (3)	0.52137 (13)	0.97039 (13)	0.0159 (7)
H66	0.7472	0.5528	0.9545	0.019*
C71	0.5542 (3)	0.74473 (12)	0.93612 (13)	0.0132 (6)
C72	0.5523 (3)	0.77807 (13)	0.88622 (14)	0.0176 (7)
H72	0.5783	0.7636	0.8519	0.021*
C73	0.5127 (3)	0.83181 (13)	0.88716 (15)	0.0217 (7)
H73	0.5089	0.854	0.8531	0.026*
C74	0.4788 (3)	0.85312 (14)	0.93750 (16)	0.0257 (8)
H74	0.4559	0.8907	0.9388	0.031*
C75	0.4779 (3)	0.81994 (14)	0.98661 (15)	0.0257 (8)
H75	0.4526	0.8346	1.021	0.031*
C76	0.5137 (3)	0.76581 (13)	0.98528 (14)	0.0197 (7)
H76	0.5106	0.7429	1.0184	0.024*
C81	0.7146 (3)	0.67248 (13)	0.88803 (13)	0.0142 (6)

C82	0.7258 (3)	0.63027 (13)	0.84829 (13)	0.0167 (7)		
H82	0.6677	0.602	0.8429	0.02*		
C83	0.8203 (3)	0.62906 (14)	0.81665 (14)	0.0225 (7)		
H83	0.8276	0.6	0.7898	0.027*		
C84	0.9043 (3)	0.67045 (14)	0.82435 (14)	0.0200 (7)		
H84	0.9685	0.6701	0.802	0.024*		
C85	0.8958 (3)	0.71218 (13)	0.86402 (13)	0.0192 (7)		
H85	0.955	0.7399	0.8696	0.023*		
C86	0.8009 (3)	0.71373 (13)	0.89587 (13)	0.0149 (6)		
H86	0.7945	0.7427	0.9229	0.018*		
N1	0.2516 (2)	0.57749 (10)	0.81489 (10)	0.0128 (5)		
N2	0.6347 (2)	0.64435 (10)	0.99603 (10)	0.0132 (5)		
F1	0.1335 (2)	0.71148 (9)	0.96105 (10)	0.0424 (6)		
F2	0.13372 (19)	0.70746 (9)	1.05954 (9)	0.0404 (6)		
F3	−0.02480 (17)	0.74020 (9)	1.00181 (8)	0.0330 (5)		
F4	0.0917 (2)	0.79785 (8)	1.06069 (8)	0.0385 (5)		
F5	0.0903 (2)	0.80160 (8)	0.96277 (8)	0.0345 (5)		
F6	0.24994 (19)	0.76911 (11)	1.02022 (10)	0.0551 (7)		
F7	0.72443 (19)	0.43486 (9)	0.74705 (9)	0.0375 (5)		
F8	0.78582 (17)	0.40997 (8)	0.84068 (8)	0.0255 (4)		
F9	0.91953 (17)	0.42305 (8)	0.77746 (8)	0.0314 (5)		
F10	0.90878 (19)	0.48342 (9)	0.85057 (8)	0.0385 (6)		
F11	0.84607 (19)	0.50836 (8)	0.75712 (9)	0.0349 (5)		
F12	0.71315 (19)	0.49579 (9)	0.82069 (10)	0.0341 (6)		
P1	0.29586 (7)	0.54624 (3)	0.87958 (3)	0.01116 (16)		
P2	0.34891 (7)	0.62997 (4)	0.81388 (3)	0.01159 (16)		
P3	0.53802 (7)	0.59136 (4)	0.99775 (3)	0.01165 (16)		
P4	0.59236 (7)	0.67322 (3)	0.92964 (3)	0.01178 (16)		
P5	0.11328 (8)	0.75458 (4)	1.01089 (4)	0.02094 (19)		
P6	0.81623 (8)	0.45921 (4)	0.79889 (4)	0.02016 (19)		
Pt1	0.441743 (9)	0.610768 (4)	0.906107 (7)	0.01061 (3)		
Cl1	0.82677 (9)	0.76853 (4)	0.71916 (4)	0.0404 (2)		
Cl2	0.92773 (14)	0.68887 (6)	0.64686 (5)	0.0751 (5)		
Cl3	0.30911 (8)	0.36043 (4)	0.97952 (4)	0.0320 (2)		
Cl4A	0.2246 (2)	0.36509 (14)	1.09592 (9)	0.0580 (9)	0.515	(3)
C02A	0.3267 (3)	0.34492 (15)	1.05375 (14)	0.0255 (7)	0.515	(3)
H02A	0.3339	0.3044	1.0574	0.031*	0.515	(3)
H02B	0.4037	0.3606	1.0711	0.031*	0.515	(3)
Cl4B	0.2955 (3)	0.40266 (14)	1.09242 (10)	0.0612 (9)	0.485	(3)
C02B	0.3267 (3)	0.34492 (15)	1.05375 (14)	0.0308 (8)	0.485	(3)
H02C	0.2727	0.3146	1.0612	0.037*	0.485	(3)
H02D	0.4091	0.3328	1.0666	0.037*	0.485	(3)

Table A 30: Atomic displacement parameters (Å^2) for [Pt(PNP-*n*Pent)$_2$].

	U^{11}	U^{22}	U^{33}	U^{12}	U^{13}	U^{23}
C1	0.0226 (13)	0.0425 (18)	0.0194 (12)	0.0050 (12)	−0.0034 (10)	−0.0088 (12)
C01	0.083 (4)	0.041 (3)	0.039 (3)	0.039 (3)	−0.010 (2)	0.001 (2)
C2	0.0335 (18)	0.0216 (18)	0.0222 (17)	0.0036 (14)	0.0069 (14)	0.0032 (14)
C3	0.041 (2)	0.031 (2)	0.0215 (17)	0.0028 (16)	0.0065 (15)	−0.0015 (15)
C4	0.0239 (19)	0.047 (3)	0.0160 (17)	0.0091 (17)	0.0024 (14)	−0.0047 (17)

C5	0.0226 (13)	0.0425 (18)	0.0194 (12)	0.0050 (12)	−0.0034 (10)	−0.0088 (12)
C6	0.0166 (16)	0.0123 (17)	0.0160 (16)	−0.0026 (12)	−0.0009 (13)	0.0025 (13)
C7	0.0225 (18)	0.0202 (19)	0.0250 (18)	0.0007 (14)	−0.0004 (15)	−0.0077 (15)
C8	0.0233 (18)	0.0207 (19)	0.0187 (17)	−0.0071 (14)	0.0020 (14)	−0.0071 (14)
C9	0.036 (2)	0.032 (2)	0.029 (2)	−0.0150 (17)	−0.0076 (17)	0.0064 (17)
C10	0.030 (2)	0.030 (2)	0.027 (2)	−0.0086 (16)	−0.0071 (16)	0.0046 (16)
C11	0.0101 (15)	0.0113 (16)	0.0160 (15)	−0.0021 (12)	0.0021 (12)	−0.0013 (12)
C12	0.0203 (17)	0.0128 (17)	0.0194 (17)	−0.0017 (13)	0.0050 (13)	0.0029 (13)
C13	0.0177 (17)	0.0214 (19)	0.0263 (19)	0.0037 (14)	0.0071 (14)	−0.0001 (15)
C14	0.0195 (18)	0.026 (2)	0.0230 (18)	−0.0019 (14)	0.0086 (14)	−0.0017 (15)
C15	0.0249 (19)	0.0208 (19)	0.0206 (17)	−0.0027 (14)	0.0051 (14)	0.0042 (14)
C16	0.0216 (18)	0.0113 (18)	0.0225 (19)	0.0015 (13)	0.0065 (15)	0.0006 (14)
C21	0.0153 (15)	0.0094 (16)	0.0124 (15)	−0.0020 (12)	0.0015 (12)	0.0025 (12)
C22	0.0170 (16)	0.0139 (17)	0.0170 (16)	−0.0016 (13)	0.0046 (13)	0.0000 (13)
C23	0.0229 (18)	0.0137 (17)	0.0240 (17)	−0.0065 (13)	0.0044 (14)	−0.0036 (14)
C24	0.0291 (19)	0.0087 (16)	0.0236 (18)	0.0034 (13)	0.0063 (14)	−0.0029 (13)
C25	0.0186 (17)	0.0160 (18)	0.0251 (18)	0.0054 (13)	0.0041 (14)	0.0001 (14)
C26	0.0176 (16)	0.0142 (17)	0.0163 (16)	−0.0019 (12)	0.0035 (12)	−0.0013 (13)
C31	0.0136 (16)	0.0159 (18)	0.0120 (16)	−0.0004 (13)	0.0020 (12)	0.0019 (14)
C32	0.0178 (17)	0.0132 (18)	0.0225 (17)	−0.0013 (13)	0.0026 (13)	0.0010 (14)
C33	0.0227 (18)	0.021 (2)	0.0282 (19)	0.0029 (14)	0.0056 (15)	−0.0078 (15)
C34	0.022 (2)	0.032 (2)	0.0168 (19)	−0.0028 (15)	0.0097 (16)	−0.0019 (16)
C35	0.0210 (17)	0.0212 (19)	0.0178 (16)	−0.0026 (14)	0.0034 (13)	0.0030 (14)
C36	0.0185 (16)	0.0130 (17)	0.0171 (16)	0.0027 (12)	0.0026 (13)	0.0009 (13)
C41	0.0145 (16)	0.0100 (16)	0.0179 (16)	0.0015 (12)	0.0049 (12)	0.0002 (13)
C42	0.0159 (16)	0.0156 (17)	0.0192 (16)	0.0038 (13)	0.0021 (13)	0.0019 (13)
C43	0.0237 (19)	0.020 (2)	0.030 (2)	0.0013 (14)	0.0115 (15)	−0.0041 (16)
C44	0.0227 (18)	0.0142 (18)	0.039 (2)	0.0065 (14)	0.0132 (16)	0.0079 (16)
C45	0.0247 (19)	0.022 (2)	0.0245 (18)	0.0082 (14)	0.0063 (14)	0.0113 (15)
C46	0.0222 (18)	0.0205 (19)	0.0191 (17)	0.0032 (14)	0.0021 (14)	0.0008 (14)
C51	0.0165 (17)	0.0075 (16)	0.0142 (16)	−0.0015 (14)	0.0009 (13)	−0.0018 (14)
C52	0.0168 (16)	0.0193 (18)	0.0165 (16)	0.0005 (13)	0.0030 (13)	0.0021 (14)
C53	0.0293 (19)	0.0210 (19)	0.0129 (16)	−0.0001 (15)	0.0033 (14)	0.0010 (14)
C54	0.031 (2)	0.0150 (18)	0.0218 (18)	−0.0013 (14)	0.0158 (15)	−0.0012 (14)
C55	0.0204 (19)	0.019 (2)	0.022 (2)	0.0018 (14)	0.0081 (16)	0.0014 (15)
C56	0.0178 (16)	0.0128 (17)	0.0184 (16)	−0.0006 (13)	0.0017 (13)	−0.0007 (13)
C61	0.0085 (14)	0.0116 (16)	0.0126 (15)	−0.0005 (11)	−0.0028 (11)	0.0004 (12)
C62	0.0182 (16)	0.0150 (17)	0.0174 (16)	0.0001 (13)	0.0030 (13)	0.0017 (13)
C63	0.0212 (17)	0.0093 (16)	0.0263 (18)	−0.0027 (13)	−0.0019 (14)	0.0015 (14)
C64	0.0247 (18)	0.0141 (18)	0.0215 (17)	0.0031 (14)	−0.0028 (14)	−0.0048 (14)
C65	0.0151 (16)	0.0218 (19)	0.0197 (17)	0.0032 (13)	0.0016 (13)	−0.0033 (14)
C66	0.0166 (16)	0.0131 (17)	0.0178 (16)	−0.0017 (12)	0.0013 (13)	0.0036 (13)
C71	0.0098 (15)	0.0085 (16)	0.0213 (17)	−0.0018 (11)	0.0025 (13)	−0.0012 (13)
C72	0.0159 (16)	0.0160 (18)	0.0214 (17)	0.0020 (13)	0.0043 (13)	0.0001 (14)
C73	0.0171 (17)	0.0118 (17)	0.036 (2)	0.0005 (13)	0.0035 (14)	0.0096 (15)
C74	0.0180 (17)	0.0115 (18)	0.047 (2)	0.0050 (13)	0.0043 (16)	−0.0001 (16)
C75	0.0254 (19)	0.020 (2)	0.032 (2)	0.0046 (14)	0.0049 (15)	−0.0057 (16)
C76	0.0208 (18)	0.0157 (18)	0.0228 (18)	0.0010 (13)	0.0033 (14)	0.0007 (14)
C81	0.0172 (16)	0.0126 (16)	0.0128 (15)	0.0037 (12)	0.0016 (12)	0.0057 (13)
C82	0.0206 (17)	0.0123 (16)	0.0163 (16)	−0.0002 (13)	0.0000 (13)	−0.0009 (13)
C83	0.0265 (19)	0.0193 (18)	0.0219 (18)	0.0061 (14)	0.0043 (15)	−0.0014 (14)

C84	0.0128 (15)	0.0237 (19)	0.0251 (18)	0.0083 (14)	0.0086 (13)	0.0070 (15)
C85	0.0169 (16)	0.0152 (18)	0.0254 (18)	−0.0008 (13)	0.0018 (13)	0.0081 (14)
C86	0.0161 (16)	0.0113 (17)	0.0172 (16)	0.0009 (12)	0.0012 (13)	0.0000 (13)
N1	0.0164 (14)	0.0105 (14)	0.0117 (13)	−0.0018 (10)	0.0029 (10)	0.0025 (11)
N2	0.0155 (14)	0.0094 (14)	0.0144 (13)	−0.0031 (10)	0.0008 (11)	0.0002 (11)
F1	0.0632 (16)	0.0221 (13)	0.0480 (14)	0.0013 (11)	0.0298 (12)	−0.0063 (11)
F2	0.0393 (14)	0.0381 (14)	0.0445 (14)	0.0116 (10)	0.0078 (11)	0.0248 (11)
F3	0.0222 (11)	0.0453 (14)	0.0309 (11)	−0.0060 (9)	0.0019 (9)	−0.0027 (10)
F4	0.0682 (16)	0.0261 (13)	0.0226 (11)	−0.0068 (11)	0.0115 (10)	−0.0082 (9)
F5	0.0593 (15)	0.0232 (12)	0.0223 (11)	−0.0004 (10)	0.0107 (10)	0.0041 (9)
F6	0.0236 (13)	0.089 (2)	0.0527 (15)	−0.0191 (12)	0.0053 (11)	0.0092 (14)
F7	0.0388 (13)	0.0365 (14)	0.0330 (12)	−0.0031 (10)	−0.0100 (10)	−0.0004 (10)
F8	0.0283 (11)	0.0167 (10)	0.0319 (11)	0.0016 (8)	0.0058 (9)	0.0050 (9)
F9	0.0334 (12)	0.0306 (12)	0.0323 (12)	0.0132 (9)	0.0122 (9)	0.0028 (9)
F10	0.0381 (13)	0.0467 (15)	0.0308 (12)	−0.0201 (11)	0.0048 (10)	−0.0113 (11)
F11	0.0504 (14)	0.0223 (12)	0.0369 (12)	0.0045 (10)	0.0239 (10)	0.0066 (10)
F12	0.0343 (13)	0.0212 (12)	0.0514 (15)	0.0085 (9)	0.0224 (11)	0.0054 (11)
P1	0.0111 (4)	0.0094 (4)	0.0131 (4)	−0.0002 (3)	0.0021 (3)	0.0003 (3)
P2	0.0131 (4)	0.0091 (4)	0.0128 (4)	−0.0005 (3)	0.0024 (3)	0.0003 (3)
P3	0.0139 (4)	0.0082 (4)	0.0131 (4)	0.0003 (3)	0.0030 (3)	0.0008 (3)
P4	0.0139 (4)	0.0084 (4)	0.0130 (4)	−0.0007 (3)	0.0016 (3)	0.0009 (3)
P5	0.0224 (5)	0.0167 (5)	0.0244 (5)	−0.0013 (3)	0.0057 (4)	0.0022 (4)
P6	0.0210 (5)	0.0155 (5)	0.0243 (5)	0.0015 (3)	0.0045 (4)	−0.0012 (4)
Pt1	0.01167 (5)	0.00794 (5)	0.01223 (5)	−0.00055 (6)	0.00167 (3)	0.00060 (6)
Cl1	0.0451 (6)	0.0342 (6)	0.0393 (5)	0.0035 (5)	−0.0036 (5)	0.0046 (5)
Cl2	0.1083 (12)	0.0499 (8)	0.0559 (8)	0.0418 (8)	−0.0303 (7)	−0.0227 (6)
Cl3	0.0380 (5)	0.0263 (5)	0.0310 (5)	0.0089 (4)	0.0017 (4)	0.0022 (4)
Cl4A	0.0499 (15)	0.098 (2)	0.0262 (11)	0.0341 (15)	0.0077 (10)	−0.0048 (12)
C02A	0.0335 (18)	0.0216 (18)	0.0222 (17)	0.0036 (14)	0.0069 (14)	0.0032 (14)
Cl4B	0.072 (2)	0.081 (2)	0.0297 (12)	0.0381 (17)	0.0039 (12)	−0.0141 (13)
C02B	0.041 (2)	0.031 (2)	0.0215 (17)	0.0028 (16)	0.0065 (15)	−0.0015 (15)

Table A 31: Bond lengths (Å) for [Pt(PNP-*n*Pent)$_2$].

Atoms	Bond length (Å)	Atoms	Bond length (Å)
C1—N1	1.481 (4)	C43—H43	0.95
C1—C2	1.535 (5)	C44—C45	1.381 (5)
C1—H1A	0.99	C44—H44	0.95
C1—H1B	0.99	C45—C46	1.385 (4)
C01—Cl1	1.737 (4)	C45—H45	0.95
C01—Cl2	1.774 (4)	C46—H46	0.95
C01—H01A	0.99	C51—C56	1.386 (4)
C01—H01B	0.99	C51—C52	1.394 (4)
C2—C3	1.516 (5)	C51—P3	1.810 (3)
C2—H2A	0.99	C52—C53	1.380 (4)
C2—H2B	0.99	C52—H52	0.95
C3—C4	1.533 (5)	C53—C54	1.397 (5)
C3—H3A	0.99	C53—H53	0.95
C3—H3B	0.99	C54—C55	1.382 (5)
C4—C5	1.534 (5)	C54—H54	0.95
C4—H4A	0.99	C55—C56	1.395 (5)

C4—H4B	0.99		C55—H55	0.95	
C5—H5A	0.98		C56—H56	0.95	
C5—H5B	0.98		C61—C66	1.393	(4)
C5—H5C	0.98		C61—C62	1.405	(4)
C6—N2	1.493	(4)	C61—P3	1.793	(3)
C6—C7	1.508	(4)	C62—C63	1.381	(4)
C6—H6A	0.99		C62—H62	0.95	
C6—H6B	0.99		C63—C64	1.383	(5)
C7—C8	1.539	(4)	C63—H63	0.95	
C7—H7A	0.99		C64—C65	1.384	(4)
C7—H7B	0.99		C64—H64	0.95	
C8—C9	1.527	(5)	C65—C66	1.383	(4)
C8—H8A	0.99		C65—H65	0.95	
C8—H8B	0.99		C66—H66	0.95	
C9—C10	1.531	(5)	C71—C76	1.380	(4)
C9—H9A	0.99		C71—C72	1.406	(4)
C9—H9B	0.99		C71—P4	1.801	(3)
C10—H10A	0.98		C72—C73	1.382	(4)
C10—H10B	0.98		C72—H72	0.95	
C10—H10C	0.98		C73—C74	1.375	(5)
C11—C12	1.389	(4)	C73—H73	0.95	
C11—C16	1.399	(4)	C74—C75	1.393	(5)
C11—P1	1.791	(3)	C74—H74	0.95	
C12—C13	1.379	(4)	C75—C76	1.378	(4)
C12—H12	0.95		C75—H75	0.95	
C13—C14	1.381	(4)	C76—H76	0.95	
C13—H13	0.95		C81—C82	1.393	(4)
C14—C15	1.387	(5)	C81—C86	1.397	(4)
C14—H14	0.95		C81—P4	1.794	(3)
C15—C16	1.381	(4)	C82—C83	1.379	(4)
C15—H15	0.95		C82—H82	0.95	
C16—H16	0.95		C83—C84	1.382	(5)
C21—C26	1.395	(4)	C83—H83	0.95	
C21—C22	1.397	(4)	C84—C85	1.378	(4)
C21—P1	1.795	(3)	C84—H84	0.95	
C22—C23	1.389	(4)	C85—C86	1.387	(4)
C22—H22	0.95		C85—H85	0.95	
C23—C24	1.378	(5)	C86—H86	0.95	
C23—H23	0.95		N1—P2	1.691	(3)
C24—C25	1.394	(5)	N1—P1	1.692	(3)
C24—H24	0.95		N2—P4	1.697	(3)
C25—C26	1.385	(4)	N2—P3	1.697	(3)
C25—H25	0.95		F1—P5	1.595	(2)
C26—H26	0.95		F2—P5	1.599	(2)
C31—C32	1.389	(4)	F3—P5	1.597	(2)
C31—C36	1.403	(4)	F4—P5	1.601	(2)
C31—P2	1.806	(3)	F5—P5	1.591	(2)
C32—C33	1.390	(4)	F6—P5	1.582	(2)
C32—H32	0.95		F7—P6	1.595	(2)
C33—C34	1.380	(5)	F8—P6	1.603	(2)
C33—H33	0.95		F9—P6	1.598	(2)

C34—C35	1.382 (5)	F10—P6	1.596 (2)
C34—H34	0.95	F11—P6	1.599 (2)
C35—C36	1.391 (4)	F12—P6	1.606 (2)
C35—H35	0.95	P1—Pt1	2.3063 (8)
C36—H36	0.95	P2—Pt1	2.2965 (8)
C41—C46	1.393 (4)	P3—Pt1	2.2994 (8)
C41—C42	1.397 (4)	P4—Pt1	2.2995 (8)
C41—P2	1.795 (3)	Cl3—C02A	1.741 (3)
C42—C43	1.388 (4)	Cl4A—C02A	1.687 (4)
C42—H42	0.95	C02A—H02A	0.99
C43—C44	1.378 (5)	C02A—H02B	0.99

Table A 32: Bond angles (°) for [Pt(PNP-*n*Pent)$_2$].

Atoms	Bond angle (°)	Atoms	Bond angle (°)
N1—C1—C2	113.8 (3)	C53—C52—C51	120.1 (3)
N1—C1—H1A	108.8	C53—C52—H52	119.9
C2—C1—H1A	108.8	C51—C52—H52	119.9
N1—C1—H1B	108.8	C52—C53—C54	119.7 (3)
C2—C1—H1B	108.8	C52—C53—H53	120.2
H1A—C1—H1B	107.7	C54—C53—H53	120.2
Cl1—C01—Cl2	111.0 (2)	C55—C54—C53	120.2 (3)
Cl1—C01—H01A	109.4	C55—C54—H54	119.9
Cl2—C01—H01A	109.4	C53—C54—H54	119.9
Cl1—C01—H01B	109.4	C54—C55—C56	120.1 (3)
Cl2—C01—H01B	109.4	C54—C55—H55	119.9
H01A—C01—H01B	108	C56—C55—H55	119.9
C3—C2—C1	112.1 (3)	C51—C56—C55	119.5 (3)
C3—C2—H2A	109.2	C51—C56—H56	120.2
C1—C2—H2A	109.2	C55—C56—H56	120.2
C3—C2—H2B	109.2	C66—C61—C62	119.4 (3)
C1—C2—H2B	109.2	C66—C61—P3	119.6 (2)
H2A—C2—H2B	107.9	C62—C61—P3	119.6 (2)
C2—C3—C4	114.4 (3)	C63—C62—C61	119.8 (3)
C2—C3—H3A	108.7	C63—C62—H62	120.1
C4—C3—H3A	108.7	C61—C62—H62	120.1
C2—C3—H3B	108.7	C62—C63—C64	120.2 (3)
C4—C3—H3B	108.7	C62—C63—H63	119.9
H3A—C3—H3B	107.6	C64—C63—H63	119.9
C3—C4—C5	112.4 (3)	C63—C64—C65	120.5 (3)
C3—C4—H4A	109.1	C63—C64—H64	119.8
C5—C4—H4A	109.1	C65—C64—H64	119.8
C3—C4—H4B	109.1	C66—C65—C64	120.0 (3)
C5—C4—H4B	109.1	C66—C65—H65	120
H4A—C4—H4B	107.9	C64—C65—H65	120
C4—C5—H5A	109.5	C65—C66—C61	120.2 (3)
C4—C5—H5B	109.5	C65—C66—H66	119.9
H5A—C5—H5B	109.5	C61—C66—H66	119.9
C4—C5—H5C	109.5	C76—C71—C72	119.4 (3)
H5A—C5—H5C	109.5	C76—C71—P4	122.5 (2)
H5B—C5—H5C	109.5	C72—C71—P4	117.7 (2)

N2—C6—C7	114.0 (3)	C73—C72—C71	120.0 (3)
N2—C6—H6A	108.8	C73—C72—H72	120
C7—C6—H6A	108.8	C71—C72—H72	120
N2—C6—H6B	108.8	C74—C73—C72	119.9 (3)
C7—C6—H6B	108.8	C74—C73—H73	120.1
H6A—C6—H6B	107.7	C72—C73—H73	120.1
C6—C7—C8	111.9 (3)	C73—C74—C75	120.3 (3)
C6—C7—H7A	109.2	C73—C74—H74	119.8
C8—C7—H7A	109.2	C75—C74—H74	119.8
C6—C7—H7B	109.2	C76—C75—C74	120.0 (3)
C8—C7—H7B	109.2	C76—C75—H75	120
H7A—C7—H7B	107.9	C74—C75—H75	120
C9—C8—C7	114.7 (3)	C75—C76—C71	120.3 (3)
C9—C8—H8A	108.6	C75—C76—H76	119.8
C7—C8—H8A	108.6	C71—C76—H76	119.8
C9—C8—H8B	108.6	C82—C81—C86	119.2 (3)
C7—C8—H8B	108.6	C82—C81—P4	120.4 (2)
H8A—C8—H8B	107.6	C86—C81—P4	120.4 (2)
C8—C9—C10	111.6 (3)	C83—C82—C81	120.8 (3)
C8—C9—H9A	109.3	C83—C82—H82	119.6
C10—C9—H9A	109.3	C81—C82—H82	119.6
C8—C9—H9B	109.3	C82—C83—C84	119.4 (3)
C10—C9—H9B	109.3	C82—C83—H83	120.3
H9A—C9—H9B	108	C84—C83—H83	120.3
C9—C10—H10A	109.5	C85—C84—C83	120.8 (3)
C9—C10—H10B	109.5	C85—C84—H84	119.6
H10A—C10—H10B	109.5	C83—C84—H84	119.6
C9—C10—H10C	109.5	C84—C85—C86	120.1 (3)
H10A—C10—H10C	109.5	C84—C85—H85	120
H10B—C10—H10C	109.5	C86—C85—H85	120
C12—C11—C16	120.1 (3)	C85—C86—C81	119.7 (3)
C12—C11—P1	119.0 (2)	C85—C86—H86	120.1
C16—C11—P1	120.0 (2)	C81—C86—H86	120.1
C13—C12—C11	120.0 (3)	C1—N1—P2	129.9 (2)
C13—C12—H12	120	C1—N1—P1	126.7 (2)
C11—C12—H12	120	P2—N1—P1	103.40 (13)
C12—C13—C14	119.9 (3)	C6—N2—P4	127.9 (2)
C12—C13—H13	120	C6—N2—P3	127.2 (2)
C14—C13—H13	120	P4—N2—P3	103.15 (13)
C13—C14—C15	120.4 (3)	N1—P1—C11	109.23 (13)
C13—C14—H14	119.8	N1—P1—C21	108.74 (13)
C15—C14—H14	119.8	C11—P1—C21	108.33 (14)
C16—C15—C14	120.2 (3)	N1—P1—Pt1	92.81 (9)
C16—C15—H15	119.9	C11—P1—Pt1	116.03 (10)
C14—C15—H15	119.9	C21—P1—Pt1	120.08 (10)
C15—C16—C11	119.3 (3)	N1—P2—C41	109.61 (14)
C15—C16—H16	120.3	N1—P2—C31	111.84 (15)
C11—C16—H16	120.3	C41—P2—C31	107.14 (15)
C26—C21—C22	120.1 (3)	N1—P2—Pt1	93.19 (9)
C26—C21—P1	118.8 (2)	C41—P2—Pt1	118.82 (11)
C22—C21—P1	120.8 (2)	C31—P2—Pt1	115.52 (11)

C23—C22—C21	119.2 (3)	N2—P3—C61	109.63 (14)
C23—C22—H22	120.4	N2—P3—C51	111.60 (14)
C21—C22—H22	120.4	C61—P3—C51	106.41 (15)
C24—C23—C22	120.5 (3)	N2—P3—Pt1	93.10 (9)
C24—C23—H23	119.7	C61—P3—Pt1	112.97 (10)
C22—C23—H23	119.7	C51—P3—Pt1	122.28 (11)
C23—C24—C25	120.6 (3)	N2—P4—C81	109.44 (13)
C23—C24—H24	119.7	N2—P4—C71	111.45 (13)
C25—C24—H24	119.7	C81—P4—C71	105.50 (14)
C26—C25—C24	119.3 (3)	N2—P4—Pt1	93.11 (9)
C26—C25—H25	120.3	C81—P4—Pt1	118.32 (11)
C24—C25—H25	120.3	C71—P4—Pt1	118.34 (10)
C25—C26—C21	120.3 (3)	F6—P5—F5	90.13 (13)
C25—C26—H26	119.9	F6—P5—F1	90.59 (14)
C21—C26—H26	119.9	F5—P5—F1	89.57 (12)
C32—C31—C36	119.7 (3)	F6—P5—F3	179.62 (16)
C32—C31—P2	120.0 (3)	F5—P5—F3	89.88 (12)
C36—C31—P2	119.4 (3)	F1—P5—F3	89.79 (12)
C31—C32—C33	120.1 (3)	F6—P5—F2	90.89 (13)
C31—C32—H32	120	F5—P5—F2	178.86 (13)
C33—C32—H32	120	F1—P5—F2	90.94 (12)
C34—C33—C32	119.8 (3)	F3—P5—F2	89.10 (12)
C34—C33—H33	120.1	F6—P5—F4	89.92 (14)
C32—C33—H33	120.1	F5—P5—F4	90.26 (11)
C33—C34—C35	121.0 (3)	F1—P5—F4	179.46 (15)
C33—C34—H34	119.5	F3—P5—F4	89.70 (12)
C35—C34—H34	119.5	F2—P5—F4	89.22 (12)
C34—C35—C36	119.8 (3)	F7—P6—F10	179.64 (15)
C34—C35—H35	120.1	F7—P6—F9	89.97 (12)
C36—C35—H35	120.1	F10—P6—F9	89.67 (12)
C35—C36—C31	119.7 (3)	F7—P6—F11	89.68 (12)
C35—C36—H36	120.2	F10—P6—F11	90.24 (12)
C31—C36—H36	120.2	F9—P6—F11	89.93 (11)
C46—C41—C42	119.5 (3)	F7—P6—F8	90.17 (12)
C46—C41—P2	121.6 (2)	F10—P6—F8	89.90 (11)
C42—C41—P2	118.9 (2)	F9—P6—F8	90.23 (11)
C43—C42—C41	120.1 (3)	F11—P6—F8	179.79 (14)
C43—C42—H42	120	F7—P6—F12	90.42 (13)
C41—C42—H42	120	F10—P6—F12	89.94 (12)
C44—C43—C42	120.0 (3)	F9—P6—F12	179.60 (14)
C44—C43—H43	120	F11—P6—F12	89.97 (11)
C42—C43—H43	120	F8—P6—F12	89.87 (11)
C43—C44—C45	120.1 (3)	P2—Pt1—P3	178.92 (3)
C43—C44—H44	120	P2—Pt1—P4	108.78 (3)
C45—C44—H44	120	P3—Pt1—P4	70.64 (3)
C44—C45—C46	120.6 (3)	P2—Pt1—P1	70.45 (3)
C44—C45—H45	119.7	P3—Pt1—P1	110.08 (3)
C46—C45—H45	119.7	P4—Pt1—P1	177.37 (3)
C45—C46—C41	119.7 (3)	Cl4A—C02A—Cl3	120.6 (2)
C45—C46—H46	120.2	Cl4A—C02A—H02A	107.2
C41—C46—H46	120.2	Cl3—C02A—H02A	107.2

C56—C51—C52	120.3	(3)	Cl4A—C02A—H02B	107.2
C56—C51—P3	119.5	(2)	Cl3—C02A—H02B	107.2
C52—C51—P3	120.2	(2)	H02A—C02A—H02B	106.8

APPENDIX B

APPENDIX B

B1. DFT calculation details

The molecular structures were optimized at the density functional theory (DFT) level using Becke's three-parameter hybrid functional with the Lee-Yang-Parr correlation functional (B3LYP). The LANL2DZ pseudopotential basis set was employed for the Pt and Pd atoms; the 6-31++G(d,p) basis set was employed for C, H, N, P and Cl atoms. All calculations were carried out using the Gaussian 03 software suite.

Table B 1: Free Energies for the DFT optimised PNP-ligands and Pt(II)/Pd(II) coordinated compounds.

Compound	Gibbs Free Energy (Hartree)
PNP-Ethyl	-1743.35807
$[PtCl_2$(PNP-Ethyl)]	-1223.11686
$[PtCl_2$(PNP-*n*Prop)]	-1262.44063
PNP-*n*Pent	-1861.30483
PNP-*c*Prop	-1781.42613
$[Pt$(PNP-*c*Prop$)_2]$	-2341.68126
$[Pd$(PNP-*c*Prop$)_2]$	-2349.24309
PNP-*c*But	-1151.27430
$[Pd$(PNP-*c*But$)_2]$	-2427.87575
PNP-*c*Pent	-1860.09176
$[Pt$(PNP-*c*Pent$)_2]$	-2498.97797
$[Pd$(PNP-*c*Pent$)_2]$	-2506.5397
PNP-*c*Hex	-1899.41774
$[Pt$(PNP-*c*Hex$)_2]$	-1378.58064
PNP-Dimprop	-1861.30152
$[PtCl_2$(PNP-Dimprop)]	-1340.47340
$[PdCl_2$(PNP-Dimprop)]	-1348.63708

B2. Cartesian coordinates for PNP-Ethyl

N	0.05160000	-0.25100000	0.91020000
P	-1.68370000	-0.20970000	1.17630000
P	0.71550000	0.01800000	-0.68950000
C	0.85850000	0.05990000	2.12430000
C	-2.33120000	-1.62930000	0.18720000
C	-3.71630000	-1.69790000	-0.05460000
C	-4.28150000	-2.81240000	-0.67500000
C	-3.47480000	-3.88810000	-1.06050000
C	-2.10150000	-3.83710000	-0.81480000
C	-1.53550000	-2.72020000	-0.19220000
C	-2.33160000	1.24770000	0.21800000
C	-2.59930000	1.25770000	-1.16230000
C	-3.08740000	2.40920000	-1.78390000
C	-3.31380000	3.57140000	-1.03820000
C	-3.05800000	3.57440000	0.33500000
C	-2.57950000	2.41710000	0.95680000
C	2.11300000	-1.19550000	-0.80570000
C	2.94170000	-1.12490000	-1.94160000
C	3.94480000	-2.06940000	-2.15950000
C	4.13520000	-3.11640000	-1.25090000
C	3.31250000	-3.20610000	-0.12720000
C	2.30940000	-2.25510000	0.09140000
C	1.65110000	1.62430000	-0.53510000
C	2.99340000	1.74200000	-0.13620000
C	3.60980000	2.99340000	-0.05670000
C	2.89450000	4.15150000	-0.37380000
C	1.56080000	4.04980000	-0.77770000
C	0.94840000	2.79710000	-0.86420000
H	0.65050000	1.08450000	2.46590000
H	-4.36020000	-0.87270000	0.23870000
H	-5.35230000	-2.84000000	-0.85740000
H	-3.91390000	-4.75570000	-1.54450000
H	-1.46320000	-4.66570000	-1.10920000
H	-0.46840000	-2.70010000	-0.00550000
H	-2.42220000	0.36500000	-1.75240000
H	-3.28910000	2.39980000	-2.85160000
H	-3.69450000	4.46530000	-1.52450000
H	-3.24030000	4.46920000	0.92350000
H	-2.40170000	2.41860000	2.02930000
H	2.80340000	-0.32270000	-2.66280000
H	4.57430000	-1.99130000	-3.04170000
H	4.91300000	-3.85500000	-1.42190000
H	3.44710000	-4.01660000	0.58410000
H	1.67460000	-2.34330000	0.96570000
H	3.56850000	0.85360000	0.10600000
H	4.64900000	3.06220000	0.25370000
H	3.37500000	5.12400000	-0.31270000
H	0.99790000	4.94270000	-1.03480000

H	-0.08470000	2.72970000	-1.19210000
C	0.66260000	-0.91650000	3.29120000
C	1.54970000	-0.55030000	4.48790000
H	-0.38860000	-0.91920000	3.59770000
H	1.32180000	0.45590000	4.85880000
H	2.61330000	-0.57290000	4.22180000
H	1.39930000	-1.25030000	5.31620000
H	0.89160000	-1.93590000	2.95680000
H	1.91170000	0.04610000	1.83090000

B3. Cartesian coordinates of PNP-*n*Pent

N	-0.00600000	-0.21270000	0.63040000
P	-0.23810000	0.23230000	-1.04770000
P	1.61180000	-0.47230000	1.26540000
C	-1.00630000	0.17730000	1.66710000
C	-1.71280000	-0.75430000	-1.58590000
C	-2.28330000	-1.79410000	-0.83850000
C	-3.31740000	-2.57570000	-1.36600000
C	-3.79810000	-2.33160000	-2.65330000
C	-3.23240000	-1.30240000	-3.41410000
C	-2.19740000	-0.52900000	-2.88840000
C	-0.96610000	1.94750000	-0.96480000
C	-0.05620000	3.02000000	-0.96330000
C	-0.50450000	4.34170000	-0.90630000
C	-1.87410000	4.61650000	-0.86540000
C	-2.79020000	3.56130000	-0.87870000
C	-2.34000000	2.23920000	-0.92660000
C	2.67830000	0.88660000	0.57380000
C	3.23740000	0.90460000	-0.71650000
C	4.02750000	1.97750000	-1.13440000
C	4.27220000	3.05190000	-0.27190000
C	3.72910000	3.04470000	1.01490000
C	2.94570000	1.96510000	1.43430000
C	2.23330000	-1.94690000	0.34220000
C	1.37930000	-2.88010000	-0.26330000
C	1.88680000	-4.05490000	-0.82720000
C	3.25610000	-4.32280000	-0.78710000
C	4.11720000	-3.40670000	-0.17360000
C	3.61060000	-2.23460000	0.38840000
H	-1.94450000	0.38540000	1.14840000
H	-1.91590000	-2.00070000	0.16040000
H	-3.74500000	-3.37490000	-0.76660000
H	-4.60050000	-2.93790000	-3.06350000
H	-3.59270000	-1.10650000	-4.42030000
H	-1.76190000	0.25910000	-3.49840000
H	1.01030000	2.81960000	-1.00670000
H	0.21620000	5.15470000	-0.90380000
H	-2.22510000	5.64400000	-0.82960000

H	-3.85730000	3.76520000	-0.85160000
H	-3.06680000	1.43280000	-0.94380000
H	3.05180000	0.08020000	-1.39650000
H	4.45120000	1.97560000	-2.13500000
H	4.88880000	3.88420000	-0.59970000
H	3.92250000	3.86970000	1.69490000
H	2.54140000	1.95600000	2.44350000
H	0.31330000	-2.68990000	-0.29960000
H	1.20660000	-4.75800000	-1.30020000
H	3.65000000	-5.23510000	-1.22570000
H	5.18490000	-3.60420000	-0.13260000
H	4.29580000	-1.53600000	0.86160000
C	-1.24060000	-0.88640000	2.74890000
C	-2.13630000	-0.39280000	3.90100000
H	-1.66810000	-1.78760000	2.29300000
H	-1.65220000	0.47280000	4.37450000
H	-2.16970000	-1.17760000	4.66920000
H	-0.27470000	-1.18540000	3.17010000
H	-0.70540000	1.12210000	2.14370000
C	-3.58070000	-0.00870000	3.52920000
H	-3.57540000	0.81210000	2.80020000
H	-4.06660000	0.39490000	4.42710000
C	-4.42530000	-1.16900000	2.98670000
H	-4.44810000	-2.00500000	3.69650000
H	-4.03670000	-1.55050000	2.03650000
H	-5.45980000	-0.85380000	2.81150000

B4. Cartesian coordinates of PNP-cProp

C	-0.81002500	0.05628800	2.25688500
H	-1.04962900	1.10701500	2.41267800
C	-0.55267900	-0.73968900	3.51242800
H	-0.55634400	-0.20214400	4.45622800
H	0.17707900	-1.54081400	3.46212500
C	-1.84670400	-0.92569300	2.76229300
H	-1.96863500	-1.84674700	2.20263600
H	-2.76697500	-0.52793900	3.18028800
C	-1.22625800	1.92276200	-0.45327100
C	-0.50753600	2.83710100	0.33348400
H	0.27608800	2.48079900	0.99400200
C	-0.77585800	4.20730800	0.26843700
H	-0.20874400	4.89401500	0.89090400
C	-1.76165700	4.69298800	-0.59347400
H	-1.97015100	5.75779200	-0.64416200
C	-2.47277600	3.79606100	-1.39613600
H	-3.23788300	4.16066600	-2.07618700
C	-2.20531200	2.42736200	-1.32898500
H	-2.76844200	1.74813000	-1.96295100
C	-2.41195500	-0.69792000	-0.54096500

C	-3.56229700	-0.20892600	0.10061100
H	-3.51543200	0.72037100	0.65902400
C	-4.77135400	-0.90271900	0.02428500
H	-5.65065300	-0.51039600	0.52811200
C	-4.85289900	-2.09848200	-0.69717600
H	-5.79527000	-2.63576500	-0.75689600
C	-3.72028600	-2.59264900	-1.34792800
H	-3.77739700	-3.51393500	-1.92099500
C	-2.51212400	-1.89264200	-1.27384200
H	-1.63714400	-2.27380900	-1.79389900
C	2.56232100	0.77295900	0.27251900
C	3.25318700	1.71628300	1.05260500
H	3.23993300	1.62326500	2.13597300
C	3.96160500	2.76435200	0.45672600
H	4.49006300	3.48283000	1.07718900
C	3.99370300	2.87855900	-0.93455000
H	4.54329200	3.69032800	-1.40289700
C	3.32018200	1.94046300	-1.72424400
H	3.34423000	2.02411700	-2.80729000
C	2.61291200	0.89510900	-1.12749800
H	2.09508900	0.17435200	-1.75131400
C	1.90891000	-2.03760200	0.14921300
C	3.16799500	-2.30519900	-0.41761000
H	3.96038100	-1.56518600	-0.35563700
C	3.41750700	-3.51400400	-1.07143600
H	4.39551200	-3.69451000	-1.50922500
C	2.41712500	-4.48532300	-1.16511000
H	2.61145100	-5.42490100	-1.67426600
C	1.16623800	-4.23752100	-0.59398200
H	0.38092500	-4.98623600	-0.65519900
C	0.91720100	-3.02872200	0.06043100
H	-0.05916100	-2.85059000	0.49979100
N	-0.06039600	-0.21247100	1.03448300
P	-0.74784300	0.13108300	-0.54464800
P	1.65554900	-0.54751300	1.21587000

B5. Cartesian coordinates of PNP-*c*But

C	0.87160000	-0.08320000	2.05280000
H	1.87890000	0.19330000	1.74170000
C	0.49390000	0.77860000	3.29080000
H	0.91800000	1.78460000	3.34770000
H	-0.58850000	0.83130000	3.42660000
C	1.11140000	-0.33550000	4.17990000
H	0.58110000	-0.58670000	5.10070000
H	2.15930000	-0.13570000	4.42030000
C	0.96310000	-1.31850000	2.98740000
H	1.76500000	-2.03620000	2.79500000
H	0.00720000	-1.84760000	3.03540000

C	-2.51800000	0.97210000	0.14760000
C	-3.13450000	1.95860000	0.93040000
H	-3.11180000	1.87080000	2.01290000
C	-3.78310000	3.04420000	0.34030000
H	-4.25620000	3.79640000	0.96360000
C	-3.82920000	3.15320000	-1.04860000
H	-4.33390000	3.99460000	-1.51290000
C	-3.22680000	2.17400000	-1.84140000
H	-3.26110000	2.25410000	-2.92340000
C	-2.57900000	1.09190000	-1.24950000
H	-2.11560000	0.33870000	-1.87500000
C	-2.05170000	-1.88450000	0.04800000
C	-3.31760000	-2.06210000	-0.53100000
H	-4.04010000	-1.25340000	-0.51380000
C	-3.66430000	-3.26950000	-1.13640000
H	-4.64710000	-3.38190000	-1.58370000
C	-2.75580000	-4.32740000	-1.16860000
H	-3.02640000	-5.26740000	-1.63860000
C	-1.49880000	-4.16830000	-0.58440000
H	-0.78560000	-4.98690000	-0.59500000
C	-1.15330000	-2.96150000	0.02110000
H	-0.17550000	-2.85620000	0.47740000
C	2.26100000	-0.94160000	-0.75030000
C	3.50040000	-0.54930000	-0.22330000
H	3.61420000	0.43650000	0.21420000
C	4.60180000	-1.40250000	-0.27400000
H	5.55230000	-1.08030000	0.14000000
C	4.48540000	-2.66420000	-0.85930000
H	5.34440000	-3.32630000	-0.90220000
C	3.26400000	-3.06350000	-1.40160000
H	3.16880000	-4.03640000	-1.87350000
C	2.16550000	-2.20580000	-1.35150000
H	1.22260000	-2.51600000	-1.79120000
C	1.42430000	1.80810000	-0.69910000
C	0.95030000	2.77760000	0.19270000
H	0.22930000	2.49860000	0.95130000
C	1.38560000	4.10080000	0.10930000
H	1.00670000	4.83550000	0.81310000
C	2.29870000	4.47990000	-0.87300000
H	2.63640000	5.50920000	-0.93910000
C	2.76960000	3.52580000	-1.77780000
H	3.47620000	3.81050000	-2.55130000
C	2.33330000	2.20590000	-1.69350000
H	2.70560000	1.47870000	-2.40900000
N	0.03610000	-0.12050000	0.83660000
P	-1.67240000	-0.39550000	1.07540000
P	0.71340000	0.09700000	-0.75610000

B6. Cartesian coordinates of PNP-*c*Pent

C	-0.89424000	-0.06859800	1.91970500
C	-0.94296100	-1.51385900	2.46678500
C	-1.50772300	-1.33727400	3.88237200
C	-0.76145500	-0.09229500	4.40627000
C	-0.57811500	0.82059900	3.16555600
C	-1.85741300	-1.21064300	-0.94292300
C	-1.34568700	-2.45183900	-1.36152100
C	-2.16801000	-3.57838700	-1.43707300
C	-3.52272600	-3.48043100	-1.10719600
C	-4.04769400	-2.25007100	-0.70218100
C	-3.22193700	-1.12532500	-0.62123200
C	-1.81457100	1.65775300	-0.89270200
C	-2.55497600	1.87424800	-2.07054600
C	-3.37156400	2.99620500	-2.21185100
C	-3.45578100	3.93931000	-1.18160500
C	-2.71647200	3.74537000	-0.01393300
C	-1.90313300	2.61524500	0.12819600
C	2.22460400	-1.47699300	-0.10908000
C	2.39137100	-2.74186400	0.47886900
C	2.77742800	-3.84738400	-0.28489600
C	3.01698800	-3.69864400	-1.65294000
C	2.86984000	-2.44182100	-2.24982600
C	2.47733200	-1.34071900	-1.48556700
C	2.53429900	1.35826100	0.23248800
C	3.92102600	1.29097300	-0.00135600
C	4.62583900	2.40440100	-0.45958100
C	3.96142500	3.61424500	-0.68686900
C	2.58890300	3.69698500	-0.44685400
C	1.88325300	2.58061000	0.01313800
N	-0.00846500	0.16022700	0.73950100
P	-0.65205000	0.21050400	-0.88357600
P	1.70458900	-0.09317600	1.02289100
H	4.45597700	0.36043200	0.16964200
H	5.69454300	2.32651300	-0.63981900
H	4.50939400	4.48111900	-1.04478900
H	2.05935900	4.62991300	-0.61954000
H	0.81890600	2.66530200	0.19585400
H	2.22204800	-2.86200900	1.54586900
H	2.89918700	-4.81712800	0.18958800
H	3.32384800	-4.55310100	-2.24976400
H	3.06009800	-2.31822100	-3.31251300
H	2.36541500	-0.37231900	-1.96082800
H	-0.29595700	-2.53682200	-1.62820000
H	-1.75216000	-4.52840800	-1.76107000
H	-4.16565000	-4.35380400	-1.17154200
H	-5.10083700	-2.16371500	-0.44839900
H	-3.64815100	-0.17574600	-0.31284000
H	-2.49307100	1.15775700	-2.88641300

H	-3.93683600	3.13810000	-3.12885100
H	-4.08702900	4.81622200	-1.29222700
H	-2.76919200	4.47217000	0.79226700
H	-1.33220000	2.48721200	1.04085900
H	-1.90311600	0.18131500	1.57862500
H	-2.58768600	-1.14262300	3.83355900
H	-1.29091700	0.40828500	5.22329300
H	0.21902000	-0.39276900	4.79410400
H	-1.36565200	-2.21897100	4.51618000
H	0.43912200	1.21782900	3.11393500
H	-1.25635300	1.68051700	3.19915300
H	-1.53294000	-2.17900200	1.83031300
H	0.07488000	-1.91790900	2.52543600

B7. Cartesian coordinates of PNP-*c*Hex

N	0.00550000	0.03770000	0.59110000
P	-1.57360000	0.58030000	1.05630000
P	0.45650000	-0.11400000	-1.06890000
C	-2.76180000	-0.59230000	0.26270000
C	-3.01440000	-0.70130000	-1.10730000
C	-3.91420000	-1.63710000	-1.58940000
C	-4.58440000	-2.48150000	-0.71240000
C	-4.35390000	-2.38080000	0.64870000
C	-3.45090000	-1.43940000	1.12860000
C	-1.85690000	2.15710000	0.14030000
C	-0.83600000	3.10110000	0.03810000
C	-1.07500000	4.35990000	-0.49120000
C	-2.34730000	4.70840000	-0.91900000
C	-3.37690000	3.78740000	-0.80590000
C	-3.13510000	2.52730000	-0.27810000
C	2.08780000	0.75030000	-1.24400000
C	2.06100000	1.97060000	-1.91700000
C	3.21920000	2.71340000	-2.11150000
C	4.43150000	2.23780000	-1.64200000
C	4.48150000	1.01420000	-0.98620000
C	3.32360000	0.27900000	-0.79410000
C	0.93120000	-1.89070000	-1.27100000
C	0.24480000	-2.89350000	-0.58950000
C	0.48670000	-4.23420000	-0.85400000
C	1.41070000	-4.60040000	-1.81950000
C	2.08410000	-3.61380000	-2.52470000
C	1.84360000	-2.27520000	-2.25600000
H	-2.50760000	-0.05590000	-1.79930000
H	-4.09190000	-1.70930000	-2.64790000
H	-5.28270000	-3.20730000	-1.09060000
H	-4.87420000	-3.02400000	1.33640000
H	-3.28450000	-1.36200000	2.18900000
H	0.15490000	2.85600000	0.37040000

H	-0.26760000	5.06760000	-0.56440000
H	-2.53440000	5.68500000	-1.32930000
H	-4.37040000	4.04580000	-1.12780000
H	-3.95260000	1.83490000	-0.19690000
H	1.12650000	2.34460000	-2.29540000
H	3.17100000	3.65250000	-2.63410000
H	5.33200000	2.80680000	-1.79260000
H	5.42190000	0.63140000	-0.63020000
H	3.39410000	-0.67530000	-0.30620000
H	-0.49350000	-2.63110000	0.14310000
H	-0.05370000	-4.98850000	-0.30940000
H	1.59860000	-5.63930000	-2.02590000
H	2.79640000	-3.88350000	-3.28470000
H	2.37460000	-1.53070000	-2.82090000
C	0.96210000	-0.25490000	1.69370000
C	1.49040000	1.02170000	2.36030000
C	2.55340000	0.70960000	3.41940000
C	2.04070000	-0.28370000	4.46340000
C	1.50340000	-1.55060000	3.79550000
C	0.42390000	-1.22420000	2.75690000
H	1.80090000	-0.75540000	1.22680000
H	0.65950000	1.54910000	2.82540000
H	1.90750000	1.67970000	1.60550000
H	2.87200000	1.63140000	3.89940000
H	3.43550000	0.29500000	2.93200000
H	1.24490000	0.18140000	5.04390000
H	2.83320000	-0.53460000	5.16430000
H	1.09480000	-2.22590000	4.54300000
H	2.32410000	-2.08230000	3.31440000
H	-0.42930000	-0.78220000	3.26140000
H	0.08040000	-2.13720000	2.28350000

B8. Cartesian coordinates of PNP-Dimprop

N	-0.02830000	-0.10470000	0.79350000
P	1.56230000	-0.80030000	1.03530000
P	-0.52760000	0.40220000	-0.80760000
C	-0.90930000	0.10100000	1.99600000
C	-0.16290000	0.71050000	3.19320000
C	2.76000000	0.39740000	0.26700000
C	2.94310000	0.59880000	-1.11260000
C	3.86730000	1.53620000	-1.57800000
C	4.62850000	2.28590000	-0.67490000
C	4.46600000	2.08920000	0.69800000
C	3.54110000	1.14850000	1.16180000
C	1.64390000	-2.23270000	-0.13320000
C	0.50920000	-3.01460000	-0.40410000
C	0.61000000	-4.19820000	-1.13970000
C	1.85100000	-4.63070000	-1.61320000

C	2.99110000	-3.86990000	-1.33890000
C	2.88970000	-2.68720000	-0.60330000
C	-0.79070000	2.23380000	-0.65270000
C	-1.63220000	2.90550000	-1.55930000
C	-1.71280000	4.29940000	-1.56710000
C	-0.94730000	5.05520000	-0.67390000
C	-0.09420000	4.40230000	0.21830000
C	-0.01260000	3.00710000	0.22310000
C	-2.28160000	-0.19820000	-1.01190000
C	-2.46150000	-1.32380000	-1.83470000
C	-3.73430000	-1.85410000	-2.06430000
C	-4.85500000	-1.25660000	-1.48290000
C	-4.69520000	-0.12420000	-0.67820000
C	-3.42160000	0.40040000	-0.44790000
H	-1.63770000	0.85280000	1.67590000
H	2.35940000	0.02430000	-1.82350000
H	3.99200000	1.68280000	-2.64740000
H	5.34660000	3.01440000	-1.04100000
H	5.06050000	2.65920000	1.40660000
H	3.42720000	0.98990000	2.23140000
H	-0.46160000	-2.69460000	-0.04120000
H	-0.28410000	-4.78270000	-1.33990000
H	1.93010000	-5.55010000	-2.18610000
H	3.96330000	-4.19500000	-1.69950000
H	3.78900000	-2.11310000	-0.40070000
H	-2.23400000	2.33940000	-2.26460000
H	-2.37560000	4.79430000	-2.27180000
H	-1.01130000	6.13950000	-0.67870000
H	0.51500000	4.97710000	0.91050000
H	0.67050000	2.51520000	0.90630000
H	-1.59550000	-1.78490000	-2.30190000
H	-3.84960000	-2.72480000	-2.70390000
H	-5.84650000	-1.66270000	-1.66250000
H	-5.56320000	0.35300000	-0.23120000
H	-3.32030000	1.29140000	0.16400000
C	-1.73480000	-1.16830000	2.36930000
C	-0.93880000	-2.26470000	3.09640000
C	-2.98370000	-0.79420000	3.18820000
H	0.30480000	1.65850000	2.91540000
H	0.61460000	0.04680000	3.57730000
H	-0.86680000	0.91520000	4.00670000
H	-2.08860000	-1.58230000	1.41750000
H	-0.62600000	-1.93840000	4.09470000
H	-0.04070000	-2.56610000	2.55060000
H	-1.56270000	-3.15660000	3.22450000
H	-3.59020000	-0.03840000	2.67730000
H	-2.72000000	-0.40450000	4.17820000
H	-3.61520000	-1.67570000	3.34420000

B9. Cartesian coordinates of [$PtCl_2$(PNP-Ethyl)]

Pt	0.00200000	0.04910000	-1.85920000
P	1.44840000	0.08280000	0.18950000
P	-1.46250000	-0.02550000	0.17050000
N	-0.01530000	0.05020000	1.21290000
C	2.44680000	1.55340000	0.78040000
C	2.47540000	-1.43050000	0.56980000
C	-2.44980000	-1.52910000	0.70060000
C	-2.50140000	1.45480000	0.63350000
C	-0.04540000	0.22480000	2.68790000
C	3.25890000	1.48790000	1.93650000
H	3.35800000	0.55760000	2.49010000
C	3.95640000	2.62880000	2.37120000
C	-3.24220000	-1.52630000	1.87120000
C	-2.35070000	-2.70040000	-0.08120000
C	3.85000000	3.83790000	1.65500000
H	4.39430000	4.71780000	1.98960000
C	3.04210000	3.90260000	0.50410000
C	2.33670000	2.76570000	0.06430000
C	3.87980000	-1.39200000	0.42520000
C	1.83350000	-2.65600000	0.84270000
C	3.99590000	-3.78510000	0.88490000
H	4.58090000	-4.69360000	1.00560000
C	2.59330000	-3.82590000	1.00860000
C	4.63620000	-2.56700000	0.58810000
H	-3.33270000	-0.62710000	2.47530000
C	-3.92820000	-2.69060000	2.25820000
H	-1.01870000	0.66120000	2.94840000
H	0.70560000	0.97920000	2.96070000
C	0.18230000	-1.06020000	3.50770000
C	-1.86750000	2.66040000	1.00020000
H	-0.78470000	2.70730000	1.07150000
C	-2.63550000	3.80920000	1.25440000
C	-3.90580000	1.41660000	0.48980000
H	4.38590000	-0.46230000	0.17900000
H	0.75120000	-2.70000000	0.91610000
H	2.95990000	4.83080000	-0.05550000
C	-3.83180000	-3.86050000	1.47750000
H	-4.36730000	-4.75880000	1.77560000
C	-3.04560000	-3.86170000	0.31020000
H	-2.97080000	-4.75890000	-0.29880000
H	1.71200000	2.82320000	-0.82460000
H	-4.40530000	0.50260000	0.17910000
C	-4.66960000	2.57130000	0.73780000
H	-2.14020000	4.73530000	1.53460000
C	-4.03740000	3.76820000	1.12560000
H	-4.62880000	4.66110000	1.31330000
H	-1.74030000	-2.70960000	-0.98180000
H	-5.74990000	2.53660000	0.62180000

H	0.10160000	-0.83040000	4.57950000
H	1.17490000	-1.48400000	3.32370000
H	-0.56550000	-1.82200000	3.26210000
H	2.09100000	-4.76700000	1.21720000
H	4.57890000	2.57350000	3.26090000
H	-4.53560000	-2.68420000	3.15990000
H	5.71680000	-2.53060000	0.47540000
Cl	0.25040000	-2.30980000	-2.56660000
Cl	-0.24840000	2.44640000	-2.43790000

B10. Cartesian coordinates of [$PtCl_2$(PNP-*n*Prop)]

Pt	-0.00550000	-0.30910000	-1.58510000
Cl	-1.79030000	-0.56110000	-3.17460000
P	1.34110000	-0.07080000	0.20740000
Cl	1.74720000	-0.62650000	-3.19890000
P	-1.33270000	0.07440000	0.19840000
N	0.01320000	0.20650000	1.28150000
C	2.49840000	1.33700000	0.28600000
C	2.24910000	-1.51690000	0.84590000
C	-2.29320000	1.62280000	0.25480000
C	-2.43370000	-1.24720000	0.80220000
C	0.03270000	0.27860000	2.75040000
C	3.26040000	1.60460000	1.43400000
C	2.60500000	2.18070000	-0.82670000
C	3.62630000	-1.65290000	0.62870000
C	1.54110000	-2.56710000	1.44740000
C	-3.67840000	1.61670000	0.04730000
C	-1.61750000	2.84840000	0.33970000
C	-3.20160000	-1.09840000	1.96840000
C	-2.48700000	-2.45240000	0.08900000
C	-0.08250000	1.68880000	3.33860000
H	0.96460000	-0.18620000	3.08940000
H	-0.77420000	-0.35340000	3.13930000
C	4.09840000	2.71500000	1.47540000
H	3.21080000	0.94190000	2.29170000
C	3.45440000	3.28630000	-0.78440000
H	2.04430000	1.95330000	-1.72670000
H	4.18170000	-0.86210000	0.13840000
C	4.28580000	-2.81520000	1.02430000
C	2.20510000	-3.72130000	1.85090000
H	0.47000000	-2.48520000	1.59470000
H	-4.21020000	0.67910000	-0.06160000
C	-4.37900000	2.81850000	-0.04310000
C	-2.32060000	4.04560000	0.25590000
H	-0.54110000	2.86610000	0.46610000
H	-3.19970000	-0.15810000	2.50950000
C	-3.99180000	-2.14970000	2.42580000
C	-3.28670000	-3.49870000	0.54650000

H	-1.92340000	-2.55330000	-0.83200000
H	-1.03210000	2.13660000	3.03190000
H	0.71000000	2.31860000	2.92090000
C	0.01310000	1.66850000	4.86620000
C	4.19490000	3.55770000	0.36510000
H	4.68340000	2.91720000	2.36660000
H	3.54100000	3.92790000	-1.65470000
H	5.35100000	-2.91450000	0.84440000
C	3.57940000	-3.84730000	1.64070000
H	1.64890000	-4.52540000	2.32120000
H	-5.45110000	2.80270000	-0.20860000
C	-3.70400000	4.03300000	0.06660000
H	-1.78850000	4.98830000	0.32780000
H	-4.58230000	-2.02840000	3.32800000
C	-4.03270000	-3.35160000	1.71550000
H	-3.33270000	-4.42370000	-0.01820000
H	-0.07400000	2.67760000	5.27830000
H	0.97020000	1.25390000	5.20160000
H	-0.78380000	1.06040000	5.30880000
H	4.85570000	4.41820000	0.39530000
H	-4.25060000	4.96740000	-0.00790000
H	-4.65600000	-4.16700000	2.06830000
H	4.09540000	-4.75090000	1.94810000

B11. Cartesian coordinates of [Pt(PNP-*c*Prop)$_2$]

C	2.33864900	2.44945200	-1.43606400
C	1.62018100	2.19998900	-2.62487900
H	0.76450200	1.52902200	-2.61840300
C	2.00450100	2.83353400	-3.81985200
H	1.44755200	2.64792200	-4.73387800
C	3.10767000	3.70874500	-3.83118100
H	3.40472500	4.19680800	-4.75536600
C	3.82654400	3.95522000	-2.64397400
H	4.67765400	4.63012200	-2.65320400
C	3.44586300	3.32899100	-1.44500500
H	4.00382000	3.52894300	-0.53414900
C	1.98123200	2.75623500	1.52791000
C	1.61962000	4.10477600	1.31519600
H	1.33488000	4.45587100	0.32664800
C	1.64573800	5.01251800	2.38957300
H	1.37768200	6.05186600	2.22227200
C	2.02843200	4.58043500	3.67388100
H	2.05801000	5.28640300	4.49914000
C	2.38200100	3.23260500	3.88489900
H	2.68701400	2.89889500	4.87299000
C	2.35281500	2.31951400	2.81636500
H	2.63814900	1.28520000	2.98190900
C	2.62610600	-2.13120800	-1.41853300

C	1.83723400	-2.03970500	-2.58511500
H	0.87704600	-1.53019400	-2.55951000
C	2.28736500	-2.62451500	-3.78205300
H	1.67628900	-2.56078300	-4.67794600
C	3.52556500	-3.29419600	-3.81811000
H	3.87354900	-3.74439000	-4.74373100
C	4.31324300	-3.38546600	-2.65263000
H	5.26734800	-3.90405800	-2.67972600
C	3.86775400	-2.80756200	-1.45172600
H	4.47990700	-2.88973000	-0.55755700
C	2.34767400	-2.46050100	1.55177900
C	2.57610600	-1.95519800	2.84886700
H	2.63932500	-0.88405600	3.01471100
C	2.74679200	-2.84065200	3.92676600
H	2.94074300	-2.45035100	4.92213000
C	2.67541900	-4.23262100	3.71689800
H	2.81279900	-4.91635200	4.54993800
C	2.43289700	-4.73571700	2.42458800
H	2.38155900	-5.80808900	2.25874700
C	2.26673200	-3.85440300	1.34033100
H	2.09199000	-4.25832500	0.34665100
N	3.01421800	0.19889900	0.40316200
P	1.85977900	1.55116600	0.11550200
P	2.04443900	-1.29649500	0.13357300
Pt	-0.00000200	-0.00001000	0.00000100
C	-2.33864000	-2.44943600	1.43606200
C	-1.62016400	-2.19994100	2.62486400
H	-0.76448600	-1.52897200	2.61835800
C	-2.00447100	-2.83345100	3.81985900
H	-1.44751300	-2.64781100	4.73387500
C	-3.10763600	-3.70866600	3.83122300
H	-3.40468200	-4.19670200	4.75542500
C	-3.82651800	-3.95517800	2.64403000
H	-4.67762400	-4.63008500	2.65328500
C	-3.44585000	-3.32898200	1.44503900
H	-4.00381700	-3.52896300	0.53419500
C	-1.98125500	-2.75624700	-1.52792500
C	-1.61973000	-4.10481000	-1.31520400
H	-1.33504600	-4.45592500	-0.32664800
C	-1.64586400	-5.01254600	-2.38958700
H	-1.37787900	-6.05191000	-2.22227900
C	-2.02848000	-4.58043400	-3.67390700
H	-2.05806500	-5.28639600	-4.49917100
C	-2.38195600	-3.23258000	-3.88493400
H	-2.68690700	-2.89884700	-4.87303600
C	-2.35275800	-2.31949700	-2.81639500
H	-2.63801700	-1.28516300	-2.98194800
C	-2.62612900	2.13118400	1.41853700
C	-1.83728400	2.03965800	2.58513600
H	-0.87711200	1.53011600	2.55955400
C	-2.28743300	2.62447100	3.78206700

H	-1.67637800	2.56072400	4.67797400
C	-3.52562300	3.29417000	3.81809900
H	-3.87362000	3.74436700	4.74371300
C	-4.31327900	3.38545100	2.65260400
H	-5.26738000	3.90405100	2.67968400
C	-3.86777200	2.80754700	1.45170700
H	-4.47990300	2.88972000	0.55752400
C	-2.34763300	2.46050500	-1.55176500
C	-2.57610500	1.95522200	-2.84885400
H	-2.63937100	0.88408300	-3.01470500
C	-2.74677000	2.84069200	-3.92674300
H	-2.94075200	2.45040700	-4.92210800
C	-2.67533900	4.23265700	-3.71686400
H	-2.81270600	4.91640100	-4.54989500
C	-2.43277400	4.73573200	-2.42455400
H	-2.38138700	5.80810100	-2.25870500
C	-2.26662800	3.85440200	-1.34030700
H	-2.09184700	4.25830900	-0.34662700
N	-3.01421900	-0.19890800	-0.40318200
P	-1.85978200	-1.55117800	-0.11552300
P	-2.04443800	1.29648000	-0.13356500
C	-4.44314100	-0.28389900	-0.13698600
C	-5.44543200	0.38869400	-1.08577000
C	-5.34831500	-1.13219900	-1.04026500
H	-4.70360400	-0.27060300	0.92072600
H	-5.06022100	0.88862700	-1.96722300
H	-6.31013800	0.86681400	-0.63653100
H	-6.14538100	-1.68915800	-0.55817800
H	-4.90064300	-1.63077300	-1.89194700
C	4.44313900	0.28387200	0.13696000
C	5.34831600	1.13220300	1.04020600
C	5.44542100	-0.38868900	1.08577700
H	4.70360400	0.27052800	-0.92075000
H	4.90064300	1.63081700	1.89186400
H	6.14538900	1.68913400	0.55809900
H	6.31012400	-0.86683600	0.63656200
H	5.06019900	-0.88858100	1.96725000

B12. Cartesian coordinates of [Pt(PNP-*c*Pent)$_2$]

C	-4.48825400	-0.48439500	-0.33644100
H	-4.64416900	-1.48564600	-0.76778400
C	-5.15420500	-0.45300200	1.06513200
H	-4.86268700	0.46200200	1.59378000
H	-4.86930100	-1.30562800	1.68954600
C	-6.66677400	-0.43157000	0.72795800
H	-7.04938100	-1.45531200	0.63405200
H	-7.25051300	0.05418200	1.51644400

C	-6.78708300	0.32017900	-0.64279100
H	-7.29547400	1.28363800	-0.53015900
H	-7.37753500	-0.26668000	-1.35497500
C	-5.33150700	0.52171400	-1.16132600
H	-4.99551000	1.54591300	-0.95718200
H	-5.24089900	0.36221800	-2.24130800
C	-2.63867400	2.17807100	1.36213800
C	-1.98556100	1.91855600	2.58623400
H	-1.14640100	1.22785300	2.62388400
C	-2.41487000	2.56023800	3.76127200
H	-1.91001700	2.36034600	4.70215100
C	-3.49535400	3.46218700	3.71778700
H	-3.82845300	3.95673600	4.62607400
C	-4.14505500	3.72516100	2.49486800
H	-4.97876600	4.42068800	2.45996300
C	-3.72106100	3.08630800	1.31740700
H	-4.23476700	3.29797200	0.38395100
C	-2.28590800	2.36709400	-1.62581200
C	-2.10114300	3.76036700	-1.48314000
H	-1.90760200	4.20158200	-0.50924400
C	-2.17983700	4.59633700	-2.61162300
H	-2.04959800	5.66871200	-2.49627900
C	-2.43424700	4.04919000	-3.88351600
H	-2.50470700	4.69863600	-4.75163500
C	-2.60261800	2.65756300	-4.02625600
H	-2.80231600	2.23167700	-5.00580800
C	-2.52249400	1.81709900	-2.90266400
H	-2.65586900	0.74696100	-3.02125900
C	-2.20325700	-2.62486300	1.28847200
C	-1.57476400	-2.31525100	2.51348900
H	-0.83599500	-1.51889300	2.56447200
C	-1.89434300	-3.04816600	3.66960800
H	-1.40693400	-2.81249700	4.61143000
C	-2.84236300	-4.08796300	3.60615300
H	-3.09116900	-4.65250700	4.50059800
C	-3.46589100	-4.40074600	2.38150300
H	-4.19463500	-5.20480100	2.33137900
C	-3.14883300	-3.67334300	1.22129700
H	-3.63208100	-3.92877000	0.28202500
C	-1.98816500	-2.70000500	-1.68630400
C	-2.68505900	-2.27899300	-2.83695200
H	-3.17210500	-1.30963700	-2.85655000
C	-2.77693700	-3.13143300	-3.95219800
H	-3.32948300	-2.81238100	-4.83161700
C	-2.16440900	-4.39919100	-3.92611800
H	-2.24010400	-5.05789100	-4.78677700
C	-1.46291300	-4.81679800	-2.77765200
H	-0.99601100	-5.79732600	-2.75176700
C	-1.37437900	-3.97225500	-1.65760700
H	-0.84575400	-4.31540100	-0.77144100
N	-3.00942000	-0.26386400	-0.38239200

P	-2.07440600	1.25026700	-0.14913500
P	-1.81633100	-1.58589400	-0.20486100
Pt	0.00000200	0.00000300	0.00000500
C	4.48825800	0.48440200	0.33647200
H	4.64416700	1.48568600	0.76774200
C	5.15422600	0.45289500	-1.06509200
H	4.86270900	-0.46215200	-1.59366800
H	4.86933300	1.30547000	-1.68957800
C	6.66679200	0.43148400	-0.72790200
H	7.04940600	1.45523200	-0.63409000
H	7.25053300	-0.05434700	-1.51633800
C	6.78708600	-0.32013800	0.64291800
H	7.29548900	-1.28360200	0.53038400
H	7.37751900	0.26679400	1.35505800
C	5.33150300	-0.52163700	1.16144900
H	4.99551700	-1.54585500	0.95738100
H	5.24088100	-0.36205800	2.24141700
C	2.63868000	-2.17804900	-1.36213900
C	1.98559000	-1.91849600	-2.58624000
H	1.14645300	-1.22776600	-2.62389200
C	2.41489700	-2.56017200	-3.76128100
H	1.91006500	-2.36024900	-4.70216500
C	3.49535100	-3.46215700	-3.71779400
H	3.82844700	-3.95670500	-4.62608300
C	4.14502300	-3.72517500	-2.49486900
H	4.97870600	-4.42073500	-2.45996000
C	3.72103300	-3.08632500	-1.31740500
H	4.23470700	-3.29803300	-0.38394100
C	2.28590600	-2.36711900	1.62579600
C	2.10118400	-3.76039200	1.48307200
H	1.90768400	-4.20157800	0.50915500
C	2.17988200	-4.59639900	2.61152600
H	2.04968000	-5.66877400	2.49614200
C	2.43425100	-4.04928800	3.88344400
H	2.50471300	-4.69876300	4.75154200
C	2.60258100	-2.65766200	4.02623500
H	2.80225000	-2.23180400	5.00580400
C	2.52245800	-1.81716200	2.90267000
H	2.65580300	-0.74702500	3.02130300
C	2.20326200	2.62485600	-1.28847700
C	1.57478200	2.31522200	-2.51349500
H	0.83602500	1.51885300	-2.56447500
C	1.89436200	3.04812700	-3.66962000
H	1.40696600	2.81244000	-4.61144400
C	2.84236700	4.08793700	-3.60616900
H	3.09117400	4.65247400	-4.50061900
C	3.46588100	4.40074300	-2.38151700
H	4.19461300	5.20480900	-2.33139600
C	3.14882300	3.67334900	-1.22130600
H	3.63205900	3.92879400	-0.28203200
C	1.98815300	2.70003900	1.68629100

C	2.68505200	2.27905800	2.83694800
H	3.17211500	1.30971200	2.85656300
C	2.77691800	3.13152100	3.95217700
H	3.32947000	2.81249400	4.83160200
C	2.16437400	4.39927100	3.92607300
H	2.24006200	5.05798900	4.78671800
C	1.46287600	4.81684700	2.77759800
H	0.99596300	5.79737000	2.75169200
C	1.37435400	3.97228200	1.65756800
H	0.84572700	4.31540500	0.77139500
N	3.00942300	0.26387100	0.38241700
P	2.07441200	-1.25025900	0.14914200
P	1.81633400	1.58590000	0.20486500

B13. Cartesian coordinates of [Pt(PNP-*c*Hex)$_2$]

Pt	0.27720000	-1.67120000	-0.71750000
Cl	-1.29180000	-3.32270000	-1.48040000
Cl	2.21050000	-2.86700000	-1.52090000
P	1.36990000	0.12680000	0.07240000
P	-1.27220000	-0.24480000	0.09570000
N	-0.08890000	0.96870000	0.49070000
C	2.35720000	1.14350000	-1.07500000
C	2.40390000	-0.05750000	1.56590000
C	-2.15690000	-0.75770000	1.60610000
C	-2.53330000	0.40640000	-1.05170000
C	-0.20220000	2.42620000	0.76180000
C	-3.39820000	-1.40010000	1.49550000
C	-1.53300000	-0.68250000	2.85770000
C	-2.37010000	0.16100000	-2.42090000
C	-3.64860000	1.13360000	-0.61130000
C	-4.01630000	-1.92790000	2.62710000
H	-3.87210000	-1.51120000	0.52740000
C	-2.15700000	-1.20520000	3.98670000
H	-0.55390000	-0.22930000	2.94790000
H	-1.53890000	-0.44740000	-2.75760000
C	-3.29370000	0.66010000	-3.33710000
C	-4.56900000	1.63220000	-1.52880000
H	-3.80910000	1.30240000	0.44720000
H	-4.97330000	-2.42920000	2.52930000
C	-3.40190000	-1.82530000	3.87490000
H	-3.16510000	0.45380000	-4.39420000
C	-4.38950000	1.40000000	-2.89410000
H	-5.42960000	2.19280000	-1.17870000
H	-5.11160000	1.78250000	-3.60830000
C	-0.55500000	4.74720000	-0.19340000
H	0.45660000	5.07610000	0.08170000
H	-0.82590000	5.30210000	-1.09760000
C	-0.53770000	3.24300000	-0.49830000

C	-1.52340000	5.07900000	0.94890000
C	2.21520000	0.68060000	2.74040000
H	1.41970000	1.41270000	2.80810000
C	3.04800000	0.47510000	3.84010000
H	-1.51640000	2.93720000	-0.87830000
H	0.19270000	3.01840000	-1.27990000
C	3.22530000	2.14250000	-0.61370000
H	3.35970000	2.30180000	0.45070000
C	3.93830000	2.92380000	-1.51980000
C	4.25180000	-1.22040000	2.61070000
H	5.03300000	-1.97150000	2.56190000
C	4.06950000	-0.47210000	3.77500000
C	3.42300000	-1.02060000	1.50950000
H	-3.88380000	-2.24000000	4.75420000
C	-1.19920000	4.25670000	2.20250000
H	-0.22090000	4.56790000	2.59380000
H	-1.92850000	4.46010000	2.99380000
C	-1.16890000	2.74890000	1.90890000
H	-0.88450000	2.19480000	2.80750000
H	-2.17670000	2.41200000	1.64230000
H	-1.66500000	-1.13980000	4.95160000
H	-2.55090000	4.86160000	0.62800000
H	-1.48680000	6.14890000	1.18110000
H	4.71490000	-0.63400000	4.63210000
H	4.60920000	3.69510000	-1.15600000
C	3.80140000	2.70140000	-2.89100000
C	2.23670000	0.91400000	-2.45180000
H	1.60810000	0.10460000	-2.80520000
C	2.95680000	1.69220000	-3.35490000
H	3.54450000	-1.62840000	0.61720000
H	0.79990000	2.73370000	1.08480000
H	4.36650000	3.30280000	-3.59590000
H	2.87050000	1.49890000	-4.41880000
H	2.89540000	1.05220000	4.74640000

B14. Cartesian coordinates of [$PtCl_2$(PNP-Dimprop)]

C	-2.40500000	-1.31640000	0.99130000
C	-2.99220000	-2.28370000	0.14540000
C	-2.59170000	-1.39360000	2.38850000
P	-1.42470000	0.03500000	0.14980000
H	-2.83540000	-2.23510000	-0.93040000
C	-3.76730000	-3.31830000	0.70240000
H	-4.21470000	-4.06200000	0.04830000
C	-3.95340000	-3.39680000	2.09570000
H	-4.54940000	-4.20040000	2.52170000
C	-3.36120000	-2.43550000	2.93810000
H	-3.49890000	-2.49410000	4.01510000
H	-2.13770000	-0.66510000	3.05380000

APPENDIX B

C	-0.03880000	1.20460000	2.47770000
N	-0.00210000	0.46270000	1.17720000
C	0.55850000	2.65210000	2.41640000
C	0.59430000	0.37020000	3.61620000
H	-1.11160000	1.32810000	2.69710000
P	1.39180000	-0.11350000	0.17720000
Pt	-0.03610000	-0.58080000	-1.62940000
C	-2.57590000	1.48680000	-0.01710000
C	2.70960000	1.18760000	-0.02020000
C	2.19400000	-1.56910000	1.02830000
C	0.04930000	3.46980000	1.21100000
C	0.25050000	3.41960000	3.72820000
H	1.64960000	2.56260000	2.32980000
H	0.54950000	4.44680000	1.18540000
H	-1.03170000	3.64820000	1.27930000
H	0.24970000	2.96600000	0.26070000
H	0.40540000	0.83310000	4.59060000
H	1.68150000	0.28820000	3.49080000
H	0.18590000	-0.64450000	3.63420000
H	-0.83270000	3.45440000	3.91660000
H	0.73570000	2.97480000	4.60470000
H	0.60330000	4.45560000	3.64800000
C	-2.49080000	2.25950000	-1.19440000
C	-3.53540000	1.80030000	0.96930000
H	-1.78510000	1.98380000	-1.97280000
C	-3.34730000	3.36150000	-1.36850000
H	-3.28790000	3.94890000	-2.28080000
C	-4.28860000	3.69100000	-0.37440000
H	-4.95210000	4.54110000	-0.51380000
C	-4.38500000	2.90670000	0.79220000
H	-5.12400000	3.14760000	1.55230000
H	-3.64370000	1.18070000	1.85560000
C	3.63420000	1.48360000	1.00570000
C	2.78660000	1.86120000	-1.25690000
H	3.59970000	0.94900000	1.95180000
C	4.61650000	2.46720000	0.80240000
H	5.32610000	2.69390000	1.59410000
C	4.68410000	3.15310000	-0.42780000
H	5.44770000	3.91100000	-0.58570000
C	3.77350000	2.84550000	-1.45540000
H	3.83580000	3.35540000	-2.41300000
H	2.10820000	1.59450000	-2.06210000
C	1.38800000	-2.48680000	1.73360000
C	3.56590000	-1.83910000	0.84030000
H	0.32250000	-2.30640000	1.84340000
C	1.95840000	-3.64920000	2.27850000
H	1.33150000	-4.35390000	2.81890000
C	3.33300000	-3.90990000	2.11040000
H	3.77160000	-4.81340000	2.52670000
C	4.13200000	-3.00610000	1.38610000
H	5.18820000	-3.21230000	1.23290000

H	4.18830000	-1.16570000	0.25860000
Cl	-1.83820000	-0.96270000	-3.22480000
Cl	1.73080000	-1.09430000	-3.21390000

B15. Cartesian coordinates of [Pd(PNP-*c*Prop)$_2$]

C	-2.51263900	-2.28942700	-1.43238200
C	-1.75098800	-2.12593300	-2.60928300
H	-0.82823600	-1.55046000	-2.59121200
C	-2.17707000	-2.72310500	-3.80896300
H	-1.58654100	-2.60282400	-4.71277800
C	-3.36504600	-3.47861500	-3.83723700
H	-3.69457500	-3.93916600	-4.76450300
C	-4.12572300	-3.64231700	-2.66186900
H	-5.04105900	-4.22694500	-2.68289600
C	-3.70389600	-3.05109800	-1.45868300
H	-4.29521400	-3.18857200	-0.55747600
C	-2.20184300	-2.62515000	1.53231200
C	-2.00181900	-4.00657700	1.31425500
H	-1.77428000	-4.38691900	0.32184500
C	-2.11661600	-4.90744400	2.38889200
H	-1.97605100	-5.97075200	2.21635400
C	-2.42265100	-4.43645000	3.68002800
H	-2.51941400	-5.13585400	4.50572300
C	-2.60996300	-3.05651800	3.89775500
H	-2.85316900	-2.69110100	4.89176000
C	-2.49262500	-2.15120600	2.82904500
H	-2.64734400	-1.09034600	3.00141500
C	-2.51342200	2.28866000	-1.43248800
C	-1.75193500	2.12526000	-2.60950300
H	-0.82907700	1.54995400	-2.59156800
C	-2.17832200	2.72231000	-3.80913800
H	-1.58791500	2.60210500	-4.71304200
C	-3.36644800	3.47758800	-3.83725200
H	-3.69622100	3.93803200	-4.76448400
C	-4.12696700	3.64119000	-2.66176400
H	-5.04241700	4.22564400	-2.68266600
C	-3.70483200	3.05010100	-1.45862500
H	-4.29601400	3.18751600	-0.55732000
C	-2.20252000	2.62460100	1.53211600
C	-2.49347700	2.15076600	2.82884300
H	-2.64819900	1.08991700	3.00127800
C	-2.61098200	3.05617000	3.89745800
H	-2.85433400	2.69083600	4.89145800
C	-2.42366600	4.43608500	3.67964000
H	-2.52056200	5.13555700	4.50526200
C	-2.11746800	4.90697700	2.38850300
H	-1.97691300	5.97027500	2.21589100
C	-2.00250600	4.00601900	1.31396300

H	-1.77486600	4.38627900	0.32154400
N	-3.02056200	-0.00042300	0.41016600
P	-1.96463500	-1.43263500	0.12329600
P	-1.96505800	1.43205200	0.12316800
C	2.51265700	2.28917800	1.43262100
C	1.75115700	2.12530400	2.60956600
H	0.82849400	1.54968900	2.59146500
C	2.17728600	2.72225900	3.80933700
H	1.58687700	2.60168300	4.71319100
C	3.36515600	3.47793400	3.83765500
H	3.69472000	3.93831900	4.76499100
C	4.12568300	3.64201300	2.66224200
H	5.04093900	4.22676600	2.68330400
C	3.70381100	3.05100700	1.45896700
H	4.29501100	3.18876900	0.55772700
C	2.20179700	2.62540400	-1.53200300
C	2.00180400	4.00679400	-1.31368500
H	1.77430600	4.38695700	-0.32119600
C	2.11658400	4.90785800	-2.38816000
H	1.97604400	5.97113700	-2.21542100
C	2.42257400	4.43709600	-3.67939200
H	2.51932400	5.13665100	-4.50496000
C	2.60985800	3.05720200	-3.89737700
H	2.85303000	2.69196400	-4.89145700
C	2.49253700	2.15169500	-2.82883100
H	2.64723300	1.09086500	-3.00140200
C	2.51349700	-2.28876300	1.43224600
C	1.75203400	-2.12550300	2.60929600
H	0.82916800	-1.55020800	2.59145000
C	2.17845300	-2.72268600	3.80885400
H	1.58806500	-2.60258500	4.71278400
C	3.36658100	-3.47796600	3.83685300
H	3.69637700	-3.93851400	4.76402600
C	4.12706300	-3.64144500	2.66132500
H	5.04250600	-4.22591400	2.68213400
C	3.70489800	-3.05022100	1.45826300
H	4.29604000	-3.18756300	0.55692100
C	2.20247400	-2.62448000	-1.53235900
C	2.49326600	-2.15055300	-2.82908900
H	2.64788600	-1.08968200	-3.00148100
C	2.61074400	-3.05589100	-3.89776300
H	2.85396800	-2.69048400	-4.89176800
C	2.42357100	-4.43583400	-3.67999800
H	2.52044900	-5.13525500	-4.50566500
C	2.11754800	-4.90682000	-2.38885400
H	1.97711100	-5.97013900	-2.21628100
C	2.00261100	-4.00592700	-1.31425600
H	1.77511500	-4.38625900	-0.32183200
N	3.02053900	0.00047400	-0.41027900
P	1.96461900	1.43264600	-0.12318900
P	1.96506400	-1.43203100	-0.12331500

C	4.45394000	0.00069200	-0.14978300
C	5.41136500	-0.76122100	-1.07709100
C	5.41108700	0.76318000	-1.07690700
H	4.71595600	0.00060700	0.90779500
H	4.99650700	-1.26049700	-1.94497800
H	6.24306900	-1.28038600	-0.61137900
H	6.24259300	1.28251800	-0.61103500
H	4.99607300	1.26252600	-1.94467600
C	-4.45394700	-0.00065300	0.14958000
C	-5.41116100	-0.76303600	1.07672200
C	-5.41142100	0.76136700	1.07674900
H	-4.71589700	-0.00067300	-0.90801400
H	-4.99620700	-1.26229700	1.94456800
H	-6.24264600	-1.28241100	0.61085100
H	-6.24308600	1.28049600	0.61092900
H	-4.99661100	1.26072700	1.94461000
Pd	-0.00000400	-0.00000200	-0.00001000

B16. Cartesian coordinates of [Pd(PNP-*c*But)$_2$]

C	1.92090500	-2.88778400	1.40188900
C	2.83156400	-3.96888900	1.34913300
H	3.36103900	-4.20771200	0.43057600
C	3.04865000	-4.75413200	2.49506000
H	3.74964100	-5.58300900	2.45487800
C	2.36014400	-4.46855400	3.69103100
H	2.52987400	-5.07978200	4.57315600
C	1.44866100	-3.39572800	3.74116600
H	0.90988400	-3.18070300	4.65966000
C	1.22947400	-2.60363600	2.60026400
H	0.51873200	-1.78136700	2.64494100
C	1.85506500	-2.75816400	-1.60503200
C	2.42002900	-2.17407900	-2.75944000
H	2.81239300	-1.16180200	-2.72956500
C	2.49374000	-2.91429300	-3.95233500
H	2.94381700	-2.46932700	-4.83550700
C	1.99704800	-4.23211500	-4.00131800
H	2.06353200	-4.80475300	-4.92228700
C	1.42107900	-4.80868200	-2.85237400
H	1.03890400	-5.82502500	-2.88560500
C	1.34471300	-4.07479700	-1.65507600
H	0.89970700	-4.53506800	-0.77668100
C	2.65402800	1.87425400	1.68722400
C	2.54408500	3.27594400	1.82612300
H	2.25151700	3.89998400	0.98565000
C	2.82540800	3.87879500	3.06552300
H	2.75416600	4.95810400	3.16682800
C	3.20436400	3.08879000	4.16822200
H	3.43017800	3.55821800	5.12172600

C	3.29769900	1.68920500	4.03063500
H	3.59528300	1.07753500	4.87783400
C	3.01957300	1.07955400	2.79504900
H	3.10726600	0.00110700	2.69395700
N	2.99380700	-0.53451200	-0.02080300
P	1.68147200	-1.75095900	-0.04976200
P	2.19323300	1.05795500	0.07748200
C	2.74407800	2.14949200	-1.32669400
C	2.02161800	2.08192000	-2.53863300
H	1.13602900	1.45508100	-2.61795000
C	2.43742100	2.83896300	-3.64801500
H	1.87798600	2.78750500	-4.57776200
C	3.57225000	3.66758000	-3.55067100
H	3.89439000	4.25266800	-4.40764600
C	4.28807900	3.74226000	-2.33899300
H	5.16203700	4.38281600	-2.26178700
C	3.87909800	2.98576900	-1.22695400
H	4.44370800	3.05415600	-0.30147900
P	-1.68147600	1.75094700	-0.04979600
P	-2.19321600	-1.05798000	0.07738200
C	-1.92094800	2.88777300	1.40184500
C	-1.85501500	2.75817500	-1.60505800
N	-2.99380100	0.53448300	-0.02084700
C	-2.65407200	-1.87432100	1.68708500
C	-2.74402000	-2.14945900	-1.32685700
C	-2.82503100	-3.87879800	3.06553200
C	-2.83147900	3.96898200	1.34899400
C	-1.22966900	2.60355000	2.60028900
C	-2.41954800	2.17399400	-2.75962800
C	-1.34502100	4.07495300	-1.65491300
C	-2.54364500	-3.27595900	1.82613900
C	-3.02018400	-1.07965500	2.79474900
C	-2.02141300	-2.08195500	-2.53871300
C	-3.87915300	-2.98560200	-1.22726300
H	-3.36081700	4.20787300	0.43037600
C	-3.04860100	4.75424400	2.49490200
C	-1.44889300	3.39565900	3.74117200
H	-0.51901700	1.78120600	2.64503800
H	-2.81161200	1.16159800	-2.72990400
C	-2.49319100	2.91425200	-3.95250000
C	-1.42132600	4.80888600	-2.85218600
H	-0.90035800	4.53530500	-0.77638500
H	-3.74949400	5.58320100	2.45464600
C	-2.36025700	4.46858300	3.69094600
H	-0.91023500	3.18057400	4.65972200
H	-2.94293000	2.46920400	-4.83580200
C	-1.99686500	4.23221900	-4.00129500
H	-1.03943600	5.82534100	-2.88527100
H	-2.75340300	-4.95807100	3.16695700
C	-3.20454900	-3.08883200	4.16806500
H	-2.25063300	-3.89996800	0.98580000

C	-3.29838300	-1.68929600	4.03032300
H	-3.10828000	-0.00125300	2.69353000
H	-1.13574600	-1.45521300	-2.61792100
C	-2.43717000	-2.83894300	-3.64815000
C	-4.28808800	-3.74203500	-2.33935800
H	-4.44389200	-3.05392100	-0.30186300
H	-3.43041500	-3.55825600	5.12155900
H	-3.59640800	-1.07766000	4.87739200
H	-1.87761800	-2.78753900	-4.57783100
C	-3.57210400	-3.66743100	-3.55094900
H	-5.16213400	-4.38248600	-2.26226400
H	-3.89420900	-4.25247400	-4.40796700
H	-2.53001300	5.07982700	4.57305400
H	-2.06330000	4.80488900	-4.92224700
C	-5.49729800	-0.00421000	0.68718100
H	-5.22131400	-1.06149500	0.74364300
H	-5.77933800	0.33709800	1.68668100
C	-6.48989700	0.26299700	-0.49419000
H	-7.09606900	-0.58327300	-0.82421000
H	-7.15037600	1.11301000	-0.29651000
C	-5.27205400	0.65249700	-1.39821000
H	-5.38291600	1.51969700	-2.05478500
H	-4.91403500	-0.20196100	-1.98240400
C	-4.43909400	0.85825100	-0.08354600
H	-4.53331400	1.90087200	0.24762100
C	5.27176300	-0.65274400	-1.39860800
H	4.91365400	0.20166200	-1.98282100
H	5.38243200	-1.52002700	-2.05510700
C	4.43908500	-0.85830900	-0.08373700
H	4.53334400	-1.90089800	0.24752100
C	6.48982300	-0.26320300	-0.49489900
H	7.09597400	0.58299100	-0.82515600
H	7.15029700	-1.11322800	-0.29725300
C	5.49749100	0.00421300	0.68664900
H	5.77973400	-0.33697300	1.68613300
H	5.22157500	1.06151900	0.74302600
Pd	0.00000400	0.00000200	0.01270500

B17. Cartesian coordinates of [Pd(PNP-*c*Pent)$_2$]

C	-4.49764500	0.45471700	0.31120800
H	-4.66367800	1.45730900	0.73545300
C	-5.15003500	0.41304200	-1.09650600
H	-4.84991600	-0.50343800	-1.61758000
H	-4.86289500	1.26388000	-1.72231600
C	-6.66545100	0.38657800	-0.77311300
H	-7.05272900	1.40913800	-0.68537700
H	-7.24015800	-0.10361300	-1.56547300

C	-6.79500000	-0.36194200	0.59845000
H	-7.29519600	-1.32935700	0.48303700
H	-7.39723000	0.22263500	1.30260200
C	-5.34347500	-0.55191700	1.13308500
H	-4.99965900	-1.57521200	0.93857300
H	-5.26546600	-0.38534200	2.21299500
C	-2.64507300	-2.20900600	-1.35524900
C	-2.00978600	-1.94229900	-2.58729700
H	-1.18223500	-1.23809000	-2.63734700
C	-2.44075100	-2.59267900	-3.75689800
H	-1.94955200	-2.38601100	-4.70350500
C	-3.50531600	-3.51276500	-3.69988600
H	-3.83983500	-4.01478100	-4.60352200
C	-4.13656300	-3.78427400	-2.46927100
H	-4.95792100	-4.49378400	-2.42372000
C	-3.71087400	-3.13585100	-1.29739800
H	-4.21076600	-3.35424900	-0.35811600
C	-2.28682400	-2.37380300	1.63237100
C	-2.07136100	-3.76457600	1.50338500
H	-1.85659600	-4.20897500	0.53535300
C	-2.14803000	-4.59374700	2.63681700
H	-1.99546400	-5.66415800	2.53094600
C	-2.42847200	-4.04244600	3.90164800
H	-2.49640100	-4.68676300	4.77377900
C	-2.62563800	-2.65340000	4.03179500
H	-2.84545200	-2.22421400	5.00557200
C	-2.54861500	-1.81973700	2.90280800
H	-2.70501500	-0.75171200	3.01191500
C	-2.23233800	2.61750100	-1.28926900
C	-1.59774700	2.31439700	-2.51286000
H	-0.85019400	1.52577300	-2.56347200
C	-1.92034600	3.04343900	-3.67071700
H	-1.42793400	2.81176000	-4.61091900
C	-2.87748000	4.07501400	-3.61012800
H	-3.12866200	4.63727000	-4.50533000
C	-3.50655700	4.38270100	-2.38703600
H	-4.24234100	5.18047800	-2.33883700
C	-3.18655800	3.65837000	-1.22548900
H	-3.67462100	3.90992900	-0.28776000
C	-2.04203800	2.69054300	1.68626500
C	-2.75580500	2.26555600	2.82542400
H	-3.23782700	1.29360100	2.83697100
C	-2.87165000	3.11684500	3.93927600
H	-3.43773100	2.79414800	4.80871700
C	-2.26550400	4.38789100	3.92478500
H	-2.35912100	5.04533700	4.78462400
C	-1.54598100	4.80961100	2.78895800
H	-1.08329800	5.79233200	2.77167800
C	-1.43303800	3.96585500	1.67045400
H	-0.88965600	4.31233500	0.79450100
N	-3.01671700	0.24424800	0.37117700

P	-2.07476100	-1.26613900	0.14731800
P	-1.83528500	1.57894400	0.20562800
C	4.49764700	-0.45471600	-0.31118600
H	4.66368300	-1.45730800	-0.73543100
C	5.15002700	-0.41304200	1.09653300
H	4.84990400	0.50343700	1.61760600
H	4.86288300	-1.26388100	1.72234000
C	6.66544600	-0.38657800	0.77315000
H	7.05272500	-1.40913800	0.68542000
H	7.24014600	0.10361500	1.56551400
C	6.79500500	0.36193900	-0.59841300
H	7.29520400	1.32935300	-0.48300000
H	7.39723700	-0.22264200	-1.30256100
C	5.34348300	0.55191700	-1.13305600
H	4.99966800	1.57521300	-0.93854300
H	5.26548100	0.38534600	-2.21296700
C	2.64506600	2.20901300	1.35525000
C	2.00977400	1.94231000	2.58729700
H	1.18222400	1.23810000	2.63734600
C	2.44073400	2.59269500	3.75689700
H	1.94953100	2.38602900	4.70350200
C	3.50529700	3.51278300	3.69988600
H	3.83981200	4.01480300	4.60352100
C	4.13654800	3.78428800	2.46927300
H	4.95790500	4.49380000	2.42372200
C	3.71086500	3.13586000	1.29740000
H	4.21076000	3.35425700	0.35811900
C	2.28683200	2.37379800	-1.63237200
C	2.07136700	3.76457100	-1.50339300
H	1.85659600	4.20897300	-0.53536400
C	2.14804000	4.59373800	-2.63682800
H	1.99547200	5.66414900	-2.53096300
C	2.42848800	4.04243100	-3.90165500
H	2.49642000	4.68674400	-4.77378900
C	2.62565600	2.65338500	-4.03179600
H	2.84547500	2.22419500	-5.00557000
C	2.54862800	1.81972600	-2.90280600
H	2.70502900	0.75170100	-3.01190700
C	2.23233300	-2.61751200	1.28926000
C	1.59774300	-2.31441300	2.51285400
H	0.85019500	-1.52578500	2.56347100
C	1.92033800	-3.04346500	3.67070500
H	1.42792700	-2.81179000	4.61090900
C	2.87746500	-4.07504600	3.61010900
H	3.12864400	-4.63731000	4.50530700
C	3.50654100	-4.38272800	2.38701500
H	4.24231900	-5.18050900	2.33881100
C	3.18654600	-3.65838600	1.22547300
H	3.67460700	-3.90994300	0.28774200
C	2.04204300	-2.69053100	-1.68627400
C	2.75579300	-2.26552700	-2.82543700

H	3.23779800	-1.29356500	-2.83698500
C	2.87164300	-3.11681000	-3.93929400
H	3.43771000	-2.79409900	-4.80873900
C	2.26551700	-4.38786600	-3.92480300
H	2.35913800	-5.04530600	-4.78464600
C	1.54601100	-4.80960300	-2.78897200
H	1.08334400	-5.79233100	-2.77169200
C	1.43306300	-3.96585300	-1.67046300
H	0.88969500	-4.31234700	-0.79450700
N	3.01671900	-0.24424700	-0.37116500
P	2.07476200	1.26614000	-0.14731600
P	1.83528600	-1.57894300	-0.20563000
Pd	0.00000000	0.00000000	0.00000000

B18. Cartesian coordinates of [$PdCl_2$(PNP-Dimprop)]

Pd	-0.00640000	-0.52780000	1.78630000
P	-1.35400000	-0.03400000	0.01890000
P	1.32160000	-0.15510000	-0.02520000
Cl	-1.76610000	-0.79610000	3.38700000
Cl	1.82050000	-0.91340000	3.27270000
N	-0.01310000	0.34990000	-1.02340000
C	-2.34340000	-1.39540000	-0.70680000
C	-2.50240000	1.37970000	0.13030000
C	2.60770000	1.13750000	0.07030000
C	2.12590000	-1.63600000	-0.73370000
C	-0.06890000	0.98520000	-2.37530000
C	-2.51010000	-1.60810000	-2.08280000
C	-2.97190000	-2.25770000	0.20440000
C	-2.40940000	2.22630000	1.24260000
C	-3.48530000	1.61800000	-0.84040000
C	3.55170000	1.33540000	-0.94870000
C	2.65350000	1.94010000	1.21700000
C	3.47250000	-1.90900000	-0.45510000
C	1.35250000	-2.60990000	-1.38110000
C	0.49640000	2.43360000	-2.42140000
H	-1.13980000	1.06770000	-2.59480000
C	0.57320000	0.08590000	-3.43890000
H	-2.03150000	-0.95910000	-2.80550000
C	-3.29760000	-2.66280000	-2.54110000
C	-3.76270000	-3.30700000	-0.26080000
H	-2.83380000	-2.10710000	1.27170000
H	-1.69410000	2.00510000	2.02660000
C	-3.26690000	3.31730000	1.36210000
H	-3.60330000	0.94150000	-1.67940000
C	-4.33580000	2.71400000	-0.72090000
H	3.55140000	0.69970000	-1.82720000
C	4.50850000	2.33920000	-0.83290000
H	1.96770000	1.74700000	2.03370000

C	3.61310000	2.94510000	1.32910000
C	4.04250000	-3.11450000	-0.86020000
H	4.07360000	-1.19460000	0.09370000
C	1.92670000	-3.80930000	-1.78950000
H	0.29760000	-2.43840000	-1.55750000
C	-0.04310000	3.33820000	-1.30910000
H	-1.12260000	3.48810000	-1.40680000
H	0.15350000	2.93520000	-0.31560000
H	0.43580000	4.32000000	-1.36700000
C	0.20980000	3.08230000	-3.78680000
H	-0.86580000	3.08860000	-4.00140000
H	0.71800000	2.58110000	-4.61350000
H	0.54670000	4.12300000	-3.78230000
H	1.58270000	2.36950000	-2.30700000
C	-3.92690000	-3.51250000	-1.63050000
H	-3.41920000	-2.81880000	-3.60820000
C	-4.22400000	3.56700000	0.37850000
H	-3.19770000	3.96050000	2.23280000
H	-5.09440000	2.89270000	-1.47580000
H	5.23650000	2.48380000	-1.62440000
C	4.53700000	3.14830000	0.30550000
H	3.64800000	3.55350000	2.22640000
H	5.08510000	-3.31430000	-0.63670000
C	3.27540000	-4.06270000	-1.53510000
H	1.31740000	-4.55160000	-2.29430000
H	-4.89580000	4.41360000	0.47770000
H	5.28920000	3.92490000	0.39860000
H	3.72090000	-5.00170000	-1.84680000
H	-4.24270000	-3.96860000	0.45250000
H	-4.53980000	-4.33340000	-1.98860000
H	1.65870000	0.03730000	-3.31460000
H	0.18930000	-0.93270000	-3.38320000
H	0.37100000	0.46630000	-4.44160000

UV - UFS
BLOEMFONTEIN
BIBLIOTEEK - LIBRARY